



**British
Geological Survey**

NATURAL ENVIRONMENT RESEARCH COUNCIL

NW UK continental margin: chronology and isotope geochemistry

BGS Commissioned Report

CR/05/095N BGS-NIGL Programme

Project 40156

BRITISH GEOLOGICAL SURVEY

BGS COMMISSIONED REPORT
CR/05/095N BGS-NIGL PROGRAMME
PROJECT 40156

NW UK continental margin: chronology and isotope geochemistry

The National Grid and other Ordnance Survey data are used with the permission of the Controller of Her Majesty's Stationery Office. Ordnance Survey licence number Licence No:100017897/2004.

Lynne Chambers, Fiona Darbyshire, Stephen Noble and Derek Ritchie

Keywords

U-Pb geochronology. Isotope geochemistry. Rockall. Hebrides.

Front cover

A photomicrograph of sample 164/25-2 in crossed polarised light. Field of View = 2 mm.

Bibliographical reference

CHAMBERS, L., DARBYSHIRE, F., NOBLE, S AND RITCHIE D. 2005. NW UK continental margin: chronology and isotope geochemistry. *British Geological Survey Commissioned Report*, CR/05/095.

Copyright in materials derived from the British Geological Survey's work is owned by the Natural Environment Research Council (NERC) and/or the authority that commissioned the work. You may not copy or adapt this publication without first obtaining permission. Contact the BGS Intellectual Property Rights Section, British Geological Survey, Keyworth, e-mail ipr@bgs.ac.uk You may quote extracts of a reasonable length without prior permission, provided a full acknowledgement is given of the source of the extract.

© NERC 2004. All rights reserved

Keyworth, Nottingham British Geological Survey 2005

BRITISH GEOLOGICAL SURVEY

The full range of Survey publications is available from the BGS Sales Desks at Nottingham, Edinburgh and London; see contact details below or shop online at www.geologyshop.com

The London Information Office also maintains a reference collection of BGS publications including maps for consultation.

The Survey publishes an annual catalogue of its maps and other publications; this catalogue is available from any of the BGS Sales Desks.

The British Geological Survey carries out the geological survey of Great Britain and Northern Ireland (the latter as an agency service for the government of Northern Ireland), and of the surrounding continental shelf, as well as its basic research projects. It also undertakes programmes of British technical aid in geology in developing countries as arranged by the Department for International Development and other agencies.

The British Geological Survey is a component body of the Natural Environment Research Council.

British Geological Survey offices

Keyworth, Nottingham NG12 5GG

☎ 0115-936 3241 Fax 0115-936 3488
e-mail: sales@bgs.ac.uk
www.bgs.ac.uk
Shop online at: www.geologyshop.com

Murchison House, West Mains Road, Edinburgh EH9 3LA

☎ 0131-667 1000 Fax 0131-668 2683
e-mail: scotsales@bgs.ac.uk

London Information Office at the Natural History Museum (Earth Galleries), Exhibition Road, South Kensington, London SW7 2DE

☎ 020-7589 4090 Fax 020-7584 8270
☎ 020-7942 5344/45 email: bgs_london@bgs.ac.uk

Forde House, Park Five Business Centre, Harrier Way, Sowton, Exeter, Devon EX2 7HU

☎ 01392-445271 Fax 01392-445371

Geological Survey of Northern Ireland, Colby House, Stranmillis Court, Belfast, BT9 5BF

☎ 028-9038 8462 Fax 028-9038 8461

Macleon Building, Crowmarsh Gifford, Wallingford, Oxfordshire OX10 8BB

☎ 01491-838800 Fax 01491-692345

Sophia House, 28 Cathedral Road, Cardiff, CF11 9LJ

☎ 029-2066 0147 Fax 029-2066 0159

Parent Body

Natural Environment Research Council, Polaris House, North Star Avenue, Swindon, Wiltshire SN2 1EU

☎ 01793-411500 Fax 01793-411501
www.nerc.ac.uk

Contents

Acknowledgments	1
Summary	2
1. Introduction	3
1.1 Previous Work	6
1.2 Characterisation of the onshore Hebridean Terrane	9
1.3 Samples Studied	14
1.4 Analytical Methods	15
2. Petrology	18
2.1 Summary	18
2.2 Petrographic Descriptions	20
3. Major and Trace Element Geochemistry	95
4. Isotope Geochemistry	110
4.1 U-Pb Geochronology	111
4.2 Common Pb Isotopic Characterisation of Rockall	134
4.3 Nd Isotope Data	138
5. Conclusions	144
5.1 Archaean Offshore Rocks	144
5.2 Proterozoic Offshore Rocks	146
5.3 Regional Correlations	147
References	153

Figures

Figure 1.1 Location of crystalline basement samples.	See pocket
Figure 1.2. The location of the Rhinns complex (Muir et al. 1994).	7
Figure 1.3. The Lewisian of Scotland (Sutton and Watson, 1951).	10
Figure 1.4. The Lewisian basement terranes of Friend and Kinny (2001).	12
Figure 3.1. An-Ab-Or diagram with field boundaries after Barker (1979).	95
Figure 3.2. Plot of CaO versus SiO ₂	101
Figure 3.3. Chondrite normalised REE plots: 57-09/536, 57-09/537, 206/7-A2 2544m, 205/16-1, 56-08/920.	102
Figure 3.4. Chondrite normalised REE plots: 204/23-1, 202/2-1, 206/8-1.	102
Figure 3.5. Chondrite normalised REE patterns: 206/8-2, 206/8-7, 206/7-A2 2599 m, 88/02, 90/14.	103
Figure 3.6. Chondrite normalised REE patterns: 154/3-1 green, 164/25-2 pale blue, 58-8/228 pink.	103
Figure 3.7. Chondrite normalised REE patterns for Stanton High samples	103
Figure 3.8. Chondrite normalised REE patterns for Rockall Bank samples.	105
Figure 3.9. Primitive mantle normalised multi-element diagram: 206/8-1A, 205/22-1 and 202/3-1.	106
Figure 3.10. Primitive mantle normalised multi-element diagrams: 206/8-8 and 204/25-1.	107
Figure 3.11. Primitive mantle normalised multi-element diagrams: 206/8-2, 205/16-1 and 56-08/920.	107
Figure 3.12. Primitive mantle normalised diagrams:	108

164/25-2 and 154/3-1.	
Figure 3.13. Primitive mantle normalised multi-element diagrams: 56-09/384, 56-09/386, 132/15-1 and 56-09/388.	109
Figure 3.14. Primitive mantle normalised multi-element diagrams: 57-15/15, 57-14/58, 56-15/18 1.65m and 56-15/18 3.02m.	109
Figure 4.1. 209/9-1 U-Pb concordia plot.	112
Figure 4.2. 206/8-1a U-Pb concordia plot.	112
Figure 4.3. 205/22-1 SEM-CL photo of a zircon.	116
Figure 4.4. 205/22-1 U-Pb concordia plot.	117
Figure 4.5. 202/2-1 SEM-CL photo of a zircon.	117
Figure 4.6. 202/2-1 U-Pb concordia plot.	118
Figure 4.7. 164/25-2: Photo of abraded grain fragments and small grains.	119
Figure 4.8. 164/25-1 U-Pb concordia plot.	119
Figure 4.9. 90/14 SEM CL zircon images.	120
Figure 4.10. 90/14 U-Pb concordia plot.	121
Figure 4.11. 56-09/536 and 537 SEM CL and plane polarised light.	123
Figure 4.12. 56-09/536 and 537 U-Pb concordia plot.	124
Figure 4.13. 56-08/921 SEM CL images.	125
Figure 4.14. 56-08/921 U-Pb concordia plot.	125
Figure 4.15. 56-08/924 SEM CL and plane polarised light.	126
Figure 4.16. 56-08/924 U-Pb concordia plot.	127
Figure 4.17. 56-09/384 Zircon crystals.	128
Figure 4.18. 56-09/384 U-Pb concordia plot.	128
Figure 4.19. 56-15/18 SEM CL image.	129
Figure 4.20. 56-15/18 U-Pb concordia plot.	129
Figure 4.21. U-Pb geochronology summary.	133

Figure 4.22. $^{206}\text{Pb}/^{204}\text{Pb}$ vs. $^{207}\text{Pb}/^{204}\text{Pb}$ common Pb whole-rock plot.	136
Figure 4.23. ϵNd versus time for the basement samples.	140
Figure 4.24. ϵNd versus $^{87}\text{Sr}/^{86}\text{Sr}$ at 1750 Ma.	142
Figure 5.1. A reconstruction of eastern Laurentia and Baltica (Park, 1994).	148
Figure 5.2. A reconstruction of Laurentia-Baltica (Winchester, 1988).	149
Figure 5.3. A palaeomagnetic reconstruction (Buchan et al., 2000).	152
Figure 5.4. A reconstruction of Laurentia-Baltica (Baba, 2002).	152

Tables

Table 1.1. Complete sample inventory	4-5
Table 3.1. Major element concentrations by XRF	96
Table 3.2. Trace element concentrations by XRF	97
Table 3.3. Trace element concentrations by ICP-MS	98
Table 3.4. CIPW NORM values	99-100
Table 4.1. Rockall Basement U-Pb data	113-115
Table 4.2. Rockall Basement Common Pb data	137
Table 4.3. Rockall Basement Sr-Nd data	139

Acknowledgments

The authors thank NIGL and BGS colleagues for their helpful discussions. Tim Brewer, Stephen Daly and Ray Scanlon are also thanked for sharing their knowledge and expertise. We acknowledge the technical support of Mark Allen, Neil Boulton, Jenny Cook, Quentin Crowley, Joanne Green, Mark Ingham, Vanessa Pashley and Aaran Sumner during this study. Alexander Henderson and Sheila Jones are thanked for their assistance in preparing materials for the final report.

The authors also gratefully acknowledge the Rockall Consortium and the BGS – NIGL programme who funded this research project.

Summary

Until recently, a significant proportion of the crystalline basement from the NW UK continental shelf was virtually terra incognita in comparison with similar rocks on the mainland. A significant increase in the geological understanding of this region's crystalline rocks is provided by new data from 42 boreholes, some of which were only drilled in 2001. The samples are from a ~550 km long transect of the UK continental shelf, extending from ~50 km west of Shetland in the northeast to Stanton High, south of the Outer Hebrides and westward to include Rockall High.

Petrography and geochemistry show the main lithologies are amphibolite to granulite facies amphibolites and gneisses, and include classic Archaean TTG's, metabasic rocks, granite (s.s), and granitic pegmatites. A long history of crustal growth is indicated by U-Pb zircon ages and Nd model ages. Archaean gneisses that developed in two main episodes dominate much of the study area. The older gneisses (c. 2.8 Ga) represent new continental crust while genesis of the later gneisses (c. 2.74-2.70 Ga) involved crustal recycling. Both groups are very similar to onshore Lewisian gneisses.

Important areas of known Proterozoic crust were also characterized, confirming the results of previous studies. Geochemistry and Nd isotope systematics of Stanton High documents extensive Archaean crust re-working in the Proterozoic, as well as addition of new continental crust. Stanton High U-Pb zircon ages (1799-1791.5 Ma) are similar to the Rhinns terrane (c. 1800 Ma). Westward, Rockall High borehole samples yield a 1744.9 Ma U-Pb age, distinct from Stanton High – Rhinns rocks. Nd data indicate addition of mantle-derived juvenile crust, as previously noted elsewhere on Rockall High. An isolated granulite facies metabasic rock on the NE portion of the Hebrides shelf was dated at 1633.5 Ma, also representing a new addition of crust.

The new data provide important constraints for regional correlations and palaeotectonic reconstructions. The Archaean rocks are almost certainly related to the Lewisian: given current models, they probably also correlate to the Nagssugtoquidian in Greenland, while the Rockall and Stanton Highs, together with the Rhinns terrane, have affinities to the Ketilidian of Greenland and the Svecofennian of Scandinavia.

1 Introduction

Much is known regarding the nature, age and characterisation of basement terranes around the margins of the North Atlantic, particularly within the NW Highlands of Scotland and Norway, but also within the conjugate margin on east Greenland, Canada and the USA. In stark contrast, almost nothing is known regarding the basement in the intervening offshore area. The samples studied in this project provide a unique and important insight into the large area of crust between the onshore conjugate margins of Greenland and Scotland. The results of this project have international relevance, making a substantial contribution to UK/Eire regional geology, and tectonic/paleocontinental reconstruction studies.

This report documents the work carried out on 42 samples provided to the authors by the BGS, the Rockall consortium and other oil companies. These crystalline basement samples from the NW UK continental margin were examined petrographically. 36 samples were selected for major and trace element geochemistry and isotope analysis in order to provide insights into their intrusive and metamorphic history.

The location of all the sample sites is shown in Figure 1.1 (location map showing the sample sites in relation to the conjugate margins of Greenland and Scotland, see pocket) and a full sample inventory can be found in Table 1.1. Whole rock Rb-Sr and Sm-Nd isotope analyses have been carried out on 35 of the samples, and whole rock Pb isotope analysis on 15 samples. U-Pb zircon ages have been obtained on 12 samples, and U-Pb titanite data for 7 of these rocks together with further zircon geochronology on an additional 3 samples obtained late in the project are still underway. The results of this ongoing work will be made available as a subsequent report, and will also include mineral (zircon) and whole rock Lu-Hf isotope data for selected samples.

Table 1.1. Complete sample inventory.				
Well	Depth (below KB* or sea bed**)	Thin section identifier (and number cut)	Rock type	Notes
220/26-1	5279.9-5280.2m	N3745	Quartzofeldspathic mylonite	
209/9-1	972.4m	N3743	Augen gneiss	
209/12-1	11520.6 ft	N3744	Biotite schist	
81/17	137.6-138.2m	N3751	Amphibolite	
208/27-2	4528-4528.75 ft	N3741 (a), N3742 (b)	Granitic gneiss (a) cataclasite (b)	
206/8-2	1864.3-1864.55m	N3736	Protomylonite	
206/8-8	2498.6-2498.95m	N3738 (a), N3739 (b) , N3740 (c)	Granitic gneiss (a) granitic gneiss (b) granitic gneiss (c)	
206/8-1A	2310.78-2310.95m	N3735	Dioritic gneiss	
206/8-7	2320.5m	N3737	Amphibolite	
206/7-2, 2A	2142.8-2143m, 2183.15-2183.3m, 2435.5-2435.65m, 2544.65-2544.85m, 2599.2-2599.4m, 2599.8-2599.95m	N4168, N4169, N4170, N4171, N4172, N4173	monzonite to granodiorite and mylonitic amphibolite	Six samples were taken over a 361.2m interval
206/7-1	1735.5-1735.6m	N4164	Tonalitic gneiss	Sample too small for geochemistry
205/16-1	4172-4172.15m	N3730 (a), N3731 (b), N3732 (c)	Pseudotachylite (a) diorite cut by pseudotachylite vein (b) diorite (c)	
205/22-1A	3225.45-3225.6m	N3733	Dioritic gneiss	
205/26-1	7002 ft	N3734	Dioritic gneiss	Sample too small for geochemistry
204/22-1	2760m	N4165	Tonalitic gneiss	Sample too small for geochemistry
204/23-1	3846.9-3847.05m	N3728	Quartzofeldspathic gneiss	
204/25-1	9416 ft	N3729	Tonalitic gneiss	
202/3-1	1774.49-1774.6m	N3727	Cataclasite	
202/2-1	4002 feet	N3810 and N3811	Quartzofeldspathic gneiss.	
202/9-1	5381 feet	N4166	Amphibolite	Sample too small for geochemistry
88/02	13.37-13.55m	N3722 (a), N3723 (b)	Quartzofeldspathic schist cut by cataclasite	
164/25-2	2727.65-2727.8m	N3725 (a), N3726 (b)	Partially retrogressed metabasic gneiss	

Table 1.1. Complete sample inventory (con't).				
Well	Depth (below KB* or sea bed**)	Thin section identifier (and number cut)	Rock type	Notes
154/3-1	8060.0-8060.2	N4167	Amphibolite	
58-08/227	0-0.38m TD			Sample too small for thin sectioning and geochemistry
58-08/228	0-1.32m TD	N3720	Granitic pegmatite	
58-08/230	0-2.04m TD	N3721	Alkali granite	
90/14	87.82m	N3724	Quartzofeldspathic gneiss	
57-09/534	0-1.33m TD	N3713	Quartzofeldspathic gneiss	Sample too small for geochemistry
57-09/535	0-1.02m TD	N3714	Quartzofeldspathic gneiss	Sample too small for geochemistry
57-09/536	0-0.50m TD	N3715	monzodiorite	
57-09/537	0-2.90m TD	N3716 (a), N3717 (b), N3718 (c)	monzodiorite	1.31-1.63 m for U-Pb
56-08/920	0-1.26m TD	N3704	diorite	
56-08/921	0-0.90m TD	N3705 (a), N3706 (b)	granodiorite	0.78m taken from (b) for geochemistry
56-08/924	0-1.69m TD	N3707	quartz monzonite protomylonitic TTG	
132/15-1	4155.55-4155.7m	N4163	Cataclasite	large calcite crystals on one surface
56-09/384	0-1.80m TD	N3708	Amphibolite gneiss	
56-09/385	0-1.33m TD			Not sampled, similar to 386
56-09/386	0-1.70m TD	N3709	Protomylonite	Sample for geochemistry 0.88-1.01 m
56-09/387	0-0.5m TD			Sample too small for thin sectioning and geochemistry
56-09/388	0-0.83m TD	N3710	Quartzofeldspathic gneiss	
56-15/18	0-4.42m TD	N3711, N3712	Tonalitic gneiss	336-374 cm half core for U-Pb
57-14/58	0-2.61m TD	N3719	Metagabbro	
57-15/15	0-0.59m TD	N3749	Trachyandesite	

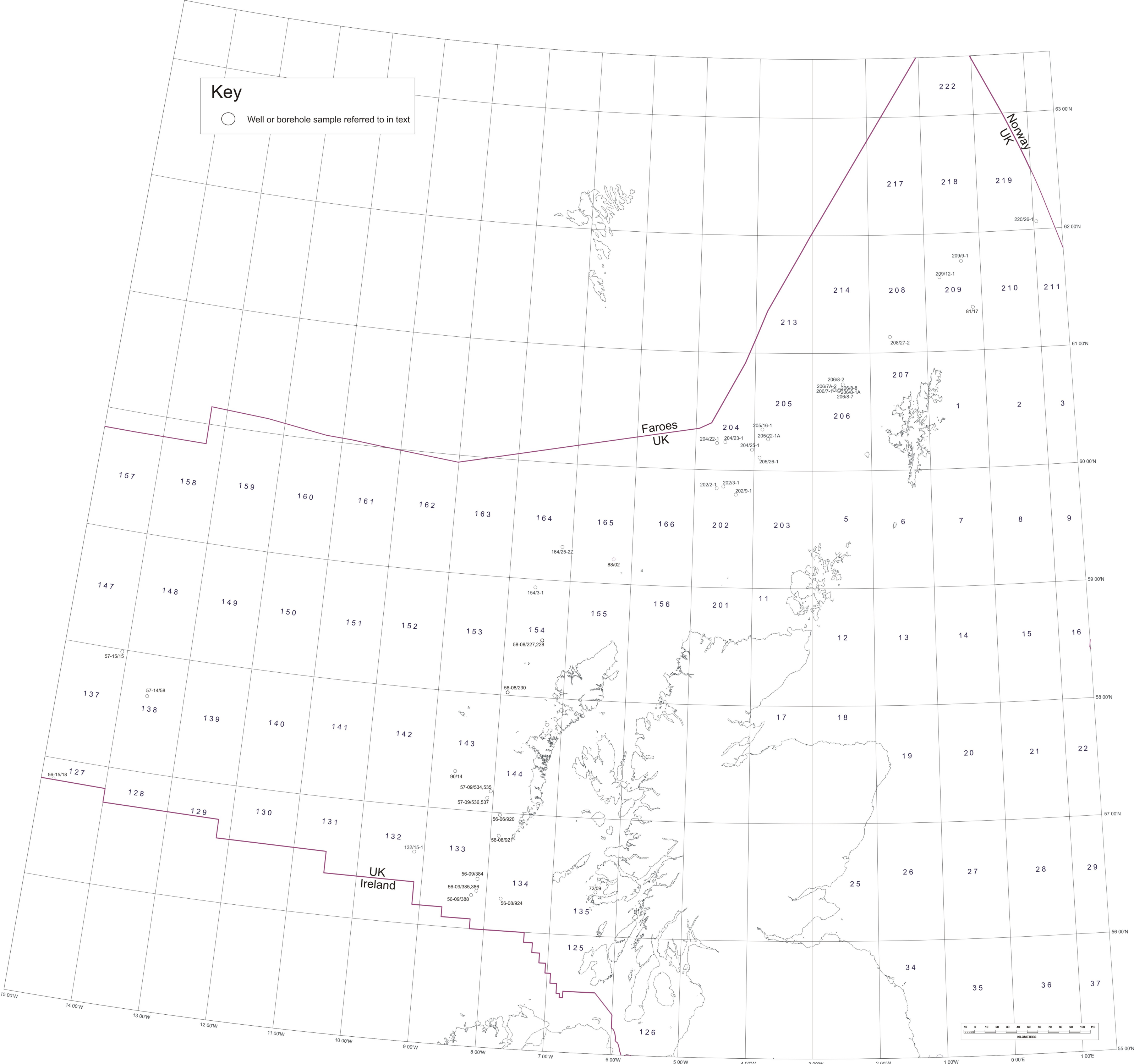


Figure 1.1. Location of crystalline basement samples recovered from wells and boreholes drilled within the NW UK continental margin

1.1 PREVIOUS WORK IN THE OFF-SHORE REGION

The basement to the west of the UK and Eire is divided into two main terranes, namely the Hebridean terrane and the Rhinns terrane (also known as the Hebridean Craton and the Rhinns Complex). Speculatively, the Archaean Hebridean Craton is thought to comprise a large part of the NW UK continental margin, with affinities to the Lewisian Gneiss Complex of NW Scotland. Within a small part of this terrane, Ritchie and Darbyshire (1984) recorded a “Scourian” Rb-Sr isochron age of c.2500 Ma for granitoids from six widely spaced commercial boreholes within the West Shetland Basin. To the north of this, Ritchie et al. (1987) documented K-Ar ages of c.400 Ma from two Caledonian granites that intrude the Archaean basement. The Rhinns terrane was identified from isotope studies of basement rocks on Islay, Colonsay, Inishtrahull and the Annagh area (e.g. Marcantonio et al. 1988; Dickin and Bowes 1991; Muir et al. 1994; Daly et al. 1995). This terrane comprises mainly deformed gabbro and syenite, with minor mafic and felsic intrusions (Figure 1.2). Isotope data indicates that the complex represents the addition of new mantle-derived crust at c. 1.8 Ga (Marcantonio et al. 1988; Muir 1990; Daly et al. 1991) rather than recycling of older Archaean crust. Formation of the Rhinns terrane at c. 1.8 Ga is contemporaneous with a widespread 1.9-1.7 Ga (Patchett and Arndt, 1986) addition of crust in the North Atlantic region. As part of this formation, the Rhinns complex provides the link between the Ketilidian province of South Greenland with the Svecofennian of Scandinavia (Muir et al. 1994). This addition of new crust is also contemporaneous with the Laxfordian “re-working” cycle within the Lewisian Complex. Onshore, growth of metamorphic hornblende during amphibolite facies metamorphism occurred at 1.71 Ga.

Recent work by Scanlon et al. (2003) on samples recovered from the Stanton High has also found juvenile Paleoproterozoic crust. They called this area, which comprises granites, amphibolite facies schists, granodiorites and syenites, the Stanton Banks Terrane. U-Pb sensitive high resolution ion microprobe (SHRIMP) zircon analyses yielded protolith ages of c. 1.79 to 1.83 Ga, similar to the nearby Rhinns terrane (Scanlon et al. 2003). In addition to these two main terranes, a separate group of basement rocks is located in an area NW of the Rhinns terrane around the Rockall High. Roberts et al. (1973), Morton and Taylor (1991) and Daly et al. (1995) carried

out geochemical and isotope investigations on borehole cores and other dive samples to characterize this region. The resulting K-Ar, Rb-Sr, Sm-Nd and Pb-Pb data indicated that the basement rocks represented a juvenile addition of crust from the mantle and thus had possible affiliation with the Rhinns terrane. For example, Rockall High samples have a ^{238}U - ^{204}Pb (μ) value of 8.03 that precludes them from representing reworked Archaean crust (Morton and Taylor, 1991). The data also suggested ages of c. 1.63 Ga, and therefore the Rockall High basement was interpreted as having formed at the same time as the Laxfordian deformation and the retrogressive metamorphism of the Lewisian (1600-1400 Ma, Park and Tarney, 1987). Dickin (1992) subsequently re-examined the Rb-Sr data set of Morton and Taylor (1991) and considered the slope of their Rb-Sr errorchron to be dominated by the most radiogenic data point, and excluding this granite sample E resulted in a recalculated age of 1720 ± 70 Ma.

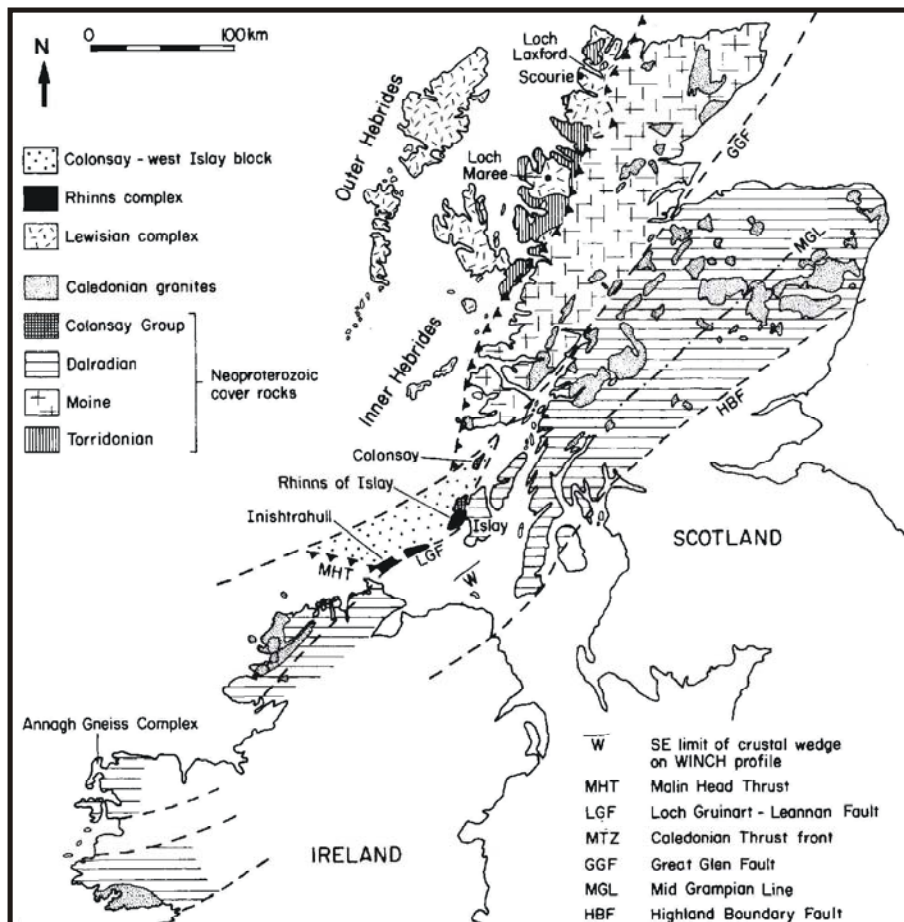


Figure 1.2: The location of the Rhinns complex reproduced from Muir et al. (1994).

Little is known about basement rocks in off-shore areas to the north the Shetlands and west of the Rockall High. It is interesting to note, however, that although the basement rocks underlying the Faeroe Islands are not exposed, whole rock Pb isotope data (e.g. $^{207}\text{Pb}/^{204}\text{Pb}$ vs. $^{206}\text{Pb}/^{204}\text{Pb}$) of the overlying basalt succession illustrates mixing of MORB and basement that is older than that of the Rockall High. West of Rockall, Morton and Hallsworth (2005) have used detrital zircon SHRIMP ages to investigate the age of the basement in the Hatton and Edoras Bank regions. There are no samples of basement itself, but zircons were recovered from sedimentary rocks found in two wells (BGS Borehole 99/2A and DSDP Site 555). Borehole 99/2A gave a mean age of 1798.5 ± 4.5 Ma (MSWD 0.69) and zircons from DSDP Site 555 gave a mean age of 1749.5 ± 2.7 Ma.

1.2 CHARACTERISTICS OF THE ONSHORE HEBRIDEAN TERRANE

The bulk of Hebridean terrane, as exposed on mainland Scotland and the Outer Hebrides, is comprised of high-grade orthogneisses that are collectively known as the Lewisian Gneiss Complex. The complex is a typical Archaean high-grade granulite gneiss terrane, and is probably one of the most extensively studied terranes of its type in the world. Despite this, the history of the Lewisian complex is difficult to unravel as intense deformation and metamorphism have affected large areas. A recent re-evaluation of the terranes that make up the Lewisian complex by Friend and Kinny (2001) has highlighted the many issues in Lewisian chronology that are still keenly debated.

Historically, the Lewisian of mainland Scotland was subdivided by their distinctive metamorphic and structural histories into three regions: Northern, Central and Southern (Peach et al. 1907; Sutton and Watson 1951). These regions were divided by shear zones and were thought to be one block of crust that had undergone successive orogenic cycles (Figure 1.3). The first occurred between 2900 and 2400 Ma and is termed the Scourian and the second, Laxfordian, occurred at 1800 Ma. These two orogenic cycles were separated by the intrusion of the Scourie dyke swarm. The deformation and field relationships of these dykes were crucial in identifying the three regions and their tectonic history.

Sutton and Watson (1951) described granulite facies rocks of the Central region (the Scourian gneisses) cut by a swarm of mafic and ultramafic dykes. In contrast, the Northern and Southern regions are composed of Scourian granulite facies gneisses that were modified during the Laxfordian when the granulite facies gneisses were transformed to amphibolite facies hornblende-biotite gneisses. These two regions are separated from the Central Region by a transition zone that is several kilometres wide. The Scourie dykes are also deformed within the Northern and Southern regions.

This stratigraphic history was revised when the work of Tarney (1963), Park (1964), Evans and Tarney (1964) and Evans (1965) showed that a significant metamorphic event took place after the prograde metamorphism of the Central Region (Badcallian) and before the intrusion of the Scourie dyke swarm. This event was termed the Inverian (Evans 1965).

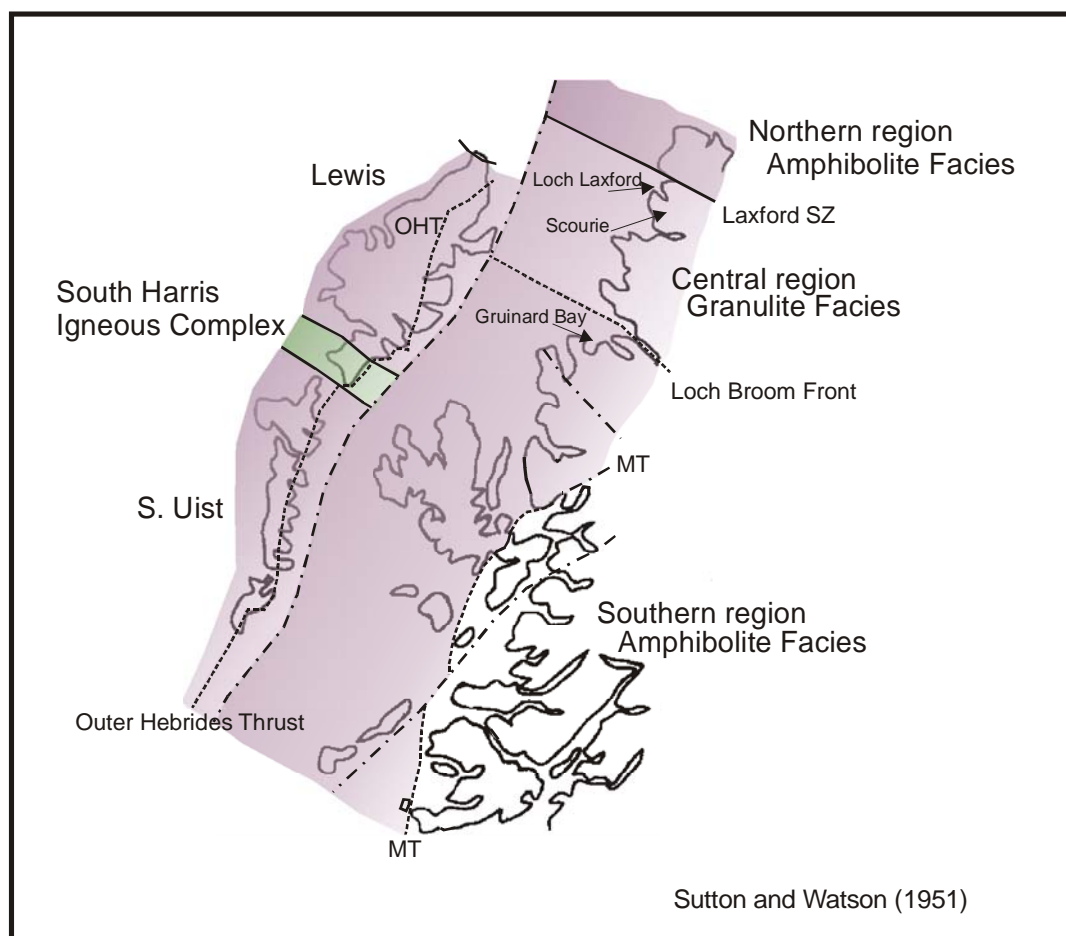


Figure 1.3. The Lewisian of mainland Scotland and the Outer Hebrides were divided into 3 regions by Peach et al. (1907) and Sutton and Watson (1951).

Most of the Scourian gneisses are banded acid to intermediate 'grey' gneisses, which are thought to have originated as plutonic igneous rocks. Chemical compositions indicate these gneisses are tonalitic to trondhjemitic. There are minor occurrences of interbanded quartzite and schist, which are probably metasediments, and some fine-grained amphibolites thought to represent metavolcanics. The association of the Scourian gneisses with metasediments is suggestive of a relationship with oceanic crust, and Tarney and Weaver (1987) proposed that a subduction zone was the only environment where large volumes of mafic material could be melted to generate tonalitic crustal material.

The timing of igneous and metamorphic events is key to unravelling the complex history of the terrane. Here we summarise some of the geochronological data used to constrain some of the events. The age of the protoliths of the Scourie gneisses, and

the Central region as a whole, has been estimated to be 2930 Ma (Nd model age; Whitehouse, 1989) and 2960-3030 (high-precision U-Pb thermal ionization mass spectrometry (TIMS) and SHRIMP; Friend and Kinny, 1995; Kinny and Friend, 1997; Corfu et al. 1998). In contrast, single titanite and zircon U-Pb analyses indicate a range in protolith ages for the other regions: 2770-2840 Ma for Northern Region gneisses, 2850-2730 Ma for Gruinard Bay in the Southern Region (Kinny and Friend, 1997; Whitehouse et al. 1997; Corfu et al. 1998).

The earliest period of deformation and granulite facies metamorphism is a characteristic feature of the Central region and is termed the Badcallian event (Park, 1970). Originally the Badcallian was thought to be c. 2.7 Ga (bulk fraction TIMS zircon ages; Pidgeon and Bowes, 1972; Lyon et al. 1973). However, Humphries and Cliff (1982) dated the closure of the Sm-Nd isotope system at 2490 Ma and more recent zircon work by Corfu et al. (1998) and Friend and Kinny (1995) illustrates that this disturbance of the U-Pb systematics corresponds to the main Badcallian event at 2490-2480 Ma. Interestingly, the Badcallian event was not found in the Northern Region (Kinny and Friend, 1997) or in the area around Gruinard Bay in the Southern region (Whitehouse et al. 1997; Corfu et al. 1998). This suggests that the event was restricted to the Central Region alone.

The significant difference in protolith ages and the lack of the Badcallian metamorphic event in the Northern and Southern Regions led Kinny and Friend (1997) to suggest that the three regions represent different crustal blocks that have been juxtaposed during the Palaeoproterozoic (Figure 1.4). The first common metamorphic event is that of the c. 1750 Ma Laxfordian amphibolite metamorphism. Friend and Kinny (2001) took this idea further and proposed that the Lewisian of mainland Scotland comprises many terranes that were juxtaposed at various times during the Proterozoic. They emphasised that these terranes underwent different accretionary and metamorphic histories, and only after juxtaposition did they share common metamorphic histories.

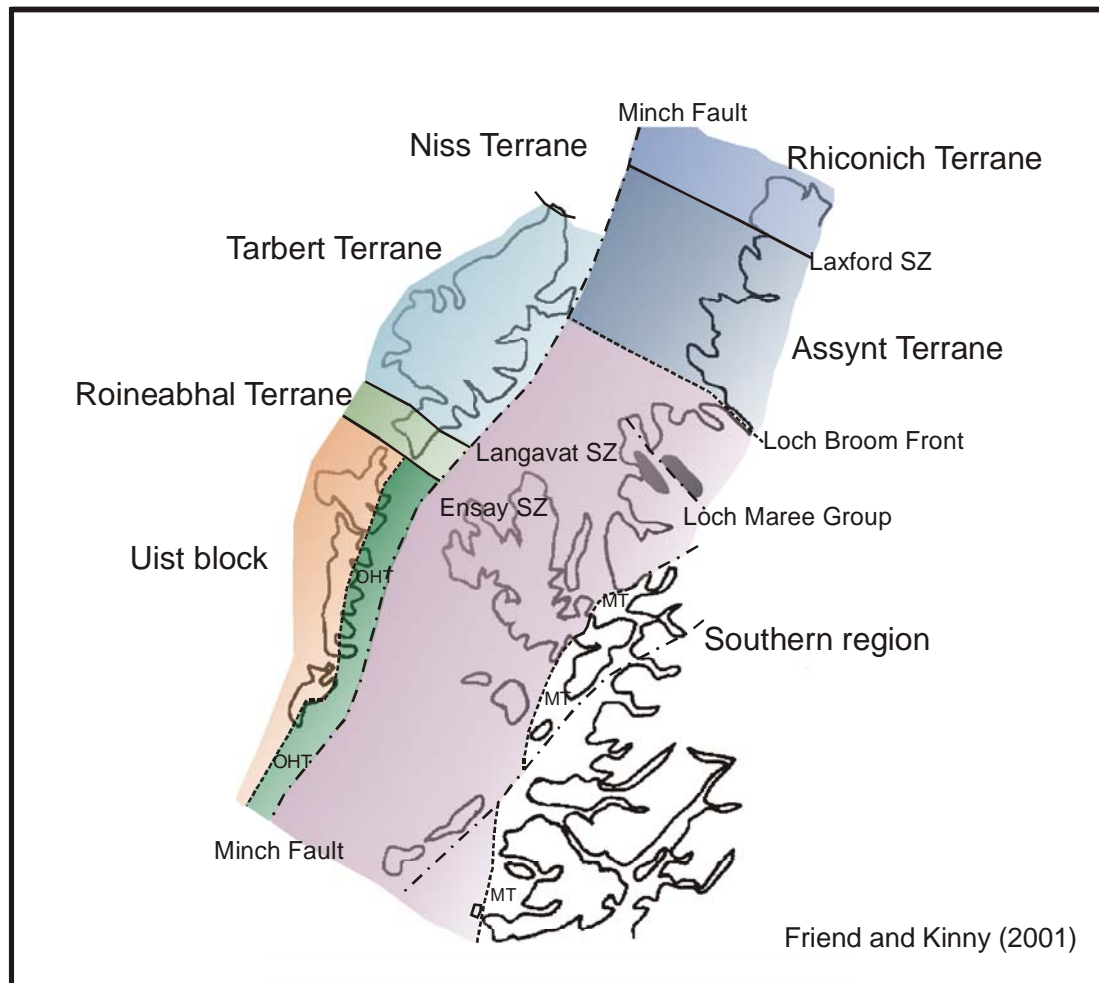


Figure 1.4. The Lewisian basement terranes of Friend and Kinny (2001).

So far only the mainland of Scotland has been discussed, but the Outer Hebrides comprises significant outcrops of Scourian granulites with amphibolite sheets associated with dykes. Deformed and amphibolite to granulite facies metamorphosed Archaean TTG's, such as those exposed on Lewis, Harris, Barra and South Uist range in age from 3125 Ma to 2730 Ma (Kinny et al., 2005; Whitehouse and Bridgwater 2001; Whitehouse 2003), some of which were metamorphosed to granulite facies between 2.8 and 2.7 Ga (the 2.49 Ga granulite facies metamorphism is absent). The significantly younger South Harris Igneous Complex is composed of anorthosite and metagabbros that are associated with tonalities and pyroxene gneisses. It is noteworthy that there are more migmatites and more supracrustal rocks on the Outer Hebrides than on the mainland. The supracrustals occur in two belts that flank the South Harris Igneous Complex.

While some geochronological evidence provided by the basement rocks of the Outer Hebrides is consistent with the arguments of Friend and Kinny (2001), other recently acquired, high quality, data serves to underline the uncertainties in their terrane model. Mason and Brewer (2005) highlight the problem in the Outer Hebrides where a proposed terrane boundary at post-1675 Ma is questioned. Friend and Kinny (2001) suggest that the Langavat Shear Zone and the associated boundary postdate c. 1675 granite pegmatites that they consider to be entirely restricted to the Tarbert Terrane and that stop at the shear zone. Dearnley (1963) and Mason et al. (2004), however, report similar pegmatites in Friend and Kinny's (2001) putative Roineabal Terrane south of the shear zone. Mason and Brewer (2005) document c. 1675 Ma TIMS U-Pb zircon ages for pegmatites just south of the shear zone. Mason and Brewer (2005) then argue that the 'Roineabal Terrane' cannot have been sutured to the rocks to the north using the Langavat Shear Zone as a terrane boundary at this time.

1.3 SAMPLES STUDIED

In the following sections of this report the samples are discussed in the order that they occur from north to south along the study area transect. Prior to any analytical work the samples were carefully examined and the presence of alteration and late fractures and their mineralogy noted. At least one thin section from each borehole sample was cut to allow a detailed examination of representative portions of the drill core.

Several thin sections were cut for some segments of drill core when they were judged to be particularly complex due to either the presence of several lithologies over a short section of core or to highlight particular deformational features.

Some petrographic descriptions are in part based on those previously reported in Phillips (2002). Many petrographic descriptions reported here, however, are new, as are all of the thin section photographs. Relatively low-resolution photographs of selected thin sections are given in Chapter 2. High quality digital files for all thin sections are given in the compact disk located in the back cover of the report.

Major and trace element geochemistry, and Sr–Nd isotope data were obtained only on material that reasonably reflected primary rock compositions. Particular care was taken to avoid surfaces affected by late alteration, which was particularly troublesome with samples cut by numerous fracture planes, but wherever possible altered portions were cut off with a trim saw prior to sample crushing.

A small subset of samples was chosen for U–Pb geochronology with the aims of maximizing geographical coverage while attempting to use material with the highest probability of success, which sometimes equated to maximum sample size to provide adequate amounts of good quality zircon.

1.4 ANALYTICAL METHODS

The various analytical techniques used in this study have methodologies that are specific to each, and in some cases are dissimilar to those used in other isotope laboratories. These methods are therefore individually described below.

1.4.1 Major and trace element geochemistry analytical techniques

All of the samples were jaw crushed in steel crushers and milled to a fine powder in agate mills. Major and trace elements were determined at the British Geological Survey by a combination of x-ray fluorescence spectrometry (XRF) and inductively coupled mass spectrometry (ICP-MS) on a single collector quadrupole mass spectrometer. Major elements were analysed by XRF on fused beads, and some trace elements analysed by XRF on pressed powder pellets. Other trace elements, including U, Th, the rare earth elements and some high field strength elements were determined by ICP-MS. Sample powders for ICP-MS were digested in concentrated HF-HNO₃ and aspirated in a dilute HNO₃ solution. The data are presented in Tables 3.1 to 3.4 and discussed in Chapter 3. Primitive mantle rare earth plots are normalized using values from Sun and McDonough (1989). Normalizing values for multi-element plots are from Nakamura (1974).

1.4.2 U-Pb Analytical Techniques

U-Pb geochronology samples (0.25-2.5 kg) were jaw-crushed and disk-milled to <420 µm using conventional techniques. Heavy mineral concentrates were prepared using a modified Superpanner©, Frantz LB-1 separator, and heavy liquids. Clear, crack-free zircon crystals and crystal fragments were handpicked under alcohol. In some cases, crystals were broken with tweezers and grain tips selected as they best represented the latest growth episode recorded by the crystal. Particular attention was paid to avoiding inherited cores unless their dating was intended.

Zircons were abraded to improve concordance (Krogh, 1982) and washed in warm distilled 4 N HNO₃ and ultra pure H₂O prior to dissolution. Samples were spiked with a mixed ²⁰⁵Pb/²³⁵U tracer and dissolved in HF-HNO₃ (Parrish, 1987) for at least 60 hours at 240 C, dried down and followed by 16 hours in HCl at 140 C to convert all dissolved salts to chloride form prior to chemistry. In some cases the dissolution

procedure was repeated to ensure complete sample dissolution. Chemical separations and TIMS analysis followed Corfu and Noble (1992) and Noble et al. (1993). Most data were collected on a VG 354 mass spectrometer fitted with a wide aperture retarding potential filter (abundance sensitivity of 54 ppb) and Philips ion counting Daly detector. A few data were collected on a ThermoElectron Triton mass spectrometer fitted with an RPQ filter (abundance sensitivity of better than 20 ppb) and an ETP discrete dynode detector, which gave data of equivalent quality to the VG 354 data set. U and Pb were loaded on degassed single Re filaments with phosphoric acid and silica gel. Data were corrected for 0.09%/AMU and 0.07%/AMU mass fractionation for Pb and U, respectively. Data obtained on the Daly detector required an additional correction for a bias relative to the Faraday cups of 0.088%/AMU for Pb and 0.04%/AMU for U. Ages are calculated using the decay constants of Jaffey et al. (1971). Uncertainties quoted for isotope ratios and ages are at the two-sigma level. Data reduction and age calculations followed Ludwig (1980, 1998, 2003).

1.4.3 Common Pb Analytical Techniques

Pb isotope ratios were determined by plasma ionisation multi-collector mass spectrometry (PIMMS) on the P54 and Axiom instruments at the NERC isotope Geosciences Laboratory (NIGL) following procedures described in Kempton and McGill (2002). Within-run standard error for Pb isotope measurements is generally less than 0.02% (2σ). Minimum uncertainties are derived from the external precision of repeated runs of NBS 981, which is better than $\pm 0.01\%$ (2σ). Instrumental mass fractionation was corrected for using a natural thallium solution mixed with the Pb samples and used as an internal monitor. A $^{203}\text{Tl}/^{205}\text{Tl}$ value of 0.41876 was used for all corrections, and was determined empirically by cross calibration with NBS 981. All sample Pb isotope ratios have been normalized using correction factors calculated from the difference between measured NBS 981 standards for each analytical session and the accepted NBS 981 values of Todt et al. (1996).

1.4.4 Rb-Sr and Sm-Nd Analytical Techniques

Concentrations of Rb and Sr for the rock samples were determined by X-ray fluorescence spectrometry using pressed pellets. For the Sr – Sm-Nd isotope ratio analyses, 150 mg samples were decomposed in Teflon bombs at 120°C for 3 days

using a mixture of concentrated hydrofluoric and nitric acids. Sample residues were converted to chloride using 6M hydrochloric acid, and strontium (Sr) and the rare earth elements (REE) were separated from the solution by conventional ion exchange techniques.

Samarium (Sm) and neodymium (Nd) concentrations were obtained by isotope dilution using a mixed ^{149}Sm - ^{150}Nd spike solution added to the samples prior to acid dissolution. Sm and Nd were separated from the bulk REE fraction on a column filled with Dowex Biobeads coated with bis Di-ethylhexyl hydrogen phosphate (HDEHP). Sr was loaded on single tantalum filaments treated with phosphoric acid. Sm and Nd were loaded in dilute HCl on tantalum evaporation filaments of a double filament assembly with a rhenium ionisation filament. Isotope analyses were made on a Finnegan MAT 262 multicollector mass spectrometer.

Errors are quoted throughout as two standard deviations from measured or calculated values. Analytical uncertainties are estimated to be 0.01% for $^{87}\text{Sr}/^{86}\text{Sr}$ and $^{143}\text{Nd}/^{144}\text{Nd}$ ratios and 1.0% for both the $^{87}\text{Rb}/^{86}\text{Sr}$ and $^{147}\text{Sm}/^{144}\text{Nd}$ ratios. Measured $^{143}\text{Nd}/^{144}\text{Nd}$ were corrected for mass fractionation relative to $^{146}\text{Nd}/^{144}\text{Nd} = 0.7219$ and $^{87}\text{Sr}/^{86}\text{Sr}$ ratios relative to $^{86}\text{Sr}/^{88}\text{Sr} = 0.1194$. Replicate analyses of a Johnson and Matthey Nd in-house standard were made during the period each batch of samples was processed, they yielded mean $^{143}\text{Nd}/^{144}\text{Nd}$ ratios of 0.511187 ± 0.0000018 ($n = 12$), 0.5111201 ± 0.000018 ($n= 23$) and 0.511197 ± 0.000017 ($n= 36$). The comparable average $^{87}\text{Sr}/^{86}\text{Sr}$ determined for the NBS 987 strontium isotope standard was 0.710256 ± 0.0000018 ($n=29$) and 0.710240 ± 0.000027 ($n=32$). Measured ratios are therefore normalised to the accepted values of 0.511125 (as calibrated against the La Jolla international Nd standard) and 0.710240.

Analytical data are presented in Chapter 4, Table 4.3. Also shown are the corresponding calculated values for ϵ_{Nd} and depleted mantle Nd model ages T_{DM} calculated according to both single and two-stage models. Where the crystallization age has been determined or can be reasonably estimated, a time dependent function for $f(\text{Sm}/\text{Nd})$ of the source is used (DePaolo et al. 1991), otherwise the measured Sm/Nd ratios are used (Borg et al 1990). ϵ_{Nd} is calculated relative to a chondritic reservoir with $^{143}\text{Nd}/^{144}\text{Nd}$ of 0.51264 and $^{147}\text{Sm}/^{144}\text{Nd}$ of 0.1967.

2 Petrography

2.1 SUMMARY

The borehole samples examined in this study span a range of lithologies, degrees of deformation and metamorphic grade. The main general characteristics of the rocks are summarized here, and individual thin section descriptions and representative photographs that describe these characteristics in detail are given below.

Most of the rocks are granitoids or granitic gneisses, with subordinate mafic rocks. The granitic rocks encountered include:

- alkali granite (e.g. 56-08/230), which is also notably unmetamorphosed,
- granitic pegmatite (e.g. 58-08/228), which is modestly deformed as recorded by kink-banded biotite books,
- tonalite – trondhjemite – granodiorite gneisses (e.g. 57-08/536 and 537) of the TTG suite, characteristic of Archaean continental crust.

In addition to TTG – type rocks are closely associated amphibolite gneisses, diorites and derivative gneisses, an association found in virtually all Archaean granitoid terranes. Also present are two mafic rocks: 57-14/58, a relatively undeformed holocrystalline gabbro, and 164/25-2, a very high-grade metabasite (metagabbro?).

Many foliated and metamorphosed rocks of broadly granitic affinity have been classified as quartzofeldspathic gneisses. These rocks are not observed in association with other lithologies of known igneous affiliation (e.g. TTG's), or have mineral textures that preclude a straightforward assignment of the protolith lithology. The inability to place these gneisses within an overall rock association, or to view detailed structural relationships in their proper context means that the gneiss protoliths are very likely to remain indeterminate.

The metamorphic grade of most of the rocks is high, when not obliterated by later low-grade retrogression or alteration, and ranges from amphibolite and upper amphibolite facies to granulite facies. Of particular note are 164/25-2 and 56-15/18 with their two-pyroxene assemblages characteristic of granulite facies, with little or

no superimposed retrogression. Other rocks, such as the majority of the TTG's, are currently at amphibolite facies, although some are probably overprinted granulite facies rocks, such the coarse-grained clinopyroxene-bearing tonalite gneiss 204/25-1. Many of the above rocks preserve a good metamorphic foliation.

Finally, a significant number of borehole samples are very strongly deformed, with mineral textures indicative of protomylonite through mylonite, ultracataclasite and psuedotachylite. Most of these deformed rocks have dioritic, granitic or quartzofeldspathic gneiss protoliths (e.g. 205/16-1, 88/02, 56-09/386). Protomylonitic to mylonitic fabrics are characterized by subgrain development in quartz, grain size reduction of ferromagnesian minerals, brittle deformation of mineral grains, up to intense dynamic recrystallisation of quartz and feldspar within narrow zones. In some rocks weakly developed shear sense indicators recording ductile deformation are preserved, e.g. S-C fabric in 56-09/924 outlined by anastomosing quartz-rich shear bands.

2.2 PETROGRAPHIC DESCRIPTIONS

Location: 220/26-1

Rock: Quartzofeldspathic mylonite

Mineralogy: major – quartz, plagioclase

minor – epidote, carbonate, opaque minerals, apatite, allanite

alteration – sericite, chlorite

Thin Section Registered Number: N3745

Description: This thin section is of a fine-grained, highly deformed, altered (sericitised and chloritised) quartzofeldspathic mylonite or protomylonite in which quartz and feldspar porphyroclasts form approximately 50 to 60% of the rock. These porphyroclasts are rounded to elliptical in shape and are wrapped by a well-developed mylonitic foliation. This fabric is defined by very narrow foliae of very fine-grained chlorite and sericitic white mica. The chloritic foliae are locally overgrown by later, apparently post-kinematic carbonate and epidote. A variably developed extensional crenulation cleavage which deforms the main mylonitic foliation yields an apparent dextral sense of shear in this plane of section.

Plagioclase is variably altered sericitic white mica, but originally formed twinned and untwinned crystals which show varying degrees of intracrystalline deformation. Relict quartz porphyroblasts and patches of quartz within the matrix are variably replaced by a fine- to very fine-grained aggregate of dynamically recrystallised quartz new grains. Relict quartz crystals are strained with intracrystalline deformation resulting in the development of an undulose extinction, deformation bands and sub-grain textures.

Chloritisation and sericitisation appear to have accompanied mylonitisation suggesting that ductile deformation occurred under greenschist or sub-greenschist facies metamorphic conditions. The rock is cut by a number of late chlorite filled fractures.

Location: 209/9-1

Rock: Augen gneiss

Mineralogy: major – quartz, K-feldspar, plagioclase, biotite

minor – epidote, apatite, opaque minerals, titanite

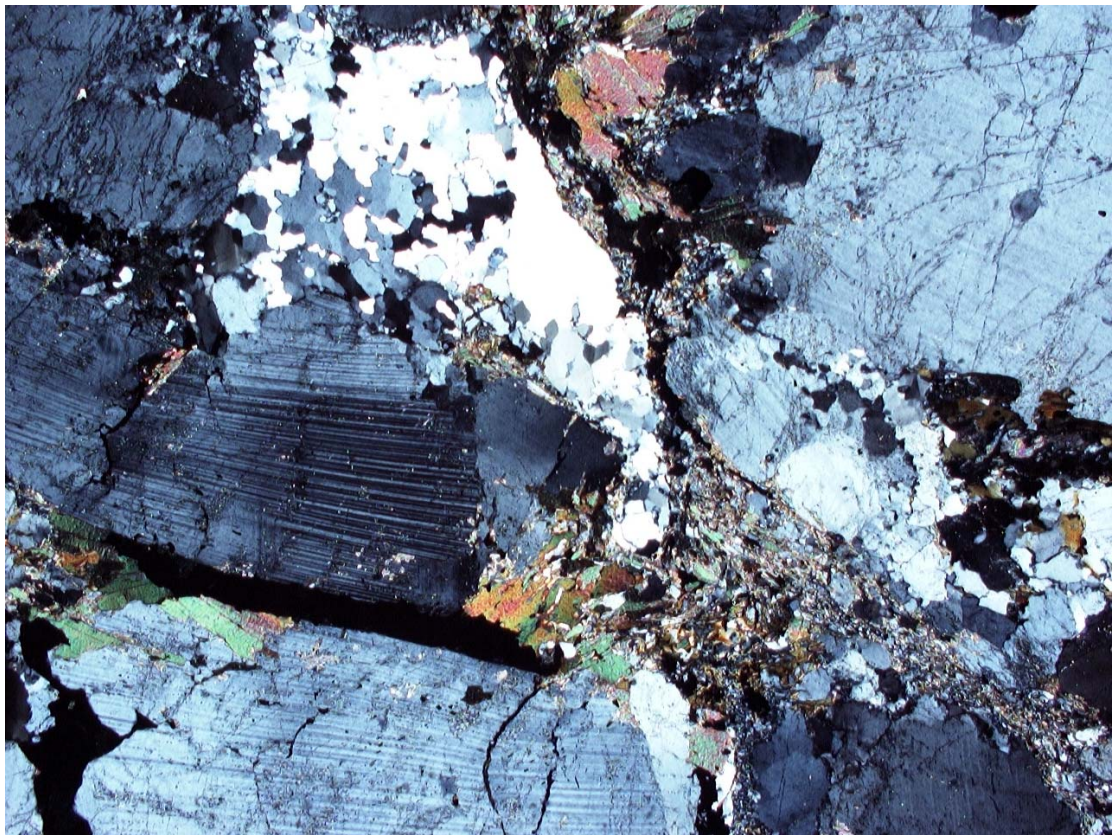
alteration – chlorite, carbonate

Registered Number: N3743

Description: This thin section is of a coarse- to very coarse-grained, inequigranular, porphyroblastic, foliated hornblende-biotite granodioritic gneissose rock. The gneissose foliation is defined by lenticular to irregular pockets of biotite and chloritised amphibole. Feldspar porphyroblasts or augen are variably shape aligned parallel to, and help define this foliation. The porphyroblasts range from 1.5 up to 5.5 mm in length and are mainly composed of anhedral to elliptical plagioclase and K-feldspar. The porphyroblasts or augen are composed of a single large feldspar or aggregate of several finer grained crystals.

The matrix to this gneissose rock is composed of recrystallised variably strained quartz and lenticular to irregular pockets of biotite and chloritised amphibole. Recrystallisation and granulation of biotite and quartz suggests that this phase of ductile deformation occurred at elevated temperatures (at least greenschist facies). These narrow (≤ 0.3 mm in width) zones of granular biotite and quartz define an anastomosing ?mylonitic foliation which wraps around the feldspar porphyroblasts. Minor cataclasis of feldspar has been recorded associated with this foliation.

Amphibole is closely associated with biotite and has been completely pseudomorphed by chlorite and carbonate (\pm opaque). The mimetic growth of chlorite locally preserves the original anhedral to subhedral shape of the amphibole crystals.



Photomicrographs of 209/9-1 (N3743) in plane and crossed polarised light. FOV = 2 mm.

Location: 209/12-1

Rock: Biotite schist

Mineralogy: major – quartz, plagioclase, biotite, muscovite

minor – apatite, zircon, opaque minerals

alteration –sericite, white mica

Thin Section Registered Number: N3744

Description: This thin section is of a coarse- to very coarse-grained, inequigranular, moderately foliated, biotite-bearing quartz-plagioclase schistose rock. A moderately well developed anastomosing schistosity is defined by thin foliae of biotite and minor/accessory muscovite. Biotite is pale yellow to dark red-brown in colour and possesses a well-developed pleochroism. The bulk of the rock is composed of plagioclase and quartz. Plagioclase forms anhedral, elongate to equant porphyroblasts which range from 1.5 to 3.0 mm in length. Plagioclase is twinned and exhibits very little alteration to sericitic white mica, in particular along fractures. These plagioclase porphyroblasts are wrapped by the biotite fabric. The porphyroblasts may also locally contain small inclusions of biotite and quartz.

The matrix to this schistose rock is composed of variably strained, anhedral quartz which possess a slightly undulose extinction. Quartz appears to be intergranular to plagioclase and biotite and may exhibit a weak shape alignment parallel to the biotite foliation. The protolith to this rock is uncertain.

Location: 81/17

Rock: Amphibolite

Mineralogy: major – amphibole, plagioclase, quartz

minor – epidote, biotite, opaque minerals, titanite

alteration – carbonate

Thin Section Registered Number: N3751

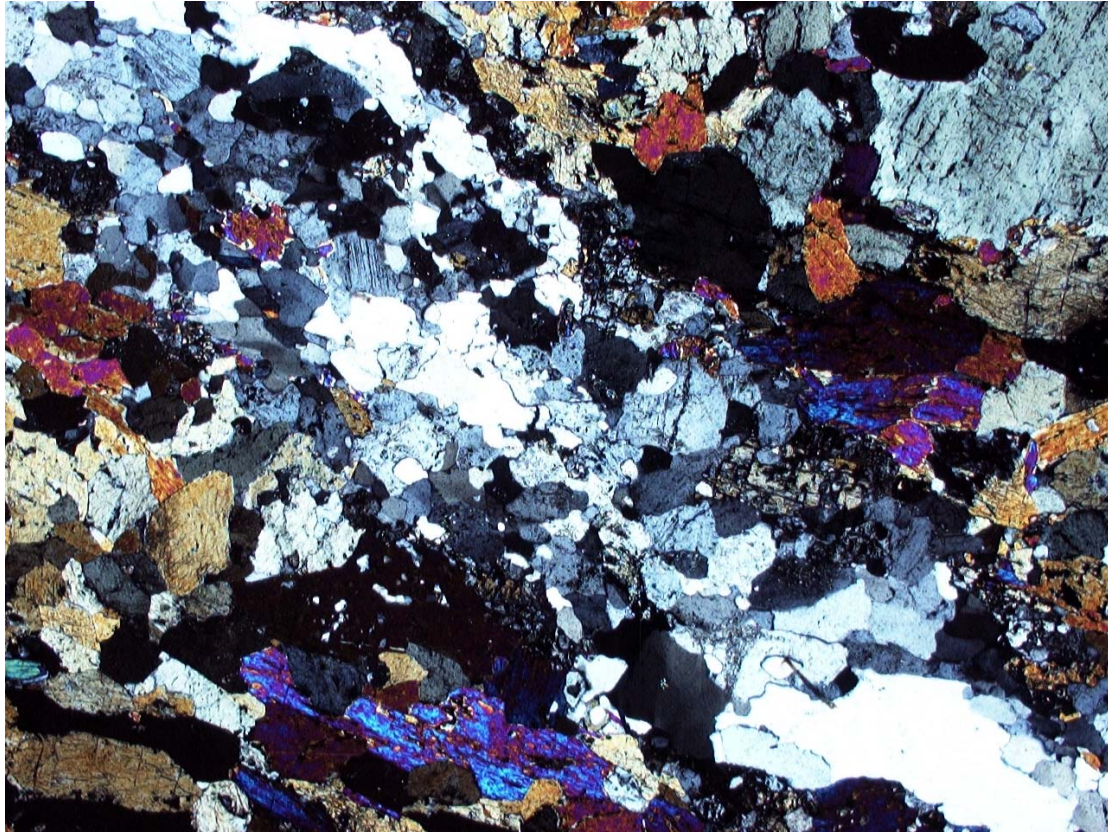
Description: This thin section is of a very coarse-grained, inequigranular, massive to weakly foliated amphibolite which is cut by a 1.5 to 2.0 mm wide plagioclase, epidote

and quartz vein. This vein is weakly zoned with an outer part which is slightly richer in plagioclase and epidote enclosing a more quartz-rich centre. Approximately 95% of the total rock is composed of amphibole with minor to accessory plagioclase and biotite. Traces of titanite and opaque minerals have also been recorded within this amphibole-rich rock. Biotite is pleochroic ranging from pale brown to brown in colour and typically forms anhedral flakes included within the larger amphibole crystals. Two textural varieties of amphibole have been recognised: (a) anhedral to irregular, very coarse-grained crystals (up to 5.0 to 6.0 mm in length); and (b) finer grained (≤ 1.5 mm in size) anhedral to subhedral, equant to prismatic crystals. These smaller crystals exhibit a locally developed preferred shape alignment and define a weakly developed foliation. Both types of amphibole are pale green, green to olive-green in colour and possess a weak to moderately developed pleochroism.

Rare fractures filled by late carbonate are present within this amphibolite.



Photomicrograph of 81/17 (N3751) in plane polarised light. FOV = 2mm.



Photomicrograph of 81/17 (N3751) in crossed polarised light. FOV = 2mm.

Location: 208/27-2(a)

Rock Type: Granitic gneiss

Mineralogy: major – quartz, K-feldspar, plagioclase

minor – apatite

alteration – carbonate, sericite, white mica

Thin Section Registered Number: N3741

Description: This thin section is of a medium- to coarse-grained, inequigranular, anhedral granoblastic, weakly banded, K-feldspar-rich granitic gneiss which is cut by a prominent band of cataclasite. The cataclasite possesses a carbonate cement and contains angular to subrounded fragments of quartz, feldspar and granitic gneiss. There is no obvious exotic material within the cataclasite with all of the fragments were derived from the adjacent granitic gneiss. The matrix of the cataclasite is

variably replaced by opaque minerals, with opaques also filling fractures within the adjacent host rock. The boundary between the cataclasite and the granitic gneiss is sharp and slightly irregular in form. Only minor fracturing has been noted within the gneiss immediately adjacent to this contact.

The granitic gneiss is mainly composed of equant to elongate K-feldspar crystals with subordinate quartz. K-feldspar and quartz are variably shape aligned parallel to a gneissose foliation which is mainly defined by elongate quartz stringers/aggregates. K-feldspar forms anhedral crystals which possess irregular to serrated grain margins and are rimmed by a mosaic of interlocking fine-grained K-feldspar and plagioclase. Quartz is strained with an undulose extinction and variably developed sub-grain textures and deformation bands. It forms anhedral crystals which appear to be intergranular to feldspar. Traces of myrmekite have been recorded within this granitic gneiss (?incipient partial melting).

Location: 208/27-2(b)

Rock Type: Cataclasite

Mineralogy: major – quartz, carbonate, opaque minerals
minor – apatite, titanite

Thin Section Registered Number: N3742

Description: This thin section is of a highly deformed, fragmentary, massive, cohesive fault breccia or cataclasite with a carbonate and opaque cement or matrix. This sample is lithologically similar to the cataclasite band cutting thin section N3741. The clasts are angular to irregular in shape and composed of broken quartz and feldspar crystal fragments as well as granitic rock and cataclasite lithic clasts. Apatite is a common accessory component.

Location: 206/8-2

Rock: Quartzofeldspathic gneiss.

Mineralogy: major – quartz, plagioclase, epidote, K-feldspar
minor – chlorite, zircon, titanite, opaque minerals
alteration – sericite, white mica, carbonate

Thin Section Registered Number: N3736

Description: This thin section is of a highly altered, recrystallised, inequigranular, sheared to protomylonitic, epidote-bearing quartzofeldspathic gneiss. This rock is mainly composed of quartz and plagioclase with minor amounts of K-feldspar. The protolith of this rock is uncertain, however, the mineralogy suggests that it is broadly granitic in composition. A weakly to moderately developed foliation within this protomylonitic rock is defined by elongate stringers of quartz and variable shape alignment of porphyroclasts. Recrystallisation during deformation resulted in grain recovery and annealing of the mylonitic fabric. The apparently contemporaneous annealing of the foliation suggests that ductile deformation may have occurred at elevated temperatures (possibly greenschist to amphibolite facies).

Plagioclase and K-feldspar form rounded to irregular porphyroclasts (range from 0.7 to *c.* 4.0 mm in diameter) which are set within a finer grained matrix of variably dynamically recrystallised quartz and feldspar. Both feldspars exhibit intracrystalline deformation which led to the development of an undulose to shadowy extinction, deformation bands, sub-grain textures and dislocations. Kinking of albite and microcline twins within the feldspar has also been noted. A number of the porphyroclasts are fractured (cataclasis/microboudinage) with the fractures filled by very fine-grained, granular-looking quartz and feldspar new grains. The margins of the feldspar porphyroclasts are irregular to serrated. A weak compositional zonation is locally preserved within some plagioclase porphyroclasts.

Quartz forms anhedral crystals which exhibit varying degrees of intracrystalline deformation; the finer grained new-grains being relatively unstrained. Relicts of larger crystals possess a well-developed undulose extinction, deformation bands and sub-grain textures.

Location: 206/8-8(a)

Rock: Granitic gneiss

Mineralogy: major – quartz, plagioclase, K-feldspar
minor – epidote, biotite, opaque minerals
alteration – chlorite, sericite, white mica

Thin Section Registered Number: N3738

Description: This thin section is of a medium-grained, inequigranular, anhedral granoblastic, crudely banded, sheared quartzofeldspathic/granitic gneissose rock which may possibly be a finer grained version of sample 206/8-2. This sample is mainly composed of plagioclase, quartz and subordinate K-feldspar. Feldspar forms clusters and chains of large anhedral crystals which are surrounded by an aggregate of finer grained, anhedral recrystallised plagioclase and K-feldspar. A weakly developed foliation is defined by these locally elongate feldspar chains as well as stringers of quartz. Both quartz and, to a lesser extent, feldspar show a preferred shape alignment parallel to this gneissose foliation.

Plagioclase forms twinned and untwinned, anhedral and irregular crystals which possess a sweeping extinction and contain numerous small inclusions of white mica and epidote. Plagioclase exhibits a dusty appearance under plane polarised light and possesses irregular, serrated grain contacts due to localised grain reduction. K-feldspar forms anhedral, perthitic to mesoperthitic crystals with a distinctive shadowy extinction. K-feldspar is less susceptible to alteration than plagioclase. Quartz is strained and variably replaced by an aggregate of fine-grained, new grains. It possess variably serrated to irregular grain contacts and forms an interlocking mosaic intergranular to feldspar. Intracrystalline deformation of quartz led to the development of deformation bands, dislocations and sub-grain textures.

Location: 206/8-8(b)

Rock Type: Granitic gneiss.

Mineralogy: (a) major – plagioclase, quartz, K-feldspar

minor – white mica, epidote, opaque minerals, biotite

alteration – chlorite, sericite, white mica

(b) major – biotite, plagioclase

minor – epidote, quartz, opaque minerals, apatite

alteration – sericite, white mica

Thin Section Registered Number: N3739

Description: This thin section is of a medium- to coarse-grained, inequigranular, massive to very weakly foliated, granitic gneissose rock which forms a band or vein in a distinctive plagioclase-biotite gneiss or hornfels. It is mainly composed of clusters or aggregates of plagioclase and subordinate K-feldspar set within a finer grained matrix dominated by variably strained quartz.

Plagioclase forms twinned and untwinned, anhedral crystals which are variably recrystallised to a fine-grained assemblage of interlocking feldspar. Both feldspar contain numerous inclusions of granular epidote and white mica. Occasional subhedral, lath-shaped plagioclase crystals also locally/rarely preserved. However, in general plagioclase possess highly irregular serrated grain boundaries. K-feldspar is weakly perthitic and exhibits a distinctive shadowy extinction and variably developed microcline twins. Quartz occurs intergranular to feldspar and possesses a well developed undulose extinction, deformation bands and sub-grain textures. A weakly developed foliation present within this gneissose rock is defined by the variable shape alignment of plagioclase and K-feldspar aggregates. This foliation occurs parallel to the margin of the granitic gneissose band.

The contact between the granitic gneiss and the adjacent plagioclase-biotite gneiss or hornfels is sharp but highly irregular in form. Elongate aggregates of fine-grained biotite extend from this hornfels into the adjacent granitic gneiss. The plagioclase-biotite gneiss/hornfels is lithologically distinctive and possesses a inequigranular granoblastic texture which is reminiscent of that formed as a result of contact

metamorphism (hornfels). It is composed of rounded to irregular plagioclase poikiloblasts within a fine-grained biotite-rich matrix. Minor amounts of epidote and quartz are present within the matrix to this apparently high-grade hornfels. Plagioclase forms rounded, anhedral, twinned and untwinned crystals which possess irregular sutured contacts. These feldspar porphyroblasts also contain numerous fine- to very fine-grained inclusions of epidote, biotite and white mica. Biotite is green-brown in colour and forms equant, stubby crystals which possess a moderately developed pleochroism. Epidote forms granular crystals replacing plagioclase and may locally form partial or complete rims upon feldspar poikiloblasts.

Location: 206/8-8(c)

Rock: Granitic gneiss.

Mineralogy: (a) major – plagioclase, quartz, K-feldspar

minor – white mica, epidote, opaque minerals, biotite

alteration – chlorite, sericite, white mica, apatite

(b) major – biotite, plagioclase

minor – epidote, quartz, opaque minerals, apatite, titanite

alteration – sericite, white mica

Thin Section Registered Number: N3740

Description: This thin section is of a medium- to coarse-grained, inequigranular, massive granitic gneissose rock which forms a band or vein in a distinctive plagioclase-biotite gneiss or hornfels.

The granitic gneissose rock is mainly composed of clusters of anhedral, rounded plagioclase which along with minor K-feldspar forms an open crystal framework. The interstices to this framework are filled by finer grained quartz. Plagioclase forms twinned and untwinned crystals which possess irregular to serrated grain boundaries. Plagioclase contain numerous fine-to very fine-grained inclusions of epidote, white mica and, in some cases, biotite. The large plagioclase crystals are enclosed within a rim or aggregate of finer grained feldspar crystals. Quartz is strained with an undulose extinction and variably developed sub-grain textures. The granitic gneiss also contains

irregular patches or elongate schlieren of variably aligned to granular biotite (\pm epidote). These biotite aggregates are interpreted as representing relict, partially digested xenoliths of the adjacent hornfels. The contact between the granitic gneiss and the adjacent plagioclase-biotite gneiss/hornfels is sharp and apparently planar in form.

The plagioclase-biotite gneiss or hornfels is composed of rounded to irregular plagioclase porphyroblasts and poikiloblasts enclosed within a biotite-rich matrix. Minor epidote and quartz are also present within the matrix. Plagioclase forms twinned and untwinned crystals which contain fine- to very fine-grained inclusions of biotite, epidote and quartz. The density of inclusions within the plagioclase poikiloblasts decreases away from the boundary with the granitic gneiss. Plagioclase forms approximately 50 to 60% of the total rock and is petrographically similar to the feldspar within the adjacent granitic gneiss. The plagioclase porphyroblasts immediately adjacent to this contact are rimmed by granular epidote.

Occasional large (≤ 0.3 mm in size) apatite crystals occur within both the granitic gneiss and hornfels.

Location: 206/8-2

Rock Type: Protomylonite

Mineralogy: major – quartz, plagioclase, epidote, K-feldspar

minor – chlorite, zircon, titanite, opaque minerals

alteration – sericite, white mica, carbonate

Thin Section Registered Number: N3736

Description: This thin section is of a highly altered, recrystallised, inequigranular, sheared to protomylonitic, epidote-bearing quartzofeldspathic gneiss. This rock is mainly composed of quartz and plagioclase with minor amounts of K-feldspar. The protolith of this rock is uncertain, however, the mineralogy suggests that it is broadly granitic in composition. A weakly to moderately developed foliation within this protomylonitic rock is defined by elongate stringers of quartz and variable shape alignment of porphyroclasts. Recrystallisation during deformation resulted in grain recovery and annealing of the mylonitic fabric. The apparently contemporaneous

annealing of the foliation suggests that ductile deformation may have occurred at elevated temperatures (possibly greenschist to amphibolite facies).

Plagioclase and K-feldspar form rounded to irregular porphyroclasts (range from 0.7 to *c.* 4.0 mm in diameter) which are set within a finer grained matrix of variably dynamically recrystallised quartz and feldspar. Both feldspars exhibit intracrystalline deformation which led to the development of an undulose to shadowy extinction, deformation bands, sub-grain textures and dislocations. Kinking of albite and microcline twins within the feldspar has also been noted. A number of the porphyroclasts are fractured (cataclasis/microboudinage) with the fractures filled by very fine-grained, granular-looking quartz and feldspar new grains. The margins of the feldspar porphyroclasts are irregular to serrated. A weak compositional zonation is locally preserved within some plagioclase porphyroclasts. Plagioclase forms twinned and untwinned crystals which exhibit a slight dusty appearance under plane polarised light.

Quartz forms anhedral crystals which exhibit varying degrees of intracrystalline deformation; the finer grained new-grains being relatively unstrained. Relicts of larger crystals possess a well-developed undulose extinction, deformation bands and sub-grain textures. The deformation bands within quartz define a weak foliation which occurs at an angle to the main mylonitic/schistose foliation. Epidote forms small granular to irregular crystals which are typically associated with bands of very fine-grained, dynamically recrystallised quartz. These narrow bands of intense grain reduction are interpreted as representing the last phase of deformation recorded by this protomylonitic rock and form an irregular to anastomosing network. Trace amounts of chlorite, opaque minerals, zircon and apatite are present within this deformed quartzofeldspathic gneiss.

Location: 206/8-1A

Rock: Dioritic gneiss.

Mineralogy: major – plagioclase, quartz, chlorite, epidote, biotite

minor –apatite, opaque minerals

alteration – sericite, white mica, opaque oxides, leucoxene, titanite, carbonate

Thin Section Registered Number: N3735

Description: This thin section is of a highly altered, very weakly foliated to massive, inequigranular dioritic rock. A very weakly developed or preserved foliation is defined by the variable shape alignment of plagioclase crystals and chains of chloritised biotite flakes. The rock is mainly composed of variably altered or recrystallised plagioclase which has been pseudomorphed by albitic plagioclase, sericitic white mica, chlorite and traces of epidote. The outline of these originally anhedral equant to prismatic crystals is locally preserved by the mimetic growth of the alteration products. Elsewhere, however, the original texture of the rock has been overprinted during hydration and alteration.

The primary ferromagnesian mineral (possibly amphibole) has been replaced by olive green biotite and chlorite. These pseudomorphs are locally composed of a one or two biotite crystals, or an aggregate of fine-grained, randomly orientated phyllosilicate flakes. These fine-grained aggregates locally form granular 'reaction rims' upon larger biotite crystals which appear to have mimetically replaced pre-existing relict amphibole. Traces of epidote and carbonate have been noted associated with biotite.

The remaining interstitial to intersertal areas are filled by strained quartz. Quartz is variably recrystallised to an aggregate of very fine-grained, granular looking crystals which typically exhibit less obvious signs of intracrystalline deformation. Primary opaque minerals are variably altered to titanite and/or leucoxene. Apatite forms a common accessory phase within this rock.

Location: 206/8-7

Rock: Amphibolite.

Mineralogy: major – amphibole, biotite, carbonate, plagioclase, quartz

minor – epidote, opaque minerals

alteration – chlorite, sericite, white mica

Thin Section Registered Number: N3737

Description: This thin section is of a fine- to very fine-grained (average grain size < 0.1 mm), highly deformed, inequigranular, schistose amphibolite which is cut by a number of carbonate and carbonate-chlorite veinlets. The rock is mainly composed of amphibole and biotite with subordinate amounts of plagioclase and minor quartz. A well-developed homogenous schistosity present within this amphibolite is defined by shape aligned, small stubby amphibole and biotite crystals. The ferromagnesian minerals occur within a very fine-grained, granular matrix of plagioclase and quartz. Biotite appears to be replacing amphibole. Amphibole is dark green in colour and is distinguished from biotite by the presence of dusty inclusions of opaque minerals. Trace amounts of pale green chlorite are also present. A crudely developed banding or mottling has been recognised within this amphibolite defined by a slight variation in modal biotite and amphibole.

The early formed schistosity was later disrupted during fracturing and the formation of the carbonate dominated veinlets. Carbonate forms anhedral, granular to elongate crystals. A number of the carbonate veins are foliated with the fabric locally passing into the schistosity developed within the amphibolite wall-rock. This relationships suggests that carbonate mineralisation/veining may have occurred during the later stages of deformation.

Location: 206/7-A2. **Depth:** 2142.8 to 2143.0 m.

Rock: Mylonitic amphibolite.

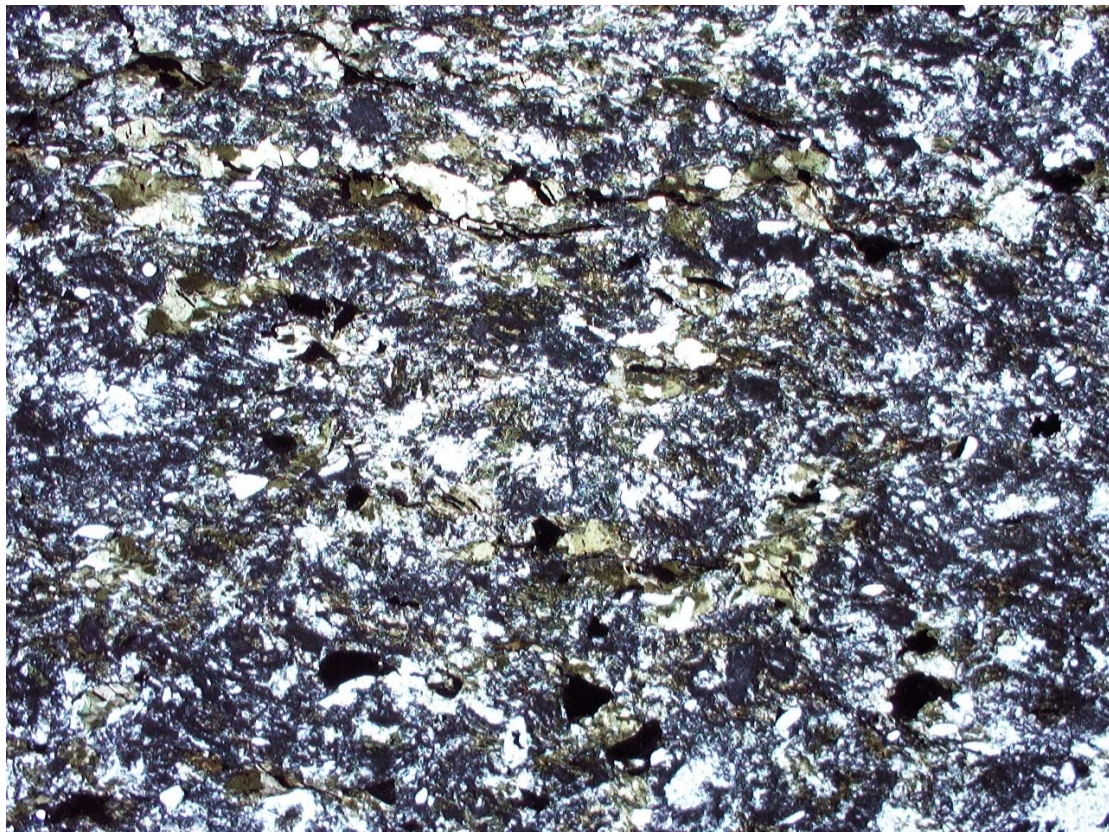
Mineralogy: major – amphibole, biotite, plagioclase, quartz, chlorite

accessory – opaque minerals, epidote, apatite

alteration – clay minerals, leucoxene, carbonate, clinozoisite

Thin Section Registered Number: N4168

Description: This thin section is of a highly altered or retrogressed hornblende-biotite schistose rock or a mylonitic amphibolite. This amphibolite contains microfractures of quartz and carbonate. Very little of the original mineralogy remains unchanged in this sample. The amphibole is pale brown to green and is often replaced by carbonate. Some rounded more resistant grains of quartz and plagioclase can be found. A mylonitic fabric is defined by stringers of fine-grained opaque minerals, chlorite and epidote.



Photomicrograph of 206/7A-2 (N4168) in plane polarised light. FOV = 2 mm.

Location: 206/7-A2. **Depth:** 2183.15 to 2183.30 m.

Rock: TTG.

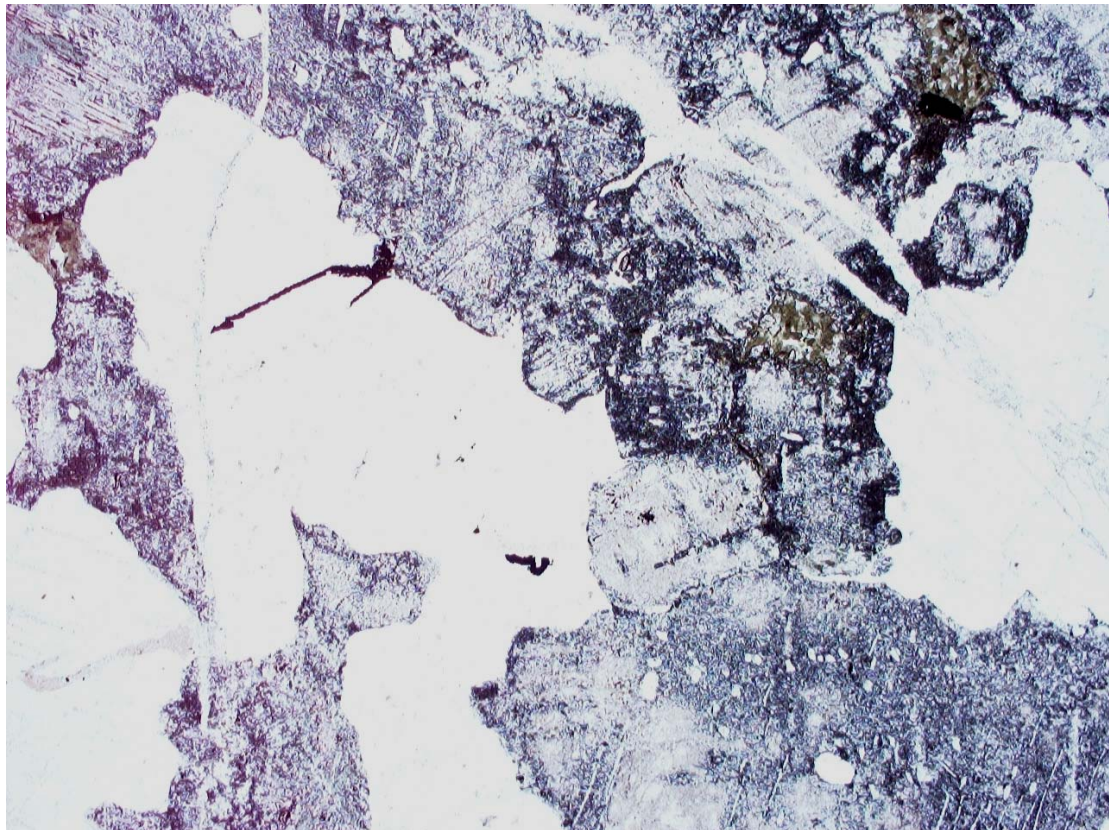
Mineralogy: major – plagioclase, quartz, K-feldspar, biotite

accessory – opaque minerals, titanite, apatite

alteration – sericite, carbonate, clinozoisite/epidote, chlorite

Thin Section Registered Number: N4169

Description: This thin section is of an altered/retrogressed, coarse grained, plagioclase-rich tonalitic rock, which is cut by thin carbonate and quartz veins. This altered sample shows a relict almost granular texture of interlocking grains. Quartz shows undulose extinction. Plagioclase and K-feldspar are slightly cloudy/dusty in appearance due to the abundance of inclusions and alteration to sericite



Photomicrograph of N4169 in plane polarised light. FOV = 2 mm.

Location: 206/7-A2. **Depth:** 2435.50 to 2435.65 m.

Rock: TTG.

Mineralogy: major – plagioclase, clinopyroxene, hornblende, biotite, actinolitic amphibole

accessory – opaque minerals, apatite, quartz

alteration – sericite, carbonate, clinozoisite/epidote

Thin Section Registered Number: N4170

Description: This thin section is of a partially retrogressed, coarse grained, pyroxene-hornblende gneissose dioritic rock. Texturally this rock is similar to N4169, however it contains pyroxene and hornblende. The relict intergranular texture is still visible. Pyroxene can be distinguished from amphibole even after alteration as fine-grained opaque minerals preserve the cleavage directions.



Photomicrograph of N4170 in plane polarised light. FOV = 2 mm.

Location: 206/7-A2. **Depth:** 2544.65 to 2544.85 m.

Rock: Dioritic gneiss

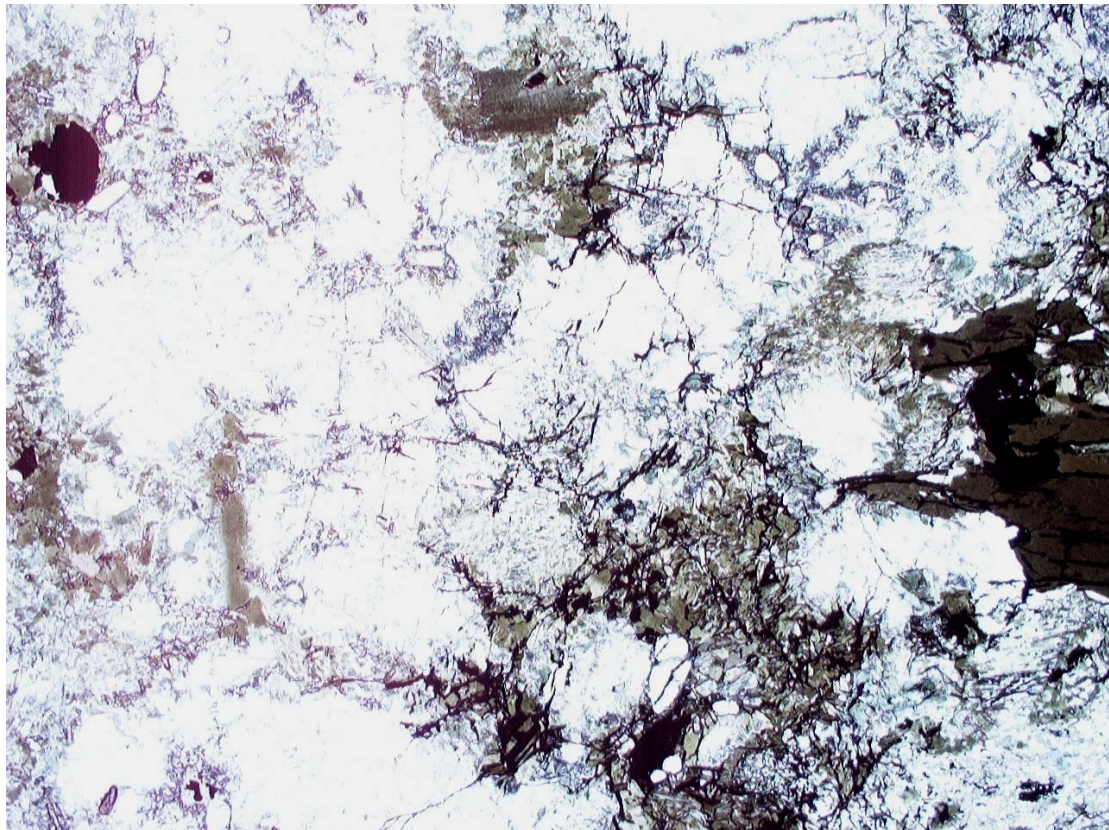
Mineralogy: major – plagioclase, biotite, hornblende, quartz, epidote, clinozoisite

accessory – opaque minerals, apatite, titanite, zircon

alteration – sericite, carbonate, leucoxene, opaque oxides

Thin Section Registered Number: N4171

Description: This thin section is of a partially retrogressed, medium grained, hornblende-biotite gneissose dioritic rock. It may represent a more felsic version of the previous thin section N4170. There are pervasive patches of very fine-grained or dynamically recrystallised quartz and feldspar. Again an intergranular texture is still visible.



Photomicrograph of N4171 in plane polarised light. FOV = 2 mm.

Location: 206/7-A2. **Depth:** 2599.2 to 2599.4 m.

Rock: TTG.

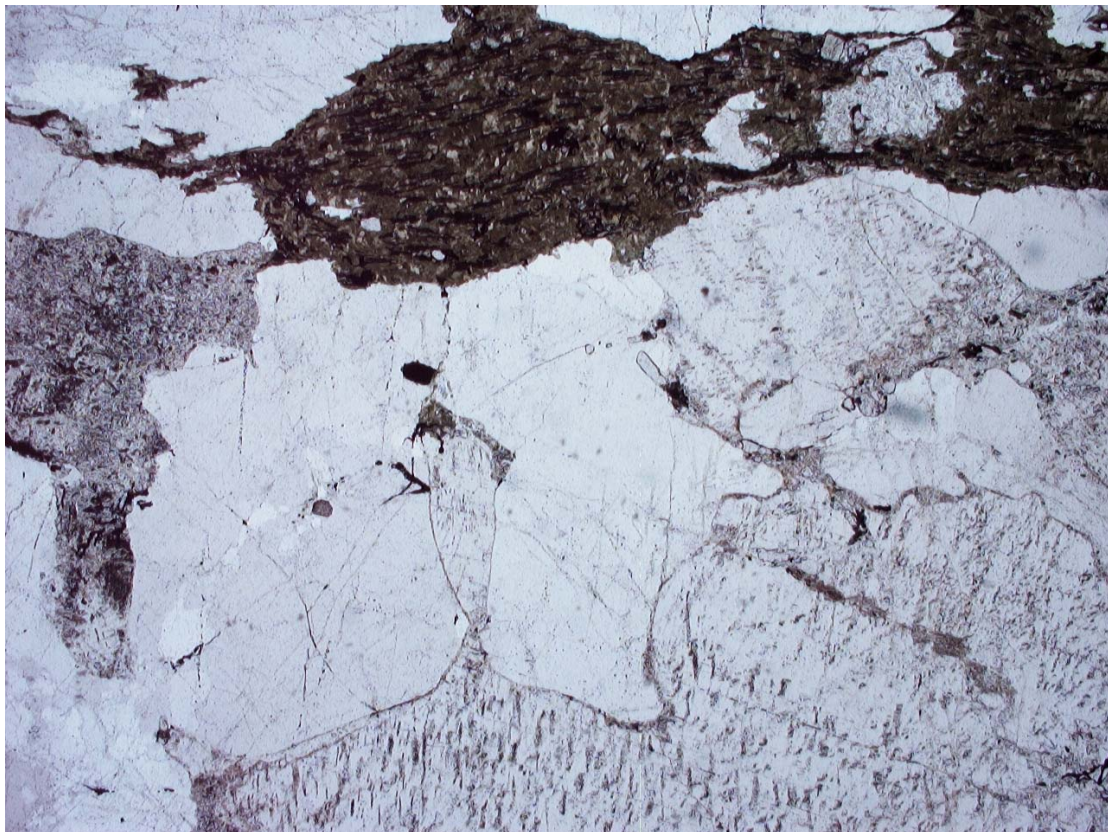
Mineralogy: major – perthitic K-feldspar (microcline), quartz, plagioclase, epidote, biotite

accessory – opaque minerals, apatite, titanite

alteration – sericite, carbonate, opaque oxide, chlorite, white mica

Thin Section Registered Number: N4172

Description: This thin section is of a very coarse grained, K-feldspar rich granitic rock. The rock is cut by an epidote-quartz-carbonate vein. The K-feldspar which makes up the majority of the sample is perthitic microcline and forms grains up to 3mm in size. Dynamically recrystallised quartz and feldspar is common around the larger grain boundaries.



Photomicrograph of N4172 in plane polarised light. FOV = 2 mm.

Location: 206/7-A2. **Depth:** 2599.0 to 2599.95 m.

Rock: Granodioritic gneiss

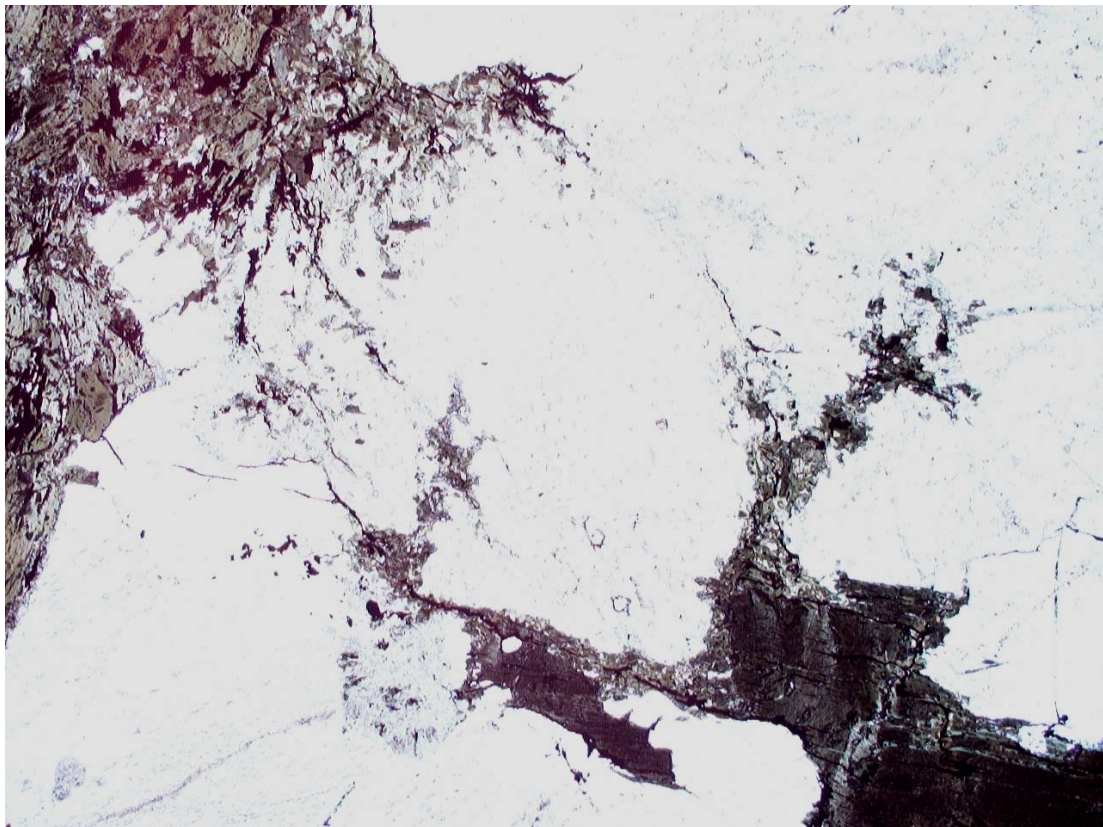
Mineralogy: major – perthitic K-feldspar (microcline), quartz, plagioclase, biotite

accessory – opaque minerals, apatite, titanite

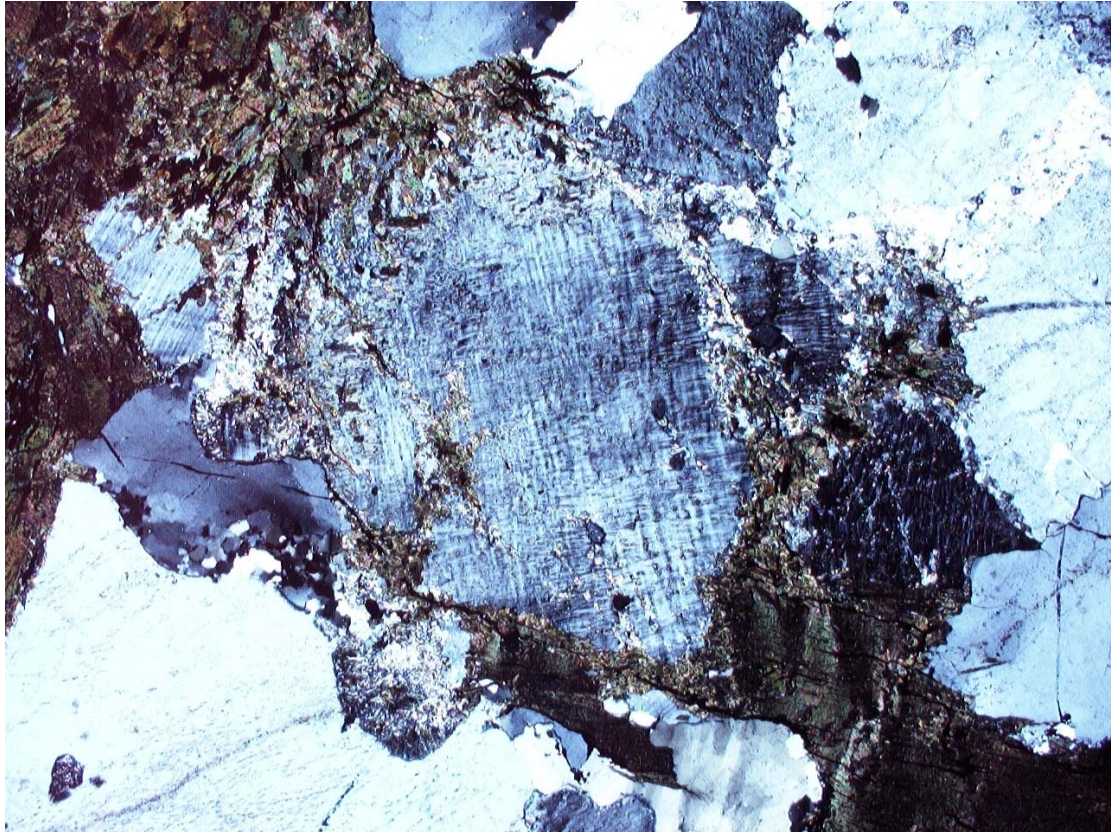
alteration – sericite, carbonate, opaque oxide, chlorite, white mica,
epidote

Thin Section Registered Number: N4173

Description: This thin section is of a very coarse grained, K-feldspar rich biotite granitic rock. It is lithologically similar to thin section N4172. The K-feldspar is perthitic microcline. Quartz and plagioclase are dynamically recrystallised in patches. This thin section is cut by microveins and in places the epidote within the vein exhibits kink banding.



Photomicrograph from 206/7-A2 (N4173) in plane polarised light. FOV = 2 mm.



Photomicrograph from 206/7-A2 (N4173) in crossed polarised light. FOV = 2 mm.

Location: 206/7-1. **Depth:** 1735.5 to 1735.6 m.

Rock Type: Tonalitic gneiss

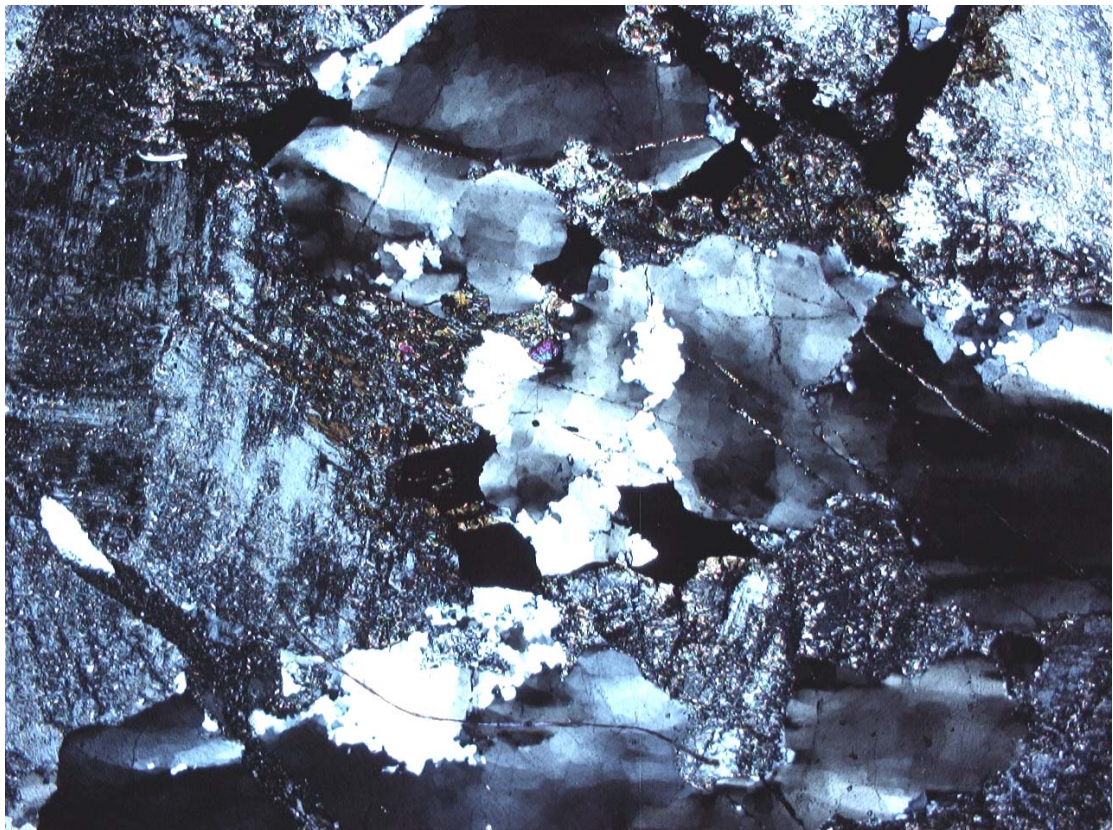
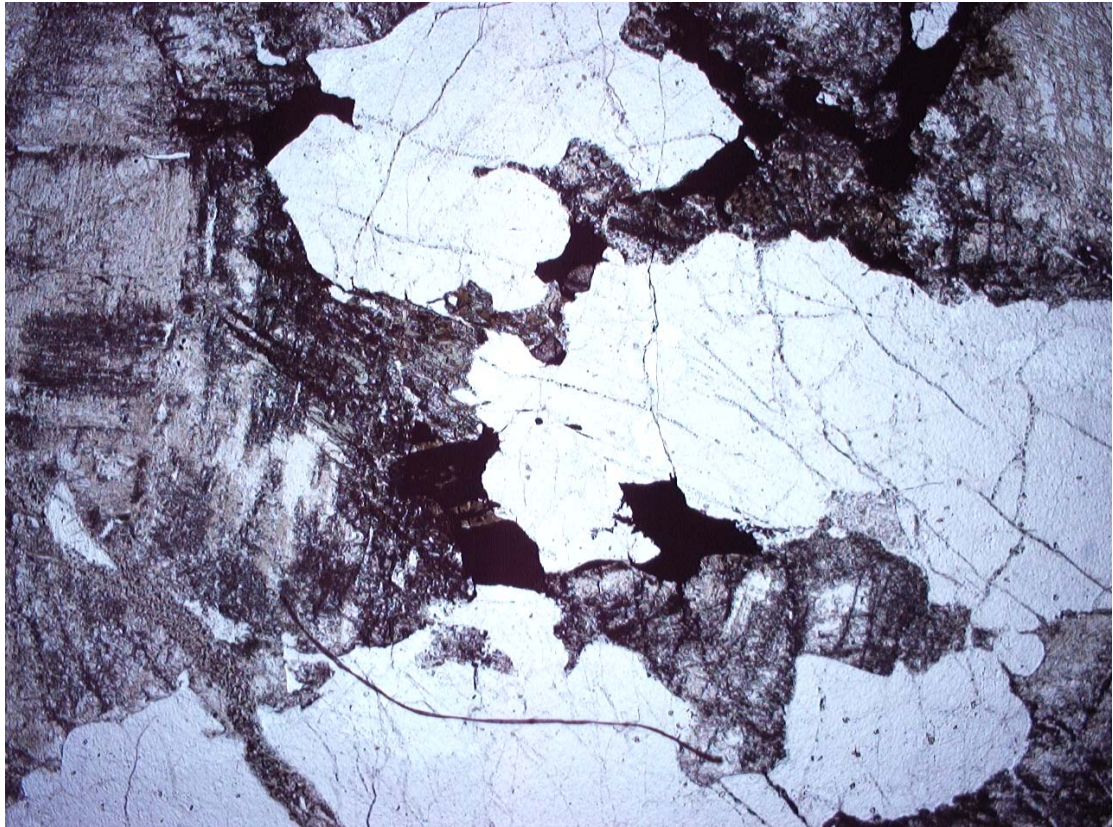
Mineralogy: major – plagioclase, quartz, carbonate, biotite, sericite

accessory – titanite, opaque minerals, apatite

alteration – chlorite, opaque oxides, white mica, leucoxene

Thin Section Registered Number: N4164

Description: This is a thin section of an altered, coarse-grained tonalitic gneissose rock which is similar to sample 204/22-1, but it lacks any obvious pseudomorphs after pyroxene. Quartz and plagioclase are the dominant phases of this rock. The plagioclase can be distinguished by its cloudy/dusty appearance. The plagioclase is altered to white mica, chlorite and biotite. Quartz commonly exhibits undulose extinction and recrystallisation along the grain boundaries. Titanite is associated with the opaque minerals. This thin section is cut by a series of quartz-carbonate veins, the largest of which is 30 microns in diameter.



Photomicrographs of 206/7-1 in plane and crossed polarised light. FOV = 2mm

Location: 205/16-1(a)

Rock: Pseudotachylite.

Mineralogy: major – quartz, feldspar, chlorite, sericite, opaque minerals

Thin Section Registered Number: N3730

Description: This thin section is of a very fine-grained to cryptocrystalline, originally glassy, devitrified quartzofeldspathic pseudotachylite. The matrix to this cohesive fault rock is composed of a dusty pale brown silicic assemblage which locally possesses a variably developed compositional/colour banding. This banding is highlighted by the variation in the intensity and style of devitrification and alteration of the matrix to sericite.

Devitrification of this originally glassy matrix resulted in the development of snowflake and spherulitic textures, as well as very fine-grained microlites. These microlites have locally nucleated upon crystal and rock fragments forming a radial fibrous rim. The fragmentary component of this fault rock is composed of angular (broken) quartz and feldspar crystal fragments, and quartzofeldspathic cataclasite. The presence of cataclasite rock fragments within this pseudotachylite suggests that the fault from which this fault rock was taken potentially had a prolonged (polyphase) history of movement.

The fragments of quartz and feldspar have undergone intracrystalline deformation resulting in the development of an undulose extinction, deformation bands and sub-grain textures. Minor rounding of some of the included fragments has been noted within this pseudotachylite, possibly due to the reaction of these clasts with the melt/matrix.

Location: 205/16-1(b)

Rock: Diorite cut by pseudotachylite vein.

Mineralogy: major – plagioclase, chlorite, quartz, K-feldspar

minor –apatite, opaque minerals

alteration – sericite

Thin Section Registered Number: N3731

Description: This thin section is of an altered/retrogressed, medium-grained, inequigranular, anhedral granular or granoblastic dioritic rock which is cut by a prominent band of cataclasite or devitrified pseudotachylite. The protolith of this broadly dioritic rock is uncertain (possibly either igneous or high-grade metamorphic rock) due to alteration leading to the overprinting of the original texture.

The bulk of the rock is composed of sericitised plagioclase with subordinate chloritised amphibole and quartz. Quartz forms anhedral strained crystals which are intergranular to plagioclase. Intracrystalline deformation of quartz resulted in the development of an undulose extinction, deformation bands and sub-grain textures. It is possible that intracrystalline deformation accompanied brittle deformation which led to the formation of the cataclasite. Plagioclase forms anhedral crystals which are almost entirely replaced by sericitic white mica. However, the mimetic growth of white mica occasionally preserves the original shape of the feldspar crystals. Amphibole originally formed equant to prismatic crystals which have been pseudomorphed by chlorite, quartz and opaque oxides. The mimetic growth of these alteration products locally preserves the cleavage and crystal shape of the amphibole. The ferromagnesian mineral originally occurred as crudely elongate clusters of several crystals. These amphibole clusters/chains define a weakly developed foliation or banding.

The boundary between the dioritic rock and the cataclasite is sharp. However, there is an increase in the intensity of brittle and intracrystalline deformation recorded by the dioritic rock adjacent to this contact. A banding present within the originally glassy matrix of this fault rock occurs parallel to the margin of the fault zone. This fault rock consists of angular to rounded fragments of monocrystalline and polycrystalline quartz, and feldspar set within a cryptocrystalline silicic matrix. Patchy silicification

and sericitisation of the matrix has been recorded. The pseudotachylite/cataclasite is cut by a number of quartz veinlets which apparently post-date deformation.

Location: 205/16-1(c)

Rock: Dioritic gneiss.

Mineralogy: major – plagioclase, chlorite, quartz

minor – clinopyroxene, apatite, titanite, opaque minerals

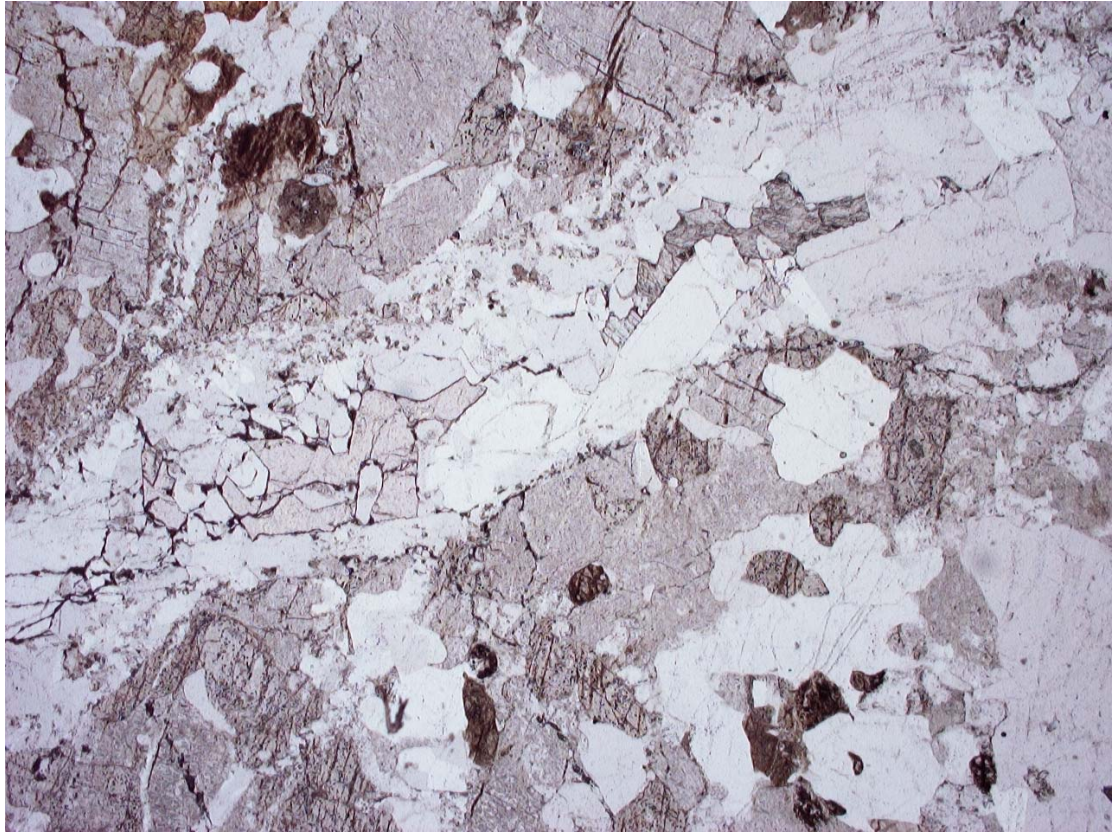
alteration – sericite, opaque oxides, carbonate

Thin Section Registered Number: N3732

Description: This thin section is of a highly altered, medium-grained, anhedral granular or granoblastic, inequigranular dioritic rock which is lithologically similar to thin section number N3731. This sample is mainly composed of altered plagioclase with subordinate chloritised ferromagnesian minerals (pyroxene, hornblende) and quartz. The original texture of the rock has been largely overprinted during the sericitisation of feldspar.

Plagioclase was the dominant feldspar and has been largely replaced by very fine-grained sericitic white mica. Plagioclase, along with the ferromagnesian minerals, originally formed an open crystal framework with the interstices filled by variably strained quartz. The ferromagnesian minerals formed equant to prismatic, anhedral crystals which are intergranular to, and may partially enclose plagioclase. These minerals included pyroxene and amphibole and are completely pseudomorphed by a very fine-grained chloritic assemblage. The pseudomorphs after pyroxene also contain small patches of fine-grained quartz and rare relict clinopyroxene. The pseudomorphs after amphibole are composed entirely of yellow-green chloritic material. The variation in the modal proportions of the ferromagnesian minerals preserves a weakly developed/preserved compositional banding.

The rock is cut by a quartz + carbonate veinlet.



Photomicrographs of 205/16-1 (c.) N 3732 in plane and crossed polarised light. FOV = 2mm.

Location: 205/22-1

Rock: Dioritic gneiss.

Mineralogy: major – plagioclase, chlorite, quartz

minor – clinopyroxene, apatite, titanite, opaque minerals

alteration – sericite, opaque oxides, carbonate

Thin Section Registered Number: N3733

Description: This thin section is of a highly altered, coarse- to very coarse-grained, anhedral granular, inequigranular dioritic rock which may possibly be a coarser grained and more mafic-rich variety of sample 205/16-1. Although altered the original igneous texture can still be recognised within this sample. The bulk of the rock is composed of coarse-grained anhedral plagioclase with subordinate intergranular highly altered amphibole and/or pyroxene. The remaining interstitial to intersertal areas are composed of variably strained quartz.

Plagioclase formed anhedral, twinned and untwinned crystals which are fractured and variably altered to chlorite (\pm sericitic white mica) along these fractures. The primary ferromagnesian minerals have been completely replaced by a fine-grained, pale green chloritic assemblage. The mimetic replacement of pyroxene has preserved possible exsolution lamellae. No obvious cleavage relationships have been preserved within these ferromagnesian minerals, consequently the relative proportions of amphibole and pyroxene are uncertain.

Trace amounts of dark brown, strongly pleochroic biotite have been recorded. Biotite forms small anhedral flakes which exhibit only minor alteration to chlorite. Interstitial quartz is strained with a well developed undulose extinction and sub-grain textures. Traces of coarse grained, intergranular, locally poikilitic K-feldspar have also been noted within this dioritic rock.

Location: 205/26-1

Rock: Dioritic gneiss.

Mineralogy: major – plagioclase, chlorite, epidote, quartz

minor –apatite, opaque minerals

alteration – sericite, leucoxene, opaque oxides, titanite, carbonate,
biotite

Thin Section Registered Number: N3734

Description: This thin section is of a highly altered, massive, medium-grained, inequigranular, anhedral granular dioritic rock which is lithologically similar to sample 205/16-1. This sample is deformed by a number of fractures which are locally marked by narrow bands (≤ 0.4 mm thick) of intense grain reduction due to localised cataclasis.

The bulk of the rock is composed of fractured, dusty looking plagioclase which is variably altered to sericite/clay minerals. The intensity of intracrystalline deformation within plagioclase increases adjacent to the bands of cataclasite/fractures. The primary ferromagnesian minerals (possibly amphibole and pyroxene) originally formed small, equant, anhedral crystals and have been completely replaced by chlorite, fine-grained granular epidote and opaque oxides. Finer grained crystals of amphibole or pyroxene are included within plagioclase. The ferromagnesian minerals typically occur as clusters or aggregates of several crystals. Trace amounts of secondary biotite has been noted included within the pseudomorphs after amphibole/pyroxene.

The remaining interstitial to intersertal areas are filled by irregular to locally weakly interlocking quartz. Quartz is deformed and possesses a well-developed shadowy extinction and sub-grain textures. Apatite is a common accessory phase within this dioritic rock. Primary opaque minerals are variably replaced by leucoxene and/or titanite.

Location: 204/22-1. **Depth:** 2760.0 m.

Rock Type: Tonalitic gneiss

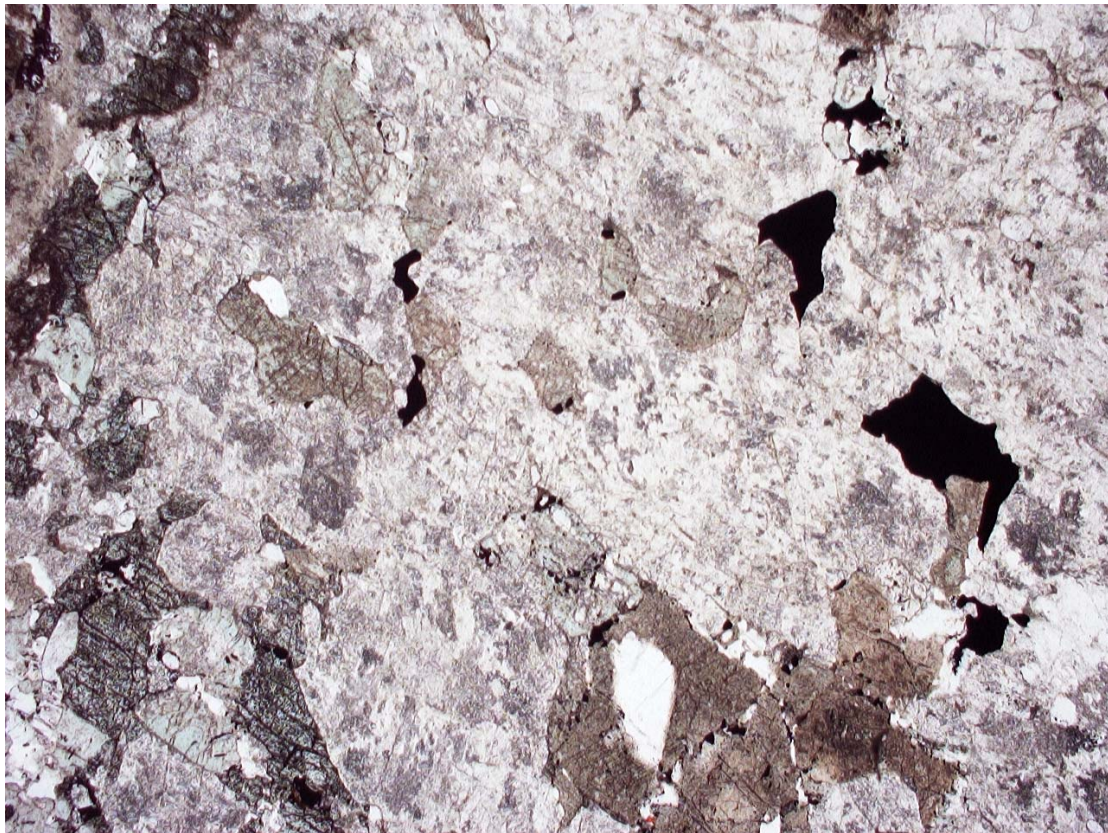
Mineralogy: major – quartz, plagioclase, carbonate, sericite, chlorite, opaque oxides

accessory – biotite, opaque minerals, apatite

alteration – leucoxene

Thin Section Registered Number: N4165

Description: This is a thin section of a highly altered (sericitised + carbonate), coarse-grained tonalitic gneissose rock (granulite facies) with pseudomorphs after pyroxene. This rock contains only 25% of its original mineralogy due to the high degree of alteration. However, the alteration itself is patchy. Quartz and plagioclase dominate the sample. Quartz shows undulose extinction and partial recrystallisation. Plagioclase is altered to white mica, but some kink banding can be seen. The pseudomorphs after pyroxene are dusty and pale brown with fine-grained opaque minerals concentrated along the cleavage planes.



Photomicrograph of 204/22-1 in plane polarised light. FOV = 2 mm.



Photomicrograph of 204/22-1 in crossed polarised light. FOV = 2 mm.

Location: 204/23-1

Rock: Quartzofeldspathic gneiss.

Mineralogy: major – plagioclase, garnet, quartz, epidote

minor – biotite, opaque minerals, K-feldspar

alteration – chlorite, sericite, white mica

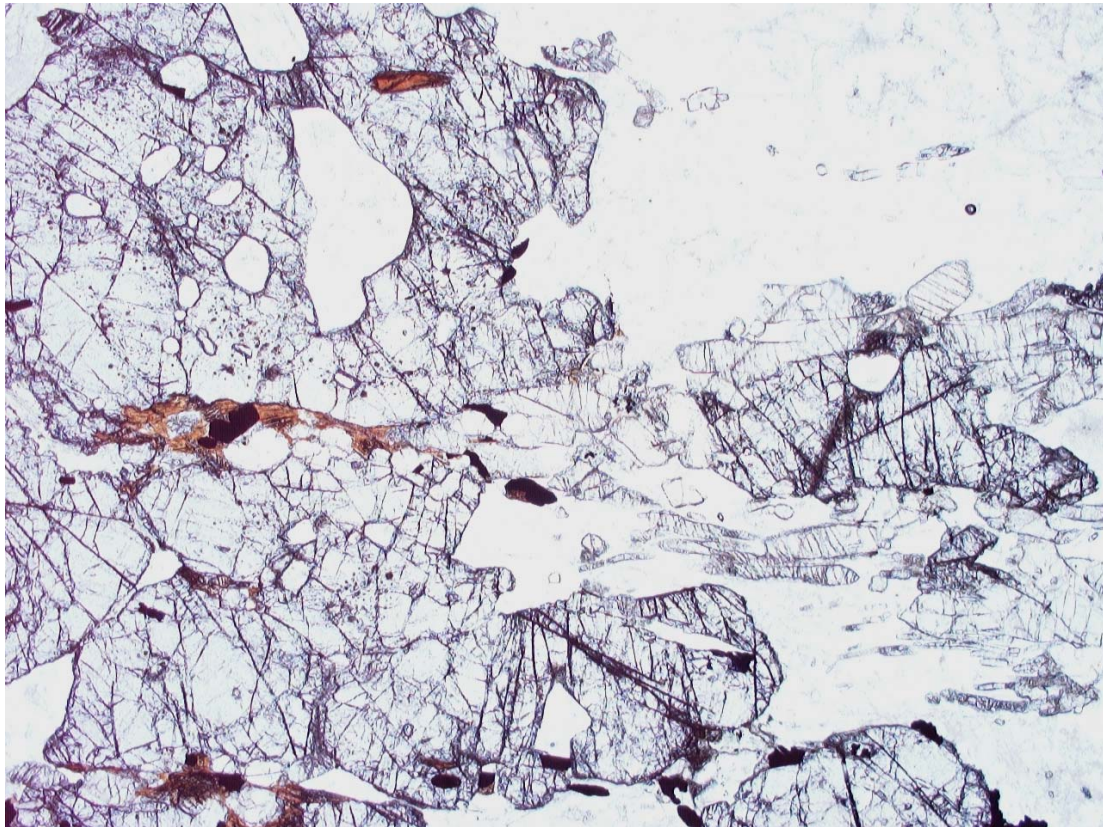
Thin Section Registered Number: N3728

Description: This thin section is of a coarse-grained, inequigranular, weakly foliated garnet-epidote quartzofeldspathic gneiss. The protolith to this gneiss was probably sedimentary in origin e.g. a calc-silicate-rich rock.

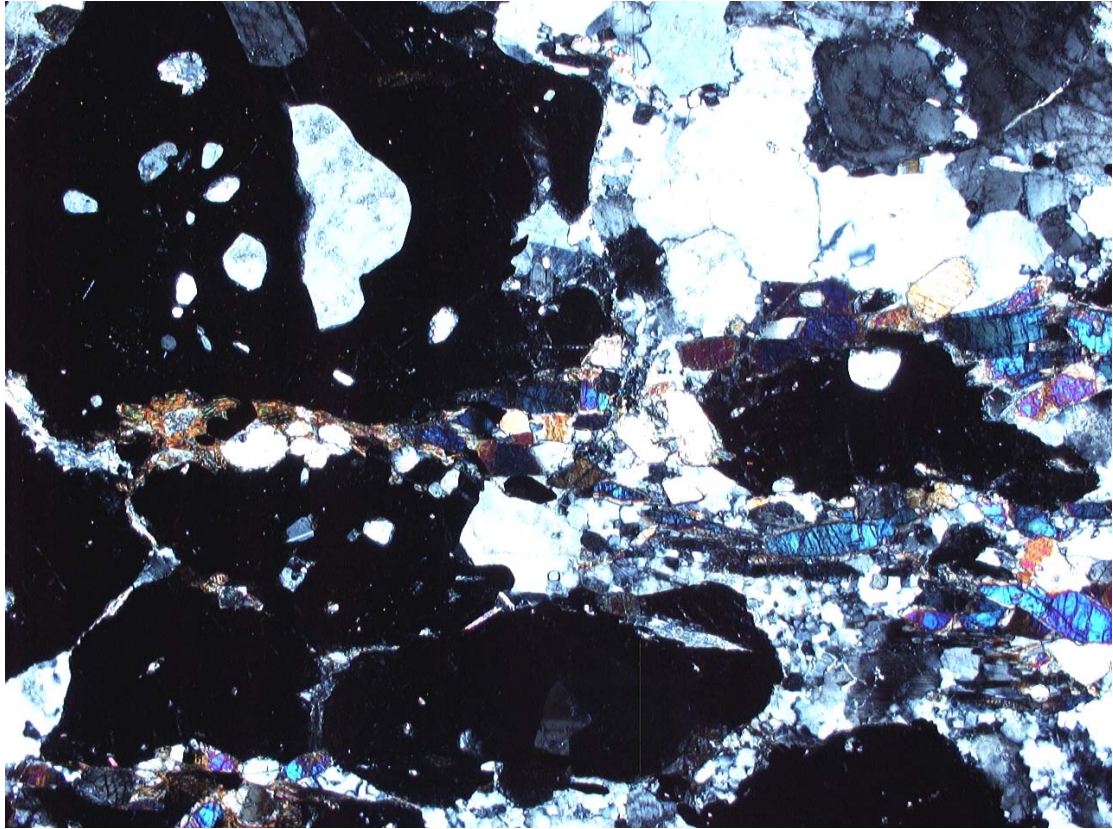
The bulk of the rock is composed of plagioclase, garnet and quartz. Plagioclase is strained with a sweeping to undulose extinction and curved twin composition planes. Feldspar is locally enclosed by a finer grained aggregate of quartz and plagioclase,

with new grains and sub-grains locally being developed along the margins of larger plagioclase crystals. Quartz forms anhedral to irregular crystals which possess an undulose extinction and variably developed sub-grain and new grain textures.

A weakly developed foliation present within this garnetiferous rock is defined by stringers of granular to elongate aggregates of epidote. The imposition of this foliation pre-dated the previously described grain reduction and intracrystalline deformation of quartz and feldspar. The epidote fabric is overgrown by large garnet porphyroblasts. Garnet forms rounded, anhedral porphyroblasts or poikiloblasts which contain small inclusions of plagioclase, quartz, epidote and opaque minerals. Garnet is dusty grey to colourless and may locally form poorly developed atoll-like crystals enclosing a core of quartz and feldspar. Occasional chloritised biotite flakes are also present within this garnetiferous gneiss.



Photomicrograph of 204/23-1 (N3728) in plane polarised light. FOV = 2mm.



Photomicrographs of 204/23-1 (N3728) in crossed polarised light. FOV = 2mm.

Location: 204/25-1

Rock: Tonalitic gneiss.

Mineralogy: major – plagioclase, quartz, chlorite, carbonate

minor – clinopyroxene, hornblende, epidote, apatite, opaque minerals

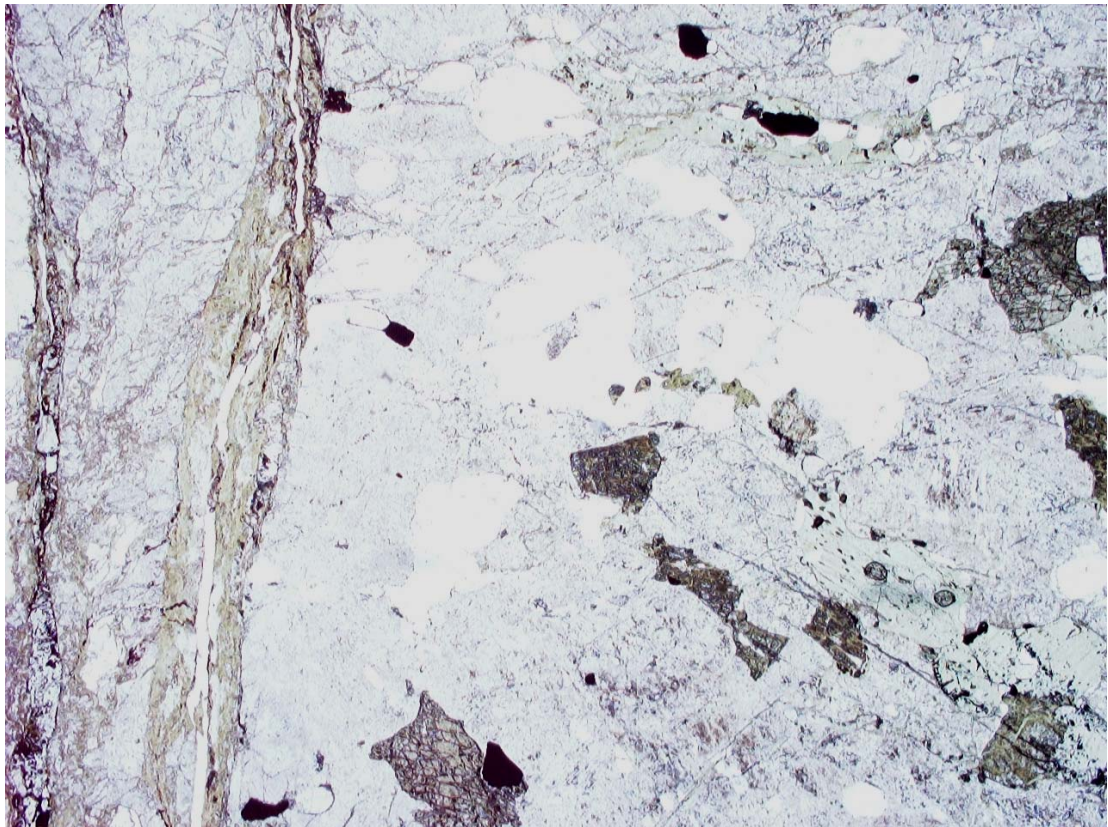
alteration – sericite/clay minerals

Thin Section Registered Number: N3729

Description: This thin section is of a coarse-grained, inequigranular, weakly foliated, retrogressed, clinopyroxene-bearing tonalitic gneiss which is deformed by a prominent brittle fracture. These fractures are associated with localised cataclasis and chlorite + carbonate alteration/mineralisation. Thin, impersistent carbonate and chlorite veinlets are present elsewhere within this sample.

The bulk of this gneiss is composed of anhedral plagioclase and subordinate quartz with minor amounts of clinopyroxene. Pale green pyroxene forms anhedral, small,

equant crystals which are variably altered to, or pseudomorphed by chlorite. Chlorite pseudomorphs after possible amphibole are also present. Plagioclase forms twinned and untwinned crystals which exhibit a dusty appearance under plane polarised light due to alteration to very fine-grained sericitic white mica. Plagioclase exhibits a weak preferred shape alignment parallel to a weakly developed gneissose foliation defined by stringers of quartz. Quartz forms anhedral strained to unstrained crystals which possess a variably developed undulose extinction. Quartz appears to be intergranular to plagioclase. Trace amounts of secondary epidote have been noted replacing plagioclase.



Photomicrograph of 204/25-1 (N3729) in plane polarised light. FOV = 2 mm.



Photomicrographs of 204/25-1 (N3729) in crossed polarised light. FOV = 2 mm.

Location: 202/3-1

Rock: Cataclasite

Mineralogy: major – quartz, plagioclase, K-feldspar, biotite

minor – muscovite, apatite, opaque minerals, clinozoisite

alteration – sericite, clay minerals, chlorite, opaque oxides, carbonate

Thin Section Registered Number: N3727

Description: This thin section is of a medium- to coarse-grained, inequigranular, massive, altered granitic rock which is deformed by an irregular network of fractures marked by narrow zones and irregular patches of cataclasite. This cataclasite is composed of broken fragments of plagioclase and quartz set within a very fine-grained to cryptocrystalline matrix of the same minerals. The rock is mainly composed of an open framework of anhedral plagioclase with the interstices filled by quartz and minor K-feldspar. The mineralogy suggests that the protolith to the rock was probably granodioritic to tonalitic in composition.

Plagioclase typically forms crude lath-shaped feldspar crystals with variably developed crystal faces that are locally preserved suggesting that the protolith may have been igneous in origin. Plagioclase ranges up to 2.0 mm in size and exhibits varying degrees of intracrystalline deformation and cataclasis. This predominantly brittle deformation resulted in the development of an undulose extinction, as well as sub-grain and new grain growth (i.e. grain reduction) along crystal boundaries.

In contrast to plagioclase, K-feldspar is unaltered and possesses variably developed microcline twins. Quartz occurs intergranular to plagioclase and forms anhedral crystals which exhibit varying degrees of intracrystalline deformation. Unusually, quartz appears to be less deformed than the typically more resistant plagioclase with intracrystalline deformation being most intense adjacent to the brittle fractures. Biotite is a minor phase within this broadly granitic rock.

Location: 202/2-1

Rock: Quartzofeldspathic gneiss.

Mineralogy: major – quartz, plagioclase, biotite, garnet

minor – K-feldspar, apatite, zircon, opaque minerals

alteration – chlorite, sericite

Thin Section Registered Number: N3810 and N3811

Description: This thin section is of a medium- to coarse-grained (average grain size *c.* 1.0 mm), anhedral granoblastic, garnet-biotite quartzofeldspathic gneiss. The bulk of the rock is composed of anhedral quartz and plagioclase. Plagioclase is relatively unaltered with very little replacement by sericite. It typically forms twinned and untwinned, anhedral crystals which possess a shadowy extinction and may contain small rounded inclusions of quartz and biotite. Plagioclase ranges up to 2.7 mm in length, but is typically ≤ 1.7 mm in size. Occasional antiperthitic plagioclase crystals were also noted. Quartz is strained with a weakly to moderately developed undulose extinction. Larger quartz crystals are variably replaced by an aggregate of finer grained crystals (new grains).

A weakly developed foliation present within this gneiss is defined by variably aligned biotite flakes. Biotite occurs as single crystals as well as clusters of several flakes. It is

pale yellow-brown to dark red-brown in colour and possess a well-developed pleochroism. Very fine-grained inclusions of opaque oxide and zircon have been noted within biotite. Garnet forms anhedral, rounded porphyroblasts (up to 3.0 mm in diameter) and poikiloblasts which locally overgrown and, therefore, post-date the imposition of the biotite fabric. These porphyroblasts contain small, rounded inclusions of quartz, plagioclase, biotite and opaque minerals. No muscovite has been recognised within this sample..



Photomicrographs of 202/2-1 (N3810) in plane polaried light. FOV = 2 mm.



Photomicrographs of 202/2-1 (N3810) in crossed polarized light. FOV = 2 mm.

Location: 202/9-1.

Rock Type: Amphibolite

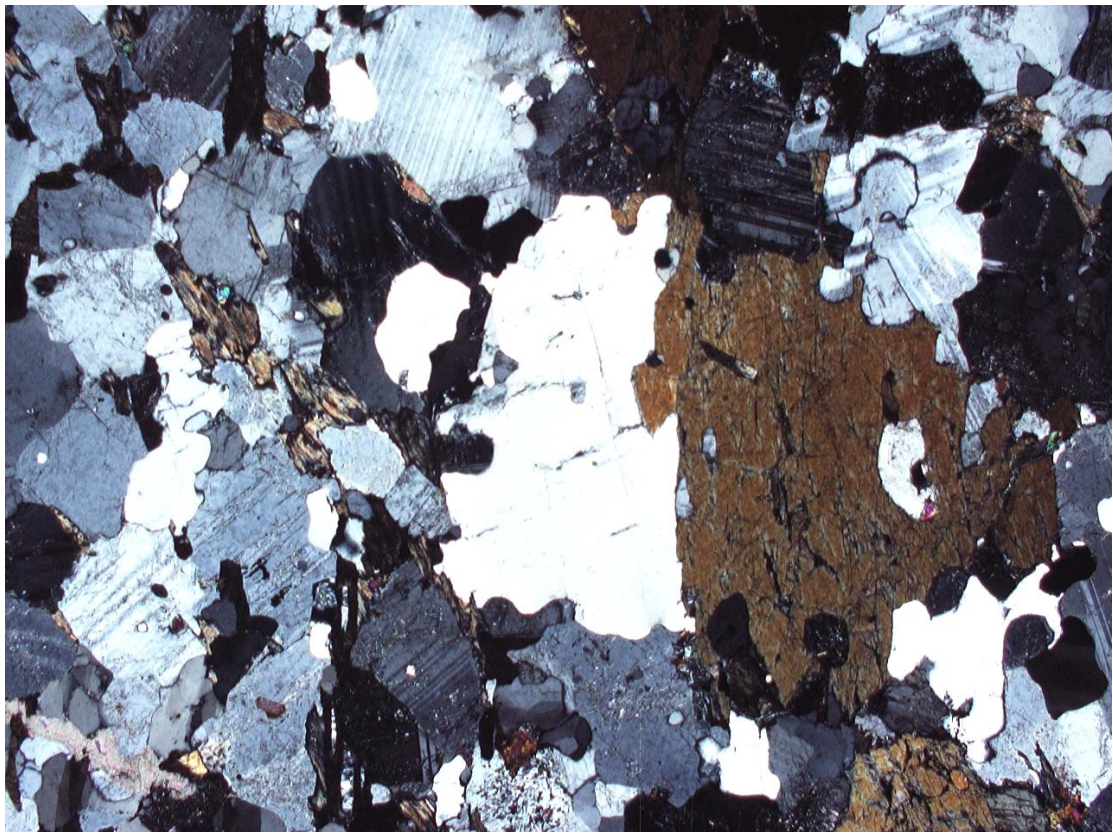
Mineralogy: major – plagioclase, amphibole, quartz, biotite

accessory – opaque minerals, epidote, apatite

alteration – chlorite, opaque oxides, sericite, epidote/clinozoisite

Thin Section Registered Number: N4166

Description: This is a thin section of a banded, medium- to coarse-grained hornblende-biotite gneissose amphibolite which is cut by a narrow cataclastic fracture. The banding in this rock is determined by the modal proportions of hornblende. The hornblende is highly pleochroic from pale straw yellow to bottle green. Plagioclase and quartz are also common in this rock, and form 90% of the leucosome. The cataclastic fracture has reduced the grain size of the original mineralogy of the rock. Biotite also forms distinctive bands within the thin section, but is also associated with the hornblende.



Photomicrographs of 202/9-1 in plane and crossed polarised light. FOV = 2mm.

Location: 88/02(a)

Rock: Quartzofeldspathic schist cut by cataclasite

Mineralogy: major – quartz, K-feldspar, biotite, plagioclase, hornblende

minor – titanite, epidote, apatite, allanite, opaque minerals

alteration – chlorite, zoisite/clinozoisite

Thin Section Registered Number: N3722

Description: This thin section is of a medium-grained (average grain size 0.3 to 0.5 mm), inequigranular, moderately foliated, anhedral granoblastic, schistose quartzofeldspathic rock. The moderately developed, homogeneous schistosity is defined by shape aligned biotite flakes and, to a lesser extent, weakly aligned feldspar and quartz crystals. The bulk of the rock is composed of quartz and feldspar. K-feldspar is the dominant feldspar, but both feldspars may contain very small inclusions of zoisite and/or clinozoisite.

Biotite forms elongate, anhedral flakes as well as needle-like crystals. Quartz forms anhedral, strained crystals in which intracrystalline deformation has resulted in the development of an undulose extinction, deformation bands and sub-grain textures. Amphibole, where present, is closely associated with biotite. Trace amounts of anhedral, late/post-kinematic epidote was noted forming small porphyroblasts which clearly overgrown the biotite fabric. Epidote was also noted forming rims upon highly altered allanite crystals. Trace amounts of anhedral titanite is spatially related to biotite.

This rock is deformed by a number of fractures defined by narrow bands or zones of cataclasite and zones of intense grain reduction. These cataclastic zones clearly represent a much later phase of brittle deformation. Along one side of the thin section is a 2.5 to 3.0 mm wide band/zone of cataclasite. This cataclasite is composed of angular to subrounded fragments of quartz and feldspar set within a turbid grey-brown, very fine-grained matrix. Occasional fragments of biotite and/or amphibole within the cataclasite have been replaced by chlorite. Crystal fragments are variably aligned parallel to the margin of this band of cataclasite. The cataclasite forms a discrete zone which apparently occurs parallel to the earlier formed schistosity. Brittle deformation leading to cataclasis post-dated the imposition of this early ductile fabric.



Photomicrographs of 88/02 (N3722) in plane and crossed polarised light. FOV = 2 mm.

Location: 88/02(b)

Rock: Quartzofeldspathic schist deformed by cataclastic fractures

Mineralogy: major – quartz, K-feldspar, plagioclase, biotite, hornblende

minor – titanite, epidote, apatite, allanite, opaque minerals, clinozoisite

alteration – chlorite, opaque minerals

Thin Section Registered Number: N3723

Description: This thin section is of a medium-grained (average grain size 0.4 to 0.6 mm), inequigranular, anhedral granoblastic, schistose quartzofeldspathic rock which is deformed by a number of fractures marked by narrow zones of cataclasite. A moderately developed, homogeneous schistosity is defined by shape aligned biotite flakes. Biotite locally contains small inclusions of opaque minerals, apatite and titanite. Titanite is closely associated with biotite. Biotite forms anhedral, elongate flakes which are locally over grown by apparently later epidote.

The bulk of the rock is composed of inequigranular, anhedral quartz and feldspar. K-feldspar is the dominant feldspar. A crudely developed or preserved zonation has been noted in both feldspars. Trace amounts of a green to blue-green, weakly pleochroic amphibole are also present within this quartzofeldspathic rock. Amphibole forms small anhedral crystals which are spatially related to biotite. Minor to trace amounts of epidote have also been recorded, with epidote locally forming rims upon altered allanite.

As previously stated the rock is deformed by a number of brittle fractures marked by < 1.0 mm up to c. 4.0 mm thick bands of cataclasite. These zones occur parallel to, and probably result from the brittle reactivation of the earlier developed schistosity. This brittle fault rock ranges from proto-cataclasite through to ultra-cataclasite due to the variation in included relict, broken quartz and feldspar crystal fragments as well as small rock fragments. The matrix to the cataclasite is composed of a turbid brown-grey, very fine-grained chloritic/clay-rich assemblage. Biotite and, where present, amphibole within the host quartzofeldspathic schist are variably altered to chlorite immediately adjacent to these brittle fractures. An asymmetrical foliation developed within the finer-grained ultra-cataclasite zones yields a possible sinistral sense of shear in this plane of section. The boundaries of the majority of the cataclasite zones

are sharp. However, in the upper part of the thin section the cataclasite comprises an anastomosing network of grain reduction composed of very fine-grained quartz and feldspar. Optical alignment of phyllosilicate minerals/clay within the matrix of the ultra-cataclasite bands locally defines a well-developed planar to anastomosing foliation.



Photomicrograph of 88/02 (N3723) in plane polarised light. FOV = 2 mm.

Location: 164/25-2(a)

Rock: Metabasic gneiss.

Mineralogy: major –plagioclase, clinopyroxene, garnet, orthopyroxene, hornblende, quartz

minor – biotite, apatite, opaque minerals

alteration – actinolitic amphibole

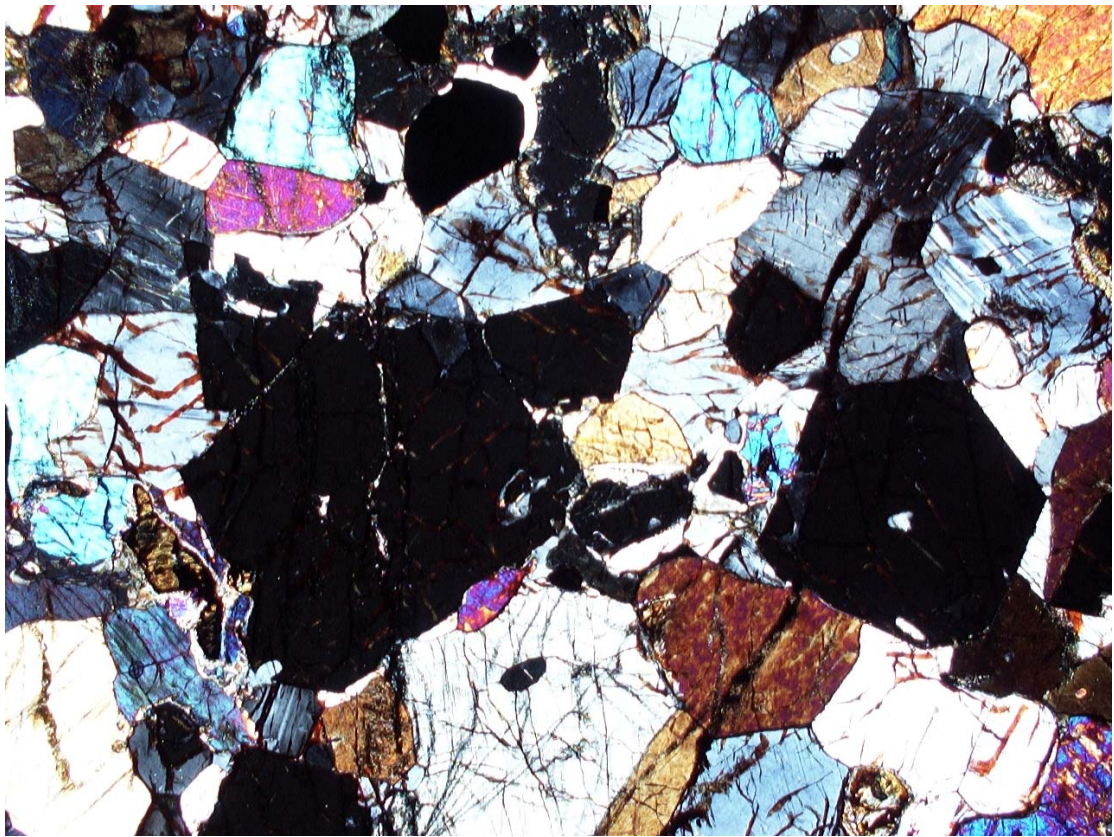
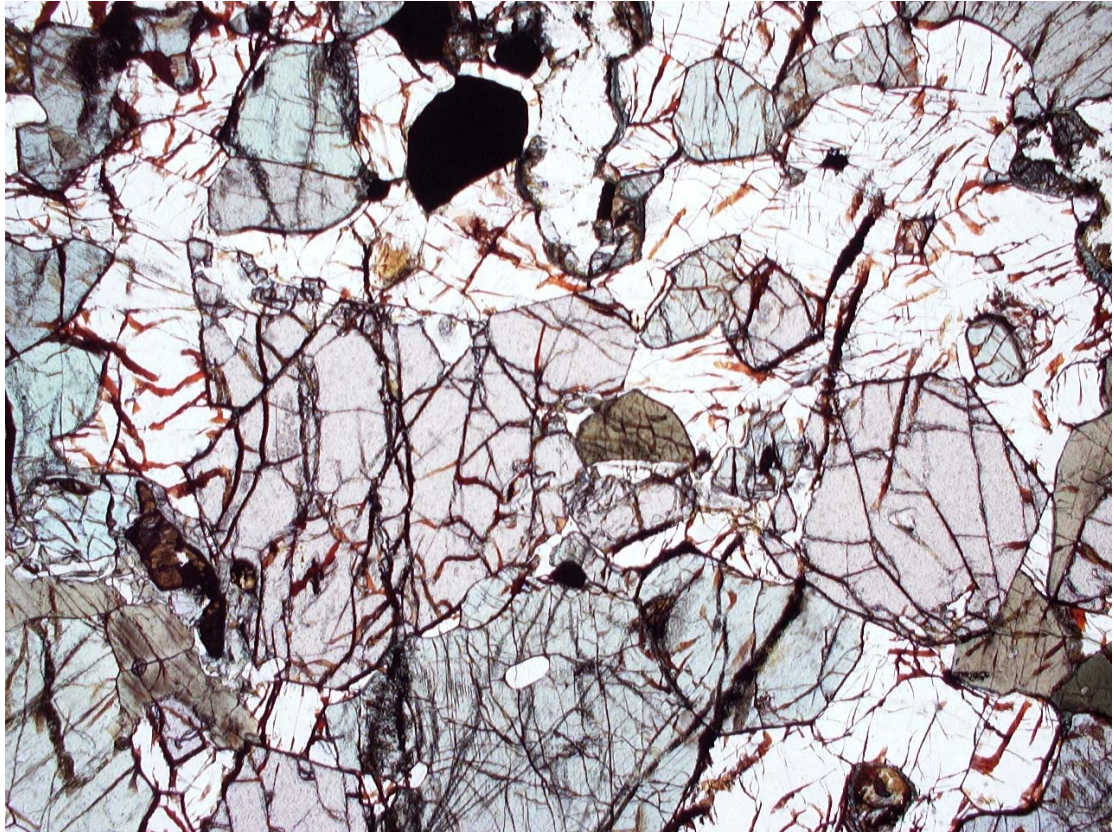
Thin Section Registered Number: N3725

Description: This thin section is of a coarse-grained, inequigranular to weakly equigranular, anhedral granoblastic, hornblende-bearing garnet-pyroxene metabasic gneiss. The protolith of this high-grade metamorphic rock was probably a basalt or gabbro. The presence of both clinopyroxene and orthopyroxene within the mineral assemblage indicate that this rock has undergone granulite facies metamorphism. However, the occurrence of hornblende within the high-grade mineral assemblage suggests that a H₂O-bearing fluid phase was present during granulite facies metamorphism.

The rock is mainly composed of plagioclase, clinopyroxene and garnet with minor amounts of orthopyroxene and quartz. Clinopyroxene is locally enclosed within a fine rim of pale green, possibly ?actinolitic amphibole; the latter possibly developing during very limited retrogression.

Unlike clinopyroxene, orthopyroxene was apparently more susceptible to alteration and is variably replaced by blue-green possibly ?actinolitic amphibole and yellow-brown bowingite/oxidised chlorite. Orthopyroxene forms single, isolated crystals or clusters of several grains which may be surrounded by, or partially enclosed within clinopyroxene. Garnet forms anhedral, pinky brown coloured, anhedral to occasionally subhedral crystals which occasionally possess well-developed crystal faces. Garnet typically occurs with, or adjacent to small pockets of plagioclase and orthopyroxene. Garnet was also noted forming more irregular crystals and rims upon opaque minerals.

Plagioclase forms anhedral crystals which appear to be intergranular to both pyroxene and garnet. Plagioclase exhibits very little alteration. Rare, small, dark brown coloured biotite flakes are present within this metabasic gneiss.



Photomicrographs of 164/25-2 (N3725) in plane and crossed polarised light. FOV = 2 mm.

Location: 164/25-2(b)

Rock: Partially retrogressed metabasic gneiss.

Mineralogy: major – plagioclase, clinopyroxene, garnet, hornblende,
orthopyroxene, quartz

minor – biotite, apatite, opaque minerals

alteration – actinolitic amphibole

Thin Section Registered Number: N3726

Description: This thin section is of a medium- to coarse-grained, granoblastic, equigranular to weakly inequigranular, partially retrogressed, weakly foliated, hornblende-bearing garnet-pyroxene metabasic gneiss. The protolith of this high-grade metamorphic rock was probably a basalt or gabbro. The presence of both clinopyroxene and orthopyroxene within the mineral assemblage indicate that this rock has undergone granulite facies metamorphism. However, the occurrence of hornblende within the high-grade mineral assemblage suggests that a H₂O-bearing fluid phase was present during granulite facies metamorphism. Subsequent retrogression resulted in the variable replacement of orthopyroxene and, to a lesser extent, clinopyroxene, hornblende and plagioclase by a pale blue-green, possibly ?actinolitic amphibole. The growth of secondary amphibole suggests that retrogression occurred under amphibolite or possible greenschist facies conditions.

A weakly developed gneissose foliation is defined by chains or elongate aggregates of pyroxene, plagioclase and amphibole. This foliation results in a weakly banded appearance to the gneiss under low magnification. Hornblende appears to be intergranular to, and occasionally partially encloses clinopyroxene indicating that amphibole growth and possibly, therefore, H₂O infiltration occurred at a later stage during granulite facies metamorphism (post-dating pyroxene growth). Traces of a symplectitic intergrowth between hornblende and quartz have also been recorded within this metabasic gneiss.

Clinopyroxene is pale green to grey green in colour and forms anhedral non-pleochroic crystals which are rimmed by later pale blue-green actinolitic amphibole. Retrogression of clinopyroxene typically occurs where it is in contact with the apparently more unstable orthopyroxene. Orthopyroxene is variably replaced, or

pseudomorphed by a very fine-grained aggregate of actinolitic amphibole. These pseudomorphs may also contain rounded, fine-grained inclusions of opaque minerals (resulting from excess Fe expelled during retrogression) and traces of yellow-brown bowlingite and/or oxidised chlorite.

Garnet is pale pink in colour and occurs as: (a) large (0.5 to 1.5 mm in diameter) anhedral to weakly subhedral porphyroblasts; as well as (b) irregular, anhedral crystals containing work-like inclusions of quartz. The second textural variety of garnet was also observed forming rims upon opaque minerals. Garnet is typically spatially related to clinopyroxene and hornblende. Plagioclase forms twinned and untwinned, anhedral crystals which locally contain thin foils of opaque along the cleavage planes. Minor quartz is present within this metabasic rock forming anhedral strained crystals which possess an undulose extinction and sub-grain textures. Trace amounts of biotite are present, typically associated with the retrogression of pyroxene to actinolitic amphibole.

Location: 154/3-1.

Rock: Amphibolite.

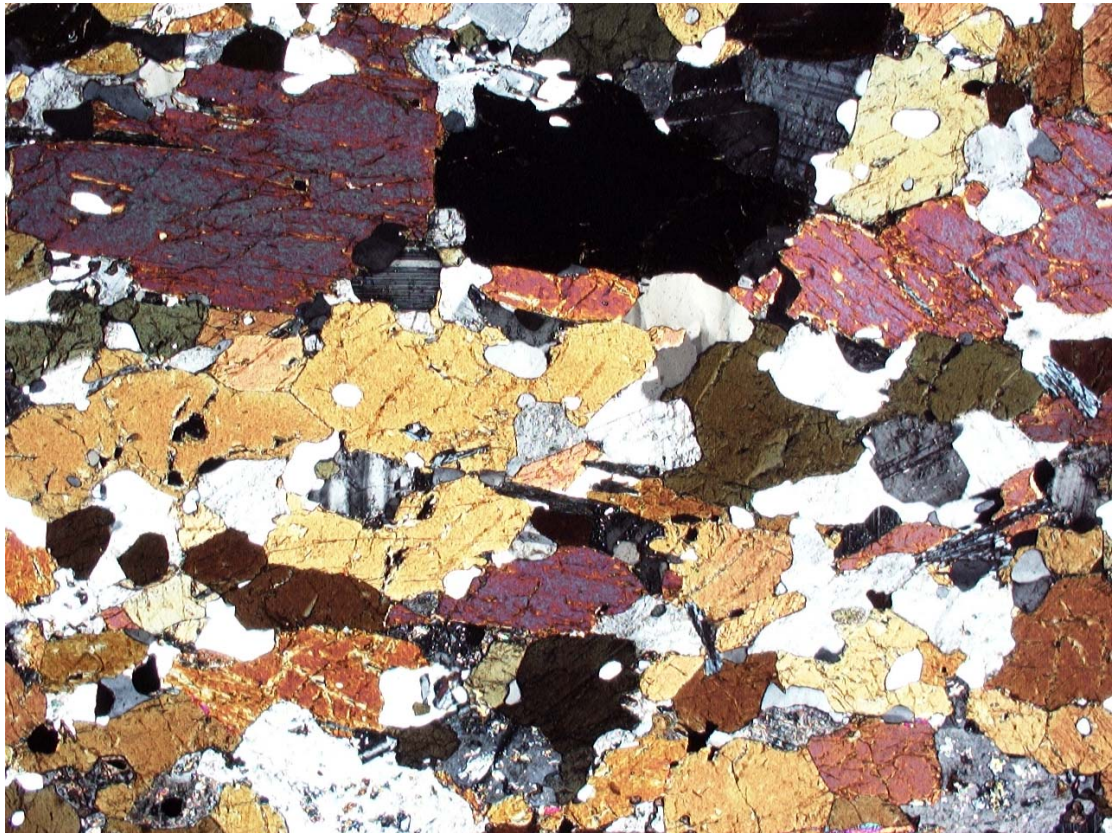
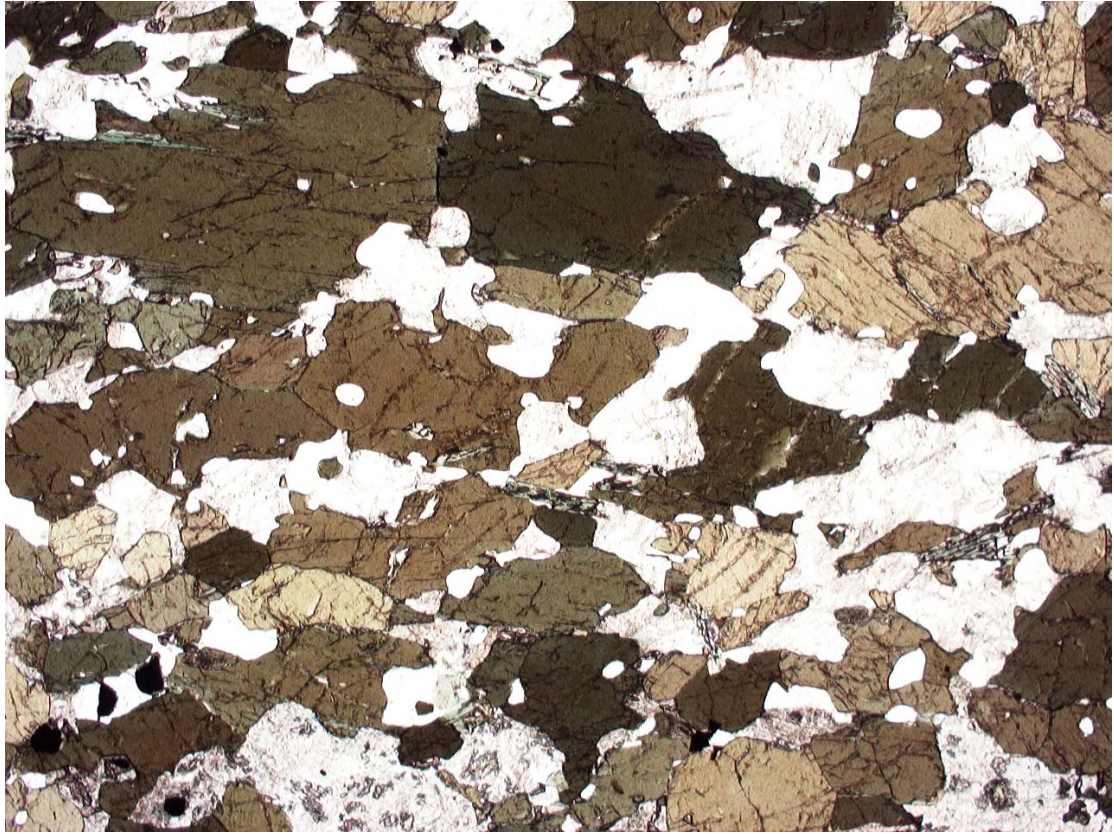
Mineralogy: major – amphibole, plagioclase, quartz, biotite

accessory – titanite, opaque minerals, apatite

alteration – chlorite, sericite, clinozoisite, white mica, opaque oxides

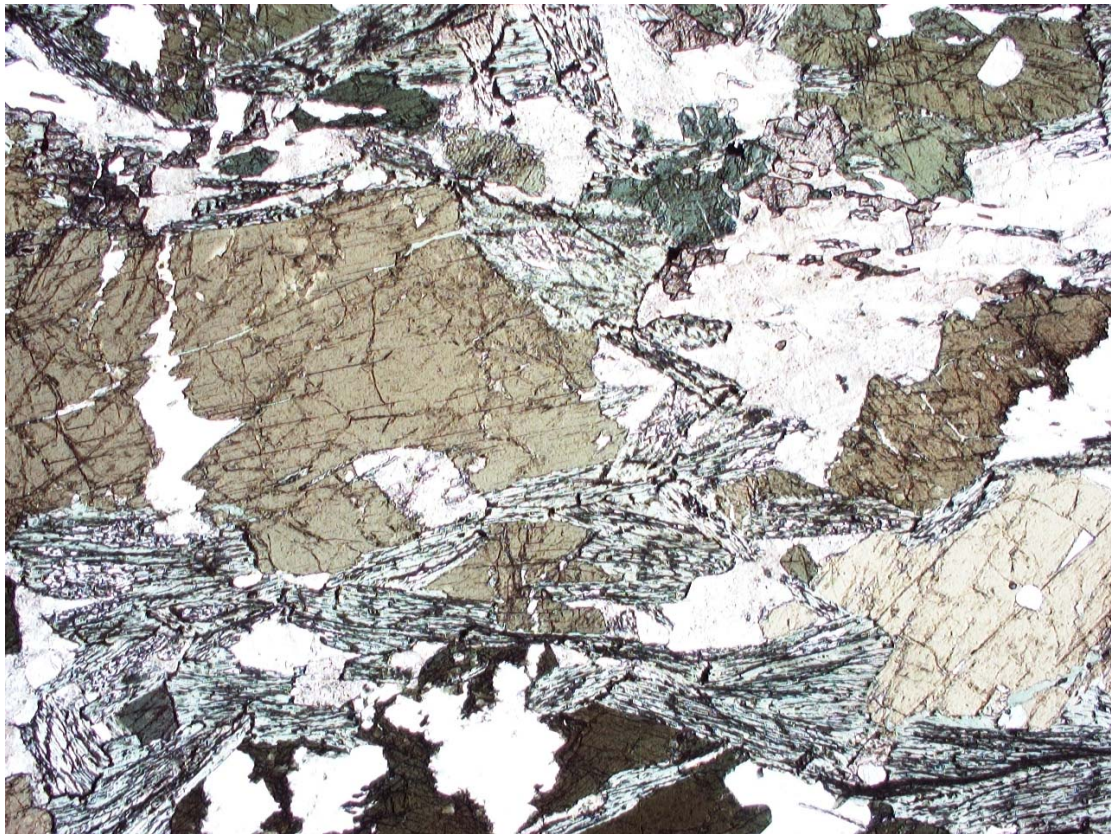
Thin Section Registered Number: N4167

Description: This is a thin section of a partially retrogressed/altered (chloritised), amphibole-biotite gneissose amphibolite. The gneissose texture of the rock is determined by the modal proportions of amphibole. The thin section can be divided into two main sections separated by a large plagioclase crystal (4 mm in size). The top of the sample (bottom of the thin section) is a fine-grained amphibolite. The amphibole is highly pleochroic from pale straw yellow to bottle green and is about 50 microns in size. There are subhedral crystals of quartz and plagioclase. Plagioclase is altered to white mica in patches, but overall this part of the sample is relatively unaltered. Rare small amphibole-quartz symplectites can also be found.

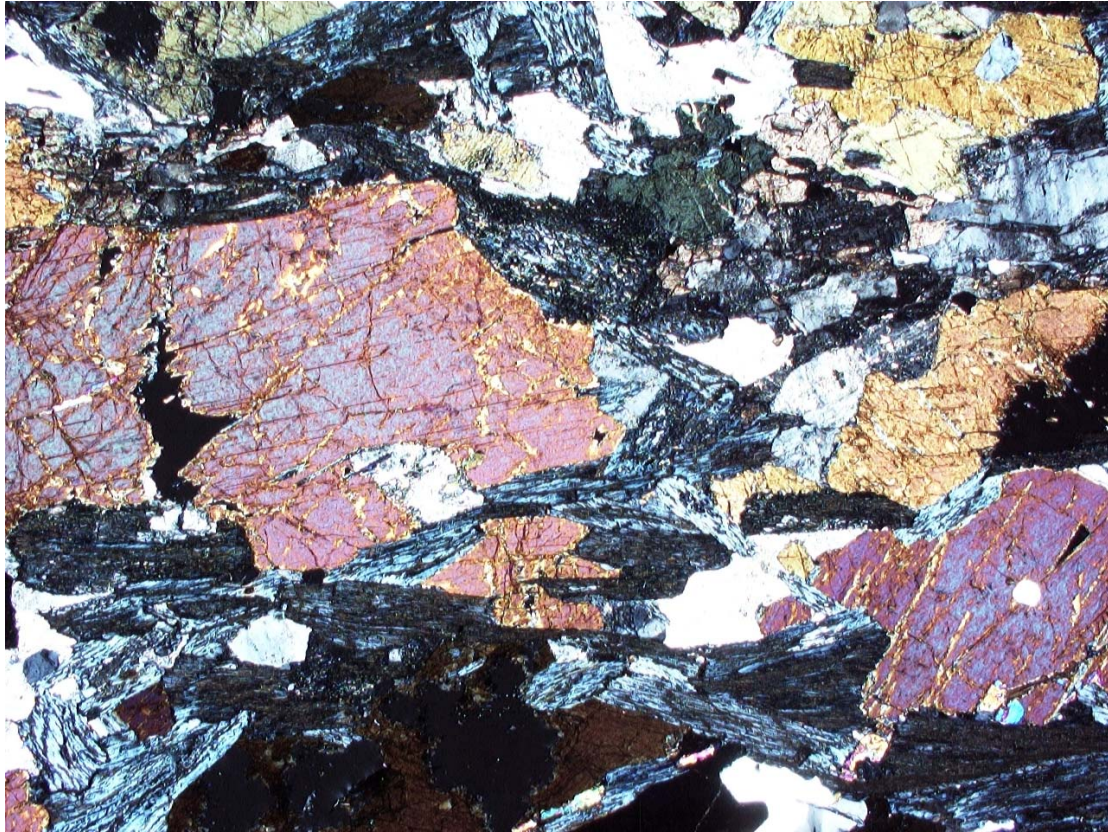


Photomicrographs of 154/3-1 from the fine-grained amphibolite in both plane and crossed polarised light. FOV = 2 mm.

The bottom of the sample (top of the thin section) is mineralogically similar to the fine-grained amphibolite already described. However, much of the amphibole (30%) has been altered to chlorite (blue interference colours) and fine-grained opaque minerals. The amphibole ranges in size from 0.5 to 1.5 mm and is still highly pleochroic from pale yellow to green. Quartz and plagioclase are also present and the plagioclase is more commonly altered to chlorite and white mica. Overall this is a coarse-grained amphibolite that has been altered or partially retrogressed.



Photomicrographs of 154/3-1 from the chloritised coarse-grained amphibolite in plane polarised light. FOV = 2 mm.



Photomicrographs of 154/3-1 from the chloritised coarse-grained amphibolite in crossed polarised light. FOV = 2 mm.

Location: 58-08/228 DR

Rock: Deformed granitic pegmatite

Mineralogy: major – quartz, biotite, K-feldspar, plagioclase

alteration – chlorite, muscovite, carbonate, opaque oxides

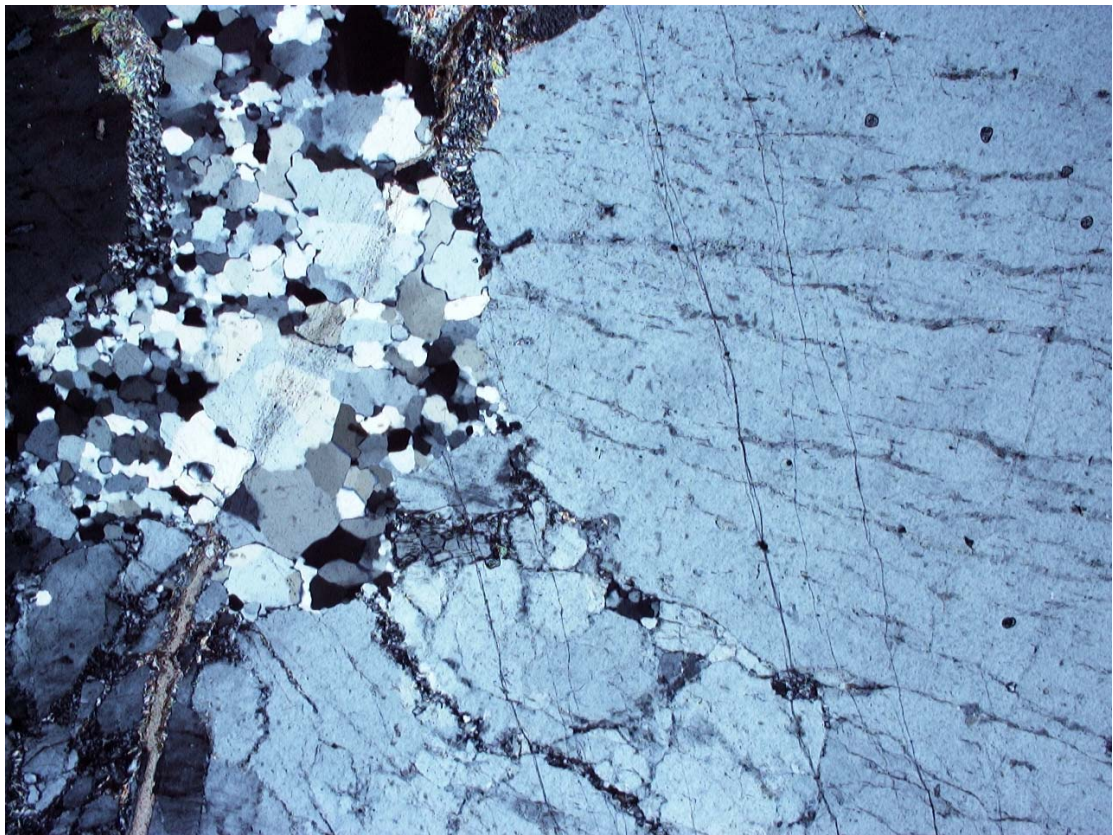
Thin Section Registered Number: N3720

Description: This thin section is of an altered, deformed, very coarse-grained granite pegmatite. The thin section is dominated by a few large crystals of K-feldspar, biotite and quartz which have all undergone varying degrees of intracrystalline deformation and/or cataclasis. Biotite is moderately pleochroic, varying from yellow-brown to brown in colour, and forms larger crystals up to *c.* 20 mm in length. Internal deformation of biotite resulted in the kinking of the basal (001) cleavage with contemporaneous chloritic alteration being focused the axial surfaces of these brittle structures. The kinks are angular in form with distinct fractures running along the

axial planes of the micro-folds. Kinking and fracturing has resulted in the fragmentation of the large crystals of biotite into a number of elongate, lenticular relicts which have undergone varying degrees of chloritisation. The originally large biotite crystals are enclosed within a reaction rim of pale green chlorite, minor muscovite/white mica and fine-grained granular carbonate; the latter appears to be replacing chlorite. Elongate quartz inclusions have also been noted along the cleavage planes within biotite.

Quartz within this pegmatitic rock has been replaced by an aggregate of variably strained new-grains and sub-grains which contain irregular to lenticular relicts of the originally larger crystals. K-feldspar (microcline) forms large (*c.* 10.0 to 20.0 mm in size) crystals which possess a distinctive undulose extinction and have undergone of cataclasis rather than ductile intracrystalline deformation. The feldspar exhibits minor alteration to white mica and/or carbonate along these fractures. A number of the fractures are defined by narrow zones of cataclasite and/or dynamic recrystallisation. These large microcline crystals are locally perthitic (vein perthite) and may also contain small crystals of rare plagioclase.

Deformation of this pegmatite appears to have been brittle in nature resulting in cataclasis of feldspar and biotite, with deformation probably accompanying alteration.



Photomicrographs of 58-08/228 in plane and crossed polarised light. FOV = 2mm.

Location: 58-08/230 DR

Rock: Alkali granite

Mineralogy: major – plagioclase, K-feldspar, amphibole, biotite

minor – opaque minerals, titanite, garnet, apatite

alteration – opaque oxides, muscovite/white mica, carbonate, sericite,
clay minerals, clinozoisite

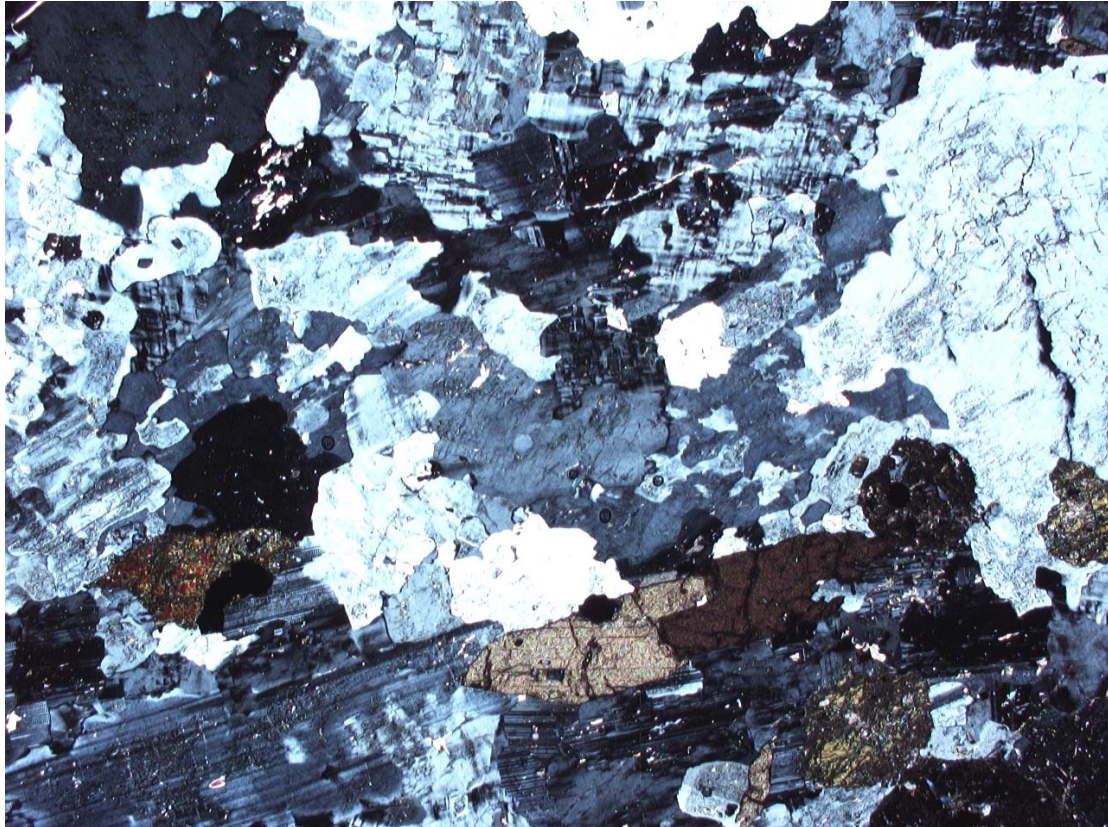
Thin Section Registered Number: N3721

Description: This thin section is of a coarse-grained, holocrystalline, inequigranular, variably recrystallised or metamorphosed, feldspathic, weakly foliated ?alkali granitic rock. The rock is mainly composed of irregular to locally interlocking plagioclase and subordinate K-feldspar with no obvious quartz present. Sub-solidus recrystallisation has resulted in the modification of the original texture of the rock. A weak pre-full crystallisation fabric is defined by the variable shape alignment of plagioclase laths.

Plagioclase forms twinned and untwinned, anhedral to irregular, lath-shaped crystals. Very fine grained muscovite or white mica flakes have been noted included within, or replacing plagioclase. A weak zonation within plagioclase is preserved by the preferential alteration of the cores of these zoned crystals. Pockets of finer grained plagioclase are also present included within intergranular poikilitic K-feldspar crystals.

Traces of opaque minerals, titanite and garnet are present within this possibly alkaline granitic rock. Garnet is yellow-brown in colour and forms small anhedral crystals.

Minor to trace amphibole is rimmed and partially replaced by bright green coloured ?chloritised biotite.



Photomicrograph of 58-08/230 in crossed polarised light. FOV = 1mm.

Location: 90/14

Rock: Quartzofeldspathic gneiss (coarser grained version of 88/02)

Mineralogy: major – quartz, plagioclase, K-feldspar, biotite, hornblende

minor – titanite, epidote, apatite, allanite, opaque minerals, clinozoisite

alteration – chlorite, sericite

Thin Section Registered Number: N3724

Description: This thin section is of a coarse-grained, inequigranular, weakly to moderately foliated quartzofeldspathic gneiss which may represent a coarser grained version of sample 88/02. However, unlike the previous samples sample 90/14 does not contain cataclasite. This sample is mainly composed of anhedral, inequigranular quartz, K-feldspar and plagioclase.

Quartz is strained with intracrystalline deformation resulting in the development of an undulose extinction, deformation bands and, in some cases, sub-grain textures.

Plagioclase is the dominant feldspar and forms twinned and untwinned crystals which exhibit minor amounts of alteration to very fine-grained sericitic white mica.

Plagioclase was also noted forming rounded to elongate, coarser grained crystals or porphyroblasts which range from 2.5 up to 4.0 mm in length. These larger crystals are shape aligned parallel to, and are wrapped by the weakly to moderately developed foliation. This coarse schistosity or gneissose foliation is defined by shape aligned biotite flakes. Biotite is locally overgrown and/or replaced by later epidote/clinozoisite. Epidote was also noted forming small, post-kinematic porphyroblasts which clearly post-date the imposition of the biotite foliation.

Apatite and titanite are common accessory phases.

Location: 57-09/536 DR

Rock: Monzodioritic gneiss.

Mineralogy: major – plagioclase, biotite, amphibole, quartz, K-feldspar

minor – opaque minerals, titanite, allanite

alteration – clinozoisite/epidote

Thin Section Registered Number: N3715

Description: This thin section is of a medium- to coarse-grained, inequigranular, moderately foliated, hornblende-biotite-bearing quartzofeldspathic gneiss. A compositional banding present within this high-grade (?upper amphibolite facies) metamorphic rock is defined by the variation in modal biotite and hornblende. A tectonic fabric is developed parallel to this banding and is defined by shape-aligned biotite flakes and, to a lesser extent, plagioclase and amphibole. Biotite is the dominant ferromagnesian mineral and locally contains inclusions of titanite and apatite.

Hornblende is associated with biotite and locally overgrown finer-grained biotite crystals it may contain small inclusions of apatite and titanite. Both apatite and titanite are common accessory phases within this gneiss.

The remainder of the rock is composed of anhedral granoblastic plagioclase with subordinate amounts of quartz and trace K-feldspar. Quartz is intergranular to

plagioclase, biotite and amphibole and forms strained anhedral crystals which possess an undulose extinction.

Location: 57-09/537 DR

Rock: Monzodioritic gneiss.

Mineralogy: monzonite: major – K-feldspar, quartz, plagioclase, biotite

minor – opaque minerals, muscovite, clinozoisite, zircon

alteration – sericite, carbonate, chlorite, opaque oxides

gneiss: major – plagioclase, K-feldspar, quartz, biotite, amphibole

minor – opaque minerals, clinozoisite, apatite, titanite

alteration – sericite, clay minerals

Thin Section Registered Number: N3718

Description: This thin section is of a monzonitic granite vein or band cutting an amphibole and biotite-bearing quartzofeldspathic rock; the latter is lithologically similar to samples 56-08/920 and 56-08/921.

The monzonitic vein or band is composed medium- to coarse-grained, anhedral granular, weakly banded, recrystallised/metamorphosed granite. The rock is mainly composed of K-feldspar and quartz with subordinate amounts of plagioclase. The banding is defined by elongate ribbons of quartz and a slight variation in the modal proportion of K-feldspar. K-feldspar is the dominant mineral phase and forms anhedral, locally perthitic crystals which possess distinctive coarse microcline twins.

The contact between the monzonite and the adjacent amphibole- and biotite-bearing quartzofeldspathic gneiss is sharp. The monzonite vein clearly cross cuts a moderately developed biotite foliation. The amphibole- and biotite-bearing gneiss appear to be broadly dioritic to granodioritic in composition and is mainly composed of plagioclase, quartz and K-feldspar with minor shape aligned biotite. Plagioclase is the dominant feldspar. Small patches of finer grained quartz, K-feldspar and, in some cases myrmekite occur intergranular to plagioclase and coarse grained K-feldspar. The myrmekite appears to be replacing the adjacent coarser grained K-feldspar and is composed of single crystals of plagioclase contain worm-like inclusions of quartz.

Opaque minerals, titanite and apatite are common accessory phases and are typically associated with biotite. Titanite forms anhedral to weakly subhedral elongate to lozenge-shaped crystals which are locally overgrown by, or included within biotite. Minor amounts of brown-green to blue-green, moderately pleochroic amphibole are present forming anhedral crystals which may partially include or overgrown biotite and titanite.

Location: 57-09/537 DR

Rock Type: Amphibolite

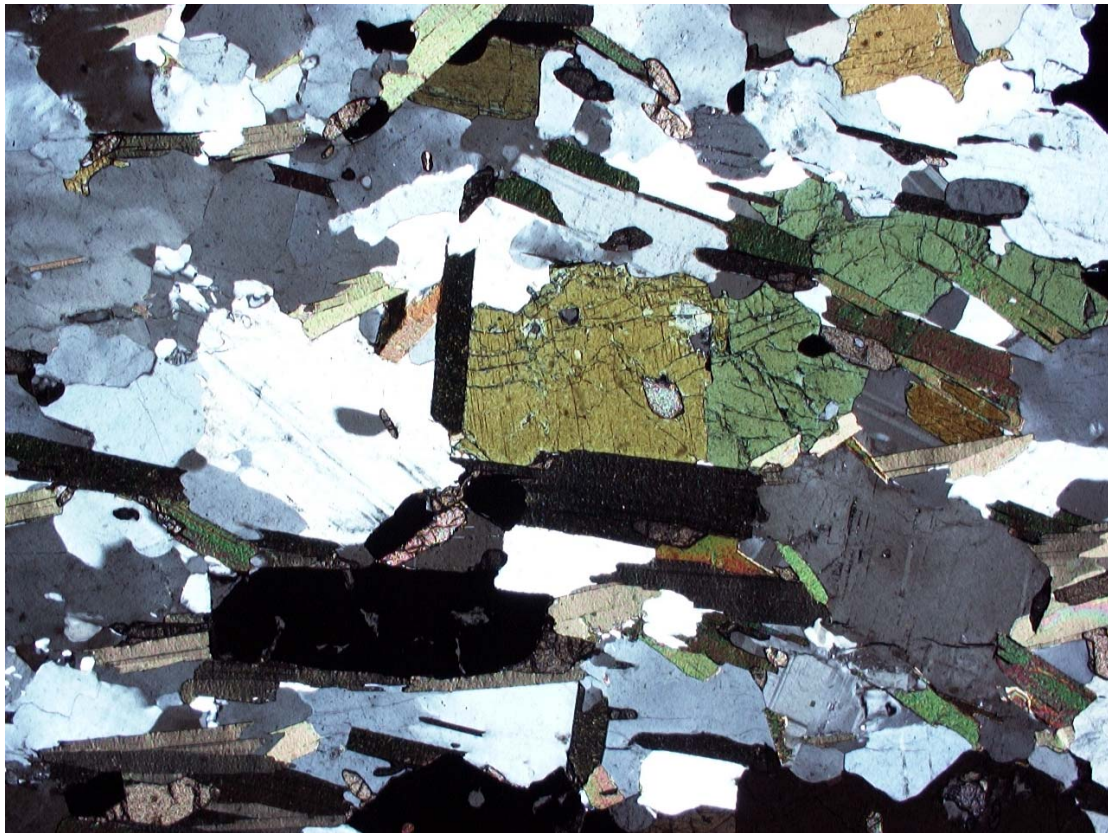
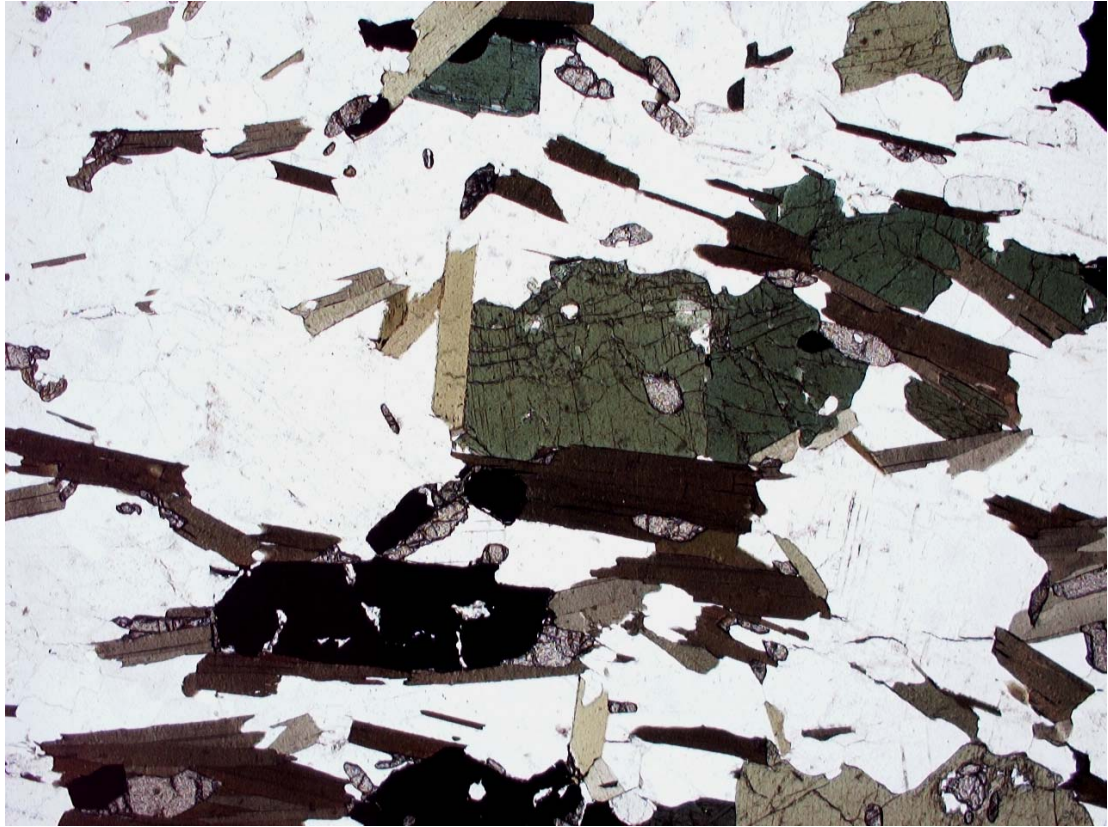
Mineralogy: major – plagioclase, biotite, amphibole, quartz, K-feldspar

minor – opaque minerals, titanite, allanite, apatite

alteration – chlorite, sericite, clay minerals, clinozoisite/epidote

Thin Section Registered Number: N3716

Description: This thin section is of a medium- to coarse-grained, inequigranular, anhedral granular, well foliated biotite-amphibolite. A well-developed homogenous tectonic foliation is defined by shape-aligned biotite and subordinate amphibole. The remainder of this high-grade (?upper amphibolite facies) metamorphic rock is composed of plagioclase and minor quartz. Apatite and titanite are common accessory phases and are both spatially related to, and may be included within biotite and amphibole. Titanite forms anhedral, rounded, irregular to weakly lozenge-shaped crystals which may be aligned parallel to the biotite fabric. Rare allanite crystals enclosed within a rim of later clinozoisite/epidote have also been recorded.



Photomicrographs of 57-09/537 (N3716) in plane and crossed polarised light. FOV = 2 mm.

Location: 57-09/537 DR

Rock: Interbanded amphibolite and quartzofeldspathic gneiss/ TTG

Mineralogy: amphibolite: major – plagioclase, biotite, amphibole, quartz, K-feldspar

minor – opaque minerals, titanite, allanite, apatite

alteration – chlorite, sericite, clay minerals, clinozoisite/epidote, carbonate

quartzofeldspathic gneiss: major – plagioclase, quartz, K-feldspar, biotite

minor – opaque minerals, titanite, amphibole, apatite, clinozoisite/epidote

alteration – chlorite, sericite, clay minerals,

Thin Section Registered Number: N3717

Description: This thin section is of a interbanded medium- to coarse-grained biotite-amphibolite and quartzofeldspathic gneiss (comparable to 57-09/535). The boundary between these two lithologies is sharp and marked by the disappearance of biotite and amphibole, and increase in modal K-feldspar.

The biotite-amphibolite possesses a well-developed, homogenous tectonic foliation which is defined by shape-aligned biotite and, to a lesser extent, amphibole crystals. This tectonic foliation occurs parallel to the compositional banding. The remainder of this high-grade metamorphic rock (upper amphibolite facies) is composed of plagioclase with minor amounts of K-feldspar and quartz. Titanite and apatite are common accessory phases with the latter locally forming larger rounded crystals up to 0.4 mm in diameter. Titanite forms anhedral, fractured weakly lozenge shaped crystals which are shape aligned parallel to the biotite fabric. Large (up to 1.7 mm in length), anhedral to weakly subhedral opaque crystals are shape aligned parallel to the biotite fabric.

The adjacent quartzofeldspathic gneiss is a medium- to coarse-grained, anhedral granular rock. The protolith of this high-grade metamorphic rock is uncertain and may have been either a granitic igneous rock or feldspathic sandstone. This gneiss is

mainly composed of an anhedral assemblage of plagioclase, K-feldspar and quartz. Plagioclase is antiperthitic and may contain coarse lamellae of microcline. K-feldspar is weakly perthitic and possesses a shadowy extinction. K-feldspar appears to be coarser grained and slightly more abundant adjacent to the boundary with the biotite-amphibolite band. Traces of epidote are present. Quartz forms anhedral strained crystals with a variably developed undulose extinction. However, quartz was also noted forming rounded, unstrained crystals (?recrystallised). Minor biotite present within this quartzofeldspathic gneiss is shape aligned and defines a weakly developed foliation, parallel to the compositional banding and fabric present within the adjacent biotite-amphibolite.

Location: 56-08/920 DR

Rock: Dioritic gneiss.

Mineralogy: major – plagioclase, quartz, biotite, amphibole

minor – clinozoisite/epidote, opaque minerals, titanite, K-feldspar, apatite

alteration – sericite, clay minerals, carbonate

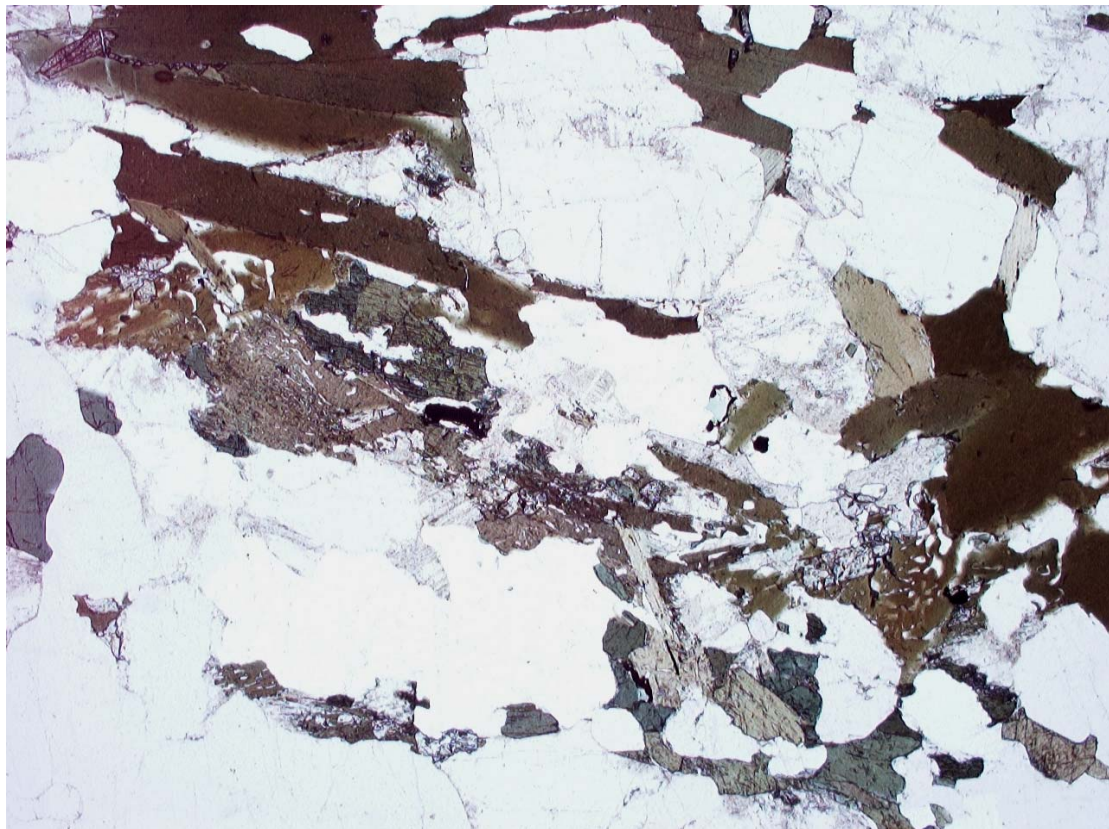
Thin Section Registered Number: N3704

Description: This thin section is of a banded, weakly foliated, medium- to coarse-grained, inequigranular, anhedral granular amphibole and biotite-bearing quartzofeldspathic gneiss. The bulk of this high-grade (?upper amphibolite facies) metamorphic rock is composed of anhedral plagioclase and subordinate quartz. The compositional banding is defined by the variation in modal biotite and amphibole. A tectonic foliation which occurs parallel to the compositional banding is defined by the alignment of biotite and, to a lesser extent, amphibole.

Plagioclase forms twinned and untwinned, anhedral crystals (≤ 4.5 mm in length, typically 1.0 to 2.0 mm in size) which exhibit a slight dusty appearance in plane polarised light due to minor alteration to sericite, clay minerals and trace carbonate. Plagioclase may locally contain rounded inclusions of quartz. Although typically unstrained, plagioclase may locally possess an undulose extinction and may locally be enclosed within a rim of untwinned albite or K-feldspar. Quartz is slightly finer

grained than plagioclase and forms anhedral crystals which possess a well developed undulose extinction, sub-grain textures and/or deformation bands. Occasional, large (5.0 to 6.0 mm in size) intergranular poikiloblastic or poikilitic quartz crystals containing inclusions of finer grained plagioclase have also been noted.

Biotite forms anhedral flakes which may contain inclusions of apatite and titanite. Biotite occurs as clusters of several crystals as well as single, isolated flakes. Worm-like or symplectitic inclusions of quartz were also noted within biotite. Green to blue-green amphibole forms anhedral crystals which are spatially related to and may partially enclose finer grained biotite. Minor secondary epidote and anhedral titanite crystals are both associated with the ferromagnesian minerals.



Photomicrograph of 56-08/920 in plane polarised light. FOV = 2 mm.

Location: 56-08/921 DR

Rock: Granitic gneiss.

Mineralogy: major – plagioclase, quartz, biotite, K-feldspar

minor – amphibole, opaque minerals, apatite

alteration – sericite, clay minerals

Thin Section Registered Number: N3705

Description: This thin section is of a medium- to coarse-grained, inequigranular, anhedral granular, banded, weakly foliated, amphibole and biotite bearing quartzofeldspathic gneiss. A compositional banding present within this high-grade (?upper amphibolite facies) metamorphic rock is defined by the variation in modal biotite and amphibole. Both ferromagnesian minerals are minor components within this gneiss. A weakly developed tectonic foliation is parallel to this compositional banding and defined by shape-aligned biotite flakes. Amphibole is an accessory phase and is restricted to one band within this gneissose rock.

The bulk of the rock is mainly composed of plagioclase and quartz with K-feldspar typically being more common within the biotite-bearing bands. Intracrystalline deformation within plagioclase resulted in the variable development of an undulose to sweeping extinction. Plagioclase may locally contain rounded inclusions of quartz. Traces of myrmekite were noted forming rims upon plagioclase. Quartz is strained with an undulose extinction and variably developed deformation bands and sub-grain textures. It is slightly coarser grained than plagioclase and forms anhedral crystals which are weakly elongate parallel to the compositional banding and tectonic foliation. K-feldspar is weakly perthitic and is locally being replaced by myrmekite.

Location: 56-08/921 DR

Rock: Granitic gneiss.

Mineralogy: major – plagioclase, quartz, K-feldspar, biotite

minor – opaque minerals, muscovite, clinozoisite, zircon

alteration – sericite, clay minerals, carbonate, chlorite, opaque oxides,
prehnite

Thin Section Registered Number: N3706

Description: This thin section is of a coarse-grained, anhedral granular, inequigranular, weakly foliated, possibly granitic, quartzofeldspathic gneiss. The rock is mainly composed of anhedral plagioclase, quartz and K-feldspar with minor amounts of biotite. A weakly developed foliation is defined by lenticular to wispy looking aggregates of biotite. Biotite is yellow-brown to red-brown in colour and exhibits minor alteration to possible prehnite along the basal (001) cleavage. Biotite within the aggregates are variably shape aligned parallel to the foliation. Biotite may locally contain inclusions of zircon and possible allanite enclosed within dark pleochroic haloes.

The bulk of the rock is composed of feldspar and quartz. Plagioclase is the dominant feldspar and it may locally exhibit minor alteration to sericite, clay minerals and carbonate. Plagioclase may locally possess moderately developed or preserved crystal faces suggesting that the protolith of this gneiss was a granitic igneous rock.

Plagioclase is locally rimmed by a clear rim of K-feldspar or albite. Myrmekite was also noted forming poorly developed rims upon plagioclase along plagioclase-K-feldspar grain contacts. The myrmekite appears to be replacing the adjacent K-feldspar. Plagioclase within this intergrowth is typically in optical continuity with the host feldspar crystal.

Quartz is coarser grained and apparently intergranular to plagioclase. It forms anhedral crystals up to *c.* 6.0 to 7.0 mm in length which are shape aligned parallel to the biotite fabric. Intracrystalline deformation within quartz resulted in the development of an undulose extinction, deformation bands and sub-grain textures.

Location: 56-09/924 DR

Rock: Protomylonitic Quartz monazite.

Mineralogy: major – K-feldspar, quartz, plagioclase, amphibole (1), amphibole (2),
biotite

minor – opaque minerals, titanite, allanite, apatite

alteration – carbonate, clinozoisite

Thin Section Registered Number: N3707

Description: This thin section is of a medium- to coarse-grained, highly deformed, banded, protomylonitic monzonitic/granitic rock. The rock is mainly composed of K-feldspar, plagioclase and quartz. A compositional banding is defined or preserved by the occurrence of amphibole and biotite. Accessory titanite and apatite are spatially related to the occurrence of these ferromagnesian minerals. The amphibole-bearing bands are finer grained than the remaining feldspathic part of this K-feldspar-rich rock. An early formed foliation which is defined by chains of amphibole and biotite, has been reactivated during a later phase of ductile deformation which resulted in mylonitisation of this broadly granitic rock. A weakly developed S-C or extensional crenulation cleavage (ECC) is defined by anastomosing bands of dynamically recrystallised quartz, feldspar and biotite. These anastomosing fabric also yield a sinistral sense of shear.

Two textural varieties of amphibole are present within this protomylonitic rock: (1) early brown-green amphibole; and (2) a later, green to blue green amphibole which appears to replacing and formed at the expense of type 1. The brown-green amphibole was noted forming anhedral lozenge-shaped crystals which are enclosed within or overgrown by beards or tails of biotite. In contrast to quartz and feldspar, amphibole has undergone more brittle/cataclastic deformation during mylonitisation. Both textural varieties of amphibole have undergone fracturing and disaggregation, with larger crystals locally being broken up into individual cleavage rhombs. Titanite is spatially related to amphibole and clearly overgrows the mylonitic foliation.

K-feldspar is fresh and possesses a distinctive shadowy extinction and diffuse microcline twins. K-feldspar is also perthitic and forms rounded to elliptical porphyroclasts which range up to 4.0 mm in length. These porphyroclasts possess

irregular serrated grain boundaries due to dynamic recrystallisation and new grain growth being focused along the grain margins. Quartz is strained with a well developed undulose extinction, deformation bands and sub-grain textures. The feldspar porphyroclasts are wrapped by a moderately well developed mylonitic foliation. This fabric is defined by narrow bands or zones of very fine-grained to cryptocrystalline, dynamically recrystallised quartz and feldspar. Relict, eye-shaped quartz and feldspar crystals are wrapped by and variably aligned parallel to this mylonitic foliation. Dynamic recrystallisation has also effected biotite to forms elongate needle-like crystals and very fine-grained irregular to ragged-looking flakes. The rock is also deformed by several narrow shear bands which occur oblique to the mainly mylonitic foliation. These shear bands are characterised by narrow zones of intense grain reduction and yield an apparent sinistral (top to left) sense of shear in this plane of section.

Location: 132/15-1.

Rock: Cataclasite.

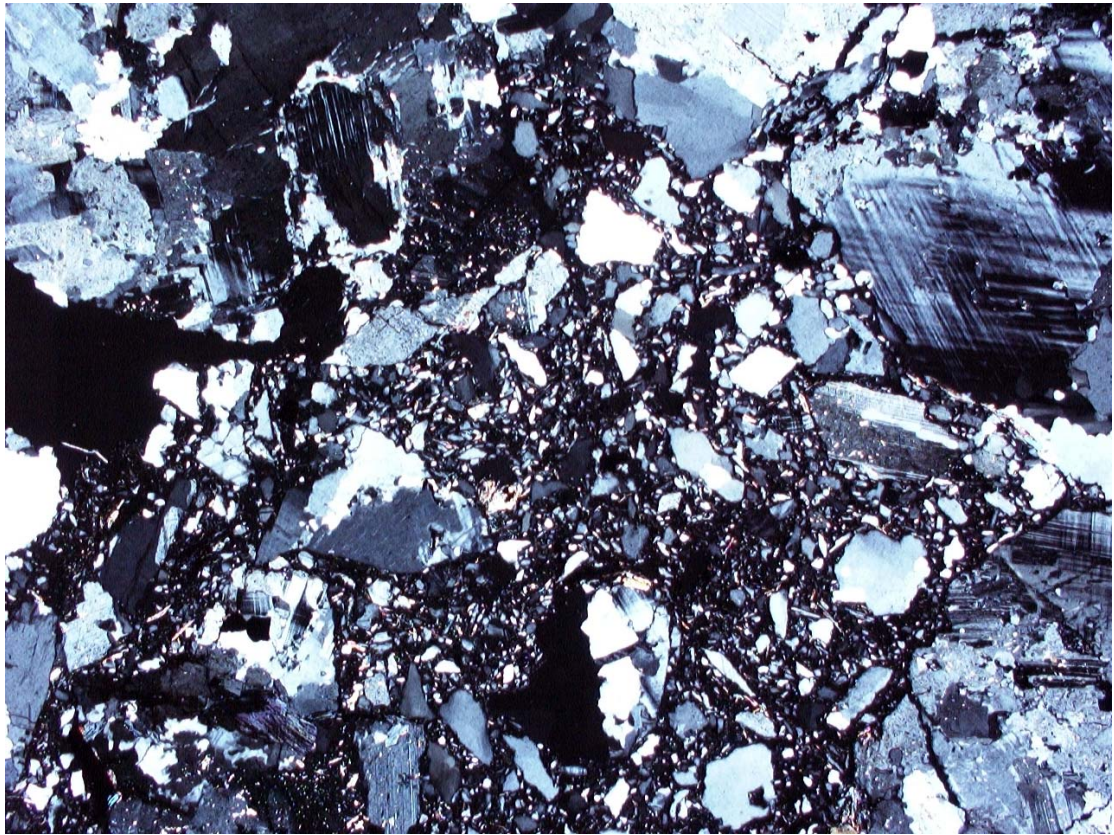
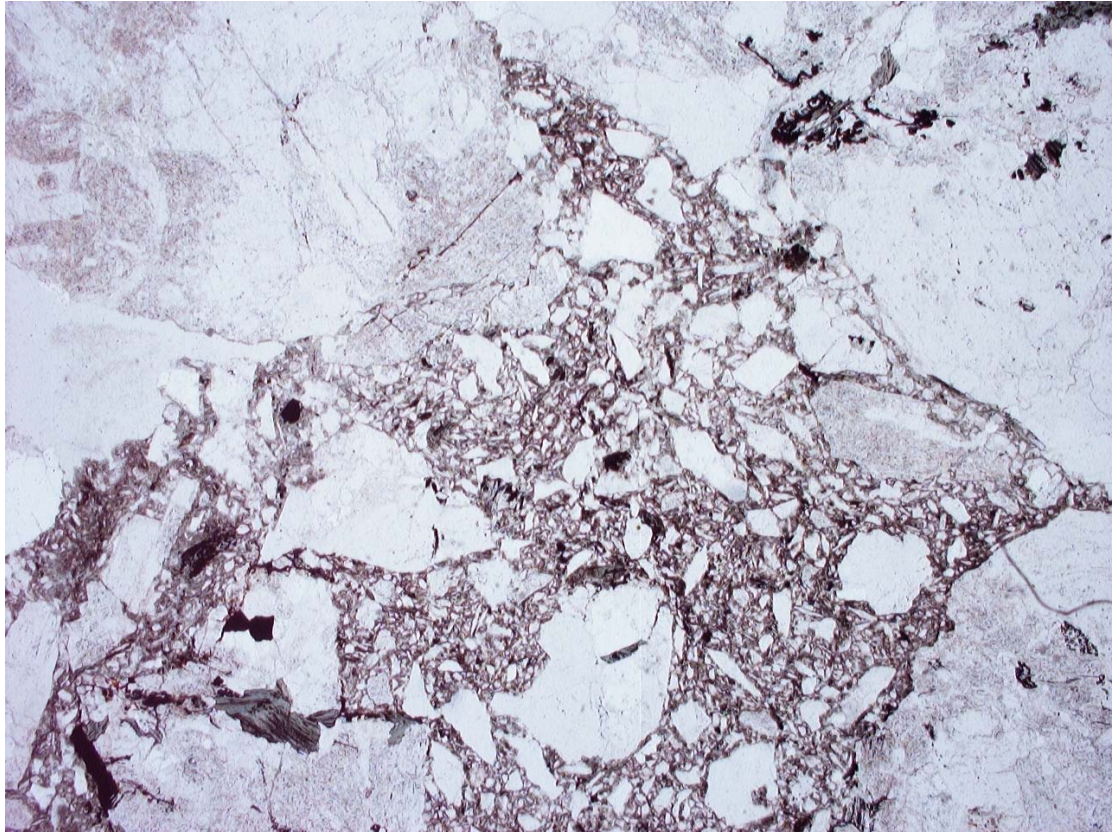
Mineralogy: major – quartz, plagioclase, K-feldspar (microcline)

accessory – muscovite, biotite, apatite

alteration – chlorite, opaque oxides

Thin Section Registered Number: N4163

Description: This is a thin section of an altered, originally amphibole-bearing, two-mica granite which is cut by a network of cataclastic fractures. In hand specimen one surface is covered by large spars of calcite up to 1cm in diameter. K-Feldspar or microcline and quartz dominate the mineralogy of this rock. Plagioclase is also common and is altered to white mica and chlorite. Quartz has been dynamically recrystallised or is fine grained and often has irregular grain boundaries. The cataclastic fracture contain granitic material from the host rock. Some clasts are highly angular and ~4 mm in size, whereas the majority are less than 50 microns. The angular nature of the clasts suggests brittle deformation.



Photomicrograph of 132/15-1 in plane and crossed polarised light. FOV = 2 mm.

Location: 56-09/384 DR

Rock: Amphibolite gneiss

Mineralogy: major –biotite, amphibole, plagioclase, quartz, epidote

minor – opaque minerals, titanite, apatite, zircon

alteration –sericite, clay minerals

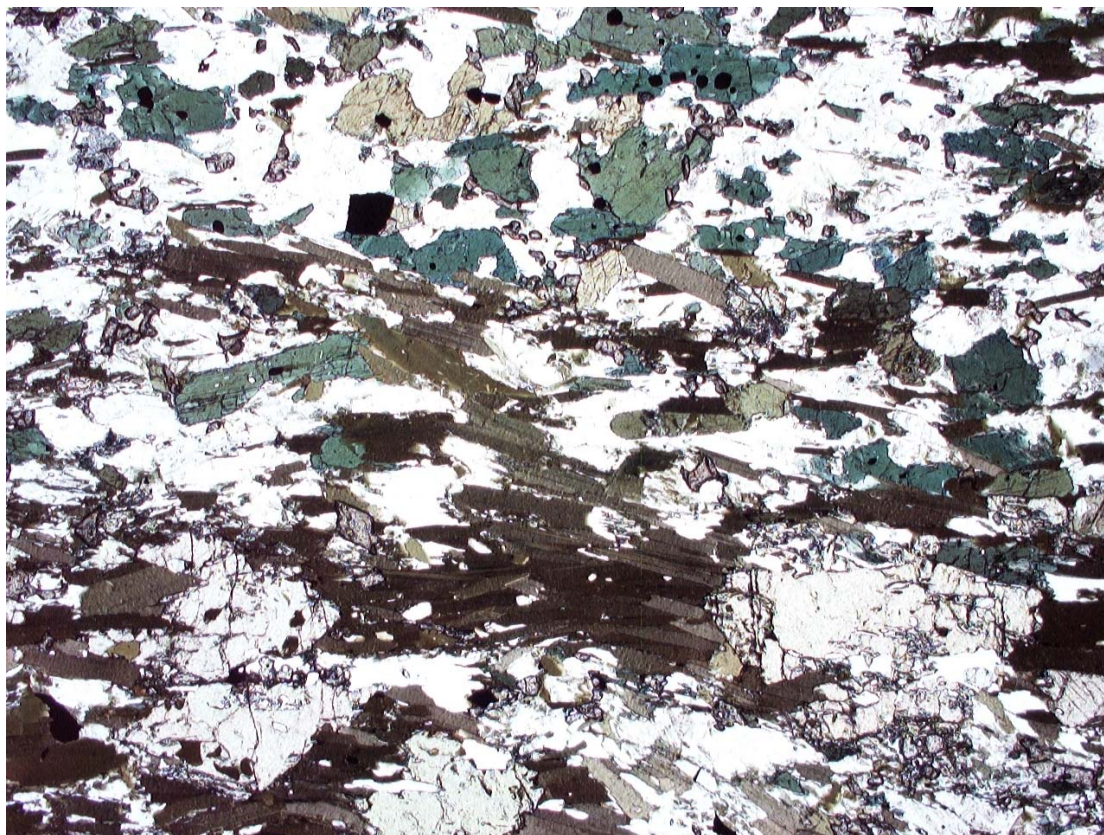
Thin Section Registered Number: N3708

Description: This thin section is of a medium-grained, foliated, inequigranular, epidote-bearing, schistose biotite-amphibolite. A well developed domainal schistosity is defined by alternating biotite-rich and amphibole-bearing domains. The biotite-rich lithons are slightly coarser grained and composed of anhedral to ragged-looking, shape-aligned biotite flakes with subordinate plagioclase and minor quartz. The foliation within the biotite-rich domains is overgrown by post-kinematic, anhedral epidote porphyroblasts. Nucleation and growth of epidote clearly post-dated the imposition of the schistosity. Epidote is weakly pleochroic and ranges from pale yellow to colourless.

The adjacent amphibole domains are composed of amphibole, plagioclase, biotite, quartz and epidote. Small anhedral titanite crystals (accessory phase) are common within these amphibole-rich domains, with titanite also locally forming irregular rims upon opaque minerals. Elongate amphibole crystals may be shape aligned parallel to the biotite fabric. Biotite within the amphibole domains is finer grained than that in the adjacent biotite lithons. Biotite within these more feldspathic domains is shape aligned parallel to the main foliation. A second, weakly developed anastomosing foliation, also defined by biotite, is preserved within the amphibole domains. This asymmetrical foliation yields a possible dextral (top to right) sense of shear in this plane of section.

The remainder of the rock is composed of anhedral to ragged-looking plagioclase with fine-grained intergranular biotite and amphibole. Minor to accessory quartz is strained with a variably developed undulose extinction. Both plagioclase and amphibole are locally being replaced by epidote. Recrystallisation associated with epidote growth appears to have resulted in the ragged appearance of many of the biotite flakes.

Possible zircon inclusions, with associated pleochroic haloes, have been recorded within biotite.



Photomicrograph of 56-09/384 in plane polarised light. FOV = 2 mm.

Location: 56-09/386 DR

Rock: Protomylonite.

Mineralogy: major – plagioclase, quartz, K-feldspar, biotite

minor – amphibole, opaque minerals, titanite, epidote, apatite, zircon

alteration – chlorite

Thin Section Registered Number: N3709

Description: This thin section is of a highly deformed, very coarse-grained, inequigranular, amphibole-bearing, protomylonitic granodioritic to monzodioritic rock. The protolith was a very coarse-grained feldspar porphyritic granitic rock with megacrysts of both plagioclase and K-feldspar. Ductile deformation resulting in

mylonitisation was partitioned into the groundmass and resulted in dynamic recrystallisation of this highly deformed igneous/meta-igneous rock.

Quartz forms large, 4.0 to 5.0 mm long, relict crystals which possess a well developed undulose extinction and deformation bands, with sub-grains and new grains being concentrated along increasingly serrated grain boundaries. These large porphyroclasts are also cut by bands of quartz new grains. Plagioclase and K-feldspar were more resistant to deformation with intracrystalline deformation largely being restricted to the development of an undulose extinction. Plagioclase forms twinned, anhedral to occasionally subhedral porphyroclasts. K-feldspar shows a higher degree of deformation and forms irregular crystals which possess a well developed shadowy extinction and irregular to serrated grain boundaries; the latter are surrounded by a mosaic of unstrained new grains. K-feldspar is locally perthitic and possesses coarse microcline twins. Poorly developed quartz pressure shadows have been noted developed upon some feldspar porphyroclasts.

The mylonitic fabric is defined by narrow, wispy zones of intense dynamic recrystallisation which are composed of very fine-grained to cryptocrystalline quartz, feldspar and granular biotite. This mylonitic fabric is locally overgrown by late, post-kinematic epidote, opaque minerals and titanite. Titanite forms anhedral crystals and was also noted forming irregular rims upon opaque minerals. Epidote is typically associated with the breakdown of biotite. Annealing of the mylonitic fabric, probably accompanying epidote growth, has resulted in a slight increase in the grain size. The very fine grained high strain zones which define the mylonitic fabric may, therefore, represent the later stages of deformation.

The matrix of this protomylonitic rock is composed of fine-grained (≤ 0.3 mm in size), variably strained quartz and feldspar. Plagioclase within the matrix may contain rounded to bleb-like inclusions of quartz resulting in a crude myrmekitic intergrowth. K-feldspar is locally being replaced by irregular patches of coarse myrmekitic intergrowth. These patches are composed of single plagioclase crystals which contain wormy to bleb-like quartz inclusions. Lenticular aggregates or clusters of biotite are variably deformed by the mylonitic foliation to form wispy-looking foliae. Biotite is green-brown in colour and forms anhedral plates and flakes which range up to 1.4 mm in length. Accessory titanite is spatially related to biotite. Blue-green amphibole is an accessory phase and is partially replaced by biotite.

Location: 56-09/388 DR

Rock: Quartzofeldspathic gneiss

Mineralogy: major – plagioclase, quartz, amphibole, biotite, K-feldspar

minor – opaque minerals, titanite, allanite, apatite, zircon

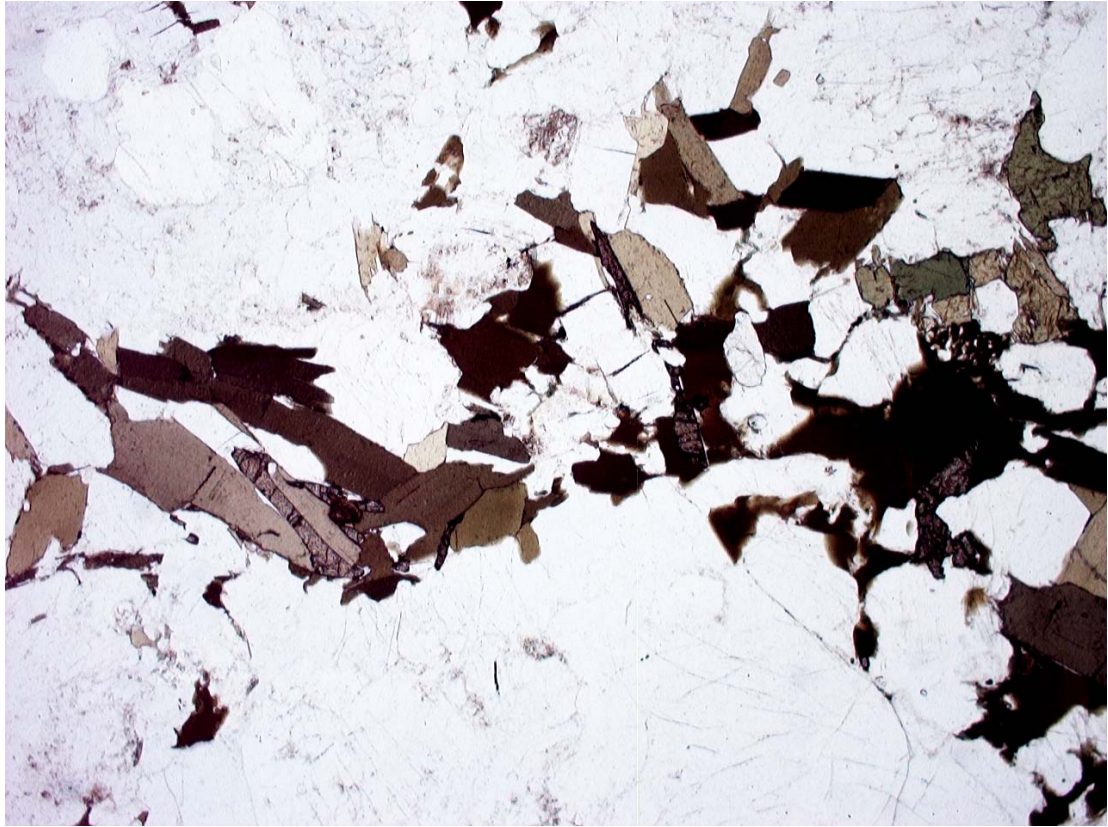
alteration –sericite, clay minerals, carbonate

Thin Section Registered Number: N3710

Description: This thin section is of a medium- to coarse-grained, inequigranular, anhedral granular, massive, amphibole-bearing quartzofeldspathic gneiss. The protolith to this broadly dioritic in composition gneissose metamorphic rock is uncertain. This high-grade metamorphic rock is mainly composed of anhedral plagioclase and quartz. Plagioclase may locally contain small rounded inclusions of quartz. Rare, crudely lath-shaped crystals of plagioclase are also present suggesting that this rock may have originally been igneous in origin (speculative). Quartz is strained and possesses a variably developed undulose extinction, deformation bands and sub-grain textures. Quartz locally forms elongate crystals which range up to 3.0 to 3.5 mm in size and may define a crude foliation or banding.

Amphibole and biotite are patchily distributed within this gneiss with the central area of the thin section being more granitic in composition. Amphibole forms clusters or chains of anhedral crystals and is spatially related to biotite. Biotite forms finer grained, anhedral to ragged looking flakes. Rare rounded to worm-like inclusions of quartz and/or feldspar have been noted within biotite resulting in a crude symplectitic intergrowth. Rounded, anhedral apatite is a common accessory phase and typically occurs associated with amphibole. Traces of secondary carbonate have been recorded associated with, or enclosed within biotite.

K-feldspar is patchily distributed and occurs associated with irregular patches of coarse- to fine-grained myrmekite and/or micrographic intergrowth. K-feldspar forms anhedral crystals which possess a shadowy extinction and coarse to diffuse microcline twins. Myrmekite forms irregular rims upon plagioclase which replace the adjacent K-feldspar. Feldspar within the myrmekite intergrowth is in optical continuity with the host plagioclase. It is possible that K-feldspar and myrmekite may be related to very localised partial melting.



Photomicrograph of 56-09/388 in plane and crossed polarised light. FOV = 2 mm.

Location: 56-15/18 DR

Rock: Tonalitic gneiss

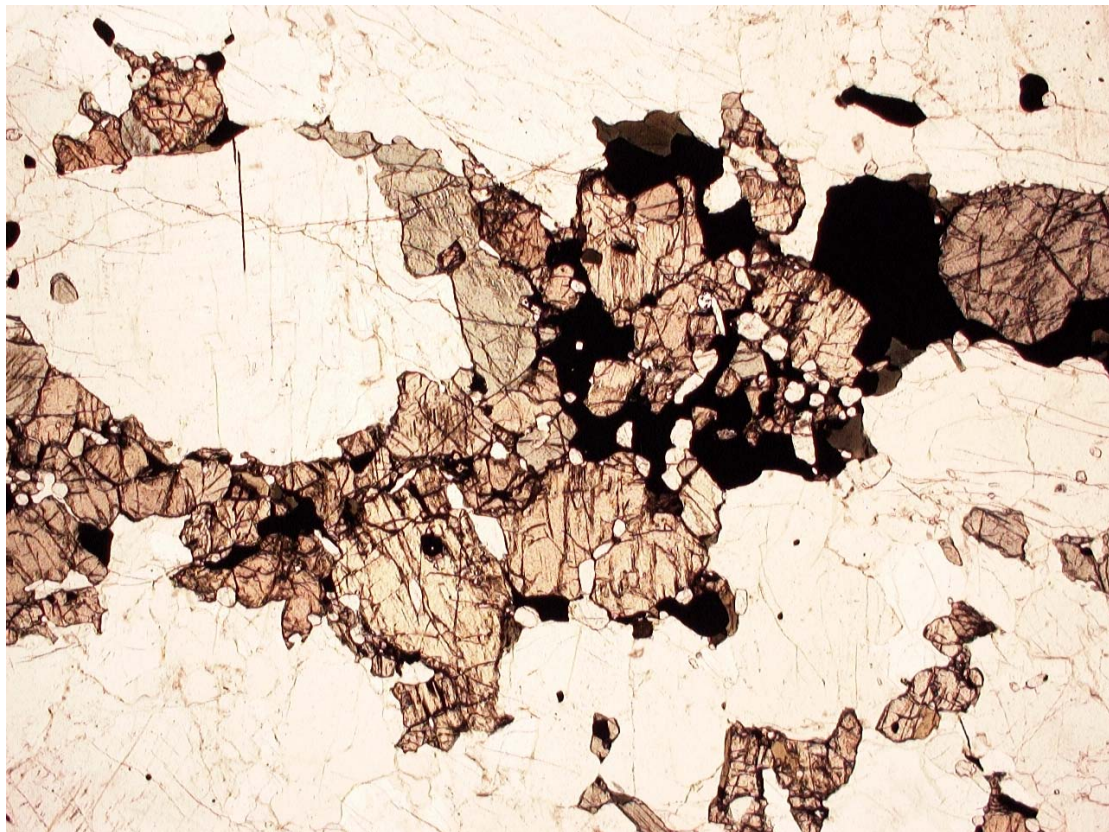
Mineralogy: major – plagioclase, quartz, clinopyroxene, orthopyroxene, K-feldspar, hornblende

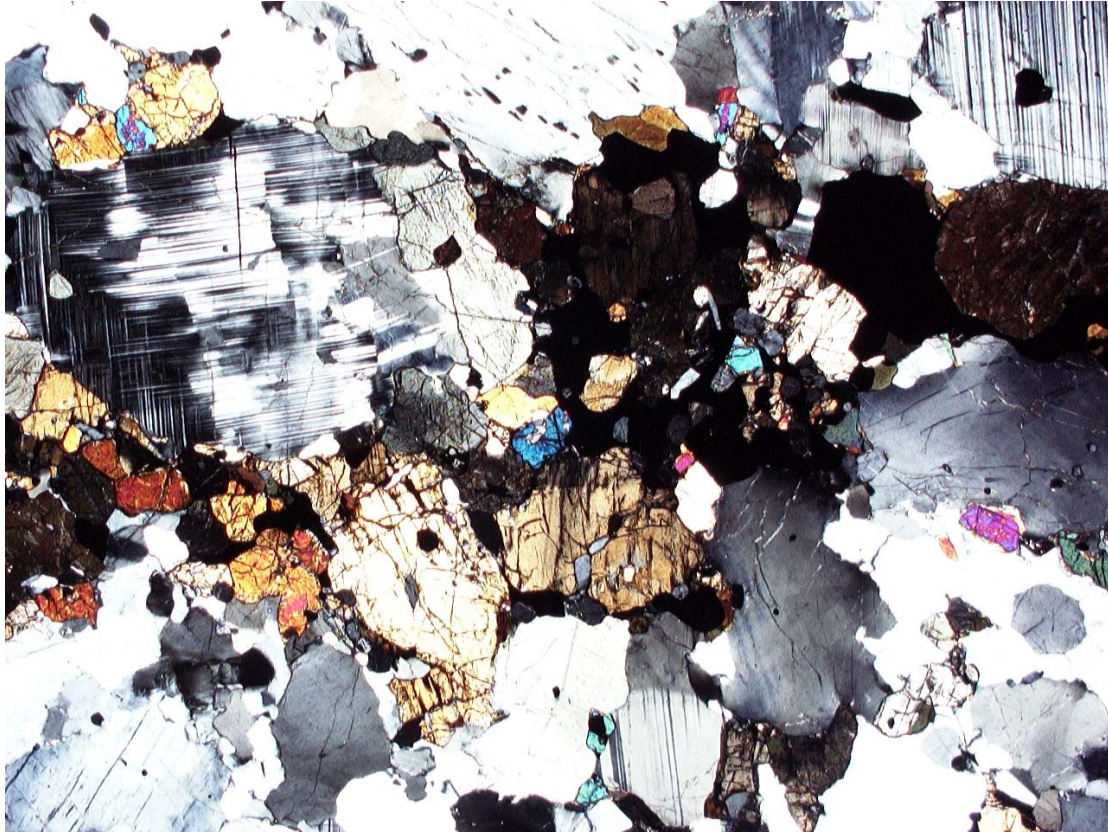
minor – opaque minerals, apatite, rutile, biotite, zircon

alteration – sericite, clay minerals

Thin Section Registered Number: N3711

Description: This thin section is of a medium- to coarse-grained, inequigranular, anhedral granoblastic, hornblende-bearing, two-pyroxene tonalitic gneiss. The presence of both clinopyroxene and orthopyroxene within the mineral assemblage of this gneiss indicates that it has undergone granulite facies metamorphism. A weak compositional banding or gneissose foliation is defined by elongate stringers or aggregates of pyroxene, opaque minerals and hornblende. The bulk of this high-grade metamorphic rock is composed of anhedral plagioclase with minor quartz and K-feldspar.





Photomicrographs of 56-15/18 (N3711) in plane and crossed polarised light. FOV = 2 mm.

Location: 56-15/18 DR

Rock: Tonalitic gneiss

Mineralogy: major – plagioclase, quartz, orthopyroxene, clinopyroxene, amphibole, K-feldspar

minor – opaque minerals, apatite, biotite

alteration – sericite, white mica

Thin Section Registered Number: N3712

Description: This thin section is of a coarse-grained, inequigranular, weakly foliated, hornblende-bearing, two-pyroxene tonalitic gneiss. The foliation within this high-grade (granulite facies) metamorphic rock is defined by stringers or chains of granular pyroxene and associated hornblende. The bulk of the rock is composed of plagioclase and quartz. Plagioclase may locally exhibit a weak preferred shape alignment parallel

to the gneissose foliation. Quartz is strained with an undulose extinction and variably developed sub-grain textures and deformation bands.

Orthopyroxene is the dominant ferromagnesian mineral and is distinguished from clinopyroxene by its straight extinction. Hornblende is associated with pyroxene, forming a granular looking rim around both orthopyroxene and clinopyroxene.

Apatite and opaque minerals are common accessory phases. Minor to trace amounts of weakly perthitic K-feldspar have also been recorded.

Location: 57-14/58 DR

Rock: Metagabbro

Mineralogy: major – plagioclase, clinopyroxene

minor – opaque minerals, apatite, amphibole, biotite

alteration – epidote, clinozoisite, carbonate, quartz, chlorite, sericite,

opaque oxides, clay minerals, titanite, leucoxene

Thin Section Registered Number: N3719

Description: This thin section is of a coarse- to very coarse-grained (average grain size 2.0 to 3.0 mm), inequigranular, anhedral granular, weakly foliated to massive, holocrystalline gabbro. The rock is mainly composed of anhedral to very weakly subhedral, elongate to lath-shaped plagioclase crystals (1.0 to 2.5 mm in length). Plagioclase forms a relatively dense crystal framework of locally shape-aligned crystals which are linked by later irregular feldspar (also plagioclase) overgrowths. It is twinned and forms simply zoned crystals which are variably replaced by anhedral to skeletal, poikiloblastic epidote (\pm carbonate, white mica and chlorite). Plagioclase may also exhibit minor alteration to sericitic white mica and/or clay minerals. The interstitial areas to this primocryst framework are mainly filled by coarse-grained, anhedral, pale brown clinopyroxene. Pyroxene is sub-ophitic and forms elongate crystals which range up to 6.0 mm in length.

Location: 57-15/15 DR

Rock: Trachyandesite

Mineralogy: major – feldspar, amphibole

minor – opaque minerals, apatite

alteration – opaque oxides, zeolite

Thin Section Registered Number: N3749

Description: This thin section is of a very fine-grained, pilotaxitic, feldspathic, anhedral granular, hypocrySTALLine to holocrystalline, inequigranular, aphyric trachyandesitic rock. This rock is mainly composed of closely packed variably shape aligned, anhedral plagioclase laths with the remaining interstitial to intersertal spaces filled by feldspar and zeolite. The zeolite is dusty yellow in colour and forms fine, fibrous crystals. Amphibole forms anhedral, granular crystals which are fractured and may locally possess a weakly pleochroism. Opaque minerals present are enclosed within a haloe of hematitic stain.

3 Major and trace element geochemistry

Major element chemical compositions of the borehole samples show a significant variation, reflecting the range of lithologies noted during petrographic examination (Tables 3.1-3.4). With respect to general chemical classification of the samples, the normative Ab-An-Or diagram after O'Connor (1965), with field boundaries by Barker (1979), may be used with a degree of caution for metamorphic rocks to provide an indication of the original magma type. Figure 3.1 shows the range in composition from tonalite to granite varieties although most samples cluster in the TTG (tonalite-trondhjemite- granodiorite) fields. However there is a wider range of SiO₂ compositions than observed in Lewisian gneisses from northwest Scotland (Rollinson, 1996). Only 206/8-2, 206/8-7, 206/7-A2 (2599 m), 205/16-1, 88/02 and 90/14 would strictly conform with the definition of TTG proposed by Defant and Drummond (1990) namely Al₂O₃ contents >15% at 70% SiO₂, Sr >300 ppm, Y < 20 ppm, Yb < 1.8 ppm and Nb ≤ 10 ppm.

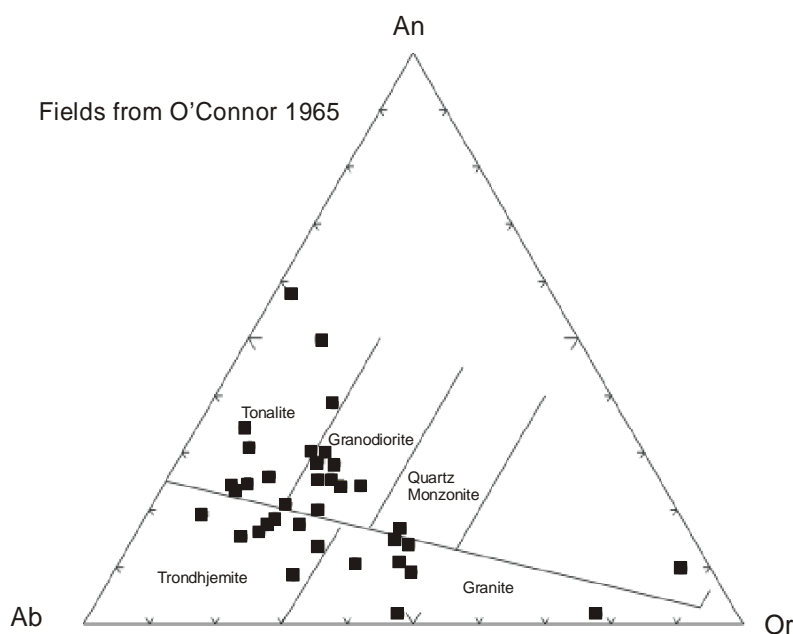


Figure 3.1. An-Ab-Or diagram with field boundaries after Barker (1979).

Table 3.1 Major element concentrations in wt% by XRF

Sample name	SiO ₂	TiO ₂	Al ₂ O ₃	Fe ₂ O _{3t}	Mn ₃ O ₄	MgO	CaO	Na ₂ O	K ₂ O	P ₂ O ₅
220/26-1	59.8	0.56	15.6	7.36	0.09	4.18	2.13	3.64	2.28	0.13
209/9-1	67.9	0.50	14.5	3.60	0.04	0.93	2.53	3.28	4.55	0.16
209/12-1 11520 - 6ft	67.5	0.64	15.2	3.90	0.05	1.34	1.69	2.66	3.93	0.12
81-17 137.6 - 138.2	49.5	0.75	7.4	9.16	0.18	15.96	12.61	1.18	0.51	0.03
208/27-2 4528-4528.75 ft	62.9	0.92	12.3	6.48	0.11	0.68	2.31	2.53	3.39	0.61
206/8-2 1864.3-1864.55m	68.9	0.27	13.7	3.34	0.03	0.71	4.18	5.04	0.89	0.09
206/8-8 2498.6-2498.95m	68.0	0.26	14.3	4.56	0.08	1.39	2.62	4.71	2.16	0.14
206/8-1A 2310.75 - 2310.95m	57.7	1.08	16.8	6.81	0.06	2.32	4.27	3.92	2.97	0.50
206/8-7 2320.5m	71.4	0.33	12.3	3.92	0.03	0.97	3.43	3.92	0.97	0.17
206/7-A2 2142.8-2143m	50.1	1.44	17.5	10.4	0.15	3.09	6.18	3.98	2.69	0.59
206/7-A2 2544.65-2544.85m	58.0	0.92	16.4	8.30	0.14	2.36	4.23	4.64	1.84	0.40
206/7-A2 2599.2-2599.4m	70.5	0.36	13.7	2.60	0.02	0.65	1.53	3.16	4.39	0.14
205/16-1 4172-4172.15m	70.9	0.59	14.1	3.89	0.02	1.41	0.75	0.13	3.77	0.18
205/22-1 3225.45 - 3275.60m	59.6	0.74	17.8	6.93	0.04	1.11	0.65	1.53	8.36	0.31
204/23-1 3846.90 - 3847.05m	50.8	1.27	23.4	10.3	0.14	4.85	2.23	3.98	1.93	0.04
204/25-1 9416 ft	62.0	0.50	16.1	4.59	0.06	1.84	3.90	5.15	1.37	0.23
202/3-1	71.2	0.21	15.3	1.63	0.02	0.51	2.14	5.06	1.84	0.07
202/2-1 4002 feet	60.8	0.90	17.3	7.55	0.08	3.54	2.98	3.23	2.19	0.10
88/02	68.5	0.38	15.4	2.80	0.04	1.42	2.98	4.36	2.28	0.13
164/25-2 2727.65-2727.8m	47.9	1.72	12.8	15.8	0.26	7.84	11.55	1.94	0.20	0.11
154/3-1 8060.0-8060.2	48.4	1.56	13.1	15.6	0.27	5.42	9.45	2.46	1.63	0.19
58-08/228DR 19 - 49cm	73.3	0.02	15.3	0.31	<0.01	0.09	2.25	5.00	2.16	0.01
58-08/230DR 0.62 - 0.86m	61.8	0.32	19.0	2.22	0.09	0.28	2.45	6.78	4.45	0.05
90/14 87.82m	69.1	0.34	15.9	2.91	0.03	0.87	3.38	4.57	1.39	0.10
57-09/537 (JD10) 0-2.90m TD	50.9	1.85	14.1	14.3	0.18	3.51	5.82	3.17	3.15	0.86
57-09/536 (JD10) 0-0.50m TD	54.0	1.54	15.1	10.5	0.15	3.38	5.88	3.61	3.02	1.09
56-08/920DR 51 - 67cm	60.6	0.55	14.3	7.90	0.17	4.06	6.42	3.92	0.98	0.05
56-08/921 (JD6) 0-0.78m TD	71.0	0.26	14.9	2.11	0.02	0.69	1.97	4.31	3.30	0.10
56-08/924 (JD4) 0.75-0.85m TD	63.7	0.70	15.6	4.82	0.06	1.02	2.62	4.60	4.68	0.22
132/15-1 4155.55-4155.7m	72.7	0.20	13.3	2.07	0.03	0.72	0.32	3.66	5.08	0.06
56-09/384DR 44 - 64cm	47.3	2.13	15.9	13.4	0.22	5.12	7.29	3.88	2.40	0.57
56-09/386 (JD1) 0.88-1.01m	70.7	0.38	13.8	2.80	0.05	0.48	1.45	3.51	5.27	0.13
56-09/388DR 0.18 - 21m	65.1	0.32	16.3	3.74	0.08	1.36	3.52	4.48	3.21	0.18
56-15/18DR 1.65 - 1.7m	56.3	1.16	18.7	7.76	0.14	1.47	5.56	4.24	3.26	0.45
56-15/18DR 3.02 - 3.36m	55.0	1.34	18.3	9.09	0.17	1.71	6.01	4.31	2.53	0.55
57-14/58 43 - 78	46.8	4.47	15.7	12.4	0.22	3.80	9.06	4.15	0.78	0.36
57-15/15 DR 19-24cm	58.3	0.61	16.8	8.17	0.19	0.94	2.31	6.08	4.19	0.19

Table 3.2 Trace element concentrations in ppm by XRF

Sample name	Sc	V	Cr	Co	Ni	Cu	Zn	Ga	Rb	Sr	Zr	Ba	Pb
220/26-1	19	106	160	19	89	15	44	18	114	221	102	447	8
209/9-1	6	44	19	8	4	9	70	17	88	472	288	2365	14
209/12-1 11520 - 6ft	7	50	38	6	9	5	62	19	120	324	217	638	18
81-17 137.6 - 138.2	42	197	606	52	523	7	77	11	4	140	27	82	1
208/27-2 4528-4528.75 ft	7	47	25	18	17	15	90	20	43	597	103	913	16
206/8-2 1864.3-1864.55m	5	32	31	6	10	7	24	17	17	364	180	234	31
206/8-8 2498.6-2498.95m	7	29	24	7	10	13	55	21	39	279	38	506	7
206/8-1A 2310.75 - 2310.95m	6	83	32	14	18	30	126	26	39	546	403	1685	82
206/8-7 2320.5m	4	38	26	10	16	5	31	17	21	356	94	206	6
206/7-A2 2142.8-2143m	17	149	37	19	29	26	217	30	49	758	290	682	30
206/7-A2 2544.65-2544.85m	18	89	32	15	22	65	170	25	14	446	245	421	10
206/7-A2 2599.2-2599.4m	<2	24	22	6	3	23	35	16	46	325	374	3660	12
205/16-1 4172-4172.15m	10	65	74	10	48	5	67	18	74	70	172	261	5
205/22-1 3225.45 - 3275.60m	10	86	40	11	25	23	81	21	78	169	197	920	5
204/23-1 3846.90 - 3847.05m	39	293	300	38	88	99	75	25	41	422	189	630	5
204/25-1 9416 ft	10	84	21	10	13	113	53	19	4	872	72	487	5
202/3-1	<2	22	17	3	5	2	35	16	38	475	83	605	6
202/2-1 4002 feet	23	189	227	31	97	37	122	21	70	303	127	703	10
88/02	3	39	36	7	18	3	49	16	67	563	126	1011	8
164/25-2 2727.65-2727.8m	38	339	242	62	148	119	127	19	1	159	84	71	2
154/3-1 8060.0-8060.2	38	275	113	52	49	234	130	17	36	227	96	329	4
58-08/228DR 19 - 49cm	<2	2	8	<2	<1	10	9	16	69	421	11	494	20
58-08/230DR 0.62 - 0.86m	<2	40	4	<2	<1	8	52	21	40	>1500	240	2631	24
90/14 87.82m	2	30	21	7	4	22	44	20	71	463	143	350	11
57-09-537 (JD10) 0-2.90m TD	15	237	64	46	73	76	191	24	93	532	200	1109	7
57-09-536 (JD10) 0-0.50m TD	16	137	25	31	21	38	160	22	90	692	230	1128	9
56-08/920DR 51 - 67cm	24	116	195	20	76	20	120	21	21	291	86	108	10
56-08-921 (JD6) 0-0.78m TD	<2	22	11	4	3	22	35	18	70	491	110	876	11
56-08-924 (JD4) 0.75-0.85m TD	5	50	35	8	6	17	49	19	76	534	567	1004	21
132/15-1 4155.55-4155.7m	2	16	13	3	2	3	43	18	211	88	175	473	16
56-09/384DR 44 - 64cm	19	186	52	44	66	33	172	21	102	661	119	817	11
56-09-386 (JD1) 0.88-1.01m	4	21	27	4	1	5	48	18	145	187	269	769	20
56-09/388DR 0.18 - 21m	7	49	32	7	8	18	58	16	47	611	104	2030	7
56-15/18DR 1.65 - 1.7m	16	40	17	8	5	16	127	24	58	630	98	2138	15
56-15/18DR 3.02 - 3.36m	20	45	22	10	5	19	152	25	49	592	103	1523	11
57-14/58 43 - 78	34	209	28	26	3	16	92	22	17	528	172	464	3
57-15/15 DR 19-24cm	6	<2	<2	<2	<1	8	127	27	51	276	612	2229	13

Table 3.3. Trace element concentrations in mg/kg by ICP-MS

Sample name	Y	Nb	Cs	La	Ce	Pr	Nd	Sm	Eu	Tb	Gd	Dy	Ho	Er	Tm	Yb	Lu	Hf	Ta	Th	U
220/26-1	17.9	21.4	0.9	12.4	27.5	3.59	15.2	3.57	0.72	0.53	3.26	3.42	0.71	2.05	0.33	2.19	0.32	3.0	1.4	5.1	1.54
209/9-1	17.9	8.6	0.1	38.7	77.9	10.4	41.0	7.24	1.57	0.72	5.44	3.77	0.69	1.83	0.26	1.51	0.22	7.2	<0.5	6.8	0.62
209/12-1 11520 - 6ft	16.5	11.3	2.5	67.8	145	15.7	58.2	9.62	1.64	0.90	6.98	4.26	0.69	1.55	0.20	1.31	0.20	5.8	<0.5	23.8	2.50
81-17 137.6 - 138.2	12.0	1.9	0.1	4.7	16.0	2.84	15.5	4.03	1.03	0.49	3.45	2.67	0.51	1.34	0.17	1.08	0.14	1.1	0.9	0.4	0.23
208/27-2 4528-4528.75 ft	28.4	11.2	0.14	33.0	56.4	8.35	35.5	7.41	2.44	1.04	7.58	5.95	1.14	2.87	0.36	2.06	0.29	3.3	0.7	4.92	1.61
206/8-2 1864.3-1864.55m	8.6	2.5	0.31	53.2	108	11.4	38.3	4.99	1.03	0.34	3.22	1.56	0.29	0.71	0.09	0.59	0.09	5.1	<0.1	21.8	1.03
206/8-8 2498.6-2498.95m	11.9	1.9	0.19	18.3	41.0	4.91	19.8	4.14	1.18	0.54	3.79	2.96	0.55	1.40	0.18	1.03	0.15	0.7	<0.1	0.32	0.24
206/8-1A 2310.75 - 2310.95m	15.0	7.9	0.3	59.9	130	14.7	56.8	8.57	1.78	0.69	6.07	3.44	0.60	1.47	0.18	1.10	0.16	9.6	<0.5	3.2	0.70
206/8-7 2320.5m	4.8	3.4	0.37	36.9	70.2	7.26	25.1	3.48	0.75	0.23	2.21	1.07	0.19	0.45	0.07	0.42	0.06	2.6	0.2	5.02	0.89
206/7-A2 2142.8-2143m	25.3	12.8	0.80	75.4	156	17.8	68.6	11.4	2.27	1.09	8.56	5.84	1.04	2.63	0.35	2.08	0.29	7.2	0.6	5.66	1.12
206/7-A2 2544.65-2544.85m	18.4	9.9	0.30	69.9	145	16.3	62.9	10.3	1.23	0.91	7.89	4.56	0.77	1.78	0.21	1.24	0.18	6.6	0.3	4.91	0.36
206/7-A2 2599.2-2599.4m	4.6	2.9	0.18	22.7	45.8	4.81	18.1	2.74	1.37	0.21	1.95	1.06	0.18	0.46	0.06	0.35	0.06	6.7	<.1	0.76	0.14
205/16-1 4172-4172.15m	17.5	8.2	0.53	50.5	105	12.1	46.1	7.88	1.96	0.73	5.78	3.82	0.72	1.90	0.28	1.77	0.25	5.1	0.4	10.9	0.54
205/22-1 3225.45 - 3275.60m	15.8	7.2	0.7	31.7	75.6	9.27	37.7	6.61	1.39	0.63	4.97	3.53	0.65	1.71	0.23	1.41	0.19	5.0	<0.5	0.7	0.20
204/23-1 3846.90 - 3847.05m	25.7	12.0	0.6	28.2	59.8	6.60	25.6	4.83	1.24	0.78	4.60	5.25	1.10	2.99	0.46	3.02	0.47	4.8	0.7	4.4	0.69
204/25-1 9416 ft	7.0	2.6	0.21	19.0	41.5	5.36	22.4	3.88	1.05	0.33	2.76	1.67	0.31	0.77	0.11	0.63	0.10	1.7	<0.1	0.09	0.07
202/3-1	2.0	1.6	0.6	7.9	16.7	1.88	7.3	1.22	0.37	0.10	0.85	0.44	0.08	0.21	0.02	0.15	0.02	2.1	<0.5	0.5	0.10
202/2-1 4002 feet	15.7	5.5	1.44	30.7	65.9	7.49	29.1	4.88	1.09	0.54	3.84	3.33	0.68	1.99	0.28	1.83	0.27	3.5	0.3	6.31	0.89
88/02	3.9	4.8	4.2	22.4	47.0	4.84	16.9	2.20	0.62	0.15	1.32	0.77	0.15	0.37	0.05	0.41	0.07	3.1	<0.5	4.5	0.77
164/25-2 2727.65-2727.8m	24.7	5.9	<0.02	6.6	17.7	2.71	14.0	4.04	1.36	0.84	5.11	5.21	1.07	2.93	0.42	2.63	0.40	2.7	0.4	0.15	0.14
154/3-1 8060.0-8060.2	25.3	7.2	0.07	17.2	39.1	5.00	22.1	4.85	1.45	0.79	5.17	5.04	1.06	3.05	0.44	2.90	0.44	2.9	0.4	1.76	0.44
58-08/228DR 19 - 49cm	0.6	0.9	0.4	0.3	0.5	0.06	0.3	0.06	0.10	0.02	0.07	0.08	0.02	0.07	0.01	0.07	0.02	0.4	<0.5	<0.1	0.88
58-08/230DR 0.62 - 0.86m	12.7	13.9	0.1	42.1	106	11.8	44.9	6.75	1.92	0.58	4.80	2.79	0.48	1.13	0.16	0.98	0.14	4.4	<0.5	4.2	1.56
90/14 87.82m	1.0	2.9	2.7	11.1	26.9	2.76	9.0	1.10	0.35	0.05	0.48	0.25	0.04	0.10	0.02	0.12	0.02	3.7	<	7.3	2.24
57-09/537 (JD10) 0-2.90m TD	20.2	15.4	0.87	54.5	135	17.3	71.3	11.4	2.46	0.94	7.89	4.75	0.85	2.11	0.28	1.81	0.26	4.5	0.8	6.10	0.71
57-09/536 (JD10) 0-0.50m TD	22.2	14.2	0.88	69.6	167	21.2	86.0	13.3	2.92	1.02	8.92	5.09	0.91	2.25	0.30	1.87	0.27	5.0	0.6	5.63	0.55
56-08/920DR 51 - 67cm	19.3	10.0	0.2	32.2	76.8	9.33	36.4	6.80	1.04	0.73	5.33	3.94	0.76	2.02	0.30	1.83	0.27	2.6	0.8	5.7	0.26
56-08/921 (JD6) 0-0.78m TD	2.0	2.0	0.31	48.4	93.6	8.86	28.2	2.90	0.73	0.14	1.39	0.53	0.08	0.20	0.02	0.17	0.03	2.9	<0.1	9.63	0.18
56-08/924 (JD4) 0.75-0.85m TD	15.3	9.2	0.13	93.9	189	17.1	54.2	6.76	0.99	0.58	4.45	3.17	0.62	1.72	0.25	1.69	0.28	15.0	0.4	14.0	1.84
132/15-1 4155.55-4155.7m	7.5	21.8	1.04	46.8	99.6	11.3	37.9	5.43	0.84	0.42	3.51	1.96	0.35	0.92	0.16	1.05	0.18	5.7	1.5	15.3	1.22
56-09/384DR 44 - 64cm	23.3	12.5	1.5	21.9	50.2	6.66	29.8	6.00	1.86	0.82	5.63	4.66	0.93	2.51	0.35	2.18	0.33	3.1	1.4	0.7	0.48
56-09/386 (JD1) 0.88-1.01m	16.8	10.0	0.43	58.8	131	12.6	42.7	6.61	0.94	0.67	4.78	3.66	0.69	1.88	0.26	1.62	0.24	7.0	0.3	8.56	0.60
56-09/388DR 0.18 - 21m	7.5	2.7	0.1	37.1	70.3	7.20	25.2	3.47	0.88	0.31	2.32	1.58	0.30	0.79	0.10	0.64	0.09	2.6	<0.5	2.9	0.34
56-15/18DR 1.65 - 1.7m	24.8	13.3	0.4	31.7	69.0	8.50	36.5	6.93	3.19	0.86	6.22	4.95	0.99	2.75	0.37	2.41	0.38	2.3	0.6	1.0	0.52
56-15/18DR 3.02 - 3.36m	32.1	16.0	0.5	36.9	85.7	10.7	46.0	8.97	3.29	1.12	7.96	6.45	1.28	3.49	0.48	3.04	0.46	2.5	0.8	1.6	0.80
57-14/58 43 - 78	34.4	7.9	0.2	11.6	31.8	4.87	24.7	6.67	2.47	1.13	7.51	7.00	1.39	3.73	0.53	3.21	0.50	4.9	0.6	0.9	0.35
57-15/15 DR 19-24cm	52.4	28	0.15	58.5	125.4	15.9	67.2	13.4	3.97	1.83	12.3	11.0	2.18	6.15	0.92	6.04	0.93	14.0	2.1	3.52	0.70

Figure 3.4. CIPW NORM data

Location	QZ	CO	OR	PL	Albite	Anorthite	LC	NE	KP	HL	TH	AC	NS	KS	WO	DI	Wollastonite	Enstatite	Ferrosilite
220/26-1	18.85	4.05	14.06	44.27	34.12	10.15	0.00	0.00	0.00	0.00	0.00	0.00	0.00	0.00	0.00	0.00	0.00	0.00	0.00
209/9-1	23.95	0.00	27.71	42.05	30.35	11.70	0.00	0.00	0.00	0.00	0.00	0.00	0.00	0.00	0.00	0.00	0.00	0.00	0.00
209/12-1	30.69	4.34	24.26	32.90	24.96	7.94	0.00	0.00	0.00	0.00	0.00	0.00	0.00	0.00	0.00	0.00	0.00	0.00	0.00
81/17	0.47	0.00	3.03	24.21	10.66	13.55	0.00	0.00	0.00	0.00	0.00	0.00	0.00	0.00	0.00	39.35	19.67	19.67	0.00
208/27-2	31.92	2.12	22.27	33.57	25.26	8.31	0.00	0.00	0.00	0.00	0.00	0.00	0.00	0.00	0.00	0.00	0.00	0.00	0.00
206/8-8	23.77	0.00	13.00	54.78	43.07	11.71	0.00	0.00	0.00	0.00	0.00	0.00	0.00	0.00	0.00	0.48	0.24	0.24	0.00
206/8-2	26.97	0.00	5.43	59.21	46.76	12.45	0.00	0.00	0.00	0.00	0.00	0.00	0.00	0.00	1.32	4.05	2.03	2.03	0.00
206/8-1a 2310.75	11.86	0.63	18.27	55.32	36.65	18.66	0.00	0.00	0.00	0.00	0.00	0.00	0.00	0.00	0.00	0.00	0.00	0.00	0.00
206/8-7	36.00	0.00	5.99	50.30	36.76	13.54	0.00	0.00	0.00	0.00	0.00	0.00	0.00	0.00	0.00	2.38	1.19	1.19	0.00
206/7-A2 2142.8m	1.48	0.00	16.54	60.10	37.20	22.90	0.00	0.00	0.00	0.00	0.00	0.00	0.00	0.00	0.00	4.01	2.00	2.00	0.00
206/7-A2 2544.65m	11.88	0.06	11.17	61.70	42.82	18.88	0.00	0.00	0.00	0.00	0.00	0.00	0.00	0.00	0.00	0.00	0.00	0.00	0.00
206/7-A2 2599.2m	30.42	1.45	27.07	36.58	29.61	6.97	0.00	0.00	0.00	0.00	0.00	0.00	0.00	0.00	0.00	0.00	0.00	0.00	0.00
205/16-1	52.96	10.54	24.26	4.04	1.27	2.77	0.00	0.00	0.00	0.00	0.00	0.00	0.00	0.00	0.00	0.00	0.00	0.00	0.00
205/22-1	16.08	6.66	51.80	15.67	14.41	1.26	0.00	0.00	0.00	0.00	0.00	0.00	0.00	0.00	0.00	0.00	0.00	0.00	0.00
204/23-1	7.72	11.76	11.41	46.57	35.76	10.81	0.00	0.00	0.00	0.00	0.00	0.00	0.00	0.00	0.00	0.00	0.00	0.00	0.00
204/25-1	15.95	0.00	8.39	65.31	47.95	17.36	0.00	0.00	0.00	0.00	0.00	0.00	0.00	0.00	0.00	0.92	0.46	0.46	0.00
202/3-1	27.86	1.39	11.07	56.64	46.29	10.35	0.00	0.00	0.00	0.00	0.00	0.00	0.00	0.00	0.00	0.00	0.00	0.00	0.00
202/2-1	21.07	4.90	13.21	44.04	29.61	14.43	0.00	0.00	0.00	0.00	0.00	0.00	0.00	0.00	0.00	0.00	0.00	0.00	0.00
88/02	24.73	0.74	13.71	54.02	39.84	14.18	0.00	0.00	0.00	0.00	0.00	0.00	0.00	0.00	0.00	0.00	0.00	0.00	0.00
164/25-2	6.07	0.00	1.20	43.62	17.69	25.93	0.00	0.00	0.00	0.00	0.00	0.00	0.00	0.00	0.00	25.25	12.62	12.62	0.00
154/3-1	5.35	0.00	9.99	43.62	22.92	20.70	0.00	0.00	0.00	0.00	0.00	0.00	0.00	0.00	0.00	21.34	10.67	10.67	0.00
58-08/228	29.14	0.70	12.93	56.73	45.48	11.24	0.00	0.00	0.00	0.00	0.00	0.00	0.00	0.00	0.00	0.00	0.00	0.00	0.00
58-08/230	0.55	0.00	26.12	68.63	60.47	8.16	0.00	0.00	0.00	0.00	0.00	0.00	0.00	0.00	0.67	1.54	0.77	0.77	0.00
90/14	27.30	1.05	8.35	58.13	41.73	16.39	0.00	0.00	0.00	0.00	0.00	0.00	0.00	0.00	0.00	0.00	0.00	0.00	0.00
57-09/536	7.72	0.00	18.33	49.86	33.31	16.55	0.00	0.00	0.00	0.00	0.00	0.00	0.00	0.00	0.00	4.86	2.43	2.43	0.00
57-09/537	6.65	0.00	19.44	45.36	29.73	15.63	0.00	0.00	0.00	0.00	0.00	0.00	0.00	0.00	0.00	6.88	3.44	3.44	0.00
56-08/920	16.08	0.00	5.85	54.15	35.57	18.59	0.00	0.00	0.00	0.00	0.00	0.00	0.00	0.00	0.00	10.62	5.31	5.31	0.00
56-08/921	26.64	1.04	19.80	48.56	39.30	9.26	0.00	0.00	0.00	0.00	0.00	0.00	0.00	0.00	0.00	0.00	0.00	0.00	0.00
56-08/924	12.51	0.00	28.11	50.34	42.00	8.34	0.00	0.00	0.00	0.00	0.00	0.00	0.00	0.00	0.00	2.47	1.24	1.24	0.00
132/15-1	28.84	1.50	30.75	34.90	33.67	1.23	0.00	0.00	0.00	0.00	0.00	0.00	0.00	0.00	0.00	0.00	0.00	0.00	0.00
56-09/384	0.00	0.00	14.45	52.41	33.31	19.10	0.00	1.32	0.00	0.00	0.00	0.00	0.00	0.00	0.00	11.49	5.75	5.75	0.00
56-09/386	25.27	0.00	31.81	38.64	32.20	6.44	0.00	0.00	0.00	0.00	0.00	0.00	0.00	0.00	0.00	0.03	0.02	0.02	0.00
56-09/388	16.83	0.00	19.20	55.79	40.72	15.07	0.00	0.00	0.00	0.00	0.00	0.00	0.00	0.00	0.00	1.13	0.57	0.57	0.00
56-15/18 1.65m	6.38	0.00	19.44	60.91	38.42	22.49	0.00	0.00	0.00	0.00	0.00	0.00	0.00	0.00	0.00	1.91	0.95	0.95	0.00
56-15/18 3.02m	6.56	0.00	15.11	62.61	39.13	23.48	0.00	0.00	0.00	0.00	0.00	0.00	0.00	0.00	0.00	2.43	1.21	1.21	0.00
57-14/58	0.04	0.00	4.77	61.28	38.55	22.73	0.00	0.00	0.00	0.00	0.00	0.00	0.00	0.00	0.00	10.66	5.33	5.33	0.00

Figure 3.4. CIPW NORM data (cont.)

Location	HY	Enstatite	Ferrosilite	OL	Forsterite	Fayalite	CS	MT	CM	IL	HM	SP	PF	RU	AP	WTAN	WTAB	WTOR
220/26-1	12.05	12.05	0.00	0.00	0.00	0.00	0.00	0.79	0.00	0.81	4.83	0.00	0.00	0.00	0.28	18.00	57.05	24.96
209/9-1	2.65	2.65	0.00	0.00	0.00	0.00	0.00	0.00	0.00	0.58	2.59	0.10	0.00	0.04	0.34	17.20	42.06	40.75
209/12-1	3.87	3.87	0.00	0.00	0.00	0.00	0.00	0.00	0.00	0.74	2.84	0.00	0.00	0.10	0.26	14.25	42.20	43.55
81/17	24.65	24.65	0.00	0.00	0.00	0.00	0.00	2.28	0.00	1.05	4.90	0.00	0.00	0.00	0.06	50.89	37.72	11.39
208/27-2	2.09	2.09	0.00	0.00	0.00	0.00	0.00	0.48	0.00	1.43	4.70	0.00	0.00	0.00	1.42	15.28	43.76	40.96
206/8-8	3.67	3.67	0.00	0.00	0.00	0.00	0.00	1.20	0.00	0.37	2.44	0.00	0.00	0.00	0.30	17.93	62.16	19.91
206/8-2	0.00	0.00	0.00	0.00	0.00	0.00	0.00	0.07	0.00	0.39	2.36	0.00	0.00	0.00	0.19	20.09	71.13	8.77
206/8-1a 2310.75	6.67	6.67	0.00	0.00	0.00	0.00	0.00	0.00	0.00	0.88	4.94	0.00	0.00	0.34	1.09	26.10	48.33	25.57
206/8-7	1.61	1.61	0.00	0.00	0.00	0.00	0.00	0.00	0.00	0.44	2.85	0.06	0.00	0.00	0.37	25.00	63.95	11.05
206/7-a 22142.8	6.88	6.88	0.00	0.00	0.00	0.00	0.00	0.20	0.00	2.09	7.41	0.00	0.00	0.00	1.28	30.73	47.06	22.21
206/7-a 22544.65	6.70	6.70	0.00	0.00	0.00	0.00	0.00	1.10	0.00	1.32	5.21	0.00	0.00	0.00	0.86	26.82	57.31	15.87
206/7-a 22599.2	1.87	1.87	0.00	0.00	0.00	0.00	0.00	0.00	0.00	0.29	1.89	0.00	0.00	0.11	0.31	11.25	45.05	43.71
205/16-1	4.24	4.24	0.00	0.00	0.00	0.00	0.00	0.00	0.00	0.31	2.95	0.00	0.00	0.29	0.41	9.82	4.24	85.94
205/22-1	3.21	3.21	0.00	0.00	0.00	0.00	0.00	0.00	0.00	0.59	5.07	0.00	0.00	0.24	0.68	1.89	20.37	77.74
204/23-1	13.40	13.40	0.00	0.00	0.00	0.00	0.00	0.34	0.00	1.77	6.95	0.00	0.00	0.00	0.08	19.33	60.26	20.41
204/25-1	4.81	4.81	0.00	0.00	0.00	0.00	0.00	0.23	0.00	0.72	3.16	0.00	0.00	0.00	0.50	24.47	63.70	11.83
202/3-1	1.43	1.43	0.00	0.00	0.00	0.00	0.00	0.00	0.00	0.29	1.16	0.00	0.00	0.01	0.15	15.91	67.06	17.03
202/2-1	9.98	9.98	0.00	0.00	0.00	0.00	0.00	0.00	0.00	1.17	5.37	0.00	0.00	0.06	0.21	25.97	50.24	23.79
88/02	3.99	3.99	0.00	0.00	0.00	0.00	0.00	0.05	0.00	0.54	1.95	0.00	0.00	0.00	0.28	21.67	57.37	20.95
164/25-2	9.37	9.37	0.00	0.00	0.00	0.00	0.00	1.99	0.00	2.43	9.84	0.00	0.00	0.00	0.23	59.18	38.07	2.74
154/3-1	4.86	4.86	0.00	0.00	0.00	0.00	0.00	2.60	0.00	2.26	9.56	0.00	0.00	0.00	0.41	39.58	41.31	19.12
58-08/228	0.25	0.25	0.00	0.00	0.00	0.00	0.00	0.00	0.00	0.02	0.22	0.00	0.00	0.01	0.02	16.77	63.94	19.29
58-08/230	0.00	0.00	0.00	0.00	0.00	0.00	0.00	1.25	0.00	0.44	0.70	0.00	0.00	0.00	0.10	8.94	62.44	28.62
90/14	2.44	2.44	0.00	0.00	0.00	0.00	0.00	0.00	0.00	0.43	2.06	0.00	0.00	0.03	0.21	25.58	61.38	13.04
57-09/536	7.16	7.16	0.00	0.00	0.00	0.00	0.00	0.00	0.00	2.19	7.51	0.02	0.00	0.00	2.34	24.97	47.36	27.67
57-09/537	6.68	6.68	0.00	0.00	0.00	0.00	0.00	0.00	0.00	2.67	10.40	0.03	0.00	0.00	1.88	24.78	44.41	30.82
56-08/920	6.02	6.02	0.00	0.00	0.00	0.00	0.00	2.50	0.00	0.77	3.90	0.00	0.00	0.00	0.11	32.07	57.83	10.10
56-08/921	1.93	1.93	0.00	0.00	0.00	0.00	0.00	0.00	0.00	0.29	1.49	0.00	0.00	0.04	0.21	14.01	56.03	29.96
56-08/924	1.63	1.63	0.00	0.00	0.00	0.00	0.00	0.00	0.00	0.86	3.42	0.20	0.00	0.00	0.47	10.97	52.05	36.98
132/15-1	2.04	2.04	0.00	0.00	0.00	0.00	0.00	0.22	0.00	0.29	1.33	0.00	0.00	0.00	0.13	1.92	49.80	48.28
56-09/384	0.00	0.00	0.00	6.50	6.50	0.00	0.00	0.25	0.01	3.02	9.34	0.00	0.00	0.00	1.21	29.41	48.33	22.26
56-09/386	1.34	1.34	0.00	0.00	0.00	0.00	0.00	0.27	0.00	0.54	1.81	0.00	0.00	0.00	0.28	9.39	44.23	46.38
56-09/388	3.23	3.23	0.00	0.00	0.00	0.00	0.00	1.06	0.00	0.45	1.93	0.00	0.00	0.00	0.38	20.74	52.82	26.43
56-15/18 1.65m	3.14	3.14	0.00	0.00	0.00	0.00	0.00	0.57	0.00	1.63	5.08	0.00	0.00	0.00	0.95	28.78	46.34	24.88
56-15/18 3.02m	3.56	3.56	0.00	0.00	0.00	0.00	0.00	0.83	0.00	1.89	5.85	0.00	0.00	0.00	1.16	31.11	48.86	20.03
57-14/58	5.53	5.53	0.00	0.00	0.00	0.00	0.00	0.00	0.00	3.23	8.91	4.82	0.00	0.00	0.78	35.60	56.93	7.47

A plot of CaO versus SiO₂ for all the samples shows the wide range in composition from alkalic to calcic (Figure 3.2). Early Proterozoic rocks from the Stanton High are similar to the Archaean samples whereas those from Rockall High are notably less calcic.

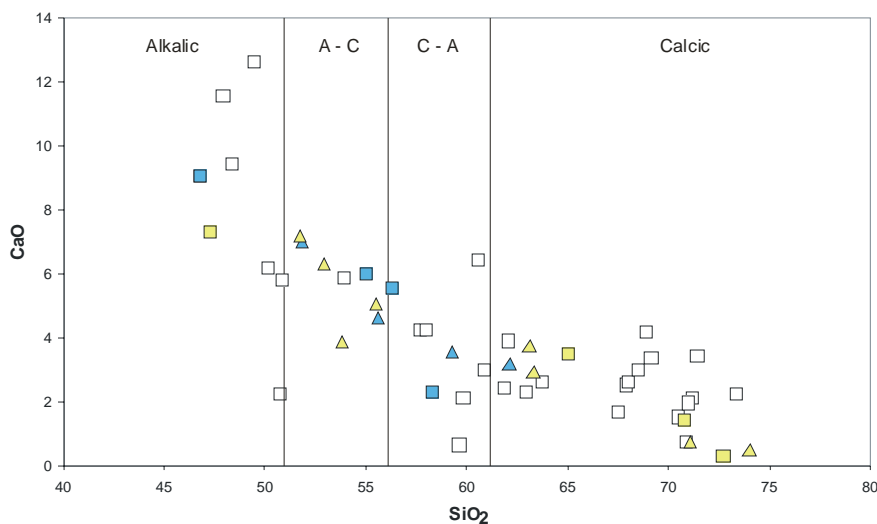


Figure 3.2. Plot of CaO versus SiO₂ with fields after Peacock (1931). Blue symbols are from the Rockall High, yellow symbols are from the Stanton High, and triangles are from Scanlon and Daly (2001). Open squares are Archaean rocks from this study.

The trace element composition of the borehole samples is as varied as their major element compositions. The differences in REE, large ion lithophile element (LILE) and U – Th compositions documented here provide valuable information regarding the identification of similarities of the borehole samples to those on the mainland.

Chondrite normalized REE profiles for the Archaean rocks vary in steepness with several samples showing a slightly negative Eu anomaly, the most pronounced being observed in 206/7-A2 2544 m (Figure 3.3).

Samples 204/23-1, 202/2-1 and 206/8-8 (Figure 3.4) are characterised by very flat patterns similar to those of Lewisian mafic gneisses (Weaver and Tarney 1987). In contrast, five samples 88/02, 90/14, 206/8-2, 206/8-7 and 206/7-A2 2599 m (Figure 3.5) exhibit a dish-shaped pattern for the heavy REE's, common in Archaean TTG and classically interpreted as reflecting the presence of garnet ± hornblende in the source. 90/14 and 207/7-A2 2599 m display positive Eu anomalies and have similar profiles to the most depleted Guinard Bay TTG's (Rollinson and Fowler 1987; Fowler and Plant 1987).

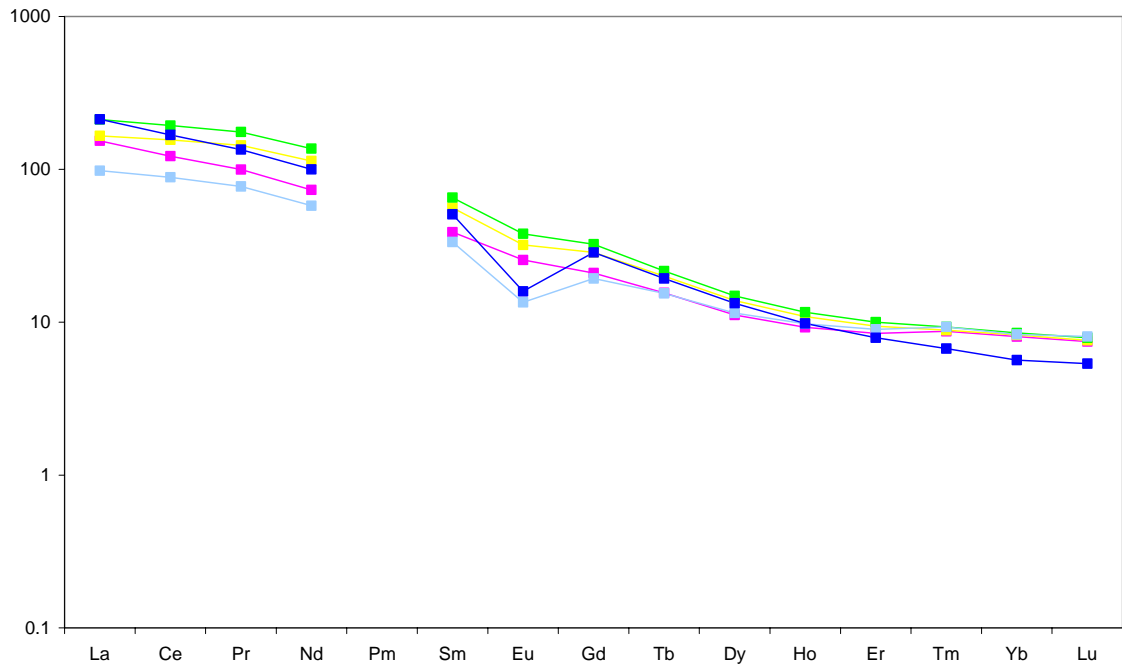


Figure 3.3. Chondrite normalised REE plots: 57-09/536 green, 57-09/537 yellow, 206/7-A2 2544 m dark blue, 205/16-1 purple, 56-08/920 pale blue.

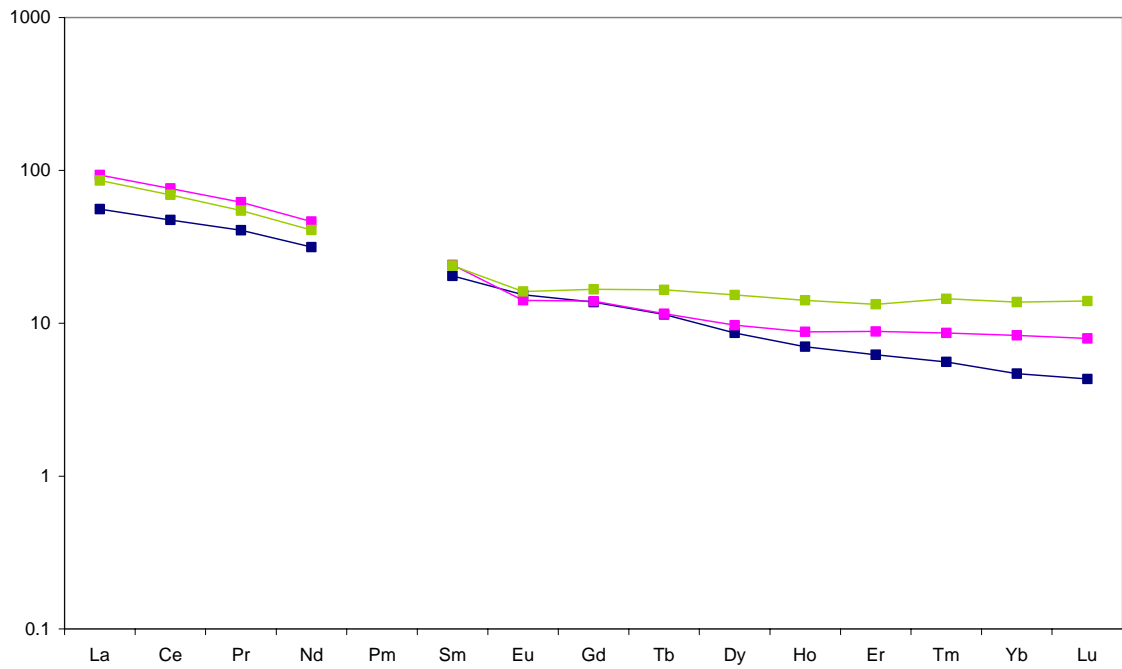


Figure 3.4. Chondrite normalised REE plots: 204/23-1 green, 202/2-1 purple, 206/8-1 blue.

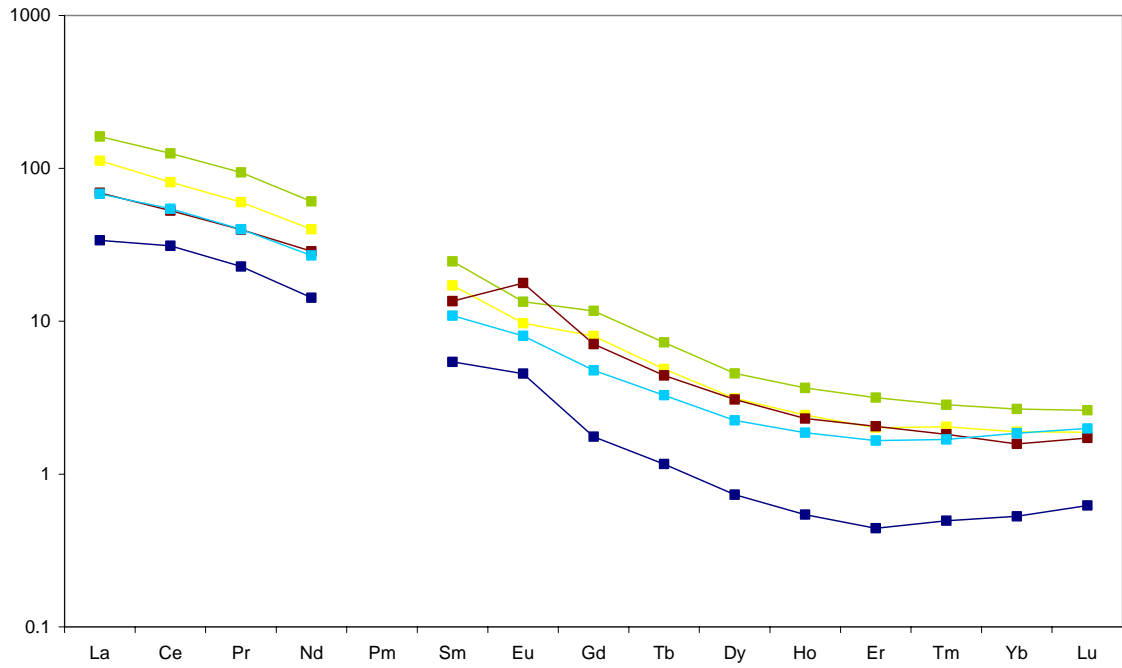


Figure 3.5. Chondrite normalised REE patterns: 206/8-2 green, 206/8-7 yellow, 206/7-A2 2599 m brown, 88/02 light blue, 90/14 dark blue.

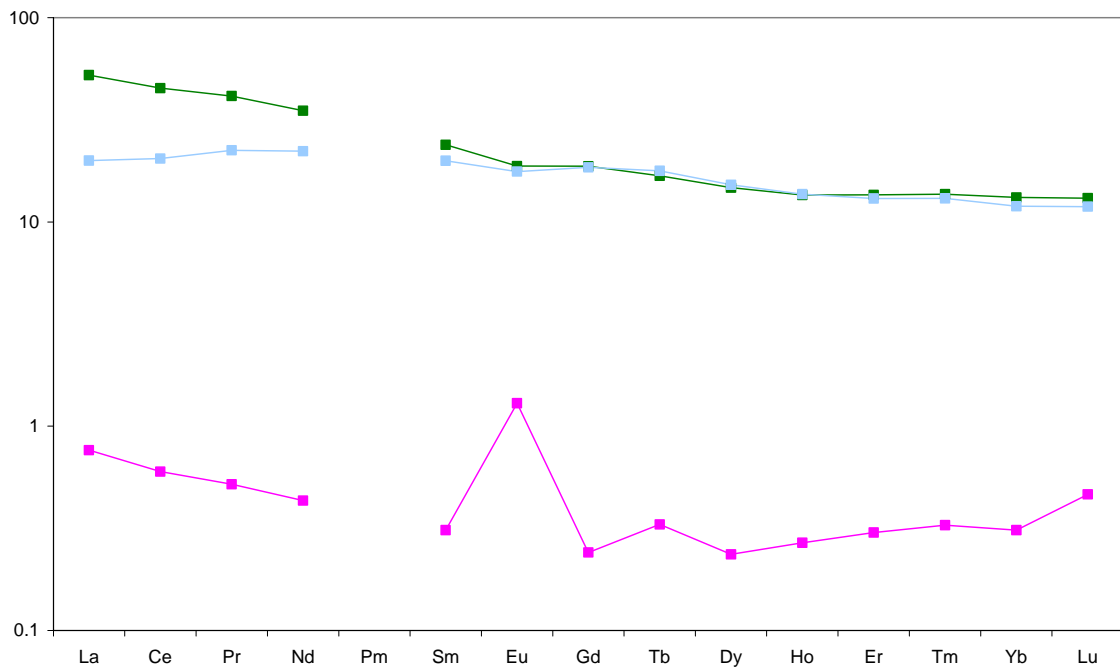


Figure 3.6. Chondrite normalised REE patterns: 154/3-1 green, 164/25-2 pale blue, 58-08/228 pink.

Samples 164/25-2 and 154/3-1 have almost identical profiles for the middle to heavy REE (Figure 3.6). However the LREE pattern for 154/3-1 is steeper reflecting the higher concentrations of these elements and indicating that this rock was derived from a more fractionated magma than 164/25-2. The granite pegmatite 58-08/228 has an extremely depleted REE signature with total elemental abundances of 1.6 and a very positive Eu anomaly. This suggests that all of the trace mineral phases have been fractionated out.

REE profiles for the four Stanton High rocks are shown in Figure 3.7 together with those for samples analysed by Scanlon and Daly (2001). Samples from this study display a general pattern of increasing steepness with increasing SiO₂ concentration. 56-09/386 and 132/15-1, with SiO₂ contents of ~70%, have negative Eu anomalies reflecting feldspar fractionation.

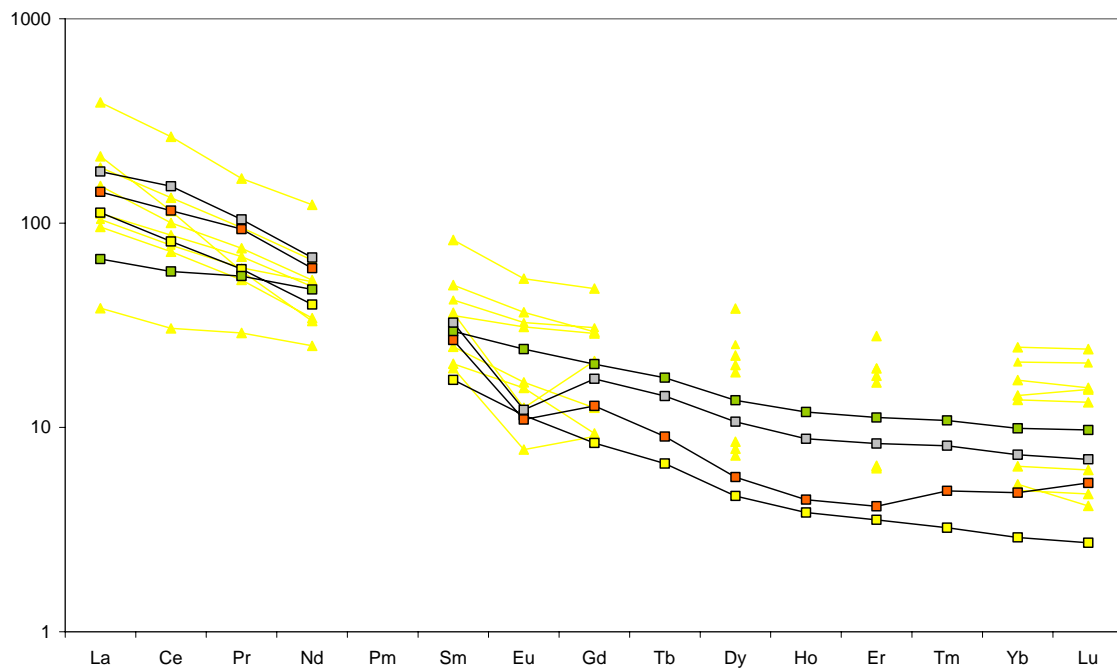


Figure 3.7. Chondrite normalised REE patterns for Stanton High samples: 56-09/384 green squares, 56-09/386 grey squares, 56-09/388 yellow squares, 132/15-1 orange squares. Data from Scanlon and Daly (2001) yellow diamonds.

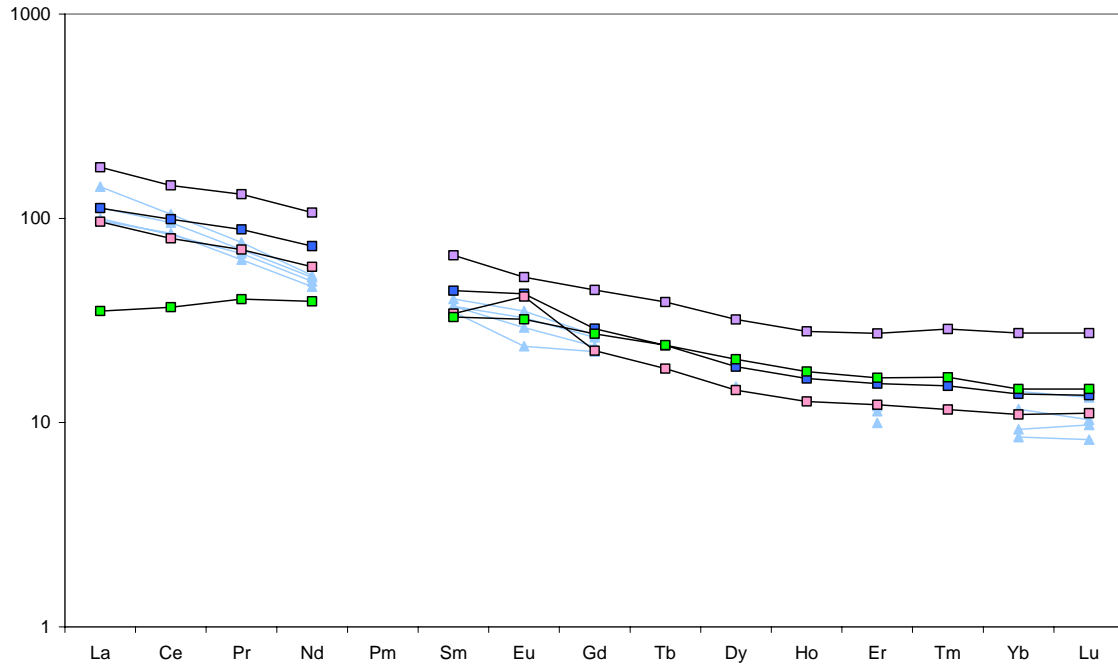


Figure 3.8. Chondrite normalised REE patterns for Rockall Bank samples: 56-15/18 1.65-1.71 m pink squares, 56-15/18 3.02-3.3 6m, dark blue squares, 57-14/58 green squares, 57/15/15 light purple squares. Data from Scanlon and Daly (2001) light blue triangles.

The Rockall Bank metagabbro 56-14/58 has a very flat REE pattern whereas the two tonalite samples from borehole 56-15/18 yield steeper profiles with positive Eu anomalies (Figure 3.8). 57-15/15 has similar slope but higher total REE concentration and no Eu anomaly.

Marked differences are observed for Rb, Th, and U between Lewisian amphibolite facies and granulite facies tonalities (Tarney and Weaver 1987) and primordial mantle multi-element plots highlight the depletion in these elemental abundances, which may amount to an order of magnitude. Rollinson (1996) plotted normalized arithmetic mean values for selected trace elements of TTG's from each region of the mainland Lewisian and observed that TTG's from the Central Region were more depleted than those from the Northern and Southern Regions. Whitehouse demonstrated that the Central Region gneisses were also depleted in Pb. There appears to be no distinct geographical pattern of depletion within the study area, 206/8-1A, 205/22-1 and 202/3-1 exhibit the classic flat bottomed Th-U trough (Figure 3.9) whereas 206/8-8, and 204/25-1 are more depleted in Th than U and hence display a V-shaped profile

(Figure 3.10). These signatures are consistent with granulite facies overprinting at some stage of the history of these rocks.

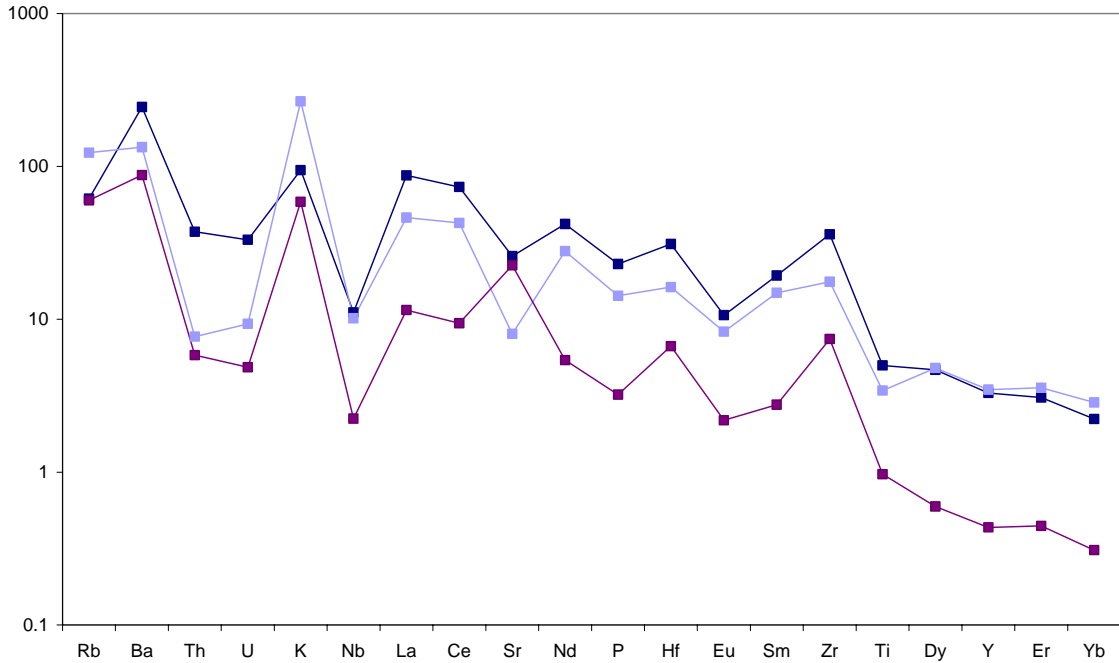


Figure 3.9. Primitive mantle normalised multi-element diagram for 206/8-1A dark blue, 205/22-1 light blue and 202/3-1 purple.

In contrast 206/8-2, 205/16-1 and 56-08/920 show enriched Th (Figure 3.11) but otherwise have patterns broadly similar to the samples exhibiting Th depletion. Most of the samples display prominent Nb and Ti troughs and K/Rb ratios range from 156 (90/14) to 2724 (204/25-1).

Samples 164/25-2 and 154/3-1 have high concentrations of V, Cr, Co, Cu and Zn and similar multi-element profiles for Sr to Yb (Figure 3.12). However the patterns for the large ion lithophile elements Rb, K, and Ba and for Th and U are very different, moreover 164/25-2 is unusual in not displaying a Nb anomaly.



Figure 3.10. Primitive mantle normalised multi-element diagrams for 206/8-8 turquoise and 204/25-1 pink.

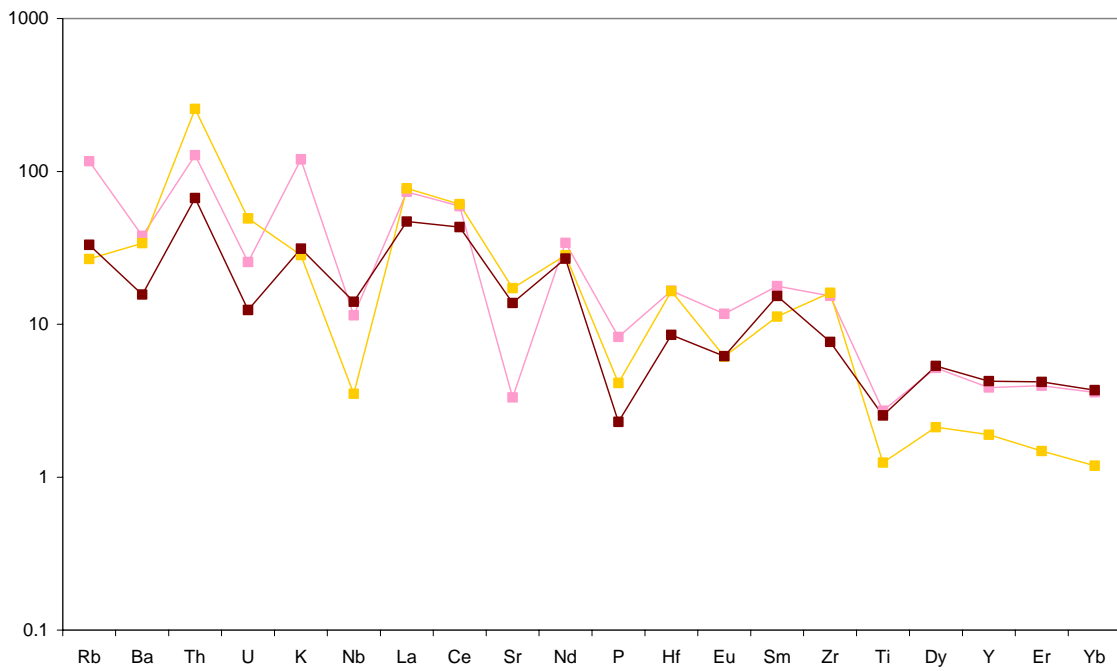


Figure 3.11. Primitive mantle normalised multi-element diagrams for 206/8-2 orange, 205/16-1 pink and 56-08/920 brown.

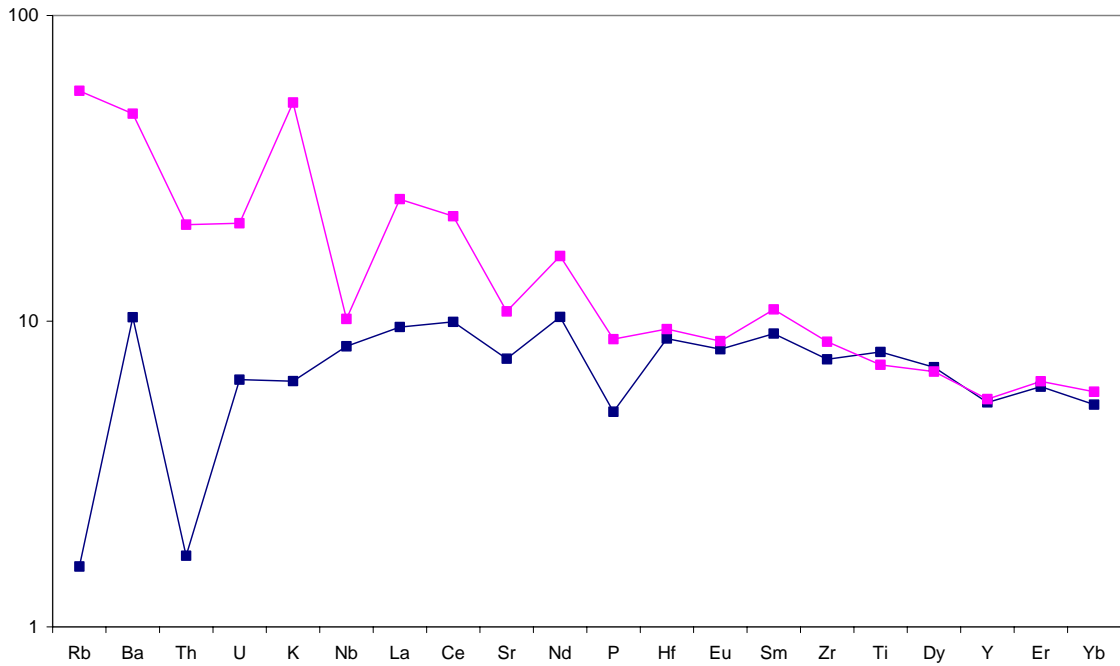


Figure 3.12. Primitive mantle normalised diagrams for 164/25-2 blue and 154/3-1 purple.

Stanton High samples 132/15-1 and 56-09/386 exhibit Th enrichment and multi elements plots that are similar to 56-08/924 whereas samples 56-09/384 and 56-09/388 display varying degrees of Th depletion (Figure 3.13). They also lack the negative P, Sr and Eu and positive Hf anomalies that characterise the Th enriched samples. These differences highlight the heterogeneous nature of the Archaean component.

Tonalite samples from location 56-15/18 on Rockall High display similar patterns of Rb, Th and U depletion to the Lewisian gneisses and these are mirrored by the metagabbro and trachyandesite samples 57-15/58 and 57-15/15 (Figure 3.14).

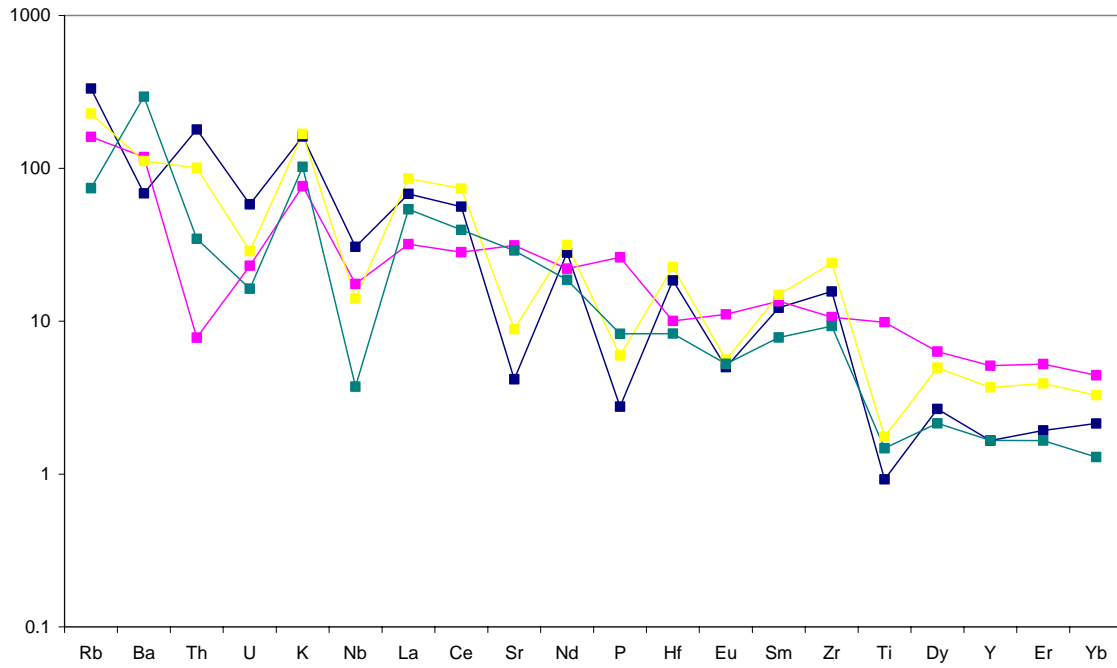


Figure 3.13. Primitive mantle normalised multi-element diagrams for 56-09/384 pink, 56-09/386 yellow, 132/15-1 blue and 56-09/388 dark green.

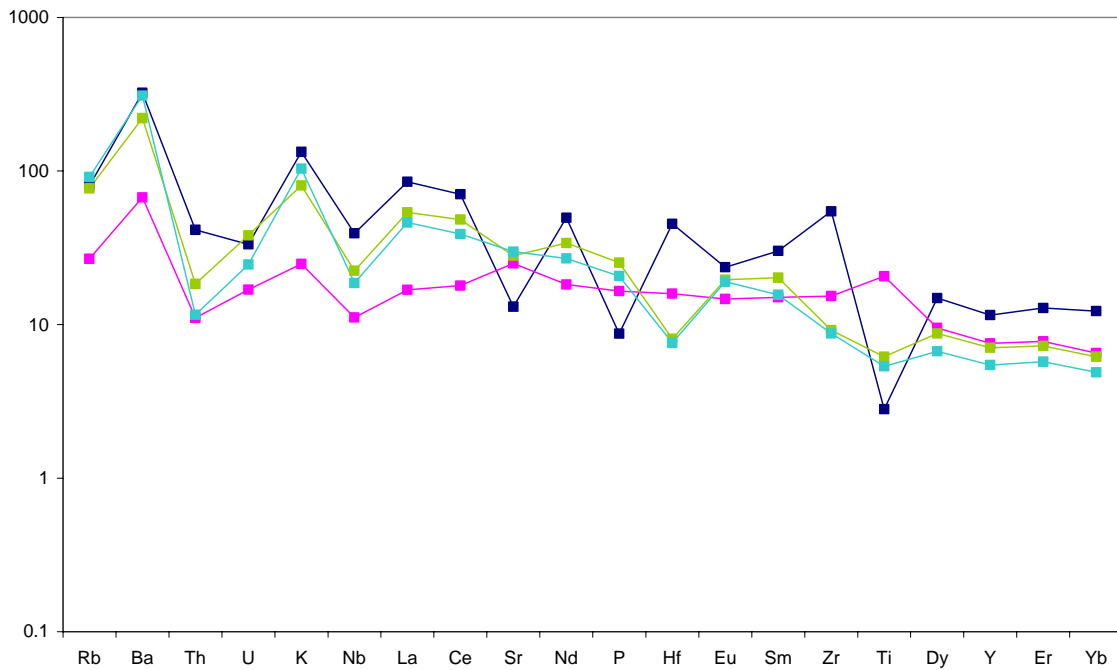


Figure 3.14. Primitive mantle normalised multi-element diagrams for 57-15/15 dark blue, 57-14/58 purple, 56-15/18 1.65 m green and 56-15/18 3.02 m turquoise.

4 Isotope Geochemistry

Isotope data obtained for the borehole samples provide information crucial to determining the age and constraining the genesis (or protoliths) of the igneous and metamorphic rocks that otherwise could not be determined in any other manner. Mineral and whole rock data for the U-Pb, Rb-Sr, Sm-Nd and Pb-Pb isotope systems is presented here. Each isotope system reveals a different aspect concerning the age or origin of the rocks.

U-Pb high precision geochronology was the dating tool of choice for this study. The relative merits of the technique are that it is based on physically robust minerals that can faithfully record mineral-forming events through time and that it can yield the most highly accurate and precise ages currently available. The technique is exclusively applied to zircon in this study although other minerals such as monazite and titanite can be dated if they are present and have suitable properties (e.g. unaltered, sufficient U and Pb for analysis). The technique is very expensive to apply and so only 12 samples were dated.

Rb-Sr and Pb-Pb isotope data were collected mainly to provide tracer information concerning potential igneous rock source regions. In the past these two isotope systems were widely used for geochronology. Hard-won experience in terranes such as the Lewisian, which is shown to be similar to many offshore rocks, has proven that these two systems can be disturbed and the mineral and whole-rock chronometers reset, either completely or in part. Their petrogenetic tracer properties are more robust and the data are mainly used to support the tracer information provided by the Sm-Nd system.

Representative samples from many of the boreholes were analysed for their Sm-Nd isotope compositions. Sm-Nd isotope systematics are very robust in many geological situations, compared to other isotope tracers, and the data are less expensive to obtain compared to U-Pb geochronology. Tracer data could therefore be obtained in a cost-effective manner for more rocks and thus provides greater geographic coverage. The data also supply important estimates, albeit model-dependent, of the ages of the rocks.

4.1 U-Pb GEOCHRONOLOGY

A total of 12 rocks were examined in detail for U-Pb geochronology. The data obtained are summarized in Table 4.1, and the results for individual samples described below. Remarkably, the data reflect UK offshore crustal growth and metamorphism spanning approximately 1.2 Ga, from Lewisian late Archaean 2.80 Ga tonalitic gneisses to 1.63 Ga mafic magmatism possibly related to Gothian – Labradorian orogenesis.

209/9-1. The data for this rock plot either on concordia or as a modestly discordant cluster (Figure 4.1). There are two concordant points with ages of 2738.3 ± 4.1 Ma and 2767.1 ± 5.6 Ma. Of the discordant data, three analyses agree within error with an average $^{207}\text{Pb}/^{206}\text{Pb}$ age of 2728.5 ± 2.3 Ma, and yield an upper intercept age of 2735 ± 13 Ma when regressed with the younger of the two concordant points. The preferred interpretation of this data set is that the age of the rock is given by the concordant 2738.3 ± 4.1 Ma analysis and that the three overlapping analyses represent 2738 Ma zircons with Pb-loss. In addition, the older concordant zircon analysis indicates inheritance, also likely present in the older two discordant analyses. A theoretical mixing line between the rock age of 2738 Ma and 2800 Ma, a potential end member age based on data for other rocks in this study, is invisible on the plot because it overlaps with the Concordia curve. Pb-loss from zircons originally at 2740 Ma and 2743 Ma along this mixing line would account for the two older discordant data points.

206/8-1A. Zircons recovered from this sample are only of moderate quality and range from turbid to relatively transparent crystals. Most grains have rounded facets and are 50-100 μm long with aspect ratios of 1:1 to 4:1, and many have opaque to rusty inclusions. Analyses of strongly abraded best quality grains yield a conservative age estimate given by an upper concordia intercept of 2801 ± 70 Ma, based on 4 single grain analyses, one of which is only modestly discordant (Figure 4.2). The regression is heavily influenced by the errors and placement of the most discordant points. As with 202/2-1, non-uniform Pb-loss has introduced significant scatter in the most discordant zircons and a large uncertainty in the age. Excluding one discordant point from the regression yields $2801.7 +5.1/-4.6$ Ma, which is probably a realistic estimate of the true age of this rock. In any case, this rock is very definitely Archaean in age.

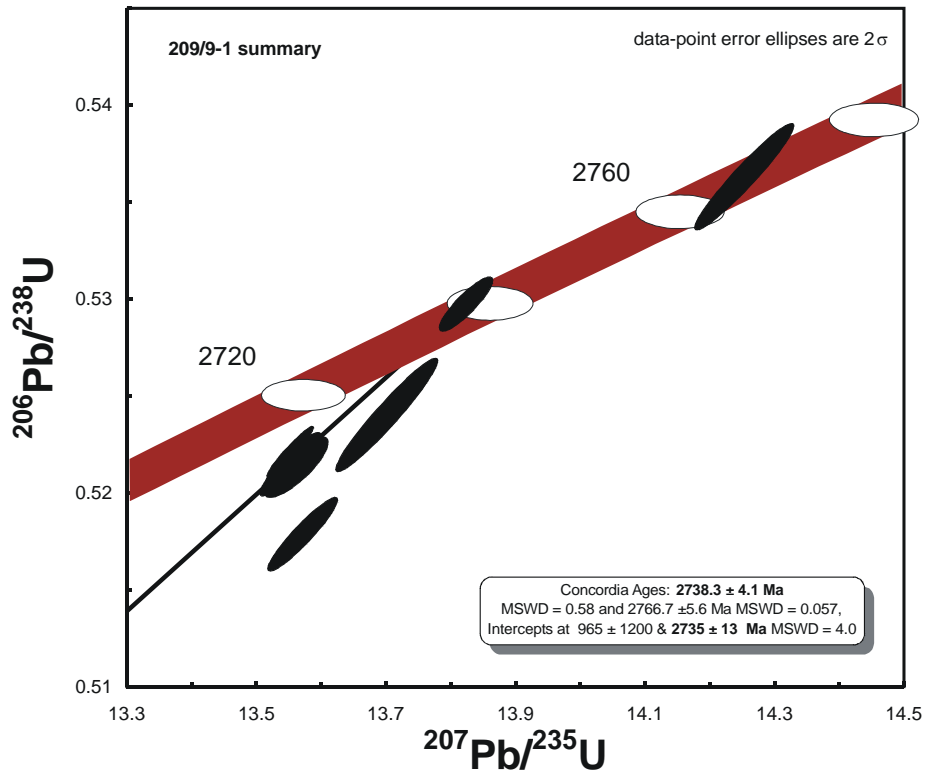


Figure 4.1. 209/9-1 U-Pb concordia plot.

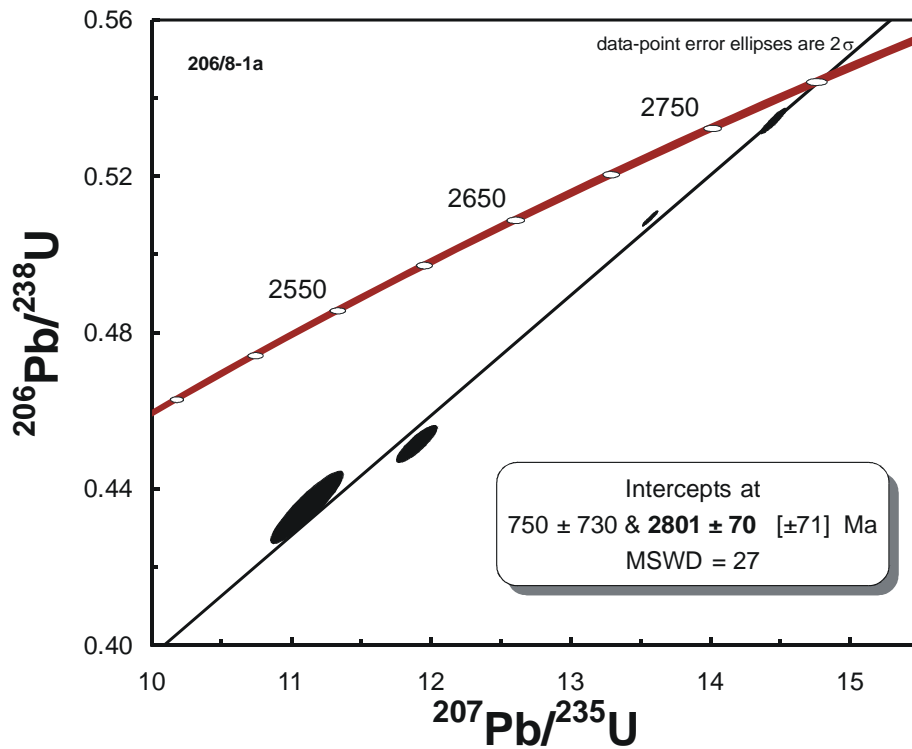


Figure 4.2. 206/8-1a U-Pb concordia plot.

Table 4.1: Rockall Basement U-Pb data

Sample [†]	Sample wt [‡] (μg)	U (ppm)	Pb (ppm)	Common Pb (pg)	²⁰⁶ Pb/ ²⁰⁴ Pb _§	²⁰⁸ Pb/ ²⁰⁶ Pb _§	²⁰⁷ Pb/ ²³⁵ U _#	²⁰⁶ Pb/ ²³⁸ U _#	²⁰⁷ Pb/ ²⁰⁶ Pb _#	²⁰⁷ Pb/ ²⁰⁶ Pb Age (Ma)	ρ**				
209/9-1															
100-09	0.7	890.0	556.4	16	1270	0.1765	13.70	± 0.48	0.5239	± 0.46	0.1897	± 0.14	2739.2	± 2.3	0.96
100-10	1.5	218.9	134.7	4.1	2531	0.1732	13.56	± 0.30	0.5212	± 0.24	0.1887	± 0.18	2730.8	± 2.9	0.81
100-12	0.4	1107	715.3	17	857.0	0.1735	14.26	± 0.44	0.5363	± 0.42	0.1928	± 0.13	2766.2	± 2.1	0.96
130-4	6.7	179.6	116.6	6.5	5855	0.2529	13.55	± 0.22	0.522	± 0.21	0.1883	± 0.06	2727.1	± 1.0	0.96
130-5	10.9	173.3	110.5	3.5	17252	0.2076	13.82	± 0.25	0.5296	± 0.22	0.1893	± 0.12	2736.1	± 1.9	0.88
130-9	9.5	234.4	151.7	5.7	12539	0.2518	13.55	± 0.29	0.5214	± 0.26	0.1885	± 0.12	2729.1	± 1.9	0.91
130-10	11.8	286.5	183.1	4.1	25838	0.2425	13.57	± 0.33	0.5177	± 0.30	0.1901	± 0.12	2743.0	± 1.9	0.93
206-8-1															
97-22	1.0	312.6	171.9	32	250.4	0.09484	11.11	± 1.94	0.4348	± 1.74	0.1853	± 0.81	2701.3	± 13	0.91
97-23	1.1	236.9	139.7	5	1734	0.08782	14.45	± 0.54	0.5340	± 0.49	0.1963	± 0.20	2796.0	± 3.3	0.93
97-24	1.4	169.8	85.43	11	584.9	0.09028	11.90	± 1.0	0.4510	± 0.85	0.1913	± 0.50	2753.8	± 8.2	0.87
130-21	3.1	314.1	179.3	11	2787	0.1083	13.57	± 0.32	0.5089	± 0.31	0.1934	± 0.08	2771.5	± 1.4	0.96
205/22-1															
97-26	0.9	151.8	106.3	5.9	718.9	0.4122	12.85	± 0.73	0.5039	± 0.70	0.1849	± 0.17	2697.3	± 2.7	0.97
97-27	1.7	38.82	23.91	7.9	264.2	0.1259	12.99	± 1.41	0.5064	± 1.33	0.186	± 0.40	2707.4	± 6.5	0.96
100-07	0.3	280.1	177.6	7.4	359.7	0.1957	13.04	± 1.14	0.5095	± 1.08	0.1856	± 0.31	2703.8	± 5.1	0.96
100-08	1.5	229.6	159.7	33	322.1	0.1771	14.34	± 0.78	0.5311	± 0.67	0.1958	± 0.40	2791.6	± 6.5	0.86
202/2-1															
97-18	4.2	216.1	97.01	28	865.0	0.1061	10.10	± 0.36	0.3895	± 0.33	0.1880	± 0.19	2724.5	± 2.4	0.92
117-10	1.0	331.3	172.2	8.1	1013	0.07919	12.50	± 0.41	0.4646	± 0.39	0.1951	± 0.20	2786.0	± 2.4	0.94
130-6	6.2	242.5	113.3	17	2248	0.06321	11.36	± 0.34	0.4284	± 0.33	0.1924	± 0.19	2762.5	± 1.4	0.97
130-7	7.9	391.7	168.1	22	3161	0.09198	10.07	± 0.34	0.386	± 0.32	0.1892	± 0.19	2734.8	± 2.0	0.93
164/25-2															
130-1	37	130	36.67	2.7	29629	0.04821	3.950	± 0.21	0.2855	± 0.20	0.1003	± 0.07	1630.2	± 1.3	0.95
130-2	13.4	90.65	26.04	3.7	5472	0.05263	4.007	± 0.35	0.2884	± 0.32	0.1008	± 0.14	1638.7	± 2.7	0.91
130-3	4.9	86.35	24.75	2.6	2720	0.05329	3.996	± 0.31	0.2885	± 0.28	0.1005	± 0.13	1632.7	± 2.5	0.90

Sample	Sample wt (μg)	U (ppm)	Pb (ppm)	Common Pb (pg)	$^{206}\text{Pb}/^{204}\text{Pb}$	$^{208}\text{Pb}/^{206}\text{Pb}$	$^{207}\text{Pb}/^{235}\text{U}$		$^{206}\text{Pb}/^{238}\text{U}$		$^{207}\text{Pb}/^{206}\text{Pb}$		$^{207}\text{Pb}/^{206}\text{Pb}$ Age (Ma)		ρ
90/14															
97-14	1.9	256.2	140.4	8.1	1783	0.04549	13.21	± 0.32	0.5103	± 0.30	0.1877	± 0.12	2722.4	± 1.9	0.93
97-17	1.1	105.6	57.8	6.1	573.8	0.04224	13.21	± 0.81	0.5051	± 0.79	0.1897	± 0.15	2739.3	± 2.5	0.98
130-17	4.2	228.4	122.1	6.4	4384	0.03641	13.05	± 0.36	0.5062	± 0.34	0.1871	± 0.12	2716.4	± 2.0	0.94
130-18	2.9	322.9	169.9	2.9	9247	0.03712	12.96	± 0.45	0.4986	± 0.43	0.1884	± 0.15	2728.7	± 2.4	0.95
130-19	4.7	185.7	104.8	26	1018	0.04102	13.63	± 0.71	0.5146	± 0.69	0.1921	± 0.17	2759.9	± 2.8	0.97
57-09/536															
101-10	1.0	275.9	171.6	13	665.5	0.1866	13.33	± 0.68	0.5169	± 0.65	0.1870	± 0.15	2686.2	± 2.4	0.98
101-12	2.2	291.7	180.5	15	1384	0.1635	13.73	± 0.34	0.5254	± 0.33	0.1896	± 0.09	2721.9	± 1.5	0.96
101-13	1.0	216.3	140.2	13	540.0	0.2438	13.29	± 0.91	0.5164	± 0.84	0.1866	± 0.30	2684.0	± 4.9	0.94
117-26	0.9	164.1	97.36	4.1	1069	0.1616	13.05	± 0.40	0.5011	± 0.37	0.1889	± 0.15	2732.3	± 2.4	0.93
57-09/537															
100-17	6.1	162.6	99.87	7.1	4301	0.1985	13.11	± 0.37	0.5138	± 0.36	0.1850	± 0.08	2698.3	± 1.3	0.98
100-19	2.8	411.2	249.4	5.1	7272	0.1629	13.63	± 0.34	0.5210	± 0.33	0.1897	± 0.07	2739.7	± 1.2	0.98
130-13	45	116.2	75.7	13	12171	0.2636	13.43	± 0.39	0.5213	± 0.37	0.1868	± 0.12	2714.1	± 1.9	0.95
130-14	35	130.5	81.42	62	2141	0.1726	13.42	± 0.50	0.5237	± 0.48	0.1859	± 0.14	2706.2	± 2.3	0.96
56-08/921															
100-13	1.0	399.4	176	8.3	1189	0.05176	9.086	± 0.37	0.4154	± 0.34	0.1586	± 0.15	2441.3	± 2.5	0.92
100-14	2.8	335.2	194.9	31	899.0	0.2024	12.86	± 0.40	0.5094	± 0.37	0.1832	± 0.16	2681.7	± 2.6	0.92
100-15	1.5	424.3	272.9	28	674.8	0.2087	13.12	± 0.48	0.5124	± 0.43	0.1858	± 0.20	2705.0	± 3.4	0.90
130-23	10.8	274.9	91.95	7.6	7427	0.1026	4.843	± 0.22	0.3199	± 0.21	0.1098	± 0.07	1796.1	± 1.3	0.94
130-22	4.5	55.27	43.07	3.9	1987	0.5295	13.47	± 0.39	0.5229	± 0.37	0.1868	± 0.13	2711.6	± 2.1	0.94
56-08/924															
101-05	1.5	497.3	165.7	7.0	2084	0.0827	4.864	± 0.30	0.3223	± 0.27	0.1094	± 0.12	1790.2	± 2.1	0.92
101-06	1.5	953.0	368.6	70	403.0	0.1338	4.888	± 0.69	0.3225	± 0.28	0.1099	± 0.64	1798.1	± 12	0.38
101-09	2.8	443.3	162.1	46	530.6	0.1077	4.860	± 0.53	0.3220	± 0.28	0.1095	± 0.45	1790.7	± 8.2	0.53
130-28	24.7	226.2	80.47	7.6	14248	0.1724	4.913	± 0.30	0.3218	± 0.28	0.1107	± 0.12	1811.1	± 2.1	0.92
130-32	12	228.0	77.16	6.2	8617	0.1169	4.860	± 0.22	0.3203	± 0.21	0.1101	± 0.07	1800.3	± 1.3	0.95
130-30	9	396.1	132.5	8.7	7945	0.09550	4.876	± 0.27	0.3215	± 0.24	0.1100	± 0.12	1799.1	± 2.2	0.89
56-09/384															
101-03	1.0	1171	401.8	28	806.4	0.07615	4.852	± 0.43	0.3212	± 0.32	0.1095	± 0.28	1791.9	± 5.0	0.76
130-11	4.6	790.4	268.3	4.6	15539	0.07279	5.455	± 0.40	0.3304	± 0.38	0.1197	± 0.13	1952.1	± 2.3	0.95
130-12	3.8	342.4	138.4	3.8	7811	0.1093	7.244	± 0.28	0.3751	± 0.25	0.1401	± 0.12	2227.9	± 2.1	0.90
130-20	13.4	577.6	198	10	15549	0.08608	5.414	± 0.32	0.3308	± 0.30	0.1187	± 0.12	1936.5	± 2.1	0.93

Sample	Sample wt (μg)	U (ppm)	Pb (ppm)	Common Pb (pg)	$^{206}\text{Pb}/^{204}\text{Pb}$	$^{208}\text{Pb}/^{206}\text{Pb}$	$^{207}\text{Pb}/^{235}\text{U}$		$^{206}\text{Pb}/^{238}\text{U}$		$^{207}\text{Pb}/^{206}\text{Pb}$		$^{207}\text{Pb}/^{206}\text{Pb}$ Age (Ma)	ρ	
56-15/18															
100-22	5.6	2954	937.4	23	12597	0.07577	4.593	± 0.18	0.3111	± 0.17	0.1071	± 0.06	1750.2	± 1.2	0.94
100-23	5.0	772.3	246.5	9.7	7457	0.08222	4.580	± 0.20	0.3110	± 0.18	0.1068	± 0.07	1746.0	± 1.3	0.94
100-24	1.8	2086	651.3	11	6755	0.06170	4.574	± 0.23	0.3106	± 0.22	0.1068	± 0.07	1745.6	± 1.2	0.95

† Sample numbers correspond to NIGL U-Pb lab run numbers.

‡ Maximum errors are $\pm 20\%$. Weights were measured on a Cahn C32 microbalance.

§ Measured ratio corrected for mass fractionation and common Pb in the $^{205}\text{Pb}/^{235}\text{U}$ spike.

Corrected for mass fractionation, spike, laboratory blank Pb and U, and initial common Pb (Stacey and Kramers, 1975, with an uncertainty of 2% propagated through calculations).

The laboratory blank Pb composition is $^{206}\text{Pb}/^{204}\text{Pb} : ^{207}\text{Pb}/^{204}\text{Pb} : ^{208}\text{Pb}/^{204}\text{Pb} = 17.46 : 15.55 : 37.32$. Quoted errors are 2 sigma (% for atomic ratios, absolute for ages).

** $^{207}\text{Pb}/^{235}\text{U} - ^{206}\text{Pb}/^{238}\text{U}$ error correlation coefficient (ρ) calculated following Ludwig (1980).

205/22-1. Three single grain analyses (see Figure 4.3) from this rock yield a concordia upper intercept age of 2700 ± 13 Ma with the lower intercept forced through 0 Ma. The three analyses are slightly discordant and overlap with each other well within analytical error (Figure 4.4). There is no evidence for a non-zero lower intercept age in this data set. A fourth analysis is significantly older and is interpreted as the product of c. 2700 Ma growth and an inherited core ($^{207}\text{Pb}/^{206}\text{Pb}$ age of 2792 Ma). A discordia regressed through all of the data would yield a much older “age” of c. 2.9 Ga, but this scenario is not likely.

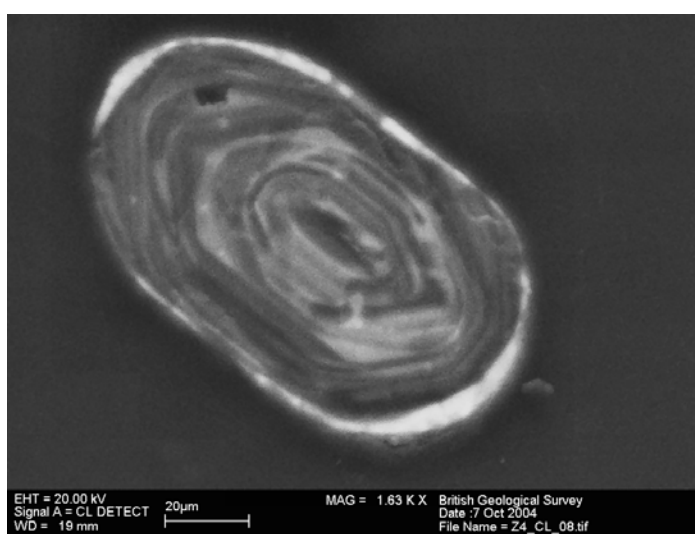


Figure 4.3. 205/22-1 SEM-CL photo of a zircon showing primary oscillatory zoning and a thin metamorphic overgrowth (bright).

202/2-1. Zircons from this sample range in quality from very poor to moderate. Almost all grains show minor turbidity and rounding of outer surfaces, and many have internal cracks. The crystals are colorless, typically 50-100 μm long with 2:1 – 5:1 aspect ratios. The best estimate of the age at 2829 ± 46 Ma is given by an upper concordia intercept of a regression through 4 data points. The data were obtained on moderate quality zircons (minimal cracks, transparent) that were abraded to remove several microns off of all outer surfaces. Despite this treatment the zircons are significantly discordant. The relatively imprecise upper intercept age is a consequence of this high degree of Pb-loss. What is not in doubt is that the zircons are Archaean, and that they are a single population.

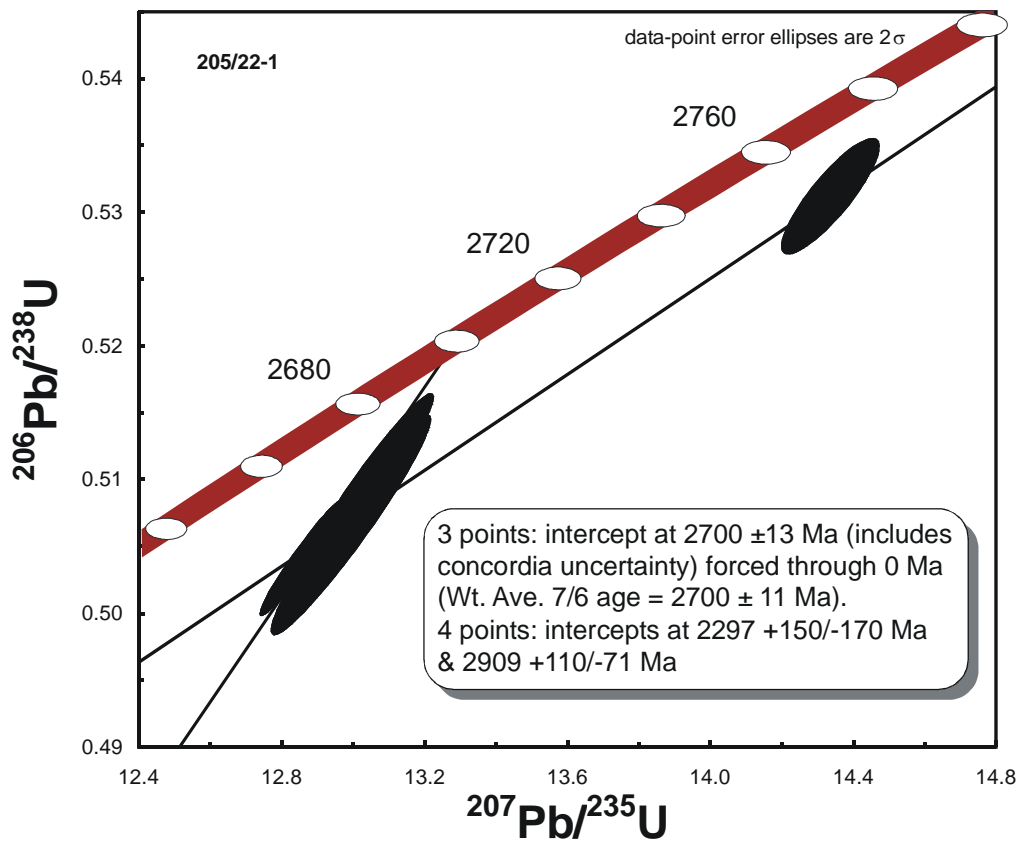


Figure 4.4. 205/22-1 U-Pb concordia plot.

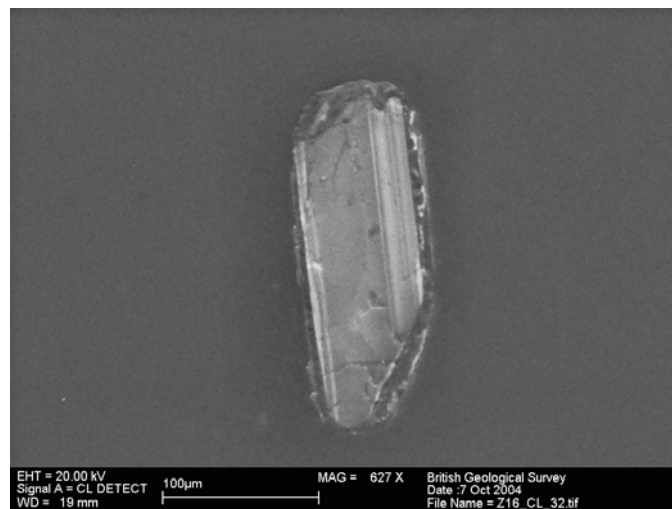


Figure 4.5. 202/2-1 SEM-CL photo of a zircon showing primary oscillatory zoning and a thin metamorphic overgrowth.

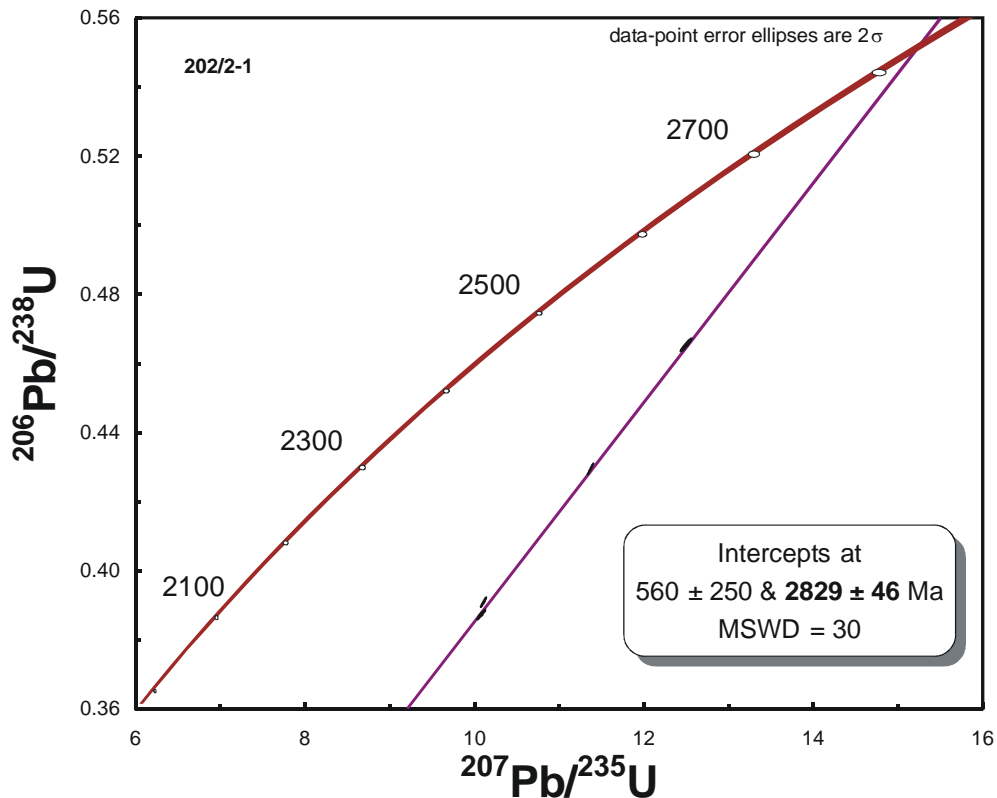


Figure 4.6. 202/2-1 U-Pb concordia plot.

164/25-2: Zircons in this sample are limpid, colorless to pale lilac flawless subrounded crystals with 1:1 to 3:1 aspect ratios. Large angular anhedral ($>100 \mu\text{m}$) fragments of very much larger grains are also present. Three multigrain fractions of 60-100 μm long limpid colorless and strongly abraded grains (Figure 4.7) were analysed and the data are illustrated in Figure 4.8. The data points have small uncertainties and are nearly concordant. One point shows minor Pb-loss, and there are two nearly overlapping ellipses within error of concordia. The age of this rock is 1633.5 ± 3.3 Ma based on the perfectly concordant analysis. The slightly older data point indicates that one of the crystals in the multigrain fraction had a very small, inherited component. Inclusion of a grain with an older core is consistent with identification under the binocular microscope of a small number of grains that had clearly visible inherited cores.



Figure 4.7. 164/25-2: Photo of abraded large grain fragments and limpid small grains. Scale bar is 300 μm .

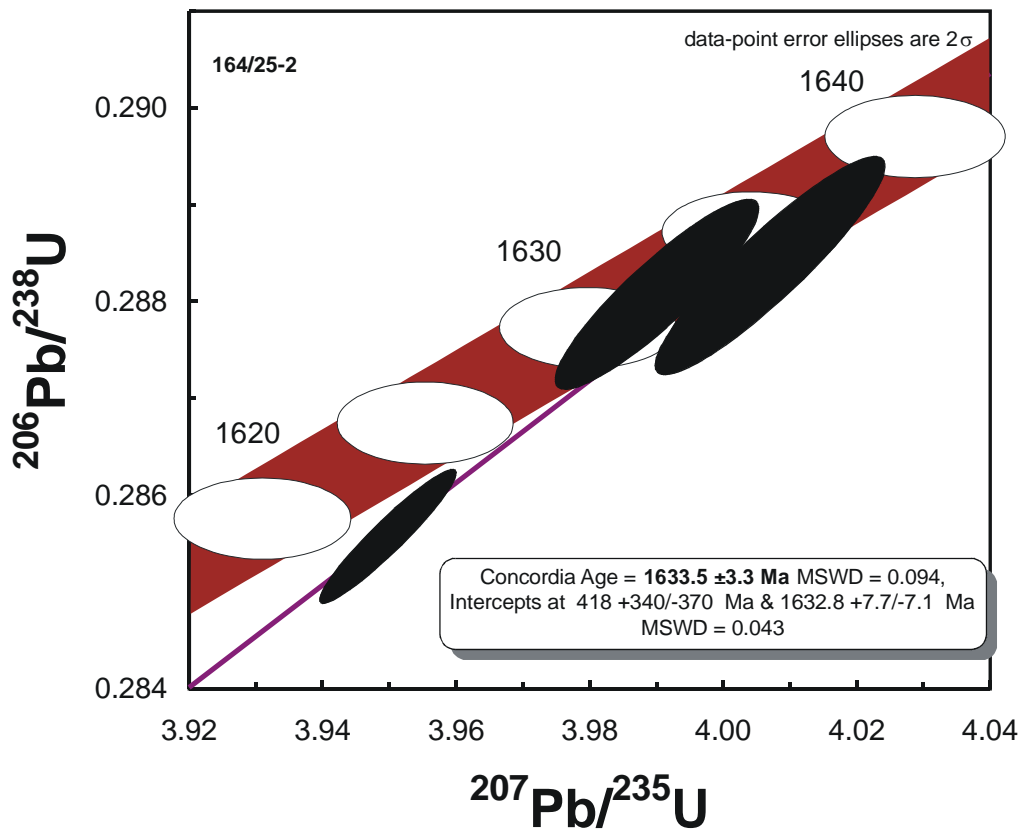


Figure 4.8. 164/25-1 U-Pb concordia plot.

90/14. Zircons from this sample have a wide range of characteristics. Some crystals have clearly visible cores and overgrowths. Others are composite crystals comprising two contrasting grains welded together along a face, or are broken crystals with healed fractures. Most grains have rounded outer surfaces while some have moderately preserved facets. Zircons analysed were limpid pale brown to colourless grains 50-80 μm long, with aspect ratios of 2:1 to 3:1 (Figure 4.9). The grains selected were judged to be from a single population based on binocular microscope observations. The resultant data show that at least two populations are present and that a unique crystallization age for the rock cannot be determined (Figure 4.10). The data are significantly discordant despite strong abrasion to remove damaged crystal domains. This degree of disturbance preserved in even the most robust parts of the crystals is suggestive of Pb-loss induced by high-grade metamorphism.

It is probable that the five single grain analyses outline two main ages of zircon growth with Pb-loss at a common time in the Proterozoic. Discordia lines regressed through the zircons give upper and lower intercepts of $2767 \pm 100/-37 \text{ Ma} - 1365 \pm 800/-590 \text{ Ma}$ and $2820 \pm 52/-31 - 1605 \pm 300-250 \text{ Ma}$. What is clear is that all of the zircons are Archaean in age, as reflected by the, albeit poorly constrained, upper intercepts.

Proterozoic-age rocks dated in this study (see below) offer a plausible time of disturbance of the U-Pb systematics in these Archaean grains, with the latest event being $c. 1745 \pm 2 \text{ Ma}$. If discordia are anchored at this lower intercept age then upper intercepts of $2767 \pm 14/-15 \text{ Ma}$ and $2838 \pm 15 \text{ Ma}$ are obtained. Both upper intercepts are plausible ages for Lewisian-type rocks. The two possible upper intercept ages could mean that 90/14 is actually a paragneiss derived from TTG protoliths of two different ages, or that it is a rather complex orthogneiss with two generations of TTG melt injection but whose textural interrelationships are completely obscured by subsequent metamorphism.

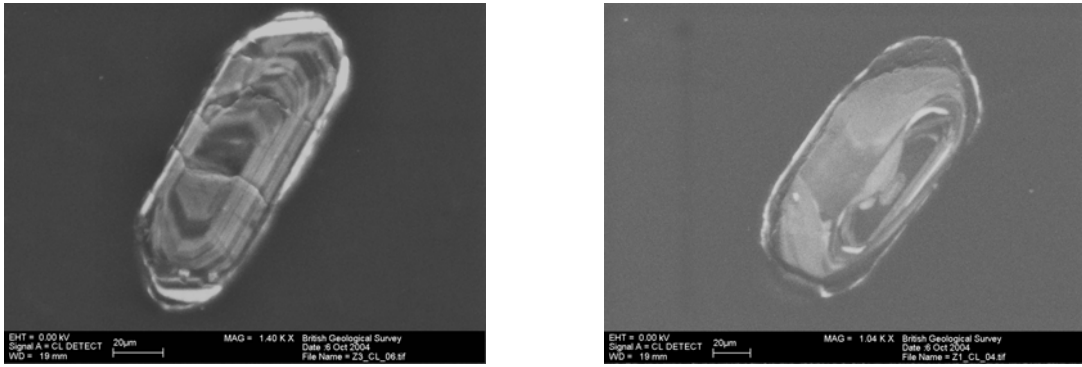


Figure 4.9. 90/14 SEM CL zircon images: (a) shows a grain with primary magmatic oscillatory zoning and a thin (bright) metamorphic overgrowth. (b) shows a grain with relict magmatic zoning in the core, surrounded by a broad sector-zoned region, and a dark outer zone of as yet unknown affinity.

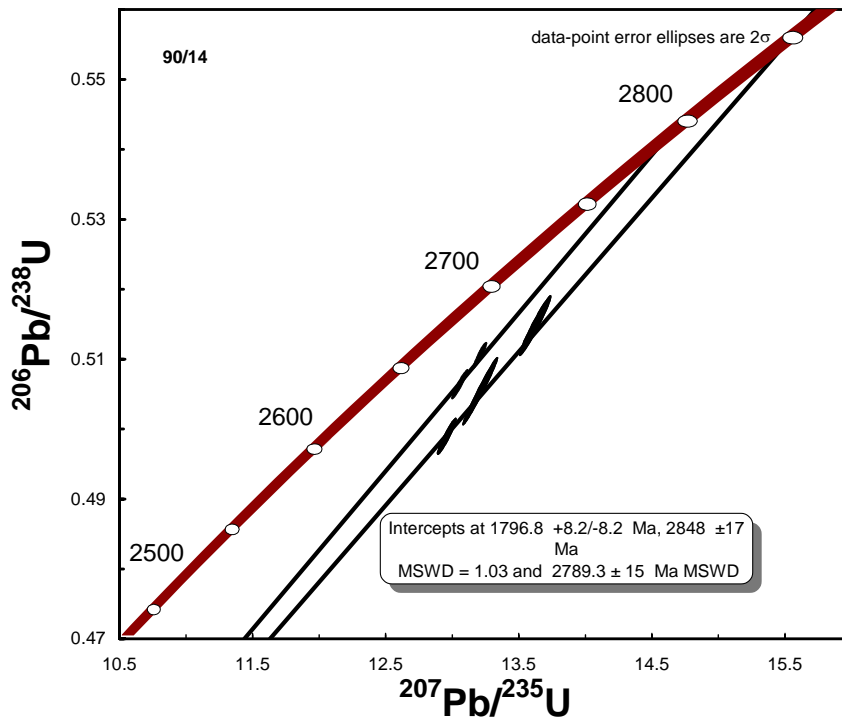


Figure 4.10. 90/14 U-Pb concordia plot.

56-09/536 and 537. Both samples were analysed to test if the gneisses were indeed similar, as expected from the proximity of the boreholes. The resulting data set is rather complex. Five analyses were obtained for sample 56-09/537. Zircons in this rock are either fragments of well-faceted $>200 \mu\text{m}$ long limpid pink acicular grains, 2:1 – 5:1 50-100 μm good quality crystals, irregular grains with thin overgrowths, or euhedral crystals with rounded cores comprising c. 50% of the grain volume (Figure

4.11). Three analyses obtained on the highest quality limpid grains have the youngest $^{207}\text{Pb}/^{206}\text{Pb}$ ages and are collinear (Figure 4.12). A discordia regressed through them gives an upper intercept age of 2704 ± 9 Ma. One of the points is concordant and yields a concordia age of 2709 ± 6 Ma. Two other data points for this rock are older, one only slightly, the other by >10 Ma, suggesting either inheritance or xenocrysts.

Zircons from sample 56-09/536 are in general much poorer in quality, cracked, and in some cases are complexly fragmented, partly resorbed and welded back together along fracture surfaces. Analysis of strongly abraded best quality grains (minimum of cracks, best faceted, euhedral) are similar to 56-09/537 in that two analyses overlap within error of the c. 2714 Ma point. Two other analyses are significantly older and interestingly they have similar $^{207}\text{Pb}/^{206}\text{Pb}$ ages to the oldest 56-09/537 analysis.

The “age” of gneiss 56-09/537 is considered to be most reliably recorded by the concordant 2709 Ma analysis. This age is based upon strongly abraded zircon grain tips and thus would record the last phase of magmatic growth in the rock. The older analyses are entire grains and record older growth episodes. Regressions through these data yield upper intercepts at 2715 and 2738 Ma; remarkably close in age to the 2713 Ma zircon in 56-09/924 and 2738 Ma zircon in 209/9-1. These older zircons could be accounted for by the gneiss recording polyphase melt injection, or a gneiss protolith representing a crustal melt derived from 2715-2738 Ma sources at 2709 Ma.



Figure 4.11. 56-09/536 and 537 SEM CL and plane light binocular views of zircons. Scale bars in PL views are 200 μm . (a) PL view of a complex composite grain from 56-09/536. (b) SEM CL image of a grain similar to (a). Note the chaotic internal zonation, sometimes noted from granulite facies grains. (c) PL image of large high quality zircons from 56-09/537. (d) SEM CL image of a high quality grain from 56-09/537, showing a low luminescence overgrowth surrounding a zoned core. The zoning probably represents granulite facies equilibration.

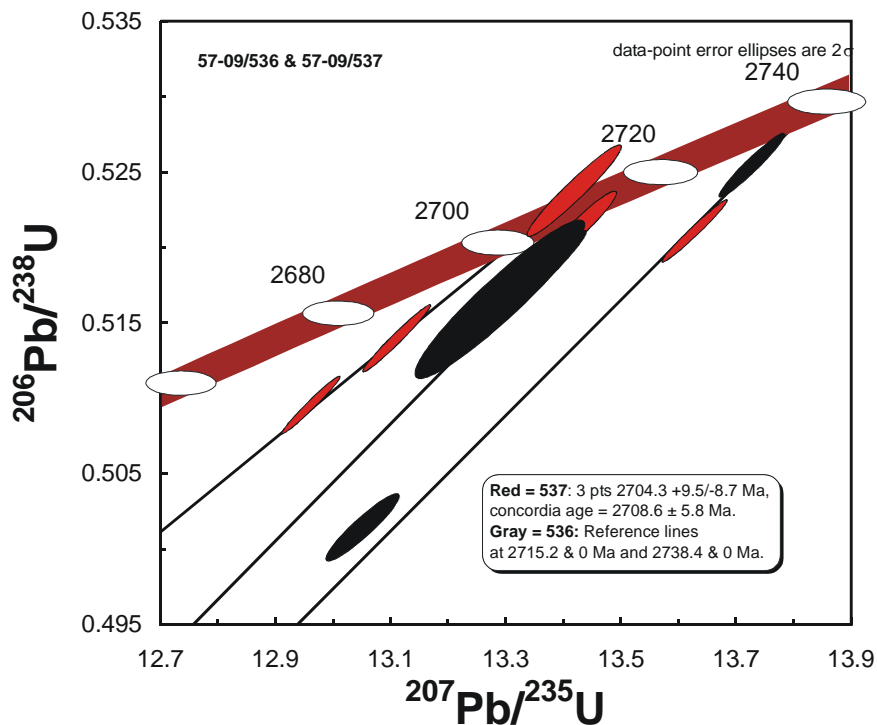


Figure 4.12. 56-09/536 and 537 U-Pb concordia plot.

56-08/921. The zircons from this sample provide very clear evidence of two main episodes of growth (Figure 4.13). Most crystals are euhedral 2:1 50-100 μm long pinkish brown crystals with no obvious core-rim relationships detected under the binocular microscope. Exceptions include some composite grains that appear to have a well faceted domain growing orthogonally away from the long surface of less well-faceted grain. The data obtained from the best quality zircons plot along a mixing line stretching between ~ 2713 Ma and ~ 1792 Ma, with the end members pinned by concordant analyses (Figure 4.14). The rest of the analyses range from modestly discordant Archaean grains to a $\sim 50\%$ discordant fraction. This latter analysis represents more or less equal amounts of Archaean and Proterozoic material. The concordant single grain analyses at the ends of the mixing line have concordia ages of 1791.5 ± 2.9 Ma and 2713.3 ± 5.2 Ma. These analyses indicate either partial melting of 2713 Ma crust at 1791 Ma, or high-grade metamorphism of an Archaean protolith at 1791 Ma that was significant enough to produce entirely new crystals.

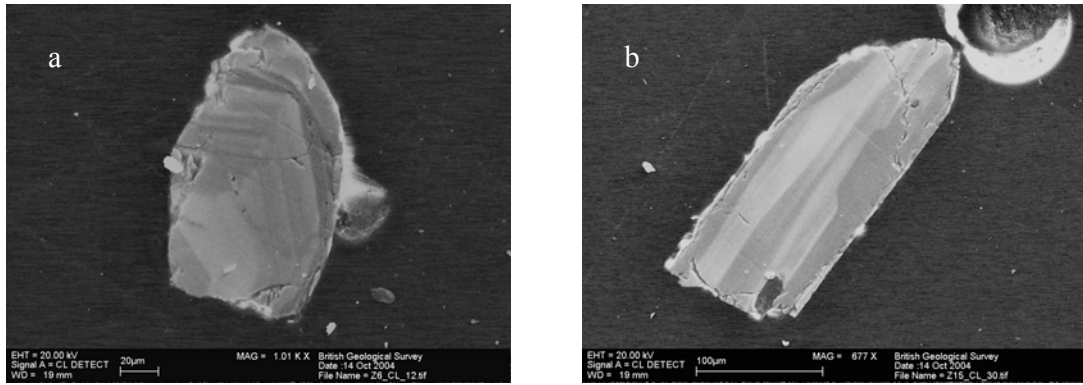


Figure 4.13. 56-08/921 SEM CL images of (a) fragment of a relatively undisturbed zircon grain tip, and (b) elongate grain with metamorphic zoning.

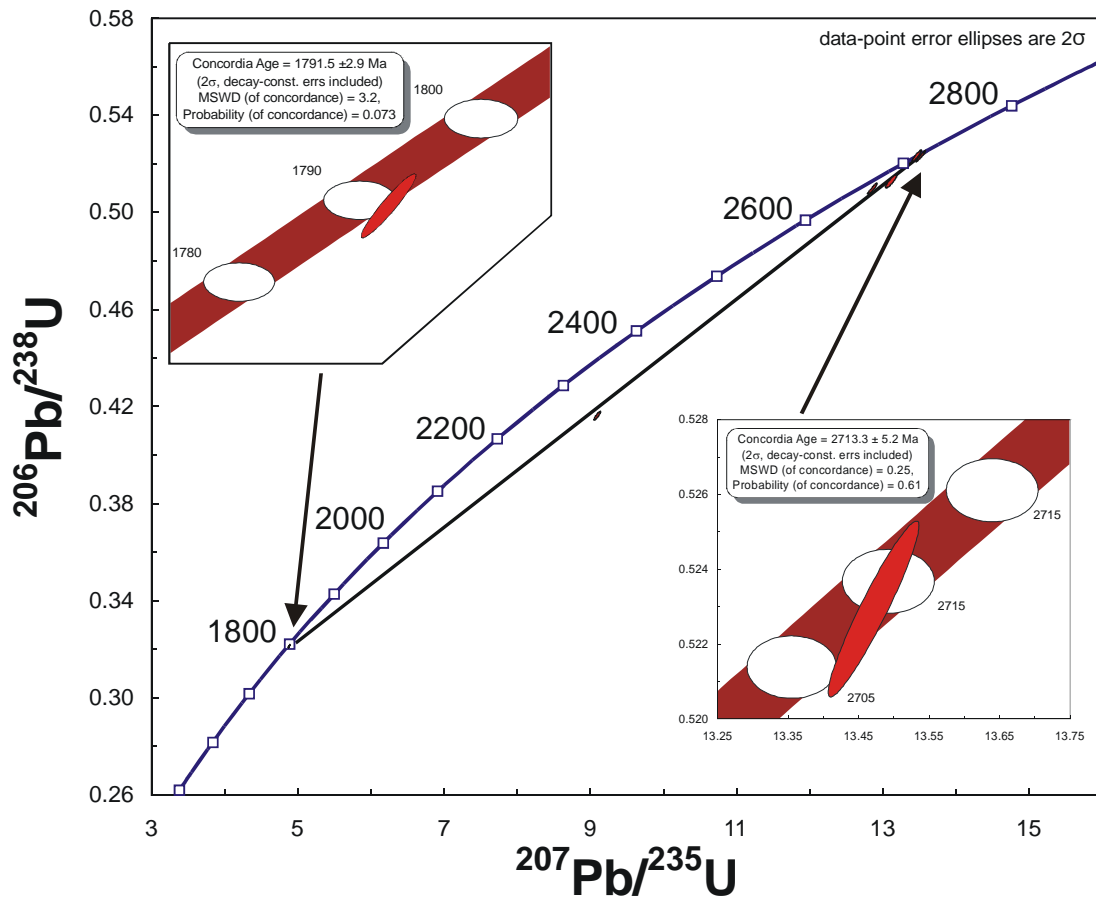


Figure 4.14. 56-08/921 U-Pb concordia plot.

56-08/924. The majority of zircons in this sample appear to be a single generation and are euhedral and sharply faceted with little or no turbidity and only a few opaque inclusions (Figure 4.15). The interpretation of the data obtained on the best quality abraded grains is straightforward. Zircons in this sample are confirmed as essentially representing a single generation with only a suggestion of Pb-loss or inheritance. Three data points are concordant and their combined concordia age is 1799 ± 2.5 Ma, within error of the best analysis (analysis with the lowest uncertainty) at 1797.8 ± 3.2 Ma (Figure 4.16). Three other points are very slightly discordant are thus not included in the calculation but indicate relatively little disturbance in this rock.

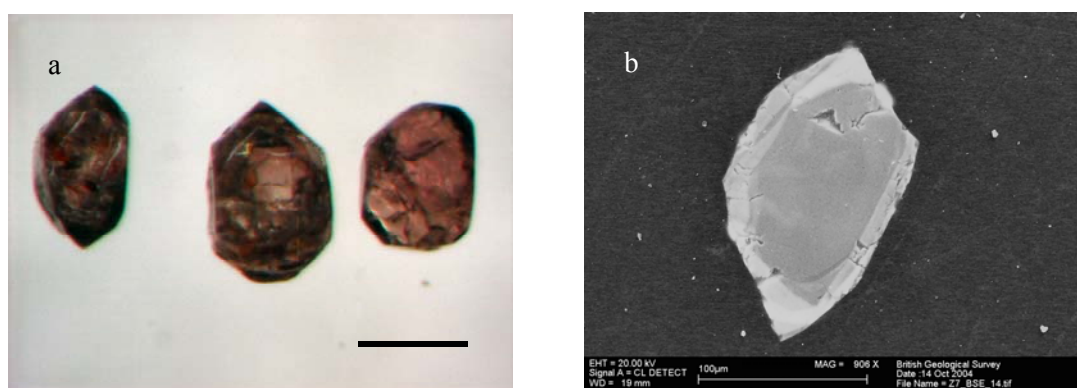


Figure 4.15. 56-08/924 SEM CL and plane light binocular views of euhedral zircon crystals. Plane light view (a) shows pristine outer surfaces. Scale bar is 200 μm . SEM CL image (b) shows little internal zoning.

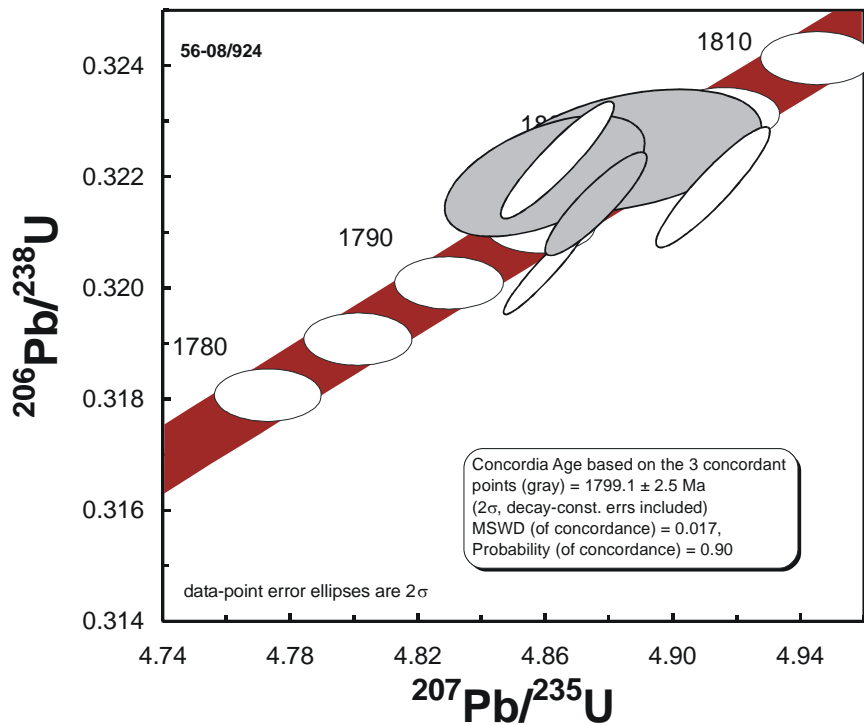


Figure 4.16. 56-08/924 U-Pb concordia plot.

56-09/384. Zircons from this rock range from flawless euhedral crystals to those with slightly cloudy to very turbid cores with flawless overgrowths (Figure 4.17). Four analyses of high-quality strongly abraded grains were obtained. One analysis is concordant at 1794.4 ± 4.2 Ma, and is interpreted as the time of latest zircon growth and the age of the rock (Figure 4.18). The other analyses are discordant and trend along a c. 1790 – 2800 Ma discordia, indicating widespread cores that are not detectable under the binocular microscope.

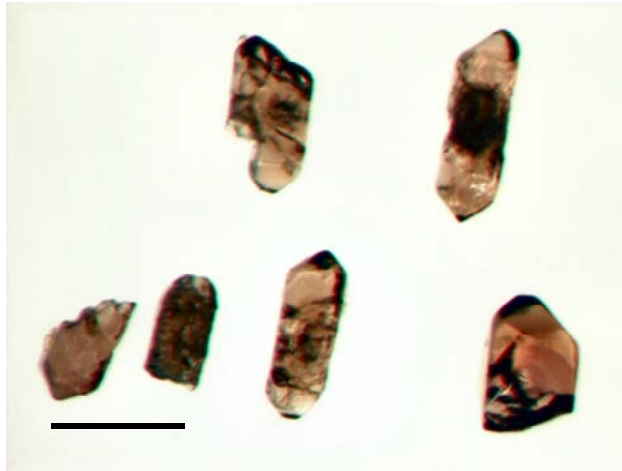


Figure 4.17. 56-09/384 Zircon crystals showing turbid cores and neocrystalline brown relatively undisturbed overgrowths. Scale bar is 200 μm .

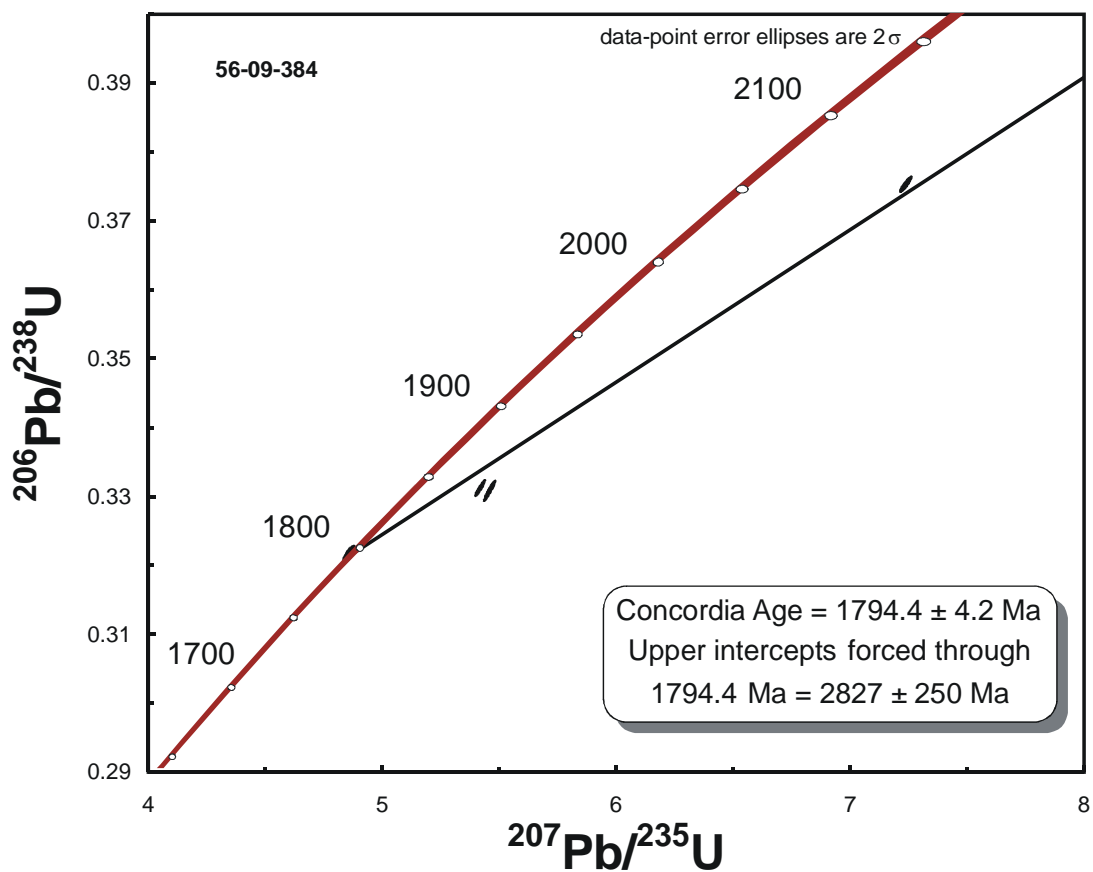


Figure 4.18. 56-09/384 U-Pb concordia plot.

56-15/18. The data interpretation for this sample is straightforward. The age is 1744.9 ± 2.2 Ma, based on the concordia age of two excellent concordant analyses obtained on high quality strongly abraded zircons (Figure 4.19). A third analysis is slightly older, indicating a very minor inherited component (Figure 4.20).

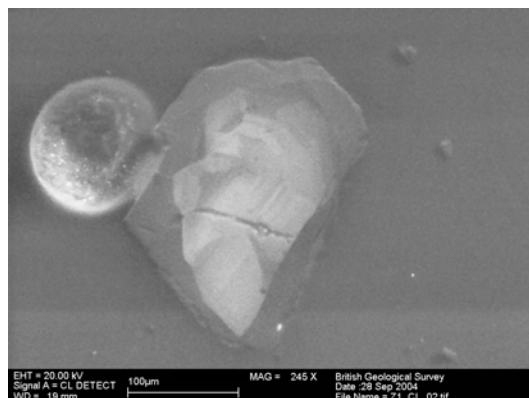


Figure 4.19. 56-15/18 SEM CL image of a subhedral grain fragment. Note the internal sector zoning and the surrounding dark region, atypical of normal igneous zoning.

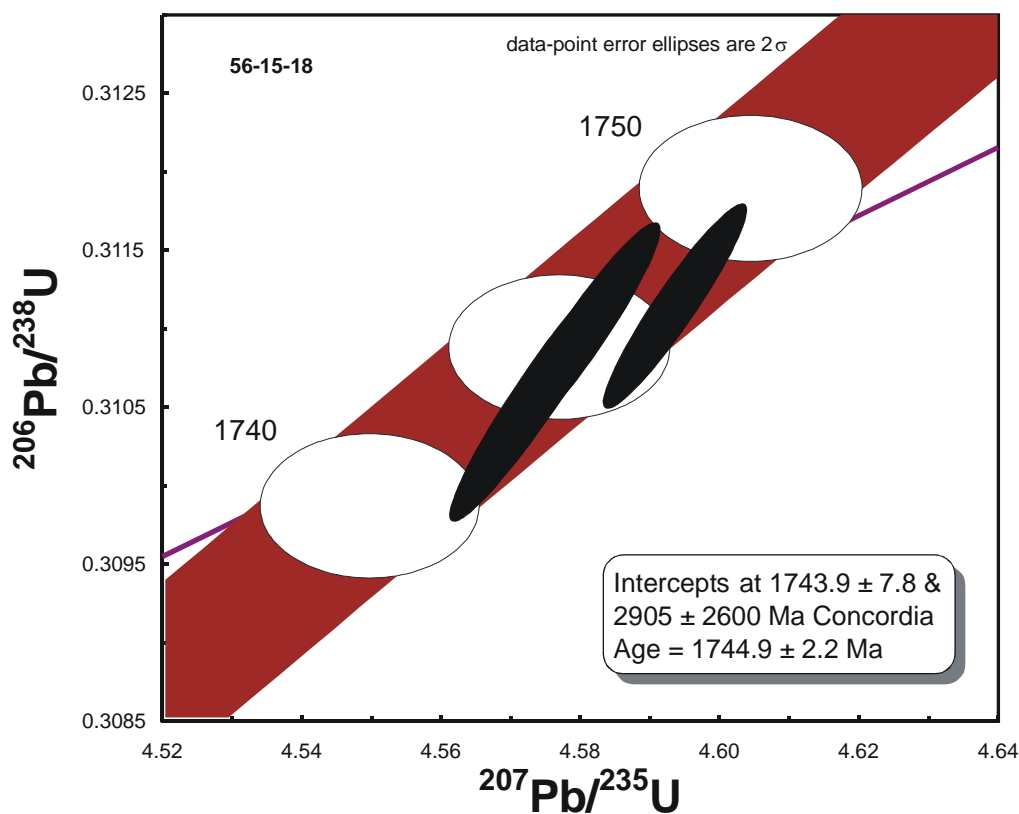


Figure 4.20. 56-15/18 U-Pb concordia plot.

4.1.1 U-Pb Geochronology Discussion

The rocks in this study can be clustered into three main groups, with two stand-alone ages. The summary concordia plot (Figure 4.21) illustrates these groupings, together with the main regional tectonothermal events.

Circa 2800 Ma gneisses are the oldest rocks dated in the offshore region. They include 202/2-1 (2829 ± 46 Ma), 206/8-1A (2801 ± 70 Ma) and 90/14. All three rocks have modestly to moderately discordant zircons with Pb-loss trajectories tending towards 0 Ma. The available SEM CL images show that the zircon overgrowths are absent or only modest. The grains are primarily magmatic with relict oscillatory zoning that is disrupted by sector and fir-tree zoning typical of granulite facies recrystallization (c.f. Corfu et al. 2003). The relict primary zoning suggests that the zircons did not crystallize under granulite facies conditions and that the metamorphism occurred later. Evidence for zircon inheritance is absent in 202/2-1 and 206/8-1a and thus there is no indication of a significant contribution to the parental TTG magmas by older intermediate to granitic crust. 90/14 is more complicated, in that the two possible upper intercepts for the data set (2848 ± 17 Ma, 2789 ± 15 Ma) could indicate the rock is a paragneiss derived from at least two Archaean protoliths, or that it is an Archaean orthogneiss with a >2.8 Ga protolith age overprinted by granulite-facies metamorphism at 2.77 Ga. Archaean metamorphism at this time has been suggested for some parts of the Gruinard Terrane (Whitehouse et al. 1997, Corfu et al. 1998). The lack of a c. 2.49 Ga lower intercept for the data arrays for these rocks suggests that the very significant 2480-2490 Ma granulite facies metamorphism ('Inverian event'), recorded throughout the central mainland Assynt terrane, did not affect these rocks (Corfu et al., 1998, Kinny et al., 2005).

A second group of Archaean rocks range in age from c. 2.74-2.70 Ga, and include 205/22-1 (2700 ± 13 Ma), 209/9-1 (2738.3 ± 4.1 Ma), 56-09/536 and 56-09/537 (2709 ± 6 Ma). All of these rocks have evidence for zircon inheritance, and the data are much less discordant than the c. 2800 Ma group. The inheritance indicates that some recycling of older continental crust was involved in the genesis of these 2.74-2.70 Ga rocks. All of the zircons have fir-tree and broad sector zoning with little or no oscillatory zoning preserved. This is good evidence for growth under, or complete overprinting by, granulite facies metamorphism. As with the 2.8 Ga TTG's above, there is no evidence for the 2.49 Ga Inverian granulite-facies event in these rocks. On

a regional scale, this data set resembles the TIMS U-Pb data for Gruinard Terrane tonalite and trondjemite gneisses reported by Corfu et al. (1998), and is likely part of a widespread Lewisian tectonometamorphic and magmatic event (Corfu et al. 1994, 1998; Love et al. 2004; Whitehouse et al. 1997).

It is noteworthy that 1.9-1.83 Ga rocks were not encountered in this study. Magmatic activity is recorded in the Outer Hebrides (Mason et al. 2004a) around 1.88 Ga. This region was then affected by ultra high-pressure granulite-facies metamorphism at c. 1.83 Ga (Baba 2003; Cliff et al. 1998). Given the aerially restricted nature of these rocks it is perhaps not surprising the drilling program did not encounter them.

The third group comprises the most southerly Hebridean terrane samples, which include those occurring on the Stanton High, crystallized or were strongly reworked at c. 1790- 1800 Ma. 56-08/921 is clearly a 2713.3 ± 5.2 Ma Archaean gneiss that suffered granulite facies metamorphism based on zircon CL textures. The evidence for crustal re-working is documented by the oscillatory-zoned 1791.5 ± 2.9 Ma neocrystalline zircon tip. Further evidence of crustal reworking at this time is given by 56-09/384 (1794.4 ± 4.2 Ma), which similarly has Archaean inheritance (2827 ± 250 Ma) but the contribution of new zircon growth in the rock suggests either more dramatic reworking, or that the rock is originated from a granodioritic melt sourced from a mixture of Archaean and Proterozoic material. 56-08/924, on the other hand, contains no evidence for significant zircon inheritance and crystallized at 1799.1 ± 2.5 Ma. This Proterozoic episode is essentially the same as the juvenile crustal additions recorded by the Inishtrahull gneisses in Ireland (1779 ± 3 Ma, Daly et al. 1991) and the $1782 \text{ Ma} \pm 5 \text{ Ma}$ Rhinns gneiss complex (Marcantonio et al. 1988).

The Rockall sample 56-15/18 (1744.9 ± 2.2 Ma) corroborates the findings of Scanlon and Daly (2001) for Rockall Bank, who obtained ages of 1755 ± 9 Ma, 1753 ± 1 Ma, and 1745 ± 2 Ma for three syenodiorites to syenites. The data unequivocally indicate that these granulite-facies metamorphosed intrusions crystallized after the Rhinns-related event. It is interesting to note that these intrusions are approximately coeval with the thermal disturbance on the mainland recorded by titanite growth in the Laxford area, interpreted as the age of docking of the putative Assynt and Rhiconich terranes along the Laxford shear zone (Kinny et al. 2005).

The youngest sample in the study, the 1633.5 ± 3.3 Ma mafic rock 164/25-2, surprisingly contained sufficient zircon for geochronology and postdates all other

Mesoproterozoic lithologies in the region. The nearest ages from the British Isles are c. 1675 Ma pegmatites from Harris (Friend and Kinny, 2001; Mason and Brewer, 2005) and a weak thermal event recorded by titanite in a Gruinard Bay trondhjemite (Corfu et al. 1998). On a regional scale, similar ages have been recorded for the Vyborg intrusive suite (1.65 – 1.62 Ga, Åhäll et al. 2000) related to Gothian orogenesis in the Baltic Shield and in the Labradorian orogeny recorded in the Grenville Province of eastern Labrador, which involved terrane accretion and crustal thickening from 1.65 – 1.63 Ga (Gower et al. 1992; Kamo et al. 1996).

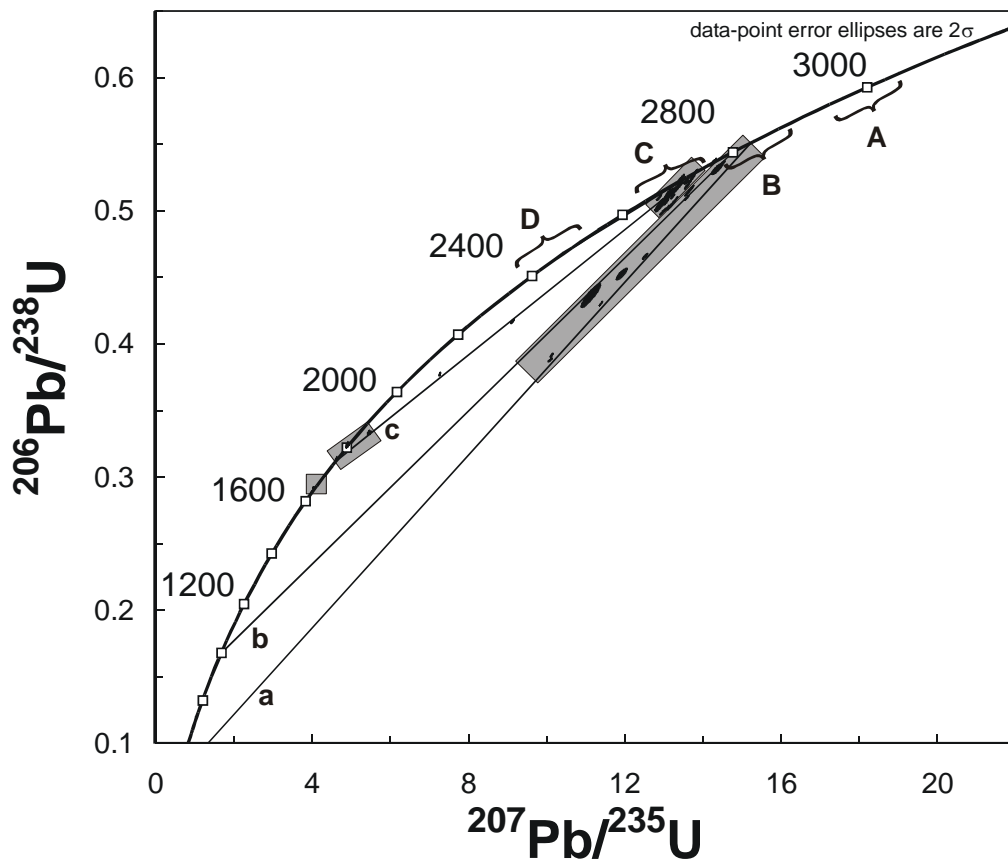


Figure 4.21. U-Pb geochronology summary. “A” indicates the age of the oldest TTG’s in the Lewisian (Assynt, Harris), “B” is the range of ages for the c. 2.8 Ga Lewisian gneisses typical of Gruinard and Outer Isles, “C” indicates the c. 2.75 Ga tonalite-trondjemite granulite facies suite and granulite facies metamorphism (Gruinard), “D” indicates the ‘Inverian’ granulite facies event. Shaded boxes highlight offshore 2.8 Ga, 2.73 Ga, 1.79-1.75 Ga and 1.66 Ga rocks. Reference lines a, b and c indicate Pb-loss or mixing arrays from 2.84 - 0.45 Ga, 2.8 – 1.0 Ga, and 2.73 – 1.79 Ga.

4.2 COMMON Pb ISOTOPE CHARACTERISTICS OF THE ROCKALL BASEMENT.

During the Rockall volcanic project, which ran concurrently with this study, a limited number of whole rock common Pb analyses were obtained on basement samples. The aim was to provide constraints on potential end-member compositions for Pb isotope basement-volcanic mixing calculations. The data are also relevant to this work and are therefore included here.

It is known from previous studies that some granulite-grade gneiss terranes have Pb isotope systematics that are difficult to impossible interpret with a single unambiguous scenario because there often several ways for the Pb-Pb system to evolve to the isotope compositions observed at the present day. The main problem stems from superposition of high-grade metamorphic events capable of significantly fractionating U-Th-Pb, coupled with differential response to these events depending upon lithology. To completely understand the common Pb system in such rocks an in-depth knowledge of the field geology is vital. In the case of the Rockall basement such a detailed study is impossible given that each borehole sample is essentially a snapshot of the basement that must be extrapolated over a considerable area. Furthermore, a detailed study would require an analytical program that is beyond the scope of the present project.

Nevertheless, useful information is provided by the present limited data set. Present day Pb isotope compositions of the basement samples are illustrated in Figure 4.22 and summarized in Table 4.2. The data plot in a diffuse group, falling generally below the Stacey and Kramers (1975) average crustal growth curve. Many samples plot within the range of Pb isotope compositions typically measured for Lewisian 2.8 Ga crust from the mainland, the Inner and Outer Hebrides (Moorbath et al. 1969, Whitehouse, 1989, 1990; Cohen, O’Nions and O’Hara, 1991; Dickin and Durant, 2002).

For a number of samples what is known from the U-Pb and Sm-Nd isotope systematics is reflected in the common Pb isotope compositions. Pb data for Archaean samples, as identified by U-Pb and Sm-Nd isotopes (e.g. 202/2-1 or 56-09/536) fall entirely within the field of typical Lewisian basement, and also relatively close to a 2.8 Ga reference line. Rocks that show evidence for metamorphic zircon growth or

that entirely crystallized at c. 1.8 Ga but also have 2.8-3.0 Ga Nd model ages (e.g. 56-08/921, 56-08/924), also have Pb isotope characteristics typical of Lewisian crust. Finally, samples that have not been dated by U-Pb but whose Nd model ages are intermediate between Archaean and mid-Proterozoic ages, and thus are suggestive of mixed Archaean-Proterozoic sources (e.g. 132/15-1), similarly have Pb isotopes characteristics consistent with either derivation entirely from an Archaean source, or mixing of Lewisian and Rhinns-type sources.

In contrast to the above, data from the 206 and 207 series boreholes plot above the typical Lewisian field and overlap with the Rhinns data field. These samples have Archaean Nd model ages. Their common Pb compositions, which are probably much less robust than the Nd systematics given the history of granulite and amphibolite facies metamorphism in the region, have either originated with much higher $^{238}\text{U}/^{204}\text{Pb}$ ratios (μ value) than the “Lewisian” compositions of some Rockall samples, or more likely, have evolved from relatively low μ -sources and then suffered a complex multistage Pb isotope history, as has been noted for some mainland Lewisian rocks.

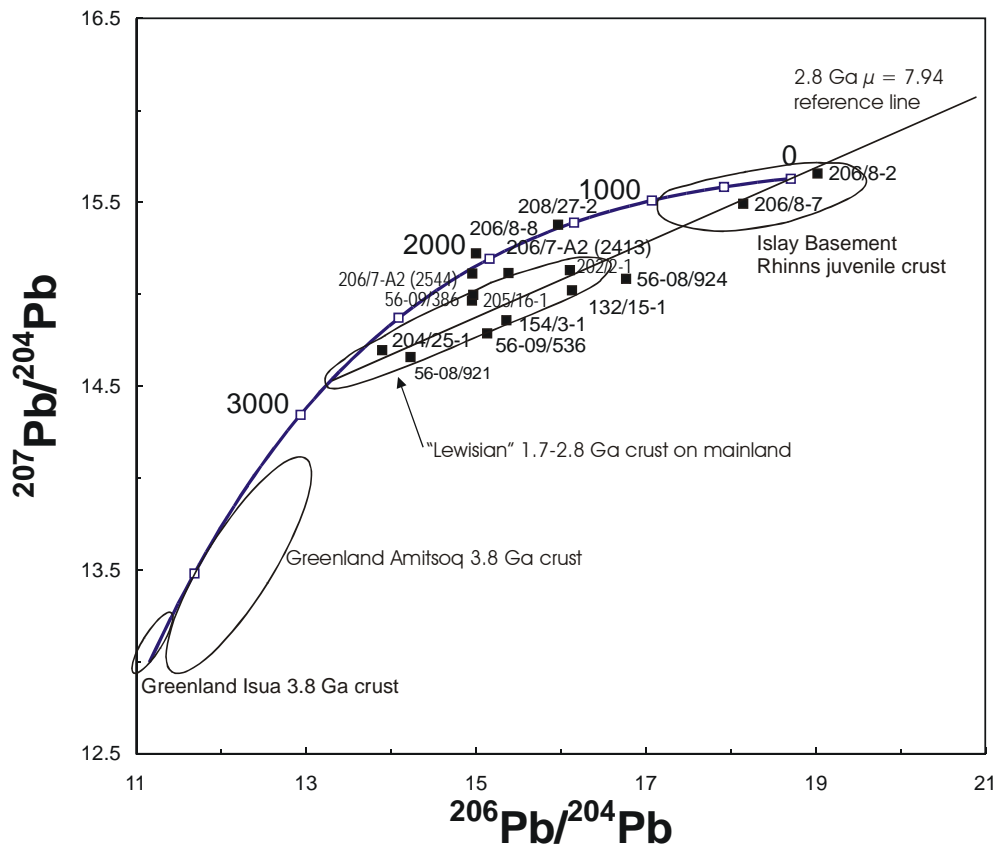


Figure 4.22. Rockall basement $^{206}\text{Pb}/^{204}\text{Pb}$ vs. $^{207}\text{Pb}/^{204}\text{Pb}$ common Pb whole-rock plot. A 2.8 Ga reference line, Stacey and Kramers (1975) crustal growth curve. Also shown is are approximate data fields for 1.8 Ga Rhinns intrusive rocks, and 3.8-3.6 Ga granulite facies Greenland crust (Frie and Rossing 2001, Kamber and Moorbath 1998).

Table 4.2. Rockall Basement Whole Rock Common Pb Data

Sample number	Pb conc in ppm	U conc in ppm	Th conc in ppm	²⁰⁶ Pb/ ²⁰⁴ Pb measured	²⁰⁷ Pb/ ²⁰⁴ Pb measured	²⁰⁸ Pb/ ²⁰⁴ Pb measured	%206	%207	%208	%204	atomic mass Pb	²³⁸ U/ ²⁰⁴ Pb	²³² Th/ ²⁰⁴ Pb
208/27-2	16	1.61	4.92	15.9639	15.3770	37.1528	0.2297	0.2213	0.5346	0.01439	207.262	6.05	19.091
206/8-2	31	1.03	21.79	19.0209	15.6560	40.8565	0.2485	0.2046	0.5338	0.01307	207.246	2.20	48.051
206/8-8	7	0.24	0.32	15.0013	15.2229	35.8609	0.2236	0.2269	0.5346	0.01491	207.266	1.95	2.780
206/8-7	6	0.89	5.02	18.1463	15.4915	48.1960	0.2191	0.1870	0.5818	0.01207	207.327	10.66	61.948
206/7-A2 (2413)	30	1.12	5.66	15.3801	15.1153	36.5837	0.2259	0.2220	0.5374	0.01469	207.267	2.20	11.470
206/7-A2 (2544)	10	0.36	4.91	14.9575	15.1125	37.8816	0.2169	0.2192	0.5494	0.01450	207.289	2.12	30.263
205/16-1	5	0.54	10.86	14.9518	14.9653	40.1687	0.2103	0.2105	0.5651	0.01407	207.313	6.58	137.953
204/25-1	5	0.07	0.09	13.8949	14.6942	33.6994	0.2195	0.2322	0.5325	0.01580	207.266	0.80	1.003
202/2-1	10	0.89	6.31	16.1018	15.1301	38.1490	0.2288	0.2150	0.5420	0.01421	207.271	5.44	39.689
154/3-1	4	0.44	1.76	15.3587	14.8581	36.5479	0.2266	0.2193	0.5393	0.01476	207.268	6.43	26.584
56-09/536	9	0.55	5.63	15.1306	14.7864	38.8496	0.2169	0.2119	0.5569	0.01433	207.297	3.70	38.955
56-08/921	11	0.18	9.63	14.2211	14.6677	38.7379	0.2072	0.2137	0.5645	0.01457	207.314	0.97	53.657
56-08/924	21	1.84	13.96	16.7619	15.0828	38.7454	0.2341	0.2107	0.5412	0.01397	207.265	5.43	42.516
132/15-1	16	1.22	15.26	16.1276	15.0214	36.6015	0.2346	0.2185	0.5324	0.01455	207.254	4.53	58.580
56-09/386	20	0.60	8.56	14.9587	14.9987	37.6315	0.2181	0.2187	0.5487	0.01458	207.287	1.79	26.232
canyon diablo meteorite				9.3066	10.2930	29.4750							

4.3 Nd ISOTOPE DATA

Four samples from the most northern quadrants of the study area, to the northwest of the Shetland Islands, display widely different Sm-Nd signatures. The quartzofeldspathic mylonite 220/26-1 yields a crustal formation age of 2.32 Ga whereas the augen gneiss 209/9-1 indicates an older protolith with a 2.98 Ga T_{DM} age. Well 209/9-1 comprises part of the Rendle granite or granodiorite dated by K-Ar at 392 ± 6 Ma (Ritchie et al. 1987) and was considered to be Caledonian in age. This age must now be interpreted as a metamorphic age in the light of the 2.8 Ga U-Pb age for 209/9-1 and the Archaean T_{DM} age. The age of 1.44 Ga for 209/12-1 indicates a significant contribution of juvenile material although the mineralogy for this biotite schist suggests the protolith may have been a feldspathic sandstone. Sample 81/17, described as an amphibolite, also yields a young crustal formation age (1.82 Ga). However this, and to a lesser extent, the age for 220/26-1 should be viewed with caution, both rocks have high $^{147}\text{Sm}/^{144}\text{Nd}$ ratios which would bias the calculation towards an older age. In order to calculate a two stage model a reasonable estimate of the crystallisation age is required but in both cases this is not known.

Further to the south on the Shetland Islands a succession of Dalradian type schists and gneisses are found on the west side of both Unst and Fetlar. Yell is mostly formed of Moine psammities interlayered with lenticular bodies of mica schists and quartzites, together with a number of Lewisian inliers (Flinn 1994). Knudsen (2000) in a provenance study of Devonian sandstones from Shetland documented a 3.05 Ga model age for an Archaean tonalite gneiss from the Wilgi Geos Group on Shetland. A psammite from the west of Yell recorded an age of 1.86 Ga and two quartzite samples from within the Whiteness and Clift Hills Divisions yielded ages of 2.15 Ga and 2.60 Ga respectively (Knudsen, 2000).

Fourteen rocks (208/27-2 to 202/2-1 Table 4.3) sampled from quadrants to the east of the Shetland Islands yield a narrow range of T_{DM} ages from 2.83 to 3.30 Ga. ϵ_{Nd} calculated using the U-Pb zircon age or, if the samples were not dated, an assumed value of either 2.7 or 2.8 Ga are generally close to 0. Samples located in quadrants 202 and 204 display more positive signatures (1.3 to 3.3) whereas sample 208/27-2

Table 4.3: Rockall Basement Sr-Nd data

Sample	Rb	Sr	⁸⁷ Rb/ ⁸⁶ Sr	⁸⁷ Sr/ ⁸⁶ Sr	Sm	Nd	¹⁴⁷ Sm/ ¹⁴⁴ Nd	¹⁴³ Nd/ ¹⁴⁴ Nd	f Sm/Nd	T _{DM} *	T _{DM} **	e _{Nd} (T)	Age#
220/26-1	114	221	1.494	0.721672	3.78	16.2	0.1408	0.512004	-0.28	2.32			
209/9-1	88	472	0.5402	0.721862	7.71	43.9	0.1061	0.510999	-0.46	3.01	2979	0.0	2738.3 ± 4.1
209/12-1	120	324	1.072	0.715786	9.66	58.7	0.0994	0.512023	-0.49	1.44			
81/17	4	140	0.0827	0.706586	4.12	15.6	0.1603	0.512468	-0.19	1.82			
208/27-2	43	597	0.2085	0.714219	7.50	36.3	0.1250	0.511105	-0.36	3.48	3295	-4.1	2800
206/8-2	17	364	0.1351	0.707933	5.21	40.7	0.0773	0.510427	-0.61	3.02	3035	-0.1	2800
206/8-8	39	279	0.4049	0.720345	4.85	23.8	0.1234	0.511249	-0.37	3.17	3072	-0.7	2800
206/8-1A	39	546	0.2067	0.711442	10.0	64.9	0.0935	0.510735	-0.52	3.03	3022	0.1	2801.7 ± 5.1/-4.6
206/8-7	21	356	0.1707	0.707924	4.02	29.4	0.0827	0.510538	-0.58	3.01	3018	0.2	2800
206/7-A2 2143m	49	758	0.1870	0.706434	11.7	70.3	0.1003	0.510913	-0.49	2.98	2953	1.1	2800
206/7-A2 2544m	14	446	0.0908	0.705532	10.8	65.5	0.0997	0.510829	-0.49	3.07	3050	-0.3	2800
205/16-1	74	70	3.062	0.717789	7.94	46.0	0.1044	0.511014	-0.47	2.94	2916	0.4	2700
205/22-1	78	169	1.336	0.711880	7.34	40.6	0.1094	0.511070	-0.44	3.00	2961	-0.2	2700 ± 13
204/23-1	41	422	0.2811	0.708151	5.26	28.3	0.1124	0.511183	-0.43	2.92			
204/25-1	4	872	0.0133	0.702025	4.48	25.5	0.1038	0.511034	-0.47	2.90	2876	1.0	2700
202/3-1	38	475	0.2315	0.709507	1.48	8.67	0.1028	0.511050	-0.48	2.85	2829	1.7	2700
202/2-1	70	303	0.6698	0.728379	4.60	27.2	0.1024	0.510959	-0.48	2.97	2941	1.6	2829 ± 46
88/02	67	563	0.3445	0.714549	2.68	21.4	0.0756	0.510440	-0.62	2.97	2967	1.3	2830
164/25-2	1	159	0.0182	0.703181	3.96	13.3	0.1799	0.512434	-0.09	3.10	2111	-0.5	1633.5 ± 3.3
154/3-1	36	227	0.4590	0.711170	4.75	21.3	0.1347	0.511661	-0.32	2.82			
58-08/228	69	421	0.4746	0.716670	0.06	0.25	0.1475	0.511525	-0.25	3.70	2874	-11.0	1700
58-08/230	40	1500	0.0771	0.704662	7.89	50.1	0.0953	0.512408	-0.52	0.88			
90/14	71	463	0.4442	0.719160	1.27	10.2	0.0750	0.510350	-0.62	3.05	3079	-0.8	2800
57-09/536	90	692	0.3766	0.715456	13.0	83.8	0.0939	0.510844	-0.52	2.90	2892	0.9	2709 ±
56-08/920	21	291	0.2089	0.712857	7.15	37.6	0.1150	0.511176	-0.42	3.01	2954	0.0	2710
56-08/921	70	491	0.4129	0.717237	3.52	35.2	0.0605	0.510513	-0.69	2.60	2890	-10.2	1791.5 ± 2.9
56-08/924	76	534	0.4120	0.714193	7.57	61.2	0.0747	0.510928	-0.62	2.40	2577	-5.2	1797.8 ± 3.2
132/15-1	211	88	7.038	0.855522	7.59	54.8	0.0836	0.510909	-0.57	2.59	2738	-7.7	1795
56-09/384	102	661	0.4468	0.715103	6.17	30.2	0.1236	0.511618	-0.37	2.54	2427	-3.1	1794.4 ± 4.2
56-09/386	145	187	2.255	0.761881	7.61	51.4	0.0895	0.510968	-0.54	2.64	2751	-7.9	1795
56-09/388	47	611	0.2227	0.712650	3.71	26.1	0.0859	0.510740	-0.56	2.84	2976	-11.6	1795
56-15/18 1.65-1.71m	58	630	0.2664	0.709627	7.57	38.6	0.1186	0.511818	-0.40	2.07	2051	1.5	1744.9 ± 2.2
56-15/18 3.02-3.36m	49	592	0.2395	0.708735	9.66	48.6	0.1201	0.511846	-0.39	2.06	2036	1.7	1744.9 ± 2.2
57-14/58	17	528	0.0931	0.705146	6.88	25.1	0.1660	0.512635	-0.16	1.49			
57-15/15	51	276	0.5345	0.704732	13.4	67.2	0.1205	0.512254	-0.39	1.38			

* Single stage TDM calculated according to Borg et al. (1991).

** Two stage TDM calculated using U-Pb or assumed age of crystallization and f(Sm/Nd) following DePaolo et al (1991).

U-Pb or assumed age.

yielded a value of -4.1. When plotted on a ϵ_{Nd} versus time diagram the growth lines fall within the field of Archaean gneisses from mainland Scotland (Figure 4.23).

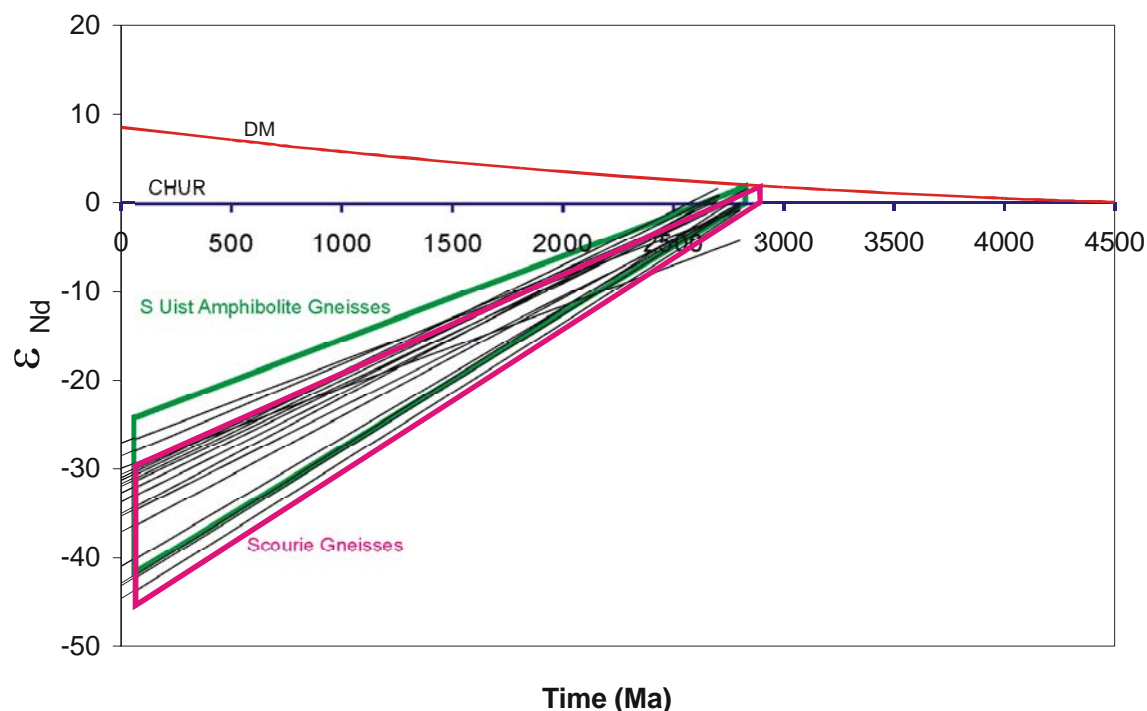


Figure 4.23. ϵ_{Nd} versus time for the basement samples. DM = Depleted mantle. CHUR = Chondritic uniform reservoir.

Sample 164/25-2 is characterised by a very high $^{147}\text{Sm}/^{144}\text{Nd}$ ratio (0.1799) and a two-stage T_{DM} age based on the U-Pb crystallisation age of 1633.5 ± 3.3 Ma indicates a 2.1 Ga protolith age. The mineralogy of this metabasic gneiss suggests a gabbroic or basaltic protolith. Cliff et al (1998) obtained Sm-Nd WR-mineral regression ages of 1.625 ± 0.016 Ga (MSWD 2.8) and 1.66 ± 0.12 Ga (MSWD 9.7) for metabasites from the Younger Basic suite on Harris. Two stage model age calculation yield protolith ages of 2.35 Ga and 2.17 Ga respectively for these rocks.

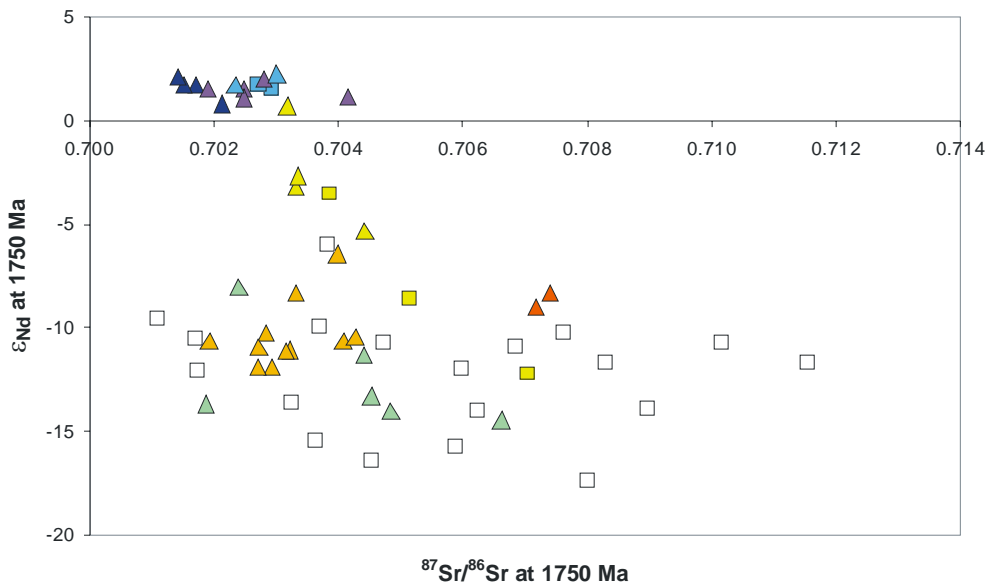
Samples 154/3-1 and 58-08/228 also have high $^{147}\text{Sm}/^{144}\text{Nd}$ ratios (0.1347 and 0.1475 respectively) and calculation of reliable model ages would be dependent on reasonable estimates of the crystallisation ages. 58-08/228 is a deformed granitic pegmatite located on the Outer Hebrides High to the west of the Isle of Lewis. Although Late Scourian pegmatites have been recorded on S Uist and Benbecula, none are found on N Uist, Harris or Lewis (Fettes et al., 1992). Laxfordian pegmatites are more abundant particularly on the west coast of Lewis and Harris and also in the Northern and Southern regions on the Scottish Mainland. A precise TIMS U-Pb age for a pegmatite from Loch Tollie near Gairloch yielded a zircon age of 1694

± 5 Ma that is interpreted as the time of intrusion (Park et al 2001). Friend and Kinny (2001) obtained a SHRIMP age of 1674 ± 3 Ma for a pegmatite from Loch Meaurach immediately NW of the Langavat Belt. Granite pegmatites from NE and SW of the main zone of type-2 tectonites within the Langavat Belt yielded U-Pb zircon ages of 1657 ± 1 Ma (Mason et al. 2004) and 1675 ± 2 Ma (Mason and Brewer, 2005) respectively. Assuming a 1700 Ma crystallisation age for 58-08/228 results in a 2.87 Ga T_{DM} age and a negative ϵ_{Nd} of -11.0 indicating a significant component of older crust.

Sample 58-08/230 is an alkali granite with a 0.88 Ga Sm-Nd model age, notably distinct from other offshore granites. Forthcoming U-Pb dating should confirm the suspected Caledonian age for this sample.

Three quartzofeldspathic gneisses (90/14, 57-09/536, and 56-08/920) sampled west of Uist yielded a tight cluster of T_{DM} ages 2.89 to 3.08 Ga demonstrating the extent of Archaean basement that appears not to have suffered reworking during the early Proterozoic. U-Pb dating of 56-08/921 highlighted early Proterozoic zircon growth but most of the zircon fractions gave c. 2.7 Ga ages, indicating reworking during metamorphism. The Nd isotope systematics similarly reflect an Archaean protolith which was reworked during the early Proterozoic. 56-08/924 also yielded an early Proterozoic U-Pb zircon age however in this case the T_{DM} of 2.58 Ga indicates mixing of juvenile material with an Archaean crustal component. Gneisses from the Outer Hebridean Lewisian complex also indicate Archaean protolith ages of 2.8-3.0 Ga, however extensive Palaeoproterozoic reworking and granite injection has affected the northern Islands of Lewis and Harris where T_{DM} ages of 2.5-2.7 Ga are reported (Whitehouse 1990; Whitehouse, 1993; Cliff et al. 1998; Whitehouse and Bridgewater, 2001).

Three samples from Stanton High (56-09/384, 386 and 388) and one from the eastern margin of the Rockall Basin (132/15-1) yield a range of negative ϵ_{Nd} values (-3.1 to -11.6) and T_{DM} ages from 2.43 to 2.98 Ga indicating a variable component of Archaean material. The oldest model age, obtained for a sample of quartzofeldspathic gneiss (56-09/388), is identical to the age reported by Scanlon and Daly (2001) for a biotite gneiss (SB3) from the Stanton High. Scanlon and Daly analysed a further seven samples from the same region and concluded from the range of T_{DM} ages (2.03



- Data from this study. Open squares Archaean rocks, Yellow squares Stanton High, Blue squares Rockall High.
- Published data. Purple triangles Islay gneisses Marcantonio 1988. Dark blue triangles Rockall Bank Morton and Taylor 1991, Orange triangles SW Tiree granulites and Red triangles Caole migmatites Whitehouse and Robertson 1995.
- Unpublished data. Light blue triangles Rockall High and yellow triangles Stanton High Scanlon and Daly 2001.

Figure 4.24. ϵ_{Nd} versus $^{87}\text{Sr}/^{86}\text{Sr}$ at 1750 Ma.

– 2.67 Ga) that, although complex, the crustal structure was mostly Proterozoic in age. They inferred a faulted boundary between these samples and SB3 to the southwest. However 56-09/386 also yields an Archaean T_{DM} age and the U-Pb systematics of 56-08/921 provide evidence of Proterozoic reworking of Archaean crust in the southerly section of the outer Hebrides High. The Nd-Sr data array (Figure 4.24) further supports the interpretation of mixing of juvenile material at 1795 Ma with a 2.9-3.0 Ga crust.

Two samples of tonalitic gneiss from different depths in the same borehole on Rockall Bank (56-15/18 depth 1.65-1.71m and 3.02-3.36m) yielded T_{DM} ages of 2.05 and 2.04 Ga. Positive ϵ_{Nd} values, which are indistinguishable within experimental error (1.5 and 1.7 respectively), reflect the predominantly juvenile nature of the crust. Morton and Taylor (1991) analysed a mafic and an intermediate granulite from this area of Rockall Bank (samples A and C) and obtained T_{DM} ages of 2.06 Ga and 2.03 Ga respectively. Scanlon and Daly (2001) studied two lengths of core (56-15/11 and 56-15/12) from localities between those of A and C and reported broadly similar T_{DM} ages (1.89-1.95 Ga) for three syenite gneiss samples. Morton and Taylor (1991) also

studied three additional samples: E with a typically granitic igneous texture located to the east of Rockall Island; a granulite and a mafic gneiss collected from the south westerly end of a northeast - southwest traverse across the top of Rockall Bank (D and B). E and D yielded T_{DM} ages of 1.98 Ga and 2.04 Ga whereas the most southerly sample, B, gave a slightly older age of 2.31 Ga. The range of model ages obtained for samples from Rockall Bank overlaps those for the Islay and Inishtrahull gneisses (2.0 – 2.22 Ga, Marcantonio et al. 1988; Dickin and Bowes 1991; Daly et al. 1991; Muir et al. 1994) and also the Annagh Division Mullet gneisses from the Erris complex in northwestern Ireland (Menuge and Daly 1990).

57-14/58 a sample of metagabbro and 57-15/15, a trachyandesite, yield Mesoproterozoic T_{DM} ages and are interpreted to be significantly younger intrusions that have differing contributions of Proterozoic crustal material.

5 Conclusions

The crystalline basement of the NW UK continental margin is composed of a varied group of igneous and metamorphic rocks, as characterized by petrography, geochemistry and isotope geochemistry from previous studies and new data presented here.

Most of the 42 boreholes investigated during this project intersected rocks that are broadly granitic in composition, and include orthogneisses and possible paragneisses. The rest of the samples cover a range of compositions from gabbros through to granitic pegmatites and alkali granite. The majority of these rocks are metamorphosed to amphibolite or granulite grade, as constrained by their dominant mineralogy, and exhibit gneissic or schistose fabrics. Some of these metamorphosed rocks suffered later alteration and brittle deformation to various degrees. The most deformed of these range from protomylonite to mylonite, cataclasites and ultracataclasites, and in the most extreme cases pseudotachylyte.

5.1 ARCHAEOAN OFFSHORE ROCKS

Archaean rocks are the dominant group, and are widespread in the central portion of the transect. They do not simply comprise one lithological group formed during a single intrusive event, but span a range of ages and of chemical compositions. The granitic rocks (s.l.) that comprise the bulk of the Archaean borehole samples are TTG gneisses or close affiliates, typical of Archaean terranes. These samples are characterized by high alumina and low Nb, they have REE patterns with variable degrees of HREE depletion, and are variably depleted and/or enriched in U and Th. Indeed, some borehole TTG's have trace element U, Th, and HREE depletion similar to that observed in the most depleted Lewisian tonalities. With respect to magma sources, these types of granitic rocks are considered to be derived by partial melting of mantle-derived basaltic protoliths, and thus are not direct mantle melts. These basaltic protoliths would have been garnet- and amphibole-bearing, and the variable degree of HREE depletion observed in the offshore TTG's reflects variable amounts of residual garnet in the melt source region. Other granitic rocks are similar to TTG's but do not conform strictly to the generally accepted definition. Some of these rocks are derived in part from TTG precursors, while others are definitely not TTG's, being

true granites in some cases, and developed from very different precursor magmas based upon their geochemical and isotope characteristics.

Crucially, Nd model ages map out the extent of the Archaean crust, and show that this material extends over a very wide area. Many of the rocks have two-stage model ages between 2.8-3.0 Ga. These model ages are consistent with widespread 2.7-2.8 Ga crust formation from slightly to modestly older basaltic precursors. These data, together with the U-Pb ages, show that previous geochronology using the K-Ar and Rb-Sr chronometers suffered variable degrees of disturbance, as late as 392 Ma in the case of K-Ar. This situation is similar to that observed on-shore. Furthermore, $>>3.0$ Ga model ages are absent from the offshore Archean crust. This is significant because it indicates that the ancient crust observed in parts of Labrador and Greenland (e.g. the Amitsôk gneisses and older crust) probably does not occur anywhere in the North Atlantic region east of Greenland.

The U-Pb data for the Archaean rocks shows they were formed at two major times. The oldest rocks crystallized at c. 2.8 Ga, and evidence of crustal recycling at this time is absent. The later rocks crystallized between c. 2.74 and 2.70 Ga. These younger gneisses show abundant evidence for crustal recycling, as indicated by zircon inheritance. The age of most of the inherited crustal material cannot be significantly older than the 2.8 Ga gneisses because the Nd model ages of the two groups of rocks are similar, and no >2.8 Ga inherited grains were observed.

The metamorphic history of these rocks is probably complex. The 2.8 Ga rocks range from amphibolite to granulite facies, and zircon textures suggest the granulite facies event probably occurred not long after crystallization. The younger gneisses definitely experienced a granulite facies event, also probably not long after crystallization. This metamorphism could be similar to that observed on parts of the Outer Hebrides and in the Gruinard Bay area on the mainland. What is significant with respect to Pb-loss trajectories is that none have lower intercepts of c. 2.5 Ga or 1.88 Ga. It can be concluded, therefore, that the prominent 2.5 Ga granulite facies event affecting the TTG's in the Assynt area, and the ~ 1.88 Ga UHP granulite facies metamorphism affecting some continental arc rocks on Harris did not affect the rocks in the offshore region.

5.2 PROTEROZOIC OFFSHORE ROCKS

Proterozoic igneous rocks are also present, and largely occur on the periphery of the offshore region of Archaean rocks. Most of these Proterozoic rocks are also dioritic to granitic (s.l.), with the notable exception of two metagabbroic rocks.

Rockall High and Stanton High basement are both characterized by dioritic to monzogranitic crust. The new Rockall borehole data indicate that the rocks were intruded at 1744.9 ± 2.2 Ma, and have Nd isotope signatures indicative of juvenile additions of crust. In contrast, the rocks of Stanton High are slightly older than those of the Rockall High and have been produced from a mixture of recycled Archaean crust and juvenile Proterozoic mantle-derived magmas. The relative proportions of recycled to juvenile components varies. This is reflected by the amount of Archaean zircon inheritance, which correlates well with the Nd model ages. Strongly reworked Archaean rocks have predominantly 2.7 Ga zircons with only minor zircon growth at 1.79 Ga, coupled with Archaean Nd model ages. A more juvenile granodiorite has little older zircon inheritance, igneous zircon growth at 1799.1 ± 2.5 Ma, and a late Archaean model age. As with the Archaean gneisses, the Rockall High and Stanton High rocks experienced upper amphibolite to granulite facies metamorphism.

In addition to mapping out the widespread Archaean crust, and the complexities of Proterozoic – Archaean crust in the Stanton High area, the Nd isotope data indicate a mixture of Archaean and younger crustal domains in the northernmost portion of the transect. This situation is perhaps not unexpected given the mixed Archaean – Proterozoic crust and their derivative Phanerozoic sediments found in the Shetlands.

Finally, a surprising result was obtained for borehole 164/25-2. This sample is a granulite facies metabasic rock with a Proterozoic two-stage Nd model age and a 1633.5 ± 3.3 Ma zircon age. An ϵ_{Nd} value of -0.5 at the crystallization age indicates a mantle-derived magma with only a modest involvement with older crust.

5.3 REGIONAL CORRELATIONS

Potential relationships between the transect samples and mainland lithologies exposed in the UK, Greenland and Labrador are currently being explored, but a number of useful points may be drawn at this stage. With respect to the Lewisian exposed on-shore, various terrane models have been proposed and are currently being tested and hotly debated. Although the terrane models are a good concept, there are numerous contentious issues concerning the on-shore Lewisian geology that require further testing and refinement before terrane definitions can be generally agreed. One of the major problems is that the terranes are defined in terms of protolith and metamorphic ages. Superposition of high- to very high-grade metamorphic events in these rocks has done much to obscure the record of the relevant events in rocks studied thus far. Until the terrane definitions improve, it would not be prudent to assign the transect samples to a particular terrane, particularly since the borehole samples are essentially pinpoints whose information must be extrapolated over a large area. What can be usefully done with the transect information available now is to use it to test and refine the current regional continental reconstruction models because a broad knowledge of the geology is probably sufficient.

With regards to palaeotectonic reconstructions on a regional scale, it is widely accepted that the Lewisian complex/terrane of NW Scotland is a small part of a wider region of Precambrian crust that extends from the Eastern Churchill Province of the Canadian Shield through to the Lapland-Kola belt of Scandinavia (Figure 5.1). Due to their similar structural histories, the Lewisian complex has been specifically linked to the Nagssugtoquidian of East and West Greenland (Park et al. 1994; Myers, 1987). Park (1994) suggested four stages in the plate tectonic history of the Lewisian complex and adjacent Palaeoproterozoic complexes of Laurentia and Baltica between 2.6 and 1.5 Ga. These are:

1. 2.6-2.4 Ga. Development of conjugate shear zones in the North Atlantic craton.
2. 2.4-2.0 Ga. Rifting and mafic dyke emplacement in the older craton, and creation of oceanic and intracontinental basins.
3. 2.0-1.8 Ga. Subduction at active margins of older cratons with the creation of magmatic arcs, collision of cratons accompanied by the closure of intra-cratonic

basins, and accretion of arcs. Intense regional deformation and high-grade metamorphism occurred at this time.

4. 1.8-1.5 Ga. Development of new active margins that are discordant to the previous ones, with a significant change in convergence direction within the amalgamated continental assembly. Metamorphic effects are more localised and less intense than 3.

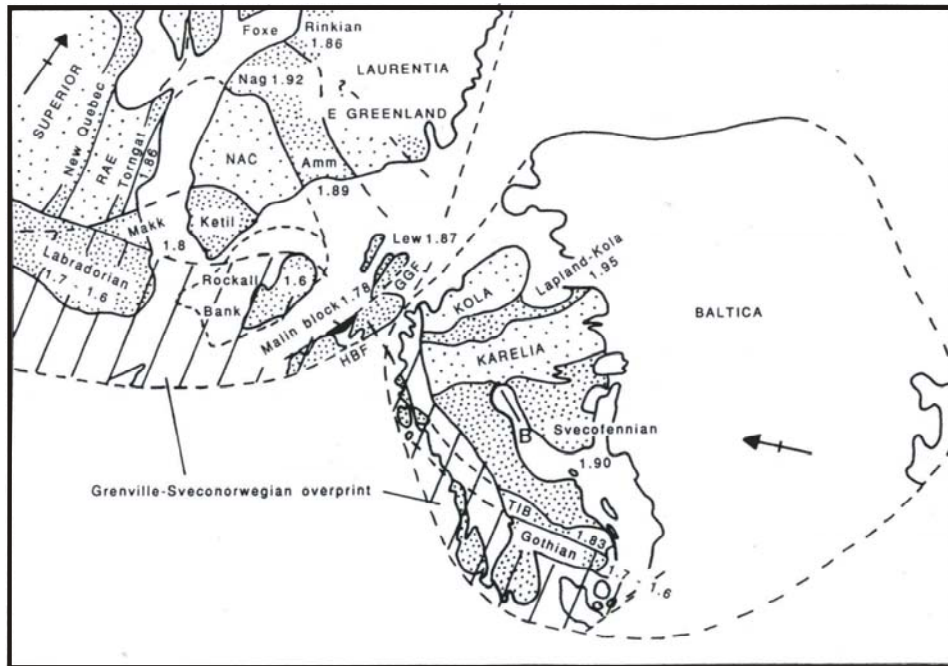


Figure 5.1. A reconstruction of eastern Laurentia and Baltica between 1.9-1.6 Ga taken from Park (1994).

Park (1994) also produced a reconstruction of the region between 1.9 and 1.6 Ga (Figure 5.1). This reconstruction modifies earlier palaeomagnetic plate reconstructions (e.g. Piper, 1982) to accommodate the northern part of Britain and Rockall. The Rhinns complex is shown in this reconstruction as the Malin Block after Muir et al. (1989). Muir et al. (1994) document the similarities between the Ketilidian of Southern Greenland and the Svecofennian of Scandinavia with the Rhinns complex. In addition, Morton and Taylor (1991) suggest that the Rockall Plateau is also similar to the Rhinns complex. Therefore in the reconstruction of Park (1994) the Rhinns complex and Rockall are linked to the Ketilidian and the Lewisian complex to the Nagssugtoquidian of Greenland. This is significant because correlation with the Ketilidian and Nagssugtoquidian requires a pinching out of the North Atlantic Craton to the west of Rockall.

Park's (1994) reconstruction is remarkably similar to that of Winchester (1988), which is shown in Figure 5.2. In this earlier model, the Rhinns complex is linked to the Ketilidian of Greenland, but Rockall is thought to be similar to the Nagssugtoquidian. The North Atlantic Craton again pinches out, but in this reconstruction it is to the south of Rockall and north of the Rhinns complex.

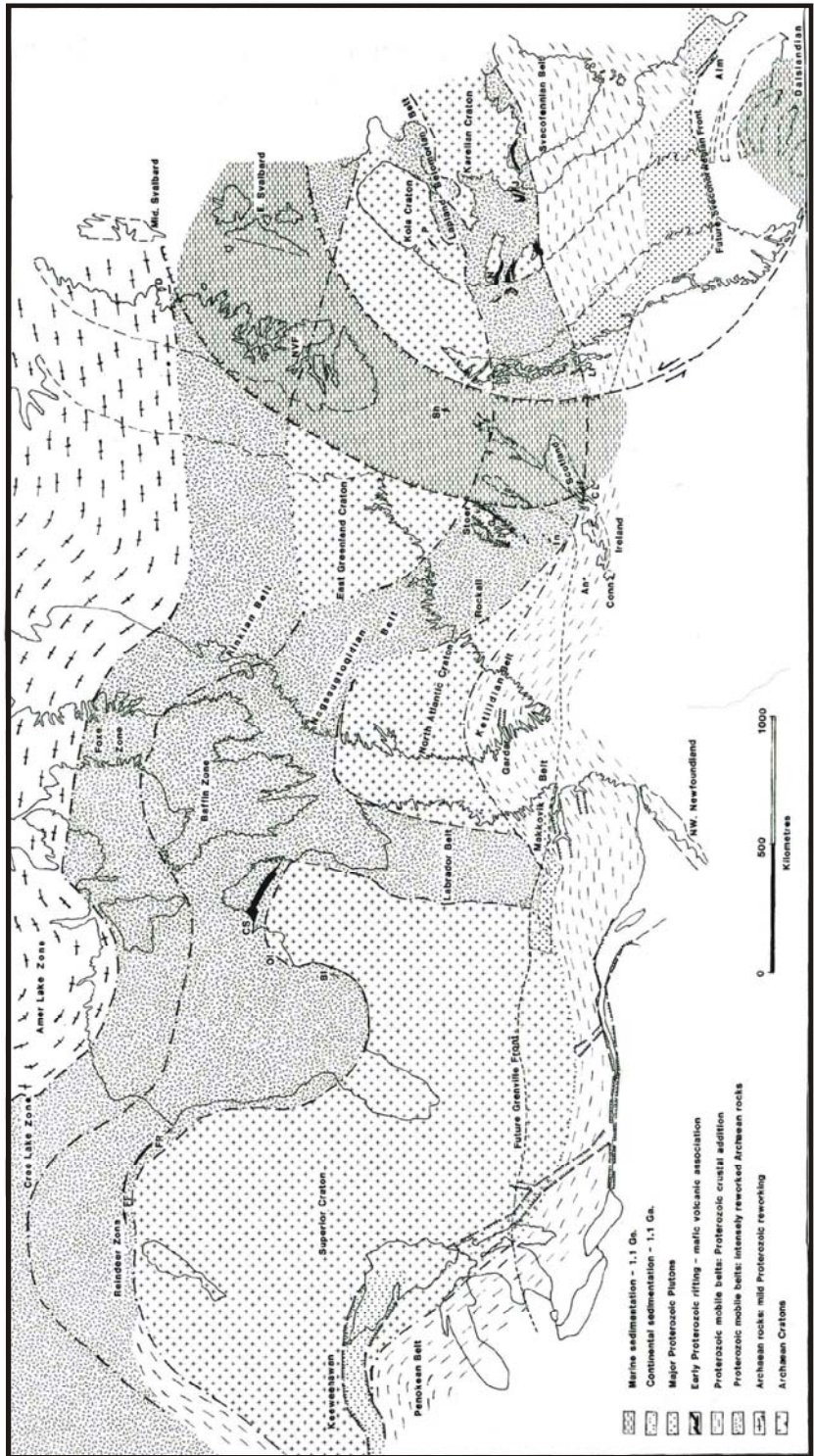


Figure 5.2. A reconstruction of Laurentia-Baltica at 1150 Ma taken from Winchester (1988).

A significant change in more recent reconstruction models (Buchan et al. 2000; Baba 2002) is the introduction on the Rockall High of an interpreted boundary between the reworked Lewisian complex to the north and the juvenile Rhinns complex in the south (Figure 5.3). This division is apparently based on work by Morton and Taylor (1991) on dredge samples recovered from Rockall Bank. Morton and Taylor (1991) document that these basement samples have little similarity to the Lewisian complex of NW Scotland and their Nd isotope data suggest an affinity with the Rhinns complex. However, while the Buchan et al. (2000) model incorporated the 1.63 Ga Rb-Sr age from Morton and Taylor (1991) which suggested that the Rockall Bank is slightly younger than the Rhinns complex (c. 1800 Ma. Marcantonio et al., 1988), it ignores the revised age of 1.72 ± 0.07 Ga by Dickin (1992). This subdivision of Rockall Bank also appears in the reconstruction of Baba (2002) as shown in Figure 5.4. Baba (2002) refines earlier reconstructions using the tectono-thermal history of South Harris, which is said to be comparable to that observed in the Lapland-Kola belt and New Quebec. Both models show the pinching out of the North Atlantic Craton to the west of Rockall. We can find no justification for this division within the area of Rockall High. U-Pb zircon data presented here for Rockall High (1744.9 ± 2.2 Ma), in conjunction with the Scanlon and Daly (2001) ages for Rockall High (4 samples giving U-Pb zircon ages of 1740 – 1770 Ma) and recent work by Morton and Hallsworth (2005) on detrital zircons from sedimentary rocks on Hatton and Eboras High (1749.5 ± 2.9 Ma and 1798.5 ± 4.5 Ma) suggest that the majority of the Rockall High is a juvenile Palaeoproterozoic terrane. The boundary between the reworked Lewisian complex and the juvenile Palaeoproterozoic crust must therefore be located elsewhere than in the Rockall area. Furthermore, Buchan et al. (2000) describe the area to the west of NW Scotland (Rhinns and Rockall) as a keystone region in plate reconstructions at 1.265 Ga. Using the new data from this study, we would suggest that Rockall High and the Rhinns complex have affinities to the Ketilidian of Greenland and the Svecofennian of Scandinavia as originally suggested by Winchester (1988) and Park (1994).

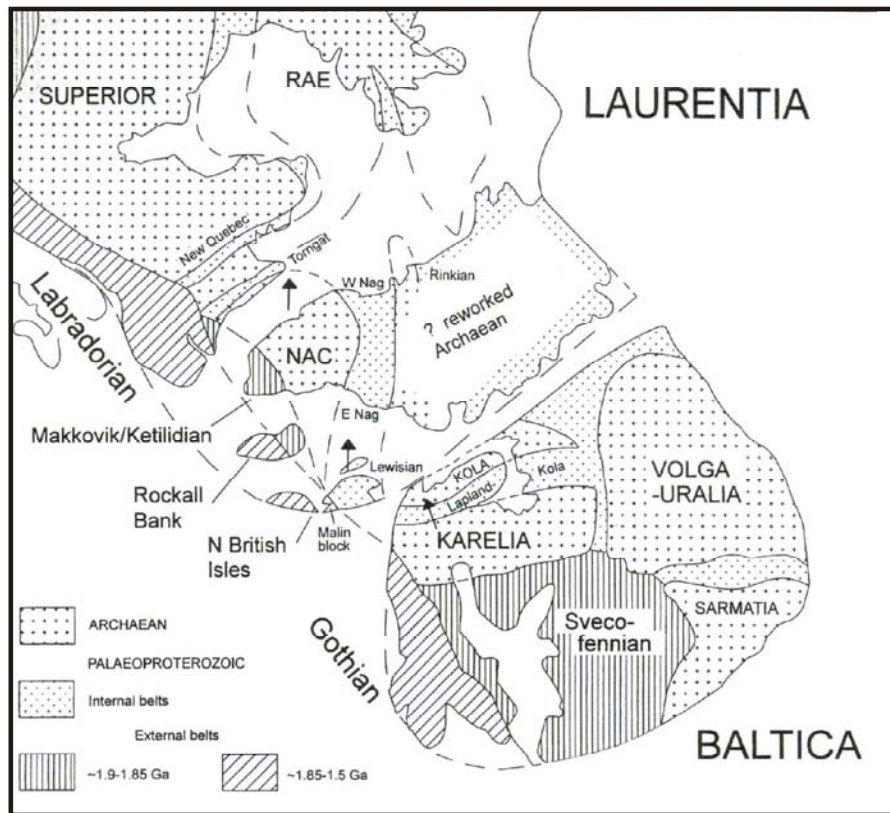


Figure 5.3. A palaeomagnetic reconstruction at 1265 Ma (Buchan et al. 2000).

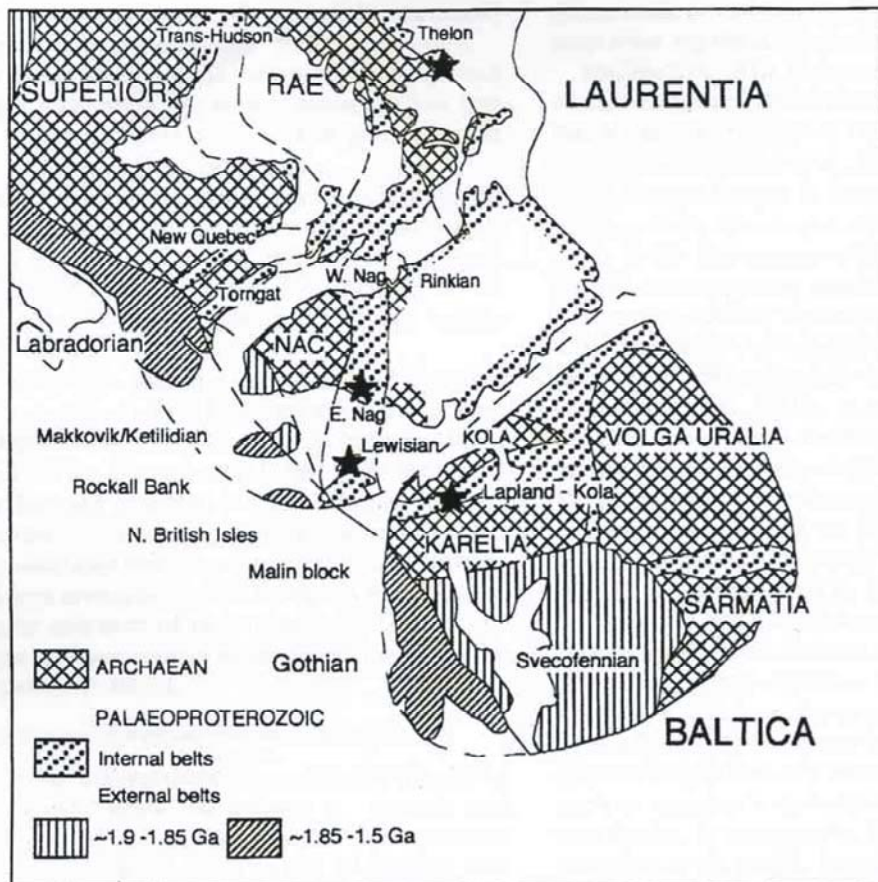


Figure 5.4. A reconstruction of Laurentia-Baltica at 1.2 Ga (Baba 2002).

References

Most of the references listed below are held in the Library of the British Geological Survey at Keyworth, Nottingham. Copies of the references may be purchased from the Library subject to the current copyright legislation.

Åhäll, K-I., Connelly, J.N. and Brewer, T.S. 2000. Episodic rapakivi magmatism due to distal orogenesis?: Correlation of 1.69 – 1.50 Ga orogenic and inboard, “anorogenic” events in the Baltic Shield. *Geology*, **28**, 823-826.

Baba, S. 2003. Two stages of sapphirine formation during prograde and retrograde metamorphism in the Paleoproterozoic Lewisian Complex in South Harris, N.W. Scotland. *Journal of Petrology*, **44**, 329-354.

Barker, F. 1979. Trondhjemite: Definition, environment and hypotheses of origin. *In* Barker, F. (ed.) *Trondhjemites, dacites and related rocks*. Elsevier, Amsterdam, 1-12.

Borg, S.G., DePaolo, D.J. and Smith, B.M. 1990. Isotopic structure and tectonics of the central Transantarctic Mountains. *Journal of Geophysical Research*, **95**, 6647-6667.

Cliff, R.A., Rex, D.C. and Guise, P.G. 1998. Geochronological studies of Proterozoic crustal evolution in the northern Outer Hebrides. *Precambrian Research*, **91**, 401-418.

Cohen, A.S., O’Nions, R.K., and O’Hara, M.J. 1991. Chronology and mechanism of depletion in Lewisian granulites. *Contributions to Mineralogy and Petrology*, **106**, 142-153.

Corfu, F. and Noble, S.R. 1992. Genesis of the southern Abitibi greenstone belt, Superior Province, Canada: Evidence from zircon Hf-isotope analyses using a single filament technique. *Geochemica et Cosmochimica Acta*, **56**, 2081-2097.

Corfu, F., Heaman, L.M., and Rogers, G. 1994. Polymetamorphic evolution of the Lewisian complex, NW Scotland, as recorded by U-Pb isotopic compositions of zircon, titanite and rutile. *Contributions to Mineralogy and Petrology*, **117**, 215-228.

- Corfu, F., Crane, A., Moser, D., and Rogers, G. 1998. U-Pb zircon systematics at Gruinard Bay, northwest Scotland: implications for the early orogenic evolution of the Lewisian complex. *Contributions to Mineralogy and Petrology*, **133**, 329-345.
- Corfu, F., Hanchar, J.M., Hoskin, P.W.O., and Kinny, P. 2003. Atlas of zircon textures. *In: J. M. Hanchar, P. W.O. Hoskin (eds.) Zircon: Experiments, isotopes and trace element investigations. Mineralogical Society of America and the Geochemical Society, Reviews in Mineralogy and Geochemistry* **53**, 183-213.
- Daly, J.S., Heaman, L.M., Fitzgerald, R.C., Menuge, J.F., Brewer, T.S. and Morton, A.C. 1995. Age and crustal evolution of crystalline basement in western Ireland and Rockall. *In Croker, P.F. and Shannon, P.M. (eds). The Petroleum Geology of Ireland's Offshore Basins, Geological Society Special Publication*, **93**, 433-434.
- Daly, J.S., Muir, R.J. and Cliff, R.A. 1991. A precise U-Pb zircon age for the Inishtrahull syentic gneiss, County Donegal, Ireland. *Journal of the Geological Society, London*, **148**, 639-642.
- Dearnley, R. 1963. The Lewisian Complex of South Harris. *Quarterly Journal of the Geological Society, London*, **119**, 243-307.
- Defant, M.J. and Drummond, M.S. 1990. Derivation of some modern arc magmas by melting of young subducted lithosphere. *Nature*, **347**, 662-665.
- DePaolo, D.J., Linn, A.M. and Schubert, G. 1991. The continental crustal age distribution: Methods of determining mantle separation ages from Sm-Nd isotopic data and application to the southwestern United States. *Journal of Geophysical Research*, **96**, 2071-2088.
- Dickin, A.P. and Bowes, D.R. 1991. Isotopic evidence for the extent of early Proterozoic basement in Scotland and northwest Ireland. *Geological Magazine*, **128**, 385-388.
- Dickin, A.P. and Durant, G.P. 2002. The Blackstones Bank igneous complex: geochemistry and crustal context of a submerged Tertiary igneous centre in the Scottish Hebrides. *Geological Magazine*, **139**, 199-207.

- Evans, C.R. 1965. Geochronology of the Lewisian basement near Lochinver, Sutherland. *Nature*, **207**, 54-56.
- Evans, C.R. and Tarney, J. 1964. Isotopic ages of Assynt dykes. *Nature*, **204**, 638-641.
- Flinn, D. 1994. Geology of Yell and some neighbouring islands in Shetland. Memoir of the British Geological Survey, Sheet 130 (Scotland).
- Friend, C.L.R. and Kinny, P.D. 2001. A reappraisal of the Lewisian Gneiss Complex: geochronological evidence for its tectonic assembly from disparate terranes in the Proterozoic. *Contributions to Mineralogy and Petrology*, **142**, 198-218.
- Frei, R. and Rossing, M.T. 2001. The least radiogenic terrestrial leads; implications for the early Archean crustal evolution and hydrothermal-metasomatic processes in the Isua Supracrustal Belt (West Greenland). *Chemical Geology*, **181**, 47-66.
- Friend, C.L.R. and Kinny, P.D. 1995. New evidence for the protolith ages of Lewisian granulites, northwest Scotland. *Geology*, **23**, 1027-1030.
- Fowler, M.B. and Plant, J.A. 1987. Rare earth element geochemistry of Lewisian grey gneisses from Gruinard Bay. *Scottish Journal of Geology*, **23**, 193-202
- Gower, C.F., Schärer, U., and Heaman, L.M. 1992. The Labradorian orogeny in the Grenville Province, eastern Labrador, Canada. *Canadian Journal of Earth Sciences*, **29**, 1944-1957.
- Humphries, F.J. and Cliff, R.A. 1982. Sm-Nd dating and cooling history of Scourian granulites. *Nature*, **295**, 515-517.
- Jaffey, A.H., Flynn, K.F., Glendenin, L.E., Bentley, W.C. and Essling, A.M. 1971. Precision measurements of half-lives and specific activities of ^{235}U and ^{238}U . *Physics Reviews* **C4**, 1889-1906.
- Kamber, B.S. and Moorbath, S. 1998. Initial Pb of the Amîsoq gneiss revisited: implication for the timing of early Archaean crustal evolution in West Greenland. *Chemical Geology*, **150**, 19-41.

- Kamo, S.L., Wasteneys, H., Gower, C.F., and Krogh, T.E. 1996. U-Pb geochronology of Labradorian and later events in the Grenville Province, eastern Labrador. *Precambrian Research*, **80**, 239-260.
- Kempton P. D. and McGill R. 2002. Procedure for the analysis of Common Pb at the NERC Isotope Geosciences Laboratory and an assessment of data quality. NIGL Report Series No. 178.
- Kinny, P.D. and Friend, C.R.L. 1997. U/Pb isotopic evidence for the accretion of different crustal blocks to form the Lewisian complex of northwest Scotland. *Contributions to Mineralogy and Petrology*, **129**, 326-340.
- Kinny, P.D., Friend, C.R.L., and Love, G.J. 2005. Proposal for a terrane-based nomenclature for the Lewisian Gneiss Complex of NW Scotland. *Journal of the Geological Society London*, **162**, 175-186.
- Knudsen, T-L. 2000. The provenance of Devonian sandstones from Shetland: a Sm-Nd and trace element study. *Scottish Journal of Geology*, **36**, 61-72.
- Krogh, T.E., 1982. Improved accuracy of U-Pb zircon ages by the creation of more concordant systems using an air abrasion technique. *Geochimica et Cosmochimica Acta*, **46**, 637-649.
- Love, G.J., Kinny, P.D., and Friend, C.R.L. 2004. Timing of magmatism and metamorphism in the Gruinard Bay area of the Lewisian Gneiss Complex: comparisons with the Assynt Terrane and implications for terrane accretion. *Contributions to Mineralogy and Petrology*, **146**, 620-636.
- Ludwig, K.R. 1980. Calculation of uncertainties of U/Pb isotope data. *Earth and Planetary Science Letters*, **46**, 212-220.
- Ludwig, K.R. 1998. On the treatment of concordant uranium-lead ages. *Geochimica et Cosmochimica Acta*, **62**, 665-676.
- Ludwig, K.R. 2003. Isoplot/Ex version 3.0. A geochronological toolkit for Microsoft Excel. Berkeley Geochronology Center Special Publication No. 4, 70p.
- Lyon, T.B.D., Pidgeon, R.T., Bowes, D.R. and Hopgood, A. 1973. Geochronological investigation of the quartzofeldspathic rocks of the Lewisian of Rona, Inner Hebrides. *Journal of the Geological Society of London*, **129**, 389-402.

- Marcantonio, F., Dickin, A.P., McNutt, R.H. and Heaman, L.M. 1988. A 1,800-million-year-old Proterozoic gneiss terrane in Islay with implications for the crustal structure and evolution of Britain. *Nature*, **353**, 62-64.
- Mason, A.J., Parrish, R.R., and Brewer, T.S. 2004a. U-Pb geochronology of Lewisian orthogneisses in the Outer Hebrides, Scotland: implications for the tectonic setting and correlation of the South Harris Complex. *Journal of the Geological Society London*, **161**, 45-54.
- Mason, A.J., Temperley, S., and Parrish, R.R. 2004b. New light on the construction, evolution and correlation of the Langavat Belt (Lewisian Complex), Outer Hebrides, Scotland: field, petrographic and geochronological evidence for an early Proterozoic imbricate zone. *Journal of the Geological Society London*, **161**, 837-848.
- Mason, A.J. and Brewer, T.S. 2005. A re-evaluation of a Laxfordian terrane boundary in the Lewisian Complex of South Harris, NW Scotland. *Journal of the Geological Society London*, **162**, 401-407.
- Menuge, J.F. and Daly, J.S. 1990. Proterozoic evolution of the Erris Complex, Northwest Mayo, Ireland: neodymium isotope evidence. *In* Gower, C.F., Rivers, T. and Ryan, B (eds) *Mid-Proterozoic Laurentia-Baltica: Geological Association of Canada Special Paper* **38**, 41-51.
- Moorbath, S., Welke, H., and Gale, N.H. 1969. The significance of lead isotope studies in ancient, high-grade metamorphic basement complexes, as exemplified by the Lewisian rocks of northwest Scotland. *Earth and Planetary Science Letters*, **6**, 245-256.
- Morton, A.C. and Taylor, P.N. 1991. Geochemical and isotopic constraints on the nature and age of the basement rocks from Rockall Bank, NE Atlantic. *Journal of the Geological Society, London*, **148**, 631-634.
- Muir, R. J., Fitches, W. R. and Maltman, A. J. 1989. An early Proterozoic link between Greenland and Scandinavia in the Inner Hebrides of Scotland. *Terra Abstracts*, **1**, 5.
- Muir, R.J. Fitches, W.R. and Maltman, A.J. 1992. Rhinns Complex: A missing link in the Proterozoic basement of the North Atlantic region. *Geology*, **20**, 1043-1046.

- Muir, R.J., Fitches, W.R. and Maltman, A.J. 1994. The Rhinns Complex: Proterozoic basement on Isaly and Colonsay, Inner Hebrides, Scotland, and on Inishtrahull, NW Ireland. *Transactions of the Royal Society of Edinburgh: Earth Sciences*, **85**, 77-90
- Myers, J. S. 1987. The East Greenland Nagssugtoqidian mobile belt compared with the Lewisian Complex. *In* Park, R. G. and Tarney, J (eds.), *Evolution of the Lewisian and comparable high grade terranes*. Geological Society of London Special Publications **27**, 235-246.
- Nakamura, N. 1974. Determination of REE, Ba, Fe, Mg and K in carbonaceous and ordinary chondrites. *Geochimica et Cosmochimica Acta*, **38**, 757-775.
- Noble, S.R., Tucker, R.D. and Pharaoh, T.C. 1993. Lower Palaeozoic and Precambrian igneous rocks from eastern England, and their bearing on Late Ordovician closure of the Tornquist Sea: Constraints from U/Pb and Nd isotopes. *Geological Magazine*, **130**, 835-846.
- O'Connor, J.T. 1965. A classification for quartz-rich igneous rock based on feldspar ratios. *United States Geological Survey Professional Paper*, 525B, B79-B84.
- Park, R.G. 1964. The structural history of the Lewisian rocks of Gairloch, Wester Ross. *Quarterly Journal of the Geological Society, London*, **120**, 397-434.
- Park, R.G. and Tarney, J. 1987. The Lewisian complex: a typical Precambrian high-grade terrain? *In* Park, R.G and Tarney, J. (eds) *Evolution of the Lewisian and Comparable Precambrian High-Grade Terrains*. Geological Society of London, Special Publications, **27**, 13-25.
- Park, R.G., Cliff, R.A., Fettes, D.G. and Stewart, A.D. 1994. Precambrian rocks in northwest Scotland west of the Moine Thrust: the Lewisian Complex and the Torridonian. *In* Gibbons, F.C. and Harris, A.L. (eds) *A Revised Correlation of Precambrian Rocks in the British Isles*. Geological Society Special Report 22, 6-22.
- Park, R.G., Tarney, J. and Connelly, J.N. 2001. The Loch Maree Group: Palaeoproterozoic subduction-accretion complex in the Lewisian of NW Scotland. *Precambrian Research*, **105**, 205-226.

- Parrish, R.R. 1987. An improved micro-capsule for zircon dissolution in U-Pb geochronology. *Chemical Geology (Isotope Geoscience Section)*, **66**, 99-102.
- Patchett, P.J. and Arnt, N.T. 1986. Nd isotopes and tectonics of 1.9-1.7 Ga crustal genesis. *Earth and Planetary Science Letters*, **78**, 329-338.
- Peach, B.N., Horne, J., Gunn, W., Clough, C.T and Hinxman, L.W. 1907. *The Geological Structure of the Northwest Highlands of Scotland*. Memoirs of the Geological Survey of Great Britain.
- Phillips, E.R. 2002. Description of thin sections. *In* Preliminary geological results of sea-bed sampling in the Hebrides-Rockall area from the *RRS James Clark Ross* in 2001. Compiled by Ken Hitchen, Eileen Gillespie and Alick Leslie. Internal Report IR/02/049. British Geological Survey.
- Pidgeon, R.T. and Bowes, D.R. 1972. Zircon U-Pb ages of granulites from the central region of the Lewisian of north-western Scotland. *Geological Magazine*, **109**, 247-258.
- Piper, J. D. A. 1982. The Precambrian palaeomagnetic record: the case for the Proterozoic supercontinent. *Earth and Planetary Science Letters*, **59**, 61-89.
- Ritchie, J.D. and Darbyshire, D.P.F. 1984. Rb-Sr dates on Precambrian rocks from marine exploration wells in and around the West Shetland Basin. *Scottish Journal of Geology*, **20**, 31-36.
- Ritchie, J.D., Hitchen, K. and Mitchell, J.G. 1987. The offshore continuation of the Moine Thrust north of Shetland as deduced from basement isotopic ages. *Scottish Journal of Geology*, **23**, 163-173.
- Roberts, D.G, Ardu, D.A. and Dearnley, R. 1973. Precambrian rocks drilled on Rockall Bank. *Nature, Physical Science*, **244**, 21-23.
- Rollinson, H.R. 1996. Tonalite-trondhjemite-granodiorite magmatism and the genesis of the Lewisian crust during the Archaean. *In* Brewer, T.S (ed.) *Precambrian Crustal evolution in the North Atlantic Region*. Special Publications, **112**, Geological Society of London. 25-42.
- Rollinson, H.R. and Fowler, M.B. 1987. The magmatic evolution of the Scourian Complex at Gruinard Bay. *In* Park, R.G. and Tarney, J. (eds) *The Evolution of the*

- Lewisian and Comparable Precambrian High Grade Terrains. Special Publications, **27**, Geological Society, London, 57-71.
- Royse K.R., Kempton P.D. and Darbyshire D.P.F. 1998. Procedure for the analysis of rubidium-strontium and samarium-neodymium isotopes at the NERC Isotope Geosciences Laboratory, NIGL Report series No. 121.
- Scanlon, R. and Daly, J.S. 2001. Progress report on BGS samples from Rockall and Stanton Banks, August 2001. unpublished 1-44.
- Scanlon, R.P., Daly, J.S. and Whitehouse, M.J. 2003. The c.1.8 Ga Stanton Banks Terrane, offshore western Scotland, a large juvenile Palaeoproterozoic crustal block within the accretionary Lewisian Complex. *Geophysical Research Abstracts*, **5**, 13248.
- Stacey, J.S. and Kramers, J.D. 1975. Approximation of terrestrial lead isotope evolution by a two-stage model. *Earth and Planetary Science Letters*, **26**, 207-221.
- Sun, S.-s. and McDonough, W.F. 1989. Chemical and isotopic systematics of oceanic basalts: implications for mantle composition and processes. *In* Saunders, A.D. and Norry, M.J. (eds), *Magmatism in the Ocean Basins*. Special Publications, Geological Society of London, **42**, 313-345.
- Sutton, J. and Watson, J. 1951. The pre-Torridonian metamorphic history of the Loch Torridon and Scourie areas in the North-west Highlands and its bearing on the chronological classification of the Lewisian. *Quarterly Journal of the Geological Society of London*, **106**, 241-307.
- Tarney, J. 1963. Assynt dykes and their metamorphism. *Nature*, **199**, 672-674.
- Tarney, J. and Weaver, B.L. 1987. Geochemistry of the Scourian complex: petrogenesis and tectonic models. *In* Park R.G. and Tarney, J. (eds), *Evolution of the Lewisian and Comparable Precambrian High Grade Terrains*, Special Publications, Geological Society of London, **27**, 45-56.
- Todt, W., Cliff, R.A., Hanser, A. and Hofmann, A.W. 1996. Evaluation of a ^{202}Pb - ^{205}Pb double spike for high-precision lead isotope analysis. *In*: *Geophysical Monograph 95, Earth Processes: Reading the Isotopic Code*, 429-437.

Whitehouse, M.J. 1989. Pb-isotopic evidence for U-Th-Pb behaviour in a prograde amphibolite to granulite facies transition from the Lewisian Complex of northwest Scotland: implications for Pb-Pb dating. *Geochimica et Cosmochimica Acta*, **53**, 717-724.

Whitehouse, M.J. 1990. Isotopic evolution of the southern Outer Hebridean Lewisian gneiss complex: constraints on Late Archaean source regions and the generation of transposed Pb-Pb palaeoisochrons. *Chemical Geology (Isotope Geoscience Section)*, **86**, 1-20.

Whitehouse, M.J. 1993. Age of the Corodale gneisses, South Uist. *Scottish Journal of Geology*, **29**, 1-7.

Whitehouse, M.J., 2003. Rare earth elements in zircon: a review of applications and case studies from the Outer Hebridean Lewisian Complex, NW Scotland. *In: Vance, D., Müller, W., and Villa, I.M. (eds.), Geochronology: Linking the Isotopic Record with Petrology and Textures. Geological Society, London, Special Publications*, **220**, 49-64.

Whitehouse, M.J. and Bridgewater, D. 2001. Geochronological constraints on Palaeoproterozoic crustal evolution and regional correlations of the northern Outer Hebridean Lewisian complex, Scotland. *Precambrian Research*, **105**, 227-245.

Whitehouse, M.J. and Robertson, C.J. 1995. Isotopic evolution of the Lewisian Complex of Tiree Inner Hebrides and correlation with the mainland. *Scottish Journal of Geology*, **31**, 131-137.

Whitehouse, M.J., Claesson, S., Sunde, T., and Vestin, J. 1997. Ion microprobe U-Pb zircon geochronology and correlation of Archaean gneisses from the Lewisian Complex of Gruinard Bay, northwestern Scotland. *Geochimica et Cosmochimica Acta*, **61**, 4429-4438.

Winchester, J A. 1988. Later Proterozoic environments and tectonic evolution in the northern Atlantic lands. *In: Winchester, J. A. (ed.) Later Proterozoic stratigraphy of the Northern Atlantic Regions. Blackie, Glasgow and London*, 253-271.